Cape Peninsula
University of Technology

ENERGY MANAGEMENT FOR A HYBRID RENEWABLE MICRO-GRID SYSTEM

by

CHRISTIAN NDEKE BIPONGO

Thesis submitted in fulfilment of the requirements for the degree

Doctor of Engineering: Electrical Engineering

In the Faculty of Engineering and the Built Environment

At the Cape Peninsula University of Technology

Supervisor: Dr Marco Adonis

Co-Supervisor: Dr Ali-Mustafa-Ali Almaktoof

Bellville
September 2024

CPUT copyright information

The thesis may not be published either in part (in scholarly, scientific or technical journals), or as a whole (as a monograph), unless permission has been obtained from the University.

DECLARATION

I, Christian NDEKE BIPONGO, declare that the contents of this thesis represent my own unaided work, and that the thesis has not previously been submitted for academic examination towards any qualification. Furthermore, it represents my own opinions and not necessarily those of the Cape Peninsula University of Technology.



02/09/2024

Signed **Date**

ABSTRACT

This study presents an energy management system (EMS) for a hybrid renewable micro-grid system. The increasing demand for energy has led to the accelerated depletion of fossil fuel reserves, outpacing their natural replenishment. It is anticipated that the available fossil fuel resources can only suffice for approximately the next 40 years, given the limitations in extracting these resources. Moreover, the widespread reliance on fossil fuels and internal combustion engines (ICE) has contributed substantially to environmental pollution and raised concerns about anthropogenic (human-induced) climate change. To address these issues, it is imperative to transit to a production system that is not based on fossil fuels as the primary energy source, hence the adoption of renewable micro-grids. The utilization of renewable micro-grids has experienced significant advancements and growth in the past decade, driven by technological maturity, the expected scarcity of fossil fuels and government policies emphasizing environmental protection.

While hybrid renewable micro-grid systems are now widely available in the market, renewable micro-grids are still considered as a promising alternative to traditional power grids. On-site hybrid micro-grids offer advantages such as minimizing disruptions, reducing costs, optimizing system component sizes to minimize operating costs, as well as ensuring access to energy sources which are affordable, reliable, and sustainable. The incorporation of an energy storage system, especially in renewable micro-grid systems, provides unconditional benefits for electric power reliability, including smoothing power fluctuations, supplying initial power during the transition from grid-connected mode to island operating mode, and offering the ability to ride through dynamic fluctuations in intermittent energy sources. Battery energy storage systems are predominantly utilized in renewable micro-grid systems. However, both renewable hybrid micro-grids and battery storage systems have shown certain limitations, not related to rising fossil fuel prices or environmental pollution but rather within the EMS. Some of these limitations include the intermittence of renewable energy sources, the efficiency dependence of the equipment on the operating point, the relationship between battery charging/discharging rates and operating conditions, overcurrent, overvoltage, state of charge (SOC), unbalanced conditions, all of which may impact battery lifetime and the reliability of hybrid micro-grids.

The main research problem focused on how to develop a real-time energy management system able to control the power flow within the hybrid renewable micro-grid system and the variable AC load as well as the utility grid. Secondly, how to control the charge and discharge

of the battery. The developed EMS algorithm including the micro-grid system was performed utilizing MATLAB/Simulink software, and Typhoon HIL's real-time digital simulator was used to test, validate and optimize their performance. This research aimed to develop a strategy to manage the energy flow within the hybrid renewable micro-grid system, which optimizes the renewable energy resources utilization and augments their incorporation into the power system. Hence, this research had as its principal objective to develop an energy management strategy capable to control the flow of energy in the hybrid micro-grid system and the main grid. The second objective of this research has been based on the control of the battery charging/discharging. To achieve these objectives, different sequences have been considered, which included the design of the components model of the hybrid micro-grid utilized in the simulation model, the development of the hybrid micro-grid simulation, the development of the hybrid micro-grid control scheme and finally, the development of the hybrid micro-grid system EMS algorithm.

To demonstrate the developed EMS control robustness and effectiveness, different cases have been utilized in the simulations, which showed its ability to handle the load in isolated as well as grid connected modes. The developed EMS control also ensures an appropriate battery operation within the hybrid micro-grid system. The main advantage of this algorithm is that it controls the flow of energy into the hybrid micro-grid and the variable AC load including the main grid; it additionally maintains a suitable battery charge/discharge, according to their conditions of operation as well as allows to keep its SOC within acceptable bounds. Additionally, the real-time experimental results obtained using the Typhoon HIL software demonstrated good performance in comparison to those achieved utilizing the Stateflow logical language in the MATLAB/Simulink software. This developed EMS algorithm was tested according to the different scenarios and shown to be extremely effective. Both results were similar and were based on the renewable energy sources production, utility grid, diesel generator, variable AC load demand and battery SOC. In discharge mode, the battery responded instantly, and during high production, it was perfectly recharged. The hybrid micro-grid and utility grid were able to share power effectively under the given conditions, which ensured the smooth operation of both sources. Finally, a higher charging power was used to charge the battery. The results indicate the feasibility of maximizing charging time using higher power, leading to improved energy density utilization and possibly increasing the longevity of the batteries.

ACKNOWLEDGEMENTS

My greatest gratitude is to Almighty God for providing me with the ability to finish my research project successfully and to the Cape Peninsula University of Technology Management for establishing a secure and supportive learning environment.

My deepest gratitude to Dr. Marco Adonis, for accepting to supervise me in this research project. His huge professional contribution, guidance and support were instrumental and motivational to the completion of this project. Working with him I have benefited academically and spiritually. This thesis has been successful because of your constant guidance.

I would like to thank my co-supervisor, Dr. Ali Almaktoof, for his guidance and invaluable assistance during this research project. His support and direction enabled me to maintain consistency and focus throughout this research phase.

I am thankful to the National Research Foundation for funding my studies.

Finally, I would want to sincerely thank my amazing family and friends for their help, understanding and encouragement over the years. I doubt I could have survived without them. I also want to express my gratitude to everyone who helped make this a reality by lending a hand in some kind.

DEDICATION

This thesis is dedicated to my father Magellan Ndeke Bipongo and my mother Lydie Kambungu your guidance and unwavering affection helped me become who I am today. To my lovely fiancée Syntyche Mujinga, my sisters Benitha, Rhema, Hervine, Dynamique and Dieudo, my uncle Andre Ndeke and his wife Sarah Pilato, my research project became more focused because of your affection.

PREFACE

The thesis delves into innovative strategies and methodologies to optimize the utilization and management of energy within hybrid renewable micro-grid systems. This comprehensive research covers various aspects of energy management, from circuit modeling to the implementation of advanced control systems, ensuring efficient integration and operation of renewable energy sources. The findings and methodologies developed throughout this research have been disseminated through several articles, reflecting the rigorous academic and practical contributions of this work. Below is a detailed overview of the published and under-review articles stemming from this research:

1. Article 1: "Basic Circuit Model of Voltage Source Converters: Methodology and Modelling"; Status: Published.

This published article presents a fundamental approach to modeling voltage source converters (VSCs), which are critical components in micro-grid systems. The methodology and modeling techniques discussed are essential for understanding and improving the performance of VSCs in hybrid renewable micro-grids.

Ndeke, C.B.; Adonis, M.; Almaktoof, A. Basic Circuit Model of Voltage Source Converters: Methodology and Modeling. AppliedMath 2024, 4, 889-907. https://doi.org/10.3390/appliedmath4030048.

2. Article 2: "Energy Management Strategy for DC Micro-Grid System with the Important Penetration of Renewable Energy"; Status: Published.

Ndeke, C.B.; Adonis, M.; Almaktoof, A. Energy Management Strategy for DC Micro-Grid System with the Important Penetration of Renewable Energy. Appl. Sci. 2024, 14, 2659. https://doi.org/10.3390/app14062659.

This published work explores strategies for managing energy within DC micro-grid systems that incorporate significant amounts of renewable energy. The study emphasizes the importance of optimal energy distribution and storage to enhance the reliability and efficiency of DC micro-grids.

3. Article 3: "Implementation of Local Controller for Micro-Grid System": Journal: Advanced Control for Applications: Engineering and Industrial Systems Journal (Wiley): Manuscript ID: ADC2-24-0110; Status: Under Review.

This article focuses on the implementation of local controllers, this article discusses their role in managing and stabilizing micro-grid systems. The paper highlights advanced control techniques that facilitate the seamless integration of various renewable energy sources, ensuring consistent and reliable energy supply. The definition and application of various primary control operations for distinct micro-grid cases that utilize a DC source and PV array are examined.

4. Article 4: "Energy Management Strategy for a Hybrid Micro-Grid System Using Renewable Energy"; Status: Published.

Ndeke, C.B., Adonis, M. & Almaktoof, A. Energy management strategy for a hybrid micro-grid system using renewable energy. Discov Energy 4, 1 (2024). https://doi.org/10.1007/s43937-024-00025-9.

This published article investigates comprehensive energy management strategies tailored for hybrid AC micro-grid systems. It addresses the challenges and solutions associated with integrating multiple renewable energy sources, aiming to optimize the overall energy efficiency and sustainability of the micro-grid.

5. Article 5: "Real-Time Energy Management System for a Hybrid Renewable Micro-Grid System"; Journal: Energy Science & Engineering Journal (Wiley); Article ID: ESE31966, Article DOI: ese3.1966; Status: Accepted.

This article introduces a real-time energy management system designed for hybrid renewable AC micro-grids. The paper details the system's architecture, functionality, and benefits, highlighting its potential to dynamically balance energy supply and demand in real-time, thereby enhancing the micro-grid's performance and resilience.

The collective insights and advancements presented in these articles significantly contribute to the field of energy management for hybrid renewable micro-grid systems. Through meticulous research and practical applications, this thesis aims to pave the way for more efficient, reliable, and sustainable energy solutions in the future. Some results that have not been published are presented in Appendices A and B. Appendix A presents the simulation results for the article 4 and Appendix B presents the simulation results for the article 5.

TABLE OF CONTENTS

DECLARATION ii

ABSTRACT iii

ACKNOWLEDGEMENTS v

DEDICATION vi

PREFACE vii

TABLE OF CONTENTS ix

LIST OF FIGURES xiii

LIST OF TABLES xiiiv

ABBREVIATIONS xv

GLOSSARY OF TERMS xvii

CHAPTER 1: INTRODUCTION 1

1.1. Background 1

1.1.1. Hybrid Micro-Grids 1

1.1.2. Energy Storage Systems 1

1.1.3. Energy Management Systems 2

1.2. Statement of the Research Problem 3

1.3. Motivation for Research 3

1.4. Existing Reviews Related to Energy Management of Micro-Grid Systems 4

1.5. Aims and Objectives of the Research 5

1.6. Research Methodology 6

1.7. Research Questions and Hypotheses 7

1.8. Significance of Research 8

1.9. Research Work Plan 9

1.10. Publications 9

1.11. Summary 10

CHAPTER 2: LITERATURE REVIEW 11

2.2.1. The Difference between a Traditional Power Grid and a Micro-Grid 13
2.2.2. Some Benefits of a Micro-Grid..... 14
2.2.3. Micro-Grid Types..... 15
2.2.3.1. The AC Micro-Grid..... 15
2.2.3.2. The DC Micro-Grid..... 16
2.2.3.3. The Hybrid Micro-Grid..... 17
2.2.4. Architecture of Micro-Grid..... 18
2.3. Distributed Generation Systems..... 19
2.4. Control Architecture in a Hybrid Micro-Grid System 20
2.4.1. Primary Control 21
2.4.2. Secondary Control..... 22
2.4.3. Tertiary Control 22
2.5. Energy Management System Algorithms for Hybrid Micro-Grid System 24
2.5.1. Battery storage optimization algorithm..... 24
2.5.2. Power flow control algorithm 25
2.5.3. Demand Response Algorithm..... 25
2.6. Energy Management System Controls for Hybrid Micro-Grid System..... 29
2.6.1 Rule-Based Control..... 29
2.6.2 Model Predictive Control 29
2.6.3 Fuzzy Logic Control..... 29
2.6.4 Artificial Neural Network Control..... 30
2.6.5 Hierarchical Control..... 30
2.7. Future Scope and Challenges..... 39
2.8. Summary 40
CHAPTER 3: FUNDAMENTAL CIRCUIT MODEL OF VOLTAGE SOURCE CONVERTERS 41
Article 1: Basic Circuit Model of Voltage Source Converters: Methodology and Modelling . 41
CHAPTER 4: ENERGY MANAGEMENT STRATEGY FOR DC MICROGRID SYSTEM 61

Article 2: Energy Management Strategy for DC Micro-Grid System with the Important Penetration of Renewable Energy 61

CHAPTER 5: HYBRID MICROGRID LOCAL CONTROLLER 85

Article 3: Implementation of Local Controller for Micro-Grid System 85

CHAPTER 6: ENERGY MANAGEMENT SYSTEM FOR A HYBRID RENEWABLE AC MICRO-GRID SYSTEM 103

Article 4: Energy Management Strategy for a Hybrid Micro-Grid System Using Renewable Energy 103

CHAPTER 7: REAL–TIME ENERGY MANAGEMENT SYSTEM FOR A HYBRID RENEWABLE AC MICRO-GRID SYSTEM 125

Article 5: Real-Time Energy Management System for a Hybrid Renewable Micro-Grid System 125

CHAPTER 8: GENERAL DISCUSSION AND CONCLUSION 147

8.1. Introduction 147

8.2. Fundamental VSC Circuit Model Connected to the LC Filter Discussion (Article 1) ... 147

8.3. Discussion of the Implementation of Energy Management Strategy for DC Micro-Grid System with the Important Penetration of Renewable Energy (Article 2) 148

8.4. Discussion of the Principal Controller Implementation for Different Hybrid Micro-Grid Applications (Article 3) 148

8.5. Discussion of the Energy Management Strategy for a Hybrid Micro-Grid System Using Renewable Energy using MATLAB/Simulink (Article 4) 149

8.6. Discussion of the Energy Management Strategy for a Hybrid Micro-Grid System Using Renewable Energy using Typhoon HIL402/404 System/Platform (Article 5) 152

8.7. Conclusions 161

CHAPTER 9: RECOMMENDATIONS FOR FUTURE WORK 165

REFERENCES 166

APPENDIX A. Additional Simulation Results for Article 4 183

APPENDIX B. Additional Simulation Results for Article 5 198

B.1: Wind Power Plant Model Simulation 198

B.2: Photovoltaic Power Plant Model Simulation 200

B.3: Diesel Generator Model Simulation 202
B.4. Battery Energy Storage Model Simulation 205
APPENDIX C: PQ control model / MATLAB/Simulink environment 207
APPENDIX D: Hybrid Micro-Grid Controller / Typhoon HIL 208
APPENDIX E: Hybrid Micro-Grid / Typhoon HIL..... 209

LIST OF FIGURES

Figure 2.1: A typical micro-grid. 12
Figure 2.2: The difference between power generation models. 14
Figure 2.3: Micro-grids Classification. 15
Figure 2.4: AC micro-grid structure. 16
Figure 2.5: DC micro-grid configuration. 17
Figure 2.6: Structure of hybrid micro-grid 18
Figure 2.7: Micro-grid architecture 19
Figure 2.8: Technologies and types of distributed generation. 20
Figure 2.9: Hierarchical control architecture. 21
Figure 2.10: Centralized tertiary controller for the converter power loss optimization 23
Figure 8.1: HIL SCADA panel interface for scenario 1. 153
Figure 8.2: HIL SCADA panel interface for scenario 2. 154
Figure 8.3: HIL SCADA panel interface for grid connected mode. 155
Figure 8.4: HIL SCADA panel interface for the third scenario. 156
Figure 8.5: HIL SCADA panel interface when the battery attained its minimum value. 157
Figure 8.6: HIL SCADA panel interface when diesel generator switched on. 158
Figure A.1: Power produced by RESs (scenario 1). 184
Figure A.2: Stateflow energy management block diagram. 185
Figure A.3: Stateflow block transition. 185
Figure A.4: Power produced by RESs (scenario 2) 186
Figure A.5: Stateflow condition / action block 187
Figure A.6: Stateflow energy management block diagram 187
Figure A.7: Stateflow block transition 188
Figure A.8: Stateflow energy management block diagram 188
Figure A.9: Stateflow block transition 189
Figure A.10: Power supplied by RESs (third scenario) 189
Figure A.11: Stateflow condition / action block 190
Figure A.12: Stateflow energy management system block diagram 190
Figure A.13: Stateflow block transition. 191
Figure A.14: Stateflow condition / action block 192
Figure A.15: Stateflow energy management block diagram 193
Figure A.16: Stateflow block transition. 193
Figure A.17: Stateflow energy management block diagram. 194

Figure A.18: Stateflow block transition. 194
Figure A.19: Stateflow energy management block diagram. 195
Figure A.20: Stateflow block transition 196
Figure A.21: Stateflow energy management block diagram. 196
Figure A.22: Stateflow block transition. 197
Figure B.1: Wind power plant rotational speed. 198
Figure B.2: Wind power plant HIL SCADA panel. 199
Figure B.3: Wind power plant HIL SCADA interface. 199
Figure B.4: Wind turbine output voltage. 200
Figure B.5: Wind turbine output power. 200
Figure B.6: PV power plant HIL SCADA panel. 201
Figure B.7: PV power plant output power. 201
Figure B.8: PV power plant HIL SCADA interface. 202
Figure B.9: Generator speed. 202
Figure B.10: Diesel generator HIL SCADA panel. 203
Figure B.11: Diesel generator output voltage. 203
Figure B.12: Diesel generator output power. 204
Figure B.13: Diesel generator HIL SCADA interface. 204
Figure B.14: Battery inverter HIL SCADA panel. 205
Figure B.15: Battery output power from the inverter. 205
Figure B.16: Battery output voltage from the inverter. 206
Figure B.17: Battery HIL SCADA interface. 206
Figure C: DC voltage regulator control diagram……..206
Figure D: Energy management control / Typhoon HIL……..206
Figure E: Developed Hybrid micro-grid. 209

LIST OF TABLES

Table 2.1: Summary of EMS/algorithms in hybrid micro-grid systems 160
Table 2.2: Summary of Previous Studies on EMS using different algorithm 3160
Table 8.1: Results Comparison 160
Table A.1: Condition Table of the EMS 183
Table A.2: Action Table of the EMS 183

ABBREVIATIONS

2 m PEM: 2 m Point Estimate Method

AC: Alternating Current

BESS: Battery Energy Storage System

CHP: Combined Heat and Power

CSP: Concentrating Solar Power

DC: Direct Current

DER: Distributed Energy Resource

DG: Distributed Generation

DR: Demand Response

EMS: Energy Management System

ESS: Energy Storage System

GA: Genetic Algorithm

HIL: Hardware-In-the Loop

Hz: Hertz

ICE: Internal Combustion Engines

kW: Kilo Watt

LCOE: Levelized Cost of Energy

MOSFET: Metal Oxide Semiconductor Field Effect Transistor

MW: Mega Watt

PV: Photo-Voltaic

DQ0: Quadrature Zero

P: Real Power

PSO: Particle Swarm Optimization

Q: Reactive Power

RES: Renewable Energy Source

SCADA: Supervisory Control and Data Acquisition

SOC: State of Charge

SST: Solid-State Transformers

SVPWM: Space Vector Pulse Width Modulation

V: Voltage

VSC: Voltage Source Converter

W: Watt

GLOSSARY OF TERMS

Battery energy storage system	A battery energy storage system is a device that uses rechargeable batteries to store electrical energy as chemical energy. It is designed to provide power when it is required, frequently during times of peak demand or power outages.
Distributed generation	Distributed generation is the power production of a variety of small-scale energy sources close to the point of use, rather than relying solely on centralized power plants that transfer electricity over long distances through the grid.
Energy demand	Energy demand is the total amount of energy needed during a given time period by different economic or social sectors. It depicts the overall amount of energy needed to satisfy different industrial, commercial, residential, as well as transportation sectors requirements.
Fossil fuel	Fossil fuels are naturally occurring hydrocarbon-based energy resources that originate from the remains of ancient plants, and marine organisms that accumulated and underwent geological transformations over millions of years.
Hybrid renewable micro-grid system	A hybrid renewable micro-grid system is an integrated energy infrastructure that combines a variety of renewable energy sources, energy storage systems and smart grid technologies to produce sustainable and dependable power to a localized area or community.
Load	A load represents the electrical demand placed on the power supply, which can vary according to the type of equipment and its operational requirements.
MATLAB/Simulink software	MATLAB/Simulink is a widely used software suite developed by MathWorks that combines numerical computing, visualization, and simulation tools. It provides an environment for algorithm development, data analysis, and model-based design for engineers, scientists, and researchers in various disciplines.
Point of common coupling	It is the point in the electrical network where two or more systems interface or share a common connection.
Real-time energy management	A real-time energy management refers to the continuous monitoring, control, and optimization of energy resources and consumption in real-time.
Renewable energy resource	A renewable energy resource refers to a natural resource that can be harnessed and converted into usable energy without being depleted or exhausted.

SCADA panel	A SCADA panel is a control center or interface used in SCADA systems to monitor and control various industrial processes or infrastructure remotely. It serves as a centralized hub for collecting data, displaying real-time information, and managing the control of multiple devices and systems.
State-flow logical programming	State-flow logical programming refers to a programming paradigm that combines state-based modelling and logical expressions to describe and control the behaviour of a system. It is commonly used in the context of modelling and simulating complex systems.
Typhoon Hardware-in-the-loop	Typhoon Hardware-in-the-loop (HIL) refers to a hardware-in-the-loop testing system developed by Typhoon HIL Inc. It is a technology utilized in power electronics field and electrical power systems to simulate and test the power electronic devices functionality and behavior, controllers, and systems in a controlled and realistic environment.
Voltage source converter	A voltage source converter is a power electronic device or system that can convert electrical power from one voltage level to another while maintaining a stable and controllable output voltage. It is widely used in different applications such as power transmission, renewable energy sources, motor drives, and reactive power compensation.

CHAPTER 1: INTRODUCTION

1.1. Background

1.1.1. Hybrid Micro-Grids

Due to the energy demand growth, fossil fuel deposits are being depleted at an ever-increasing rate. Hence it is predicted that the available fossil fuel can only meet our energy demand for the next 40 years because we will not have the capacity to get the fossil fuel out of the ground in the distant future. Additionally, the use of fossil fuel and internal combustion engine (ICE) has contributed significantly to environmental pollution and looming concerns of anthropogenic (man-made) climate change. Because of these problems, it is critical that we adopt and develop a production system that will not depend on fossil fuel as the principal source of energy, hence, the adoption of renewable micro-grid (Zia at al., 2018). The use of renewable micro-grids has seen significant development and growth in the past decade due to technology maturity, anticipated scarcity of fossil fuel and government policies on environmental protection (Han et al., 2017).

Renewable micro-grids are considered a better alternative to traditional power grids (Raya-Armenta et al., 2021). A hybrid micro-grid system is a local energy system that employs a blend of several energy production sources, such as biomass, solar photovoltaic (PV), micro-hydro, wind, and fossil fuel-based generation (diesel, for example). An on-site hybrid micro-grid offers several benefits, primarily related to increased energy reliability, efficiency, minimizing long-term energy expenses and optimizing system component sizes as well as environmental sustainability (Zebra et al., 2021). According to the load type, hybrid micro-grid systems can generate power in direct current (DC) or in alternating current (AC) forms.

1.1.2. Energy Storage Systems

An energy storage system (ESS) is a device or system that stores energy in any form and delivers it in the same or different form based on the application's need (Parhizi et al., 2015). The use of an ESS, particularly in renewable micro-grid systems offers an unconditional advantage in electric power reliability. An ESS is essential when it comes to reducing power quality issues, smoothing the fluctuation of the power, providing a primary micro-grid control, supplying initial energy when transiting from grid-connected mode to island operating mode, and it also provides the capacity to ride through when intermittent energy sources experience dynamic fluctuations and allows the dispatchable operation of distributed generation (DG) (Faisal et al., 2018). ESS can be categorized in different technologies based on the methods utilized to store energy, which include compressed air storage, superconducting magnetic

storage, pumped hydropower, super-capacitor, flywheel energy storage, and secondary batteries (Bradbury, 2015).

Super-capacitors, flywheels and battery technologies are the energy storage system types mostly utilized in renewable micro-grid systems and batteries are the most employed in micro-grid applications (Prashant & Atma, 2016). Batteries offer a wide range of benefits across various applications and industries because of their capacity to both store and discharge electrical energy. Batteries can be utilized to provide a capacity reserve for future energy demands or they can be employed as the primary storage method (Nadeem et al., 2019). In general, battery operation needs specific attention. However, renewable hybrid micro-grids as well as battery storage systems, have shown some serious limitations not related to increased fossil fuel prices or environmental pollution rather within the energy management system (EMS). Some of these limitations relate to the intermittence of renewable energy, the dependence of the efficiency of the equipment on the operating point, the relation between the battery charging/discharging rate on their operating conditions, overcurrent, overvoltage, SOC, unbalanced situations that may generally affect the battery lifetime and the hybrid micro-grid reliability. Therefore, an EMS is necessary to offer a proper hybrid renewable micro-grid operation and optimize its functionality.

1.1.3. Energy Management Systems

An energy management system in a micro-grid system is a critical component responsible for optimizing energy usage, enhancing system stability, and ensuring efficient operation (Morstyn et al., 2019). An EMS optimizes the utilization of available energy resources within the micro-grid by coordinating the operation of renewable energy sources, energy storage systems, and conventional generators and ensures that energy is produced and consumed efficiently. An EMS also continuously monitors energy supply and demand, dynamically adjusting energy flow and distribution to prevent fluctuations that could destabilize the grid. This enhances the reliability of power delivery to end-users. An EMS provides a holistic approach to optimizing energy use, reducing costs, enhancing environmental sustainability, and improving overall operational efficiency. These systems are valuable tools for organizations and individuals looking to address energy challenges while gaining a competitive edge in an increasingly energy-conscious world (Chowdhury et al., 2020).

Nowadays, consideration is focused on EMS utilized in hybrid renewable micro-grids. To maintain the stability and reliability within the system, energy management systems application is crucial in hybrid renewable energy systems (Feng et al., 2019). It also helps in decreasing the energy produced cost and in increasing the hybrid unit's lifetime, more particularly energy

storage systems. A real-time and reliable EMS is necessary to integrate hybrid renewable energy sources and the ESS, due to the rapid expansion in renewable energy resources (Totem, 2019). Much research has been carried out to increase the effectiveness of EMS action and operation, but further development is still needed. These studies rely on balance situations, deterministic calculations, and imprecise models. As a result, new research must be conducted to raise the reliability of micro-grid systems.

1.2. Statement of the Research Problem

The main research problem is how to develop real-time energy management for a hybrid renewable micro-grid system that controls the energy flow between the renewable energy sources of the hybrid micro-grid system and the load directly connected to these sources and connected to the utility grid. The second research problem is how to control the battery energy storage system charging and discharging.

1.3. Motivation for Research

The motivation for developing an EMS for a hybrid renewable micro-grid system stems from the urgent need to transition towards sustainable energy sources. Traditional energy grids heavily rely on fossil fuels, contributing to environmental degradation and climate change. By focusing on hybrid renewable micro-grids, which combine renewable energy sources like solar and wind with energy storage systems, the research helps to promote sustainable energy practices and reduce carbon emissions. Renewable energy sources are intermittent and variable, posing challenges to their seamless integration into existing power grids. Developing an EMS for hybrid renewable micro-grids seeks to address these challenges by optimizing the utilization of renewable energy resources. By intelligently managing the operation of renewable energy sources and battery storage systems, this maximizes renewable energy penetration while maintaining grid stability and reliability. Hybrid micro-grids offer a promising solution for improving energy access, especially in remote or underserved regions where traditional grid infrastructure is lacking. By developing a real-time EMS for hybrid renewable micro-grids, it enhances the energy access by providing reliable and affordable electricity to communities. Additionally, the resilience of hybrid micro-grids during natural disasters or grid outages is a key motivation. An effective EMS can ensure continuity of power supply, thereby enhancing the resilience of communities and critical infrastructure. The rapid advancement of renewable energy technologies, energy storage systems, and smart grid technologies presents opportunities for innovation in energy management. Developing a real-time EMS for hybrid renewable micro-grids involves leveraging these technological advancements to design

efficient and scalable solutions. This research helps to contribute to the advancement of knowledge and technology in the field of renewable energy and micro-grid systems.

1.4. Existing Reviews Related to Energy Management of Micro-Grid Systems

A summary of the existing research on EMS of micro-grid systems based on RESs and many different tools as well as techniques is outlined below:

1. Chaouachi et al. have proposed a generalized formulation for intelligent energy management of a micro-grid (Chaouachi at., 2017). They developed an artificial intelligence method in cooperation with multi-objective optimization based on linear programming. These developed techniques aim to reduce the operating cost and the levels of emission for a micro-grid, including its pre-operational variables such as the future availability of renewable resources and load demands. The results have positively demonstrated the cost reduction of energy produced and the lifetime augmentation of different hybrid devices, more specifically for energy storage systems (batteries).
2. Garcı´a et al. (García et al., 2018) have demonstrated the performance improvement of the hybrid renewable energy system by combining two different methods for energy management, which included the optimization with fuzzy logic control. The principal objective of their study was how to manage uncertainties occurring from renewable production and load demand predictions. These methods have shown an efficient hybrid renewable energy system.
3. Serban (Serban et al., 2017) have implemented an original hardware-in-the loop (HIL) solution for real-time tests and optimization of the frequency control mechanism in isolated micro-grids. The production system was based on renewable energy sources combined with batteries.
4. Baziar (Baziar & Kavousi-Fard, 2019) developed a probabilistic structure focused on the 2 m Point Estimate Method (2 m PEM). This method has been proposed to take into consideration the uncertainties in the optimum energy management of the renewable micro-gird systems.
5. A control management of a hybrid system has been implemented by Dagdougui et al. (Dagdougui et al., 2015) using a real-time mathematical optimum solution. Their generation system included hydropower, wind power and fuel cells and the study was based in Afourar village, in Morocco. Different operation system scenarios have been considered, either operating in grid connected mode or isolated mode according to

any settled point of time. Another main aspect was how to control the production power with the load demands.

6. Pablo et al. (Pablo et al., 2015) have developed an optimal EMS for a stand-alone hybrid micro-grid system, the proposed strategy was focused on fuzzy logic control. The aim of the study was to meet the power requirements of the load and maintain the energy storage systems SOCs, which comprised the battery and hydrogen within a specific range. The outcomes demonstrate that the strategy was successful in maximizing the lifetime of energy storage devices and utilization costs. The authors recommended using other techniques, such as the grid-connected mode to assess the effectiveness of the suggested energy management system.
7. Fathima and Palanisamy (Fathima & Palanisamy, 2015) proposed a review on optimization in micro-grids with hybrid energy systems. The researchers have concluded that future studies need to be done, which will support to improve the power quality of the hybrid renewable energy sources and surmount the shortcomings of the current scenario like system optimization.
8. Lanre et al. (Lanre et al, 2016) presented a review on EMS in hybrid renewable energy systems. Their research showed that in order to reduce system costs and minimize adverse effects, it is crucial to optimize component size and implement an energy management system.

However, Lanre Olatomiwa et al., (Olatomiwa et al., 2021) presented a review on EMS in hybrid renewable energy systems. The EMSs of smart grids were given special attention in this study. The development of energy management systems is also demonstrated using fuzzy logic approaches. According to the report, to connect hybrid renewable resources with energy storage systems, real-time and efficient energy management solutions are now essential. Most research on the energy management system for hybrid renewable energy systems has been conducted in islanded mode, with just a small number of cases focusing on grid connected systems, according to this comprehensive assessment. Therefore, it is critical to develop new plans and methods for managing and controlling the flow of energy in a hybrid renewable micro-grid system connected to the grid.

1.5. Aims and Objectives of the Research

To maximize the use of renewable energy sources and strengthen their integration into the power system, this research aims to develop an energy management system for a hybrid renewable micro-grid system. This is done by using different load scenarios.

The main objective of this research is to develop an energy management strategy that regulates the energy transfer between the hybrid micro-grid system and the load in both grid-connected and isolated modes. The second research objective is to control the battery energy storage system charging and discharging. Additionally, this thesis has the objective to use the results and perform a comparative analysis with the results obtained from other similar research studies.

To achieve the different objectives mentioned above, various tools, algorithms and techniques are implemented and applied, which aim to predefine optimal design criteria both in real-time and offline. The approaches include the method of optimization, parallel metaheuristic technique, model predictive control, and evolutionary algorithms. The tools used to develop the energy management strategy comprise MATLAB/Simulink and Typhoon HIL's real-time digital simulator. The proposed energy management strategy is based on Stateflow logical programming environment. The parallel metaheuristic technique is an algorithm that turns multiple metaheuristic searches in parallel by using parallel computing techniques.

The objectives are conducted through the following sequences:

- A hybrid micro-grid components model used in the simulation model is designed and developed using MATLAB/Simulink software
- A simulation of a hybrid micro-grid is developed using MATLAB/Simulink software
- A control system scheme for the hybrid micro-grid is developed using Stateflow logical programming environment
- An energy management system algorithm for the hybrid micro-grid system is developed using Typhoon HIL's real-time digital simulator.
- A hybrid micro-grid with battery energy storage system simulation is designed and developed using MATLAB/Simulink software and validated in Typhoon Hardware-in-loop (HIL) simulation package with HIL402 configuration in the virtual environment.

In addition, to allow users to access and modify any control parameter within the hybrid micro-grid, the algorithm model needs to be adaptable.

1.6. Research Methodology

The EMS is typically utilized to plan programs and manage power generation for a variety of power grid applications. It is also recognized as a different method for managing electrical loads in micro-grids (Morstyn et al., 2019). However, the new practice of micro-grids defines more the energy management systems. The main objective of this study is to provide an

EMS controller capable of ensuring adequate power distribution that will promote the application of a hybrid micro-grid system for RES applications. This will offer an improved value and trigger significant interest in the use of renewable micro-grid applications.

This study examines a hybrid micro-grid system with a hierarchical control scheme that consists of a central controller and a local controller. The central controller coordinates the hybrid micro-grid protection devices and handles the secondary and tertiary control layers, while the local controller controls the power flow of all distributed generation devices. This ensures optimal operation and reliability under varying production and demand conditions, as well as suitable protection against utility grid faults and failures.

The choice of a real-time simulation tool is considered to develop the hybrid micro-grid central controller due to the response time which is in the order of minutes. The selected software is the Typhoon Hardware-in-the-loop (HIL). This enables the HIL test of the controller and enables the control of the power converter via its digital signal processor (DSP) interface board. Additionally, the Typhoon HIL software tool chain includes a Supervisory Control and Data Acquisition (SCADA) panel, which is fundamental to manage micro-grid operations and sending commands to local controllers.

1.7. Research Questions and Hypotheses

The research is required to provide answers to the following questions:

- How can the hybrid micro-grid be made more efficient by the developed EMS?
- To ensure an optimal performance of the micro-grid, how can the defined software model determine the control algorithm?
- According to the actual micro-grid EMS, how is the developed energy management algorithm able to improve the effectiveness of the hybrid renewable micro-grid system?
- Does integrating the EMS algorithm contribute to improve the deployment of renewable energy resources into hybrid micro-grid systems?
- By introducing the implemented hybrid renewable micro-grid EMS algorithm, can the system enhance the integration of renewable energy resources into the power system and optimize their deployment?
- To increase the use of hybrid micro-grid, how is the definition of the algorithm made?
- Is the developed energy management algorithm significantly contributing to the hybrid renewable micro-grid system reliability?

It is hypothesised in this research that the whole hierarchical structure of the hybrid micro-grid is implemented in a decentralized method. In addition, the power supply source sizes, type of energy management configuration, power electronic converters, and the system design are projected to be the most significant factors to consider in the power distribution and functionality of the entire system. Although, an efficient energy management system coupled with effective real-time performance significantly improves the synchronized operation with the main grid. The developed hybrid renewable micro-grid system includes solar power, wind power, a battery energy storage system and a diesel generator.

1.8. Significance of Research

Hybrid micro-grid systems are a key factor in the shift to sustainable energy sources, resiliency, and efficient power infrastructure, ensuring a cleaner, more dependable energy supply in the future. The new method of micro-grids, however, focusses on the EMS. In this regard, diverse research has been conducted in accordance with EMS, and it has been discovered that EMS of micro-grids presents several obstacles. The effectiveness and operation of an EMS are rarely used in the current literature, or the precision of an EMS is insufficient. For instance, the correlation between the operating conditions of the battery energy storage systems (BESSs) and their rates of charging and discharging, has an impact on the efficiency dependence of the equipment on the operating point, state of charge, system degradation, and imbalance situations. Hence, an EMS is important to offer an optimal hybrid renewable micro-grid operation and optimize its performance.

The aim of this research is to optimize the utilization of renewable energy sources while ensuring stability, reliability, and efficiency of the hybrid micro-grid operation. By implementing a sophisticated control algorithm, the aim is to seamlessly integrate various renewable energy sources (RESs), such as solar and wind, with a battery energy storage system and diesel generator. The primary goal is to minimize reliance on fossil fuels, reduce carbon emissions, and promote sustainability by maximizing the utilization of clean energy resources within the hybrid micro-grid. This research offers several significant contributions such as developing an EMS controller that optimizes energy usage within the hybrid micro-grid, ensuring that energy is produced and consumed efficiently.

By coordinating the operation of renewable energy sources, energy storage systems, and demand-side management strategies, the controller minimizes energy wastage and improves overall system efficiency. Additionally, this research implements comprehensive control in real-time and management systems to adaptively respond to variation in renewable energy generation and load demands. By addressing these aspects, the research aims to promote

wider adoption of sustainable energy practices by offering useful guidance for the design and hybrid micro-grid systems operation. The outcome of this research adds value to existing available academic literature in the quest to plan programs and projects that lead to accelerate the adoption and use of hybrid renewable energy sources for sustainable development and effective sources of power production.

1.9. Research Work Plan

To achieve the research objectives, the project was conducted in the following sequence:

Chapter 1: This section introduces the background, the research problem statement, aims and objectives. It also provides the methodology and the significance of the research. This assists in garnering relevant information that gives an advanced understanding of EMS for hybrid renewable micro-grid applications.

Chapter 2: This section gives an overview of the hybrid micro-grid systems. A literature review of the micro-grid energy management systems is assessed.

Chapter 3: The basic circuit concept of the VSC with an output LC filter is reviewed in this section. The basic theory and design of the behaviour of VSC as an active rectifier with DC bus control and as an inverter integrating the derived control loops in grid-feeding and grid-forming modes are also presented.

Chapter 4: This section presents the EMS control algorithm for DC micro-grid system.

Chapter 5: The implementation of a local controller for micro-grid system is presented in this Section.

Chapter 6: This section presents the EMS strategy for a hybrid renewable AC micro-grid system.

Chapter 7: In this section, the real-time energy management system for a hybrid renewable AC micro-grid system is presented.

Chapter 8: This section contains the general discussion and conclusions of this thesis.

Chapter 9: This section presents some recommendations for further studies.

1.10. Publications

Ndeke, C.B.; Adonis, M.; Almaktoof, A. Basic Circuit Model of Voltage Source Converters:

Methodology and Modeling. AppliedMath 2024, 4, 889-907. https://doi.org/10.3390/appliedmath4030048

Ndeke, C.B., Adonis, M. & Almaktoof, A. Energy management strategy for a hybrid micro-grid system using renewable energy. Discov Energy 4, 1 (2024). https://doi.org/10.1007/s43937-024-00025-9.

Ndeke, C.B.; Adonis, M.; Almaktoof, A. Energy Management Strategy for DC Micro-Grid System with the Important Penetration of Renewable Energy. Appl. Sci. 2024, 14, 2659. https://doi.org/10.3390/app14062659.

1.11. Summary

The background information on hybrid micro-grids, energy storage systems, and energy management systems is provided in this chapter. The research problem statement and motivation are presented. Also, some reviews that are currently available on EMS of micro-grid systems are introduced. Following that, the aims and objectives as well as the research methodology are summarised. Additionally, the significance of the research is presented. Finally, the thesis structure is described and publications resulting from this study are presented.

CHAPTER 2: LITERATURE REVIEW

2.1. Overview

The hybrid micro-grid system uses distributed generation (DG) systems with a variety of renewable and non-renewable sources. Four energy storage technologies are studied in this research, which are compressed pressurised air storage and mechanical flywheel, gravitational pumped storage systems and chemical batteries.

To connect the main grid and end user loads to distributed energy resources, a DC to AC VSI is utilized. The DC voltage from the renewable energy sources (RESs) is converted to AC form using the inverter, which interfaces with the AC voltage of the load and the main grid. In addition, an inverter regulates the voltage, frequency, active power, and reactive power to help stabilize the grid. Moreover, converters allow batteries to connect to the grid. Finally, an EMS is essential for the hybrid micro-grid system to operate at its best, increasing dependability and lowering operating costs, thus, a brief review on EMS algorithms and controls is presented.

2.2. Concept of Hybrid Micro-Grid

A hybrid micro-grid is a localized energy system that integrates multiple sources of energy generation, storage, and distribution to provide reliable and sustainable power to a specific area or community (Agrawal & Mittal, 2011). The concept of a hybrid micro-grid arises from the need to address challenges associated with traditional centralized power grids, such as reliance on fossil fuels, vulnerability to disruptions, and limited access in remote areas. A hybrid micro-grid operates either in conjunction with or independently of the main grid, offering flexibility and stability to meet various energy needs. The concept of a hybrid micro-grid represents a decentralized, flexible, and sustainable approach to energy management, offering resilience, reliability, and environmental benefits to communities and regions around the world (Lotfi & Khodaei, 2017).

To guarantee that the system performs as intended, a control technique is required. It is crucial that the system and power electronics work together as a single unit when they interface. The control system has many advantages because it also makes it possible to preserve the particular energy source and the quality of power (Totem, 2019). A typical configuration of a micro-grid system is shown in Figure 2.1.

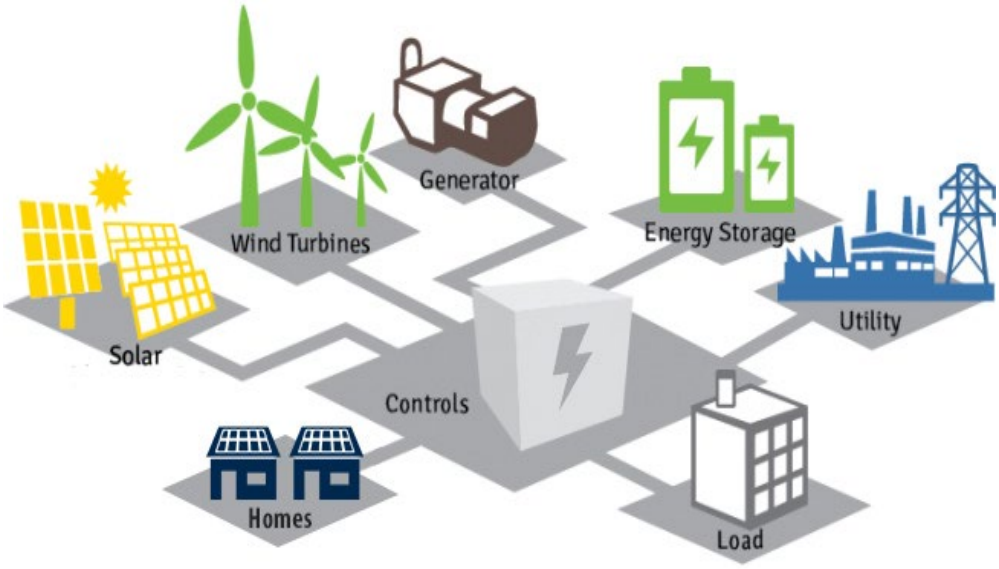


Figure 2.1: A typical micro-grid (Totem, 2019).

The renewable energy resources offer a path toward a more sustainable, environmentally responsible, society conscious and economically viable energy future. The transition to renewables becomes an increasingly attractive and feasible option for addressing global energy challenges because of technological growth and the cost reduction (Chowdhury et al, 2019). Since a decentralized power production moves generation close to the consumption point, this increases the system dependability because isolated portions of the network are less likely to be affected by faults that occur somewhere. As transmission losses are decreased, it also improves the system's efficiency (Jones & Chowdhury, 2018).

Due to the unstoppable rise in global energy demand, which differs between countries and continents, the integration of hybrid micro-grid systems is getting more attention. Hybrid micro-grid systems are designed to be scalable and modular, allowing for easy expansion or modification to meet changing energy demands. New renewable energy sources or storage technologies can be seamlessly integrated into existing systems, enhancing flexibility and adaptability (Hirsch et al, 2018). Community engagement and ownership are central to the concept of hybrid micro-grids. By involving local stakeholders in the planning, development, and operation of the micro-grid, a sense of ownership and responsibility is fostered, leading to greater support and sustainability of the system (Carpintero-Rentería et al, 2019).

2.2.1. The Difference between a Traditional Power Grid and a Micro-Grid

In a traditional power grid, electricity flows in one direction, from the power plants to the point of consumption. The produced power is managed to ensure supply meets demand in real-time, balancing generation and consumption across the network. Differently to a conventional grid, micro-grids can operate in various modes depending on the circumstances. They can be connected to the main grid, allowing for the exchange of electricity, or operate autonomously in islanded mode during grid outages or disruptions (Islam et al., 2014).

The characteristics of hybrid micro-grid systems listed below are typically categorized as the primary distinctions from the conventional power grid, the motivations and goals of a micro-grid in various nations are not exactly the same (Feng et al., 2018):

- ✓ Ameliorate the ability of intermittent RESs and allow the power grid to adjust various energy source systems.
- ✓ Practically eliminates the possibility of widespread, protracted power outages, with the exception of significant physical damage.
- ✓ Increase the economy while cutting prices, emissions, and energy usage.

For the electrical system to operate safely and steadily as well as to administer resources as efficiently as possible, the power grid distribution is a crucial component. The conventional power grid is unable to fulfil the needs satisfied by the micro-grid improvement due to the distributed generation widespread access, intermittent renewable energy sources, increasing demand on the dependability of energy production, and economy (Richter et al, 2012). According to its incorrect restoration procedure, which necessitates rapid action, typically human and in real-time, the whole restore processing is significantly simpler in a micro-grid structure since there are less factors that can be controlled (Islam et al., 2014). Figure 2.2. presents the difference between traditional and micro-grid systems.

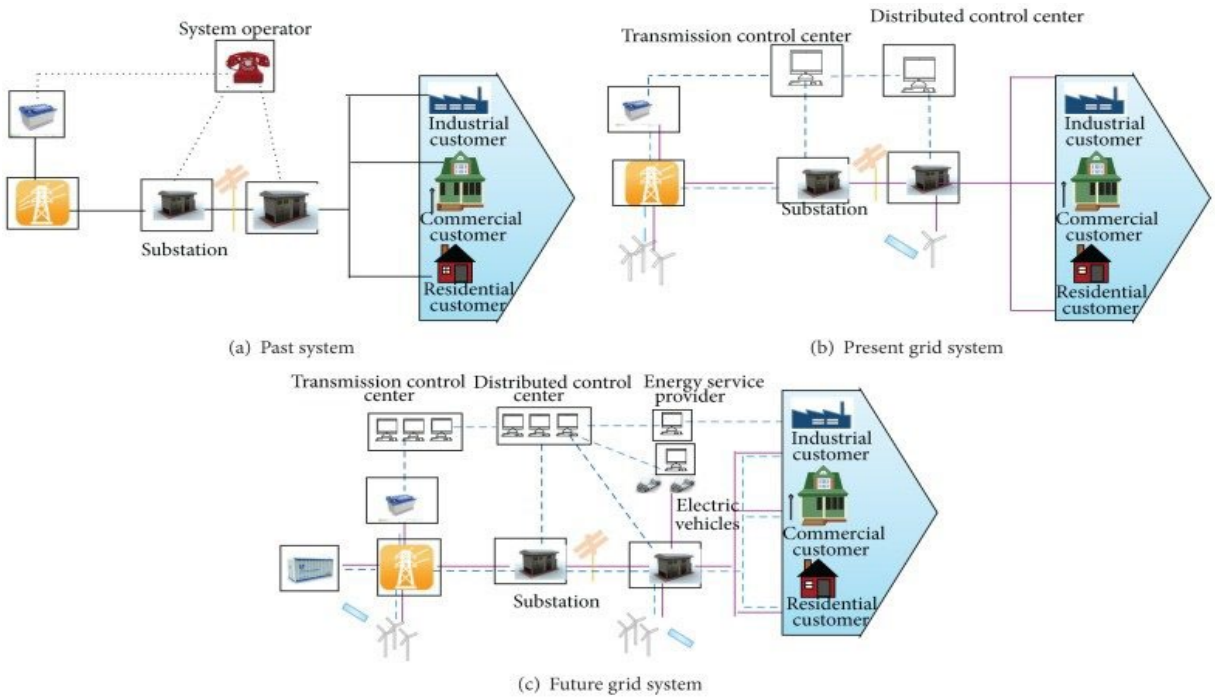


Figure 2.2: The difference between power generation models (Islam et al., 2014).

2.2.2. Some Benefits of a Micro-Grid

When compared to other technologies, the deployment of micro-grid system provides a number of advantages, the most well-known are (Chowdhury et al., 2019):

- Because it uses micro-sources, which have little to no emissions, a micro-grid decreases pollutants from an environmental protection perspective.
- By operating in parallel with the main grid, the micro-grid enables the main grid to sustain additional loads. The surplus of micro-grids generation can assist in preventing power grid failures and overload issues.
- The transmission line size and the installation are reduced as well as the utilization of fossil energy.
- The micro-grid supplies load continuously in grid-connected mode and isolated mode. This characteristic makes it more dependable and enables it to supply important loads with high-quality electricity.
- When using the combination of heat and power, micro-grid systems become more advantageous than thermal energy conservation. The micro-source in a micro-grid makes it easy to complete this operation. To maximize energy efficiency, the micro-source could be placed closer to the thermal and electrical demands.

2.2.3. Micro-Grid Types

Micro-grids offer a flexible and scalable approach to energy management and distribution, with different types catering to various applications, locations, and objectives. They can operate in grid-connected mode and isolated mode. Grid-connected micro-grids are interconnected with the main utility grid and can import or export power as needed. They can operate in parallel with the main grid, providing benefits such as load balancing, peak shaving, and grid support services. Grid-connected micro-grids often incorporate renewable energy sources such as solar photovoltaics (PV), wind turbines, or hydroelectric generators, along with conventional generators such as diesel generators or gas turbines. Islanded micro-grids are capable of operating independently from the main utility grid, forming an "island" of electrical infrastructure that can continue to supply power to local loads even during grid outages. (Ahmed et al., 2020). Additionally, micro-grid systems are divided in three groups, which include AC micro-grid, DC micro-grid and hybrid micro-grid. Figure 2.3 gives a detailed micro-grid system classification.

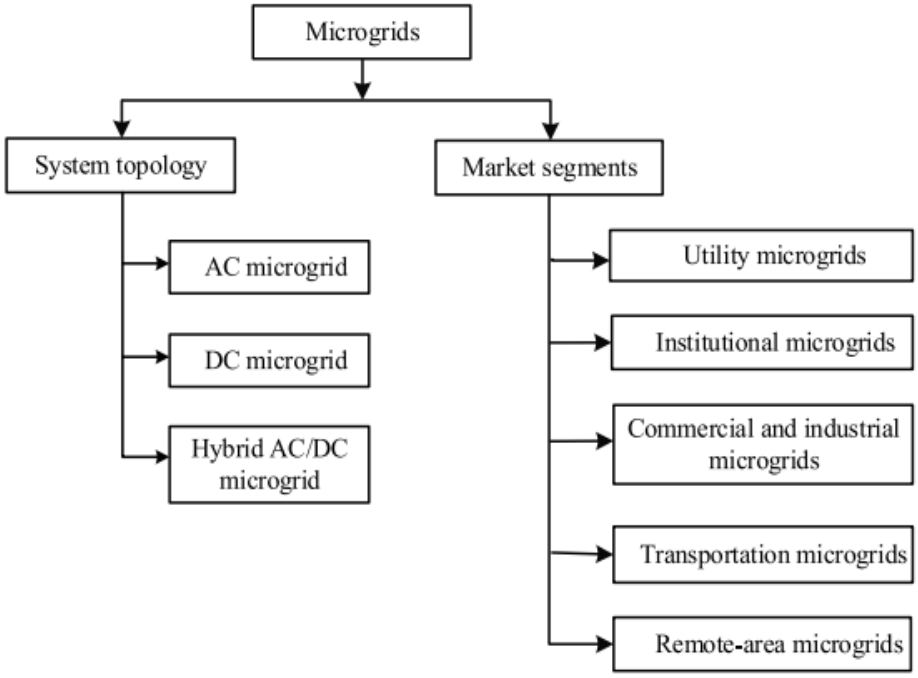


Figure 2.3: Micro-grids Classification (Ahmed et al., 2020).

2.2.3.1. The AC Micro-Grid

An AC micro-grid includes renewable and non-renewable energy, loads, and power electronic converters which connect everything to a common AC bus. Its principal disadvantage is how challenging it is to operate and control. Figure 2.4 depicts an example of an AC micro-grid.

Based on the distribution system, there are three different categories of AC micro-grids: single phase, three phase without neutral point lines, and three phase with neutral point lines (Shahgholian, 2021).

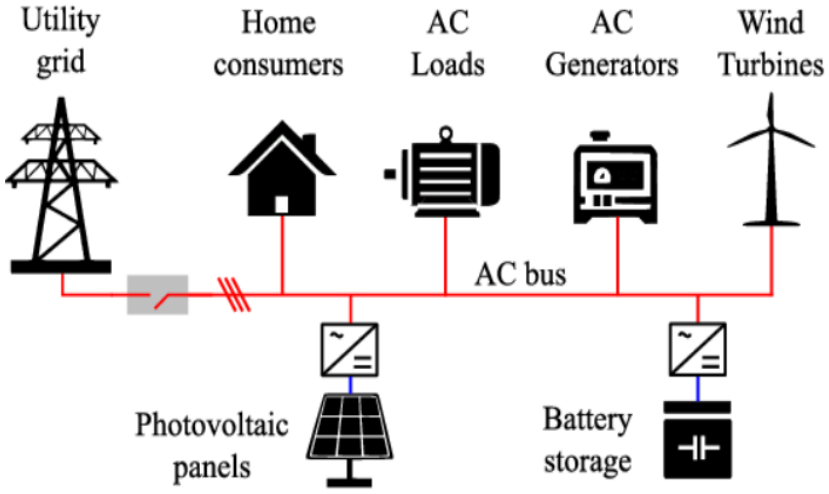


Figure 2.4: AC micro-grid structure (Semenov et al., 2018).

It is necessary for all connected devices in AC micro-grids to synchronize to a specific voltage and frequency. The order of the phases takes on more importance in three-phase systems. Any unwanted power flow between the connected sources is prevented as a result. The standardization, protection, control, and stability of AC micro-grids have improved due to their extensive operational history (Ishaq et al., 2022). To increase the flow of power in distribution networks and decrease power losses into transmission lines, power grids for medium and low voltage distribution are connected to AC micro-grids. However, they also bring with them new issues like reactive power shortage, power quality issues, synchronization of distributed energy resources, and system stability, which can be resolved by applying advanced control techniques (Yousef et al., 2022).

2.2.3.2. The DC Micro-Grid

The concept of DC micro-grid is attracting more attention than conventional AC micro-grids due to several advantages, which include no conflicts with harmonics or frequencies, no requirement of synchronization in isolate mode, and there are no issues with reactive power control (Al-Ismail, 2021). Additionally, DC micro-grids offer fewer conversion steps, fewer maintenance and operating expenses, and no impact on the skin effect and no power loss due to corona. DC micro-grids are constituted of battery storage systems, DC continuous loads,

and distributed renewable energy sources. To provide DC micro-grids with more effectively generated power that is sent to the load portion, few conversation steps are required. DC micro-grid systems have recently been used to supply DC power to aircraft, commercial buildings, telecommunications towers, electric vehicles, data centres, and government buildings (Prince et al., 2022). DC micro-grids are generally divided into two broad categories based on operating conditions: grid-connected and isolated modes. The DC micro-grids configuration depends on renewable energy sources to reduce the carbon footprint. A DC micro-grid uses inverters to provide power to AC loads and to connect AC sources to the DC bus rectifiers are utilized (see Figure 2.5).

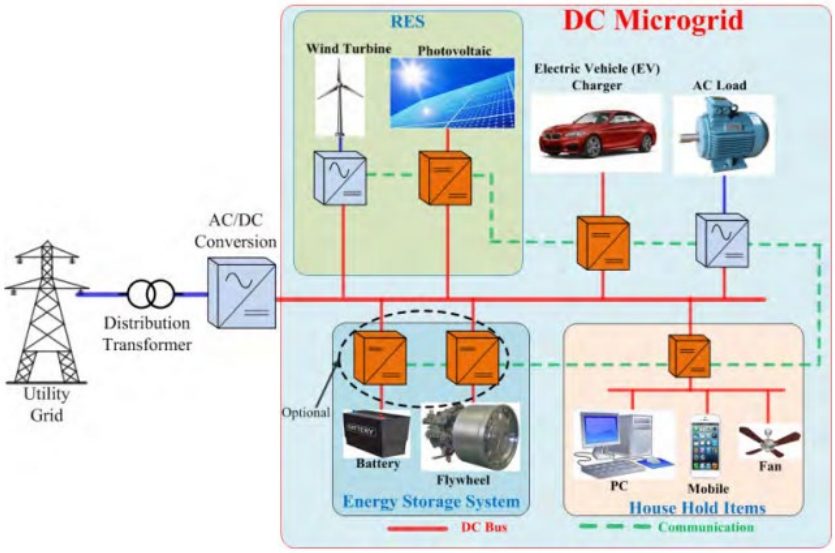


Figure 2.5: DC micro-grid configuration (Kumar et al., 2017).

However, integrating RESs with DC micro-grids reduces system reliability because of the variable conditions of renewable sources. To solve reliability problems, some fossil fuels like diesel or gas, are used together with RESs in DC micro-grids (Ghorashi et al., 2022). On the one hand, integrating multiple energy storage systems like super-capacitors and batteries may increase the DC micro-grids reliability to a good scope, on the other hand, control problems become complex for a such case (Yuan et al., 2022).

2.2.3.3. The Hybrid Micro-Grid

The hybrid micro-grid is an integrated electrical distribution system that combines alternating current (AC) and direct current (DC) components to efficiently manage power generation, storage, and consumption within a localized area. The AC/DC hybrid configuration enables the

incorporation of diverse energy sources, including renewable energy systems, energy storage devices, and traditional generators, while optimizing energy conversion, distribution, and control. (Fuxing et al., 2021). By integrating both AC and DC components, hybrid micro-grids minimize energy conversion losses and improve overall system efficiency compared to traditional AC-only or DC-only systems (Pragya & Thakur, 2022). Hybrid micro-grids offer greater flexibility in managing energy flows, allowing for optimized utilization of renewable energy sources, energy storage, and backup generation to meet varying demand and supply conditions. Figure 2.6 illustrates a hybrid micro-grid structure.

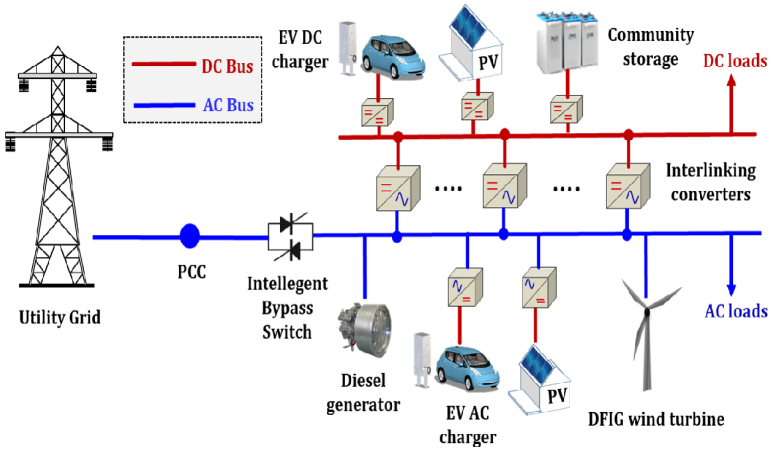


Figure 2.6: Structure of hybrid micro-grid (Rahman, 2018).

A hybrid micro-grid guarantees a stable operation inside each micro-grid. The hybrid configuration improves micro-grid resilience by diversifying energy sources and distribution pathways, reducing vulnerability to single-point failures and grid disturbances. They can be scaled up or down to accommodate changing energy needs and technological advancements, making them suitable for a wide range of applications from small-scale community micro-grids to large industrial complexes (Ashagire et al., 2021).

2.2.4. Architecture of Micro-Grid

The micro-grid architecture is composed with the following elements (Avendano, 2022):

- Distributed energy resources,
- Energy storage system,
- Control components

These above components are connected to a low voltage grid dispatching. Figure 2.7 presents a micro-grid system architecture. Micro-grid architecture refers to the structure and layout of a localized power distribution system that integrates various components to generate, store, and

distribute power energy within a defined area. Micro-grid architecture typically includes a combination of power generation sources, energy storage systems, loads, control systems, and communication infrastructure (Bhavaraju et al., 2022). The Point of Common Coupling (PCC) plays a crucial role in micro-grid architecture as it serves as the interface between the micro-grid and the main utility grid or other interconnected systems. The PCC is the location where power flows between the micro-grid and the external grid, allowing for import and export of electricity as needed (Altaf & Member, 2022).

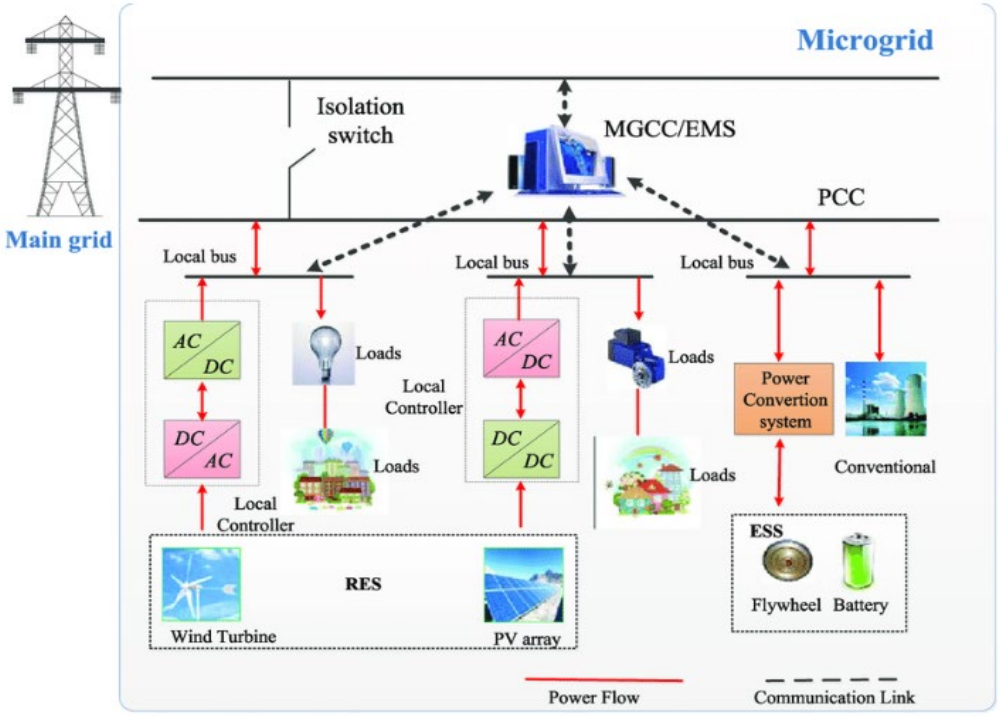


Figure 2.7: Micro-grid architecture (Han et al., 2018).

2.3. Distributed Generation Systems

Distributed generations (DGs) refer to electrical energy sources, which are directly connected to the grid customer site (Malik et al., 2022). It uses a variety of renewable and non-renewable sources. Renewable energy sources refer to power sources that use renewable energy methods to produce electricity, including PV, solar thermal, wind, biomass, tidal, and geothermal power. Non-renewable sources, on the other hand, rely on raw materials that are not renewed by nature to generate electricity (Adajah et al., 2021).

Recent studies indicate that approximately 80% of the global population are connected to the grid, but the rest 20% might be effectively supplied by distributed generation systems. Different

research demonstrated many interests have been given to distributed generation, which makes it to be more attractive than the traditional power grid (Oymak et al., 2022). Most of the known benefits include short transmission lines (reduce complexity and transmission losses), reduction in costs of transmission operation, gas emissions and amelioration in power supply security. Additionally, distributed generation modifies environmental impacts like emission control by using renewable energy sources such as solar, wind, biomass, etc. (Ufa et al., 2022). Figure 2.8 presents a distributed generation structure.

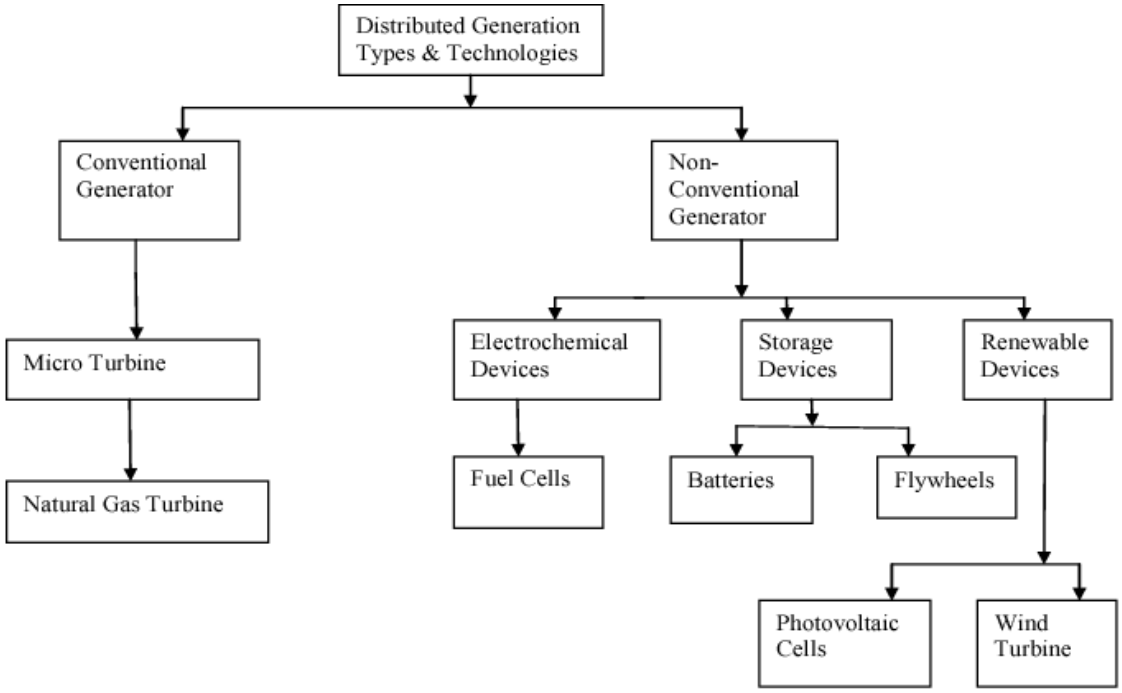


Figure 2.8: Technologies and types of distributed generation (Yadav & Srivastava, 2014).

Despite the significant benefits of distributed generation, integrating it into the current distribution networks is still difficult due to a number of technical, economic, and environmental obstacles. If distributed generations are built and designed incorrectly, voltage volatility, significant power losses, low power quality, and protection deterioration may occur in power distribution grids. The utilization of distributed generation systems will be increased if these issues are resolved (Ishaq et al., 2022).

2.4. Control Architecture in a Hybrid Micro-Grid System

In order to support and coordinate the hybrid micro-grid system, which offers complete system stability, various control levels such as micro source and central controllers are typically used. Figure 2.9 shows the primary, secondary, and tertiary controls in a hierarchical control

system. The primary control is responsible for initial power sharing and current/voltage controls. The secondary control, which is higher than the primary control and aids in improving performance sharing and compensating for voltage, comprises of the initial power sharing and current/voltage regulations. Finally, the tertiary control focuses on power management, energy management and economic dispatch (Bidram & Davoudi, 2012).

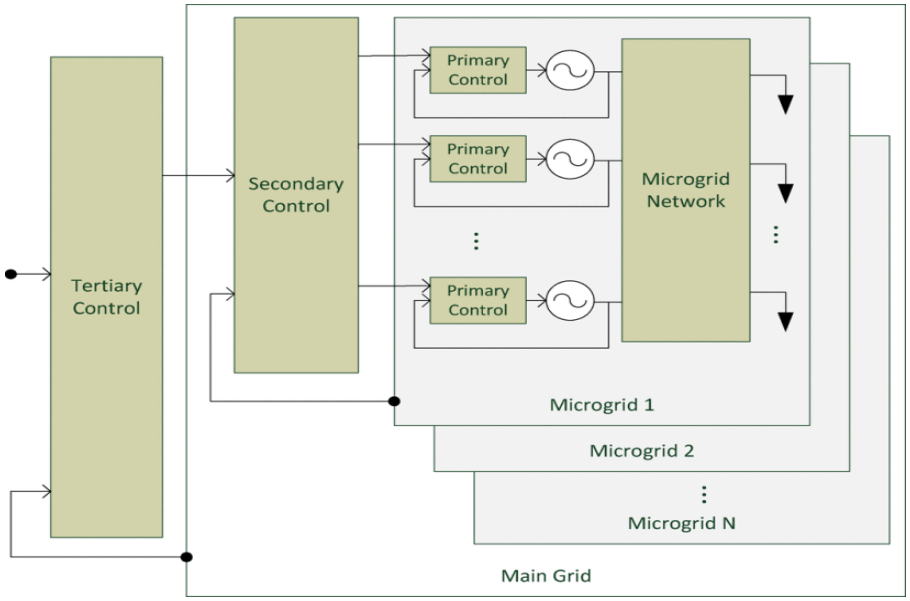


Figure 2.9: Hierarchical control architecture (Olivares et al., 2014).

2.4.1. Primary Control

When it comes to power converter control, the two main components are droop control (preliminary power sharing) and inner loops (current/voltage regulation).

Alternating current can be controlled in a synchronous rotating frame by the inner loops of a voltage control device, such as a three-phase voltage source converter (VSC). The linear controllers adjust the current within a specified range and provide the necessary voltage after the measured currents convert a three-phase stationary frame into a synchronous rotational frame. For a pulse-width modulation (PWM), the voltage needs are thus inversely transformed into three-phase modulation indices (Olivares et al., 2014).

Since there is no need for communication lines, voltage droop control is often used. The most popular method for "droop control" involves adding a "virtual resistance" to the existing system. While the virtual resistance is unaffected by operating conditions and is an ideal value that cannot result in any real power loss, the real resistance is not a fixed value that could be modified by environmental factors and would cause "real" power losses that should be

minimized. This hypothetical resistance is also known as the gain of droop, statistic constant, or coefficient of droop. AC systems were the first to use droop control (Guerrero et al., 2013).

In DC micro-grids, basic droop control can be achieved as current droop/power mode, combining voltage-mode drooping techniques such as V – I and V – P, as well as current – voltage (I – V) and power voltage (P – V) techniques (Olivares et al., 2014). These control techniques assess the DC voltage and analyse the injected current/power depending on the droop characteristic. As can be seen, I-V and P-V both performed similarly (Beerten & Belmans, 2013). Evidence can be found in the fact that both models are nearly same and only differ slightly when small voltage errors are considered. In this context, current/power mode approaches can be represented by the I-V droop. Like that, voltage mode techniques can be used to study the V-I droop feature (V-I and V-P).

2.4.2. Secondary Control

To maintain the bus voltage for a droop-controlled DC micro-grid at nominal value, a secondary control level is added to the micro-grid. This establishes the primary control reference and keeps the controlled parameter within an optimum range (Dragicevic et al., 2014).

As a result, secondary control, contrary to voltage and frequency regulation in AC micro-grids, aims to reduce voltage differences and enhance power quality (Naeinian, 2016). A centralized, distributed, or decentralized control strategy can be used to implement secondary control from the perspective of the communication link (Sahoo et al., 2018).

2.4.3. Tertiary Control

The main goal of the tertiary control is to regulate energy and power to accomplish objectives, such as balanced energy storage, lower power flow losses, and lower operating costs. The objective of a central tertiary controller is to maximize the system efficiency based on the converters' efficiency curve, as illustrated in Figure 2.10. The total demand, micro-grid voltage, and converter efficiency curves are determined by an optimization technique, such as a partial swarm optimization or genetic algorithm, in order to optimize the converter output power (Bompard et al., 2021).

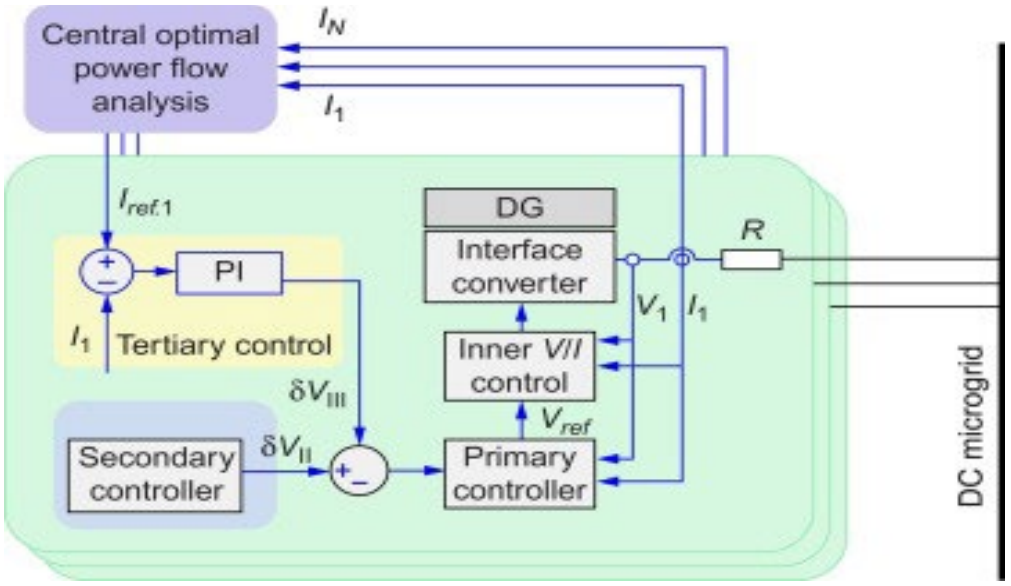


Figure 2.10: Centralized tertiary controller for the converter power loss optimization (Hu et al., 2021).

A tertiary controller is required because a hybrid micro-grid can attain its economical and ideal operation with two initial level controllers for voltage and current management. In a hybrid micro-grid system, the tertiary controller has evolved into a necessary instrument for power and energy management. To increase the overall efficiency of a hybrid micro-grid, energy management and power flow control are required (Hu et al., 2021). To achieve the objective, the tertiary controller employs a variety of optimization strategies.

When multiple hybrid micro-grid systems are connected in a group, the main objective of the tertiary controller is to synchronize individual incremental costs while controlling power flow and load sharing amongst the converters. Furthermore, based on the preferences for production costs, a tertiary controller is used to update the set point of the secondary controller by adjusting each converter's loading ratio (Abhishek et al., 2020). A tertiary controller can achieve the best power production dispatch by eliminating voltage fluctuations and adjusting the voltage operating point, in contrast to a secondary controller.

Several distributed control architectures have been developed by researchers for hybrid micro-grid systems that are controlled by various methods (Al-Ismail, 2021). The main contribution of these research is the design and implementation of two (local and central) smart controller approaches for energy management system in a hybrid micro-grid. The controllers are developed to operate with hybrid micro-grid systems that manage battery energy systems, allowing the micro-grid voltage and frequency to change depending on the

system load and solar radiation. The effectiveness of the suggested approaches has been assessed utilizing a variety of load dynamics in various scenarios depending on the metrology conditions. The findings obtained using the suggested controllers have ensured the operational safety and a high degree of hybrid micro-grid stability. The resulting simulation results also show that, for effectiveness and precision, the fuzzy logic method outperformed the PID and artificial neural network (ANN) techniques.

2.5. Energy Management System Algorithms for Hybrid Micro-Grid System

To optimize micro-grid performance, the energy management system of a hybrid micro-grid usually consists of several interconnected algorithms (Bateman, 2018). It is possible to integrate and modify these algorithms to meet the specific needs of a given micro-grid by employing a variety of software tools and computer languages to implement them (Halifa et al., 2016). Some of the typical algorithms utilized in an EMS for a hybrid micro-grid are as follows:

2.5.1. Battery storage optimization algorithm

The ideal charging and discharging schedules for the batteries in the micro-grid are determined by this algorithm, which also takes into account the availability of renewable energy sources and the anticipated energy demand (Dolara et al., 2016). An expanding area of study and development in energy management is battery storage optimization algorithms. These algorithms strive to manage the charge and discharge cycles of batteries intelligently to optimize the efficiency and dependability of energy storage devices. The ability of battery storage optimization algorithms to lower energy costs for consumers is one of their main benefits (Shi et al., 2023). These algorithms can assist in lowering peak energy use and avoiding costly demand charges by controlling the charging and discharging of batteries in real-time. Also, by storing excess energy during times of low demand and using it later, they can aid in lowering the overall energy consumption of buildings and houses (Moghimi et al., 2018).

There are several different types of battery storage optimization algorithms, including rule-based algorithms, model-based algorithms, and machine learning algorithms. Rule-based algorithms are relatively simple and rely on a set of predefined rules to manage battery charging and discharging. Model-based algorithms are more complex and use mathematical models to predict energy demand and optimize battery performance. Machine learning algorithms are even more advanced and use artificial intelligence techniques to learn from data and continuously improve performance. The effectiveness and dependability of energy

storage systems could be greatly enhanced by battery storage optimization techniques. There will be a greater need for complex algorithms as more households and buildings embrace these systems. We can anticipate even more sophisticated algorithms in the future that optimize energy storage and lower customer expenses by utilizing real-time data and machine learning approaches (Haider et al., 2020).

2.5.2. Power flow control algorithm

This algorithm regulates the power flow inside the micro-grid to maintain the voltage and frequency within reasonable bounds and to maintain the stability and dependability of the system. These algorithms aid in controlling electricity flow, preventing overloading, and enhancing system effectiveness (Feng et al., 2022). Power flow control algorithms are in a variety of forms, each with advantages and disadvantages. The common generation control algorithm is among the most often used algorithms for controlling the flow of power. In order to maintain a balance between generation and load, this algorithm is developed to regulate the output of generators in a power system (Fazeli et al., 2014).

As it is simple to implement and has been around for a while, the common generation control algorithm is widely employed in power systems. In large, complicated power systems, where conventional approaches might not be adequate, the advanced power flow control algorithm is especially helpful (Balamurugan, 2019). For managing the flow of electricity in power systems, power flow control algorithms are a crucial instrument. They aid in preventing overloads, enhancing system effectiveness, and guaranteeing that consumers will have a consistent supply of electricity (Pohl et al., 2018). The algorithm picked will depend on the requirements of the power system, and it is important consider this thoroughly to ensure that the chosen algorithm is appropriate for the task at hand.

2.5.3. Demand Response Algorithm

This algorithm enables the micro-grid to adapt to variations in demand by altering the functioning of the various generators and storage devices in order to maintain a balance between supply and demand (Hadi et al., 2014). Demand response (DR) algorithms have drawn more attention recently as a means of enhancing the dependability and effectiveness of electricity systems. These algorithms are made to automatically modify how much electricity is used in response to variations in supply and demand, thereby lowering peak demand and enhancing grid stability (Priya et al., 2020). Depending on the application and algorithm design, the efficiency of DR algorithms can vary.

Some algorithms may work better in an office or commercial environment, while others may work better in a home or small-scale application (Pi et al., 2021). The accuracy of the data inputs and the sophistication of the algorithm's predictive models are other factors that frequently affect the performance of a DR algorithm. A more sustainable and effective energy system will require the creation of efficient DR algorithms (Ali et al., 2022). We may anticipate seeing more advanced and efficient DR algorithms emerge as data analytics and machine learning continue to advance, helping to optimize energy use and lessen environmental impact.

Table 2.1 summarizes the advantages and disadvantages of these different EMS algorithms for the hybrid micro-grid.

Table 2.1: Summary of EMS/algorithms in hybrid micro-grid systems

EMS/Algorithms	**Advantages**	Disadvantages
Battery storage optimization algorithm (Wong & Ramachandaramurthy, 2021) (Mohamadi & Noshahr, 2020)	• Increased efficiency: they can help to maximize the efficiency of battery systems by reducing the amount of energy wasted and ensuring that the batteries are charged and discharged at the optimal times. • Reduced energy cost: They can assist utilities in making financial savings by lowering the demand for backup power and optimizing resource use. • Improved battery lifespan: By reducing the number of charge and discharge cycles required. • Enhanced reliability: they can help to ensure that battery systems are always charged and ready to use when needed, providing a more reliable source of backup	• Complexity: Battery storage optimization algorithms are often complex and require a high level of technical expertise to develop and implement. • Limited accuracy: While battery storage optimization algorithms can be highly accurate, they are still subject to limitations and errors. • Cost: Implementing battery storage optimization algorithms can be expensive, as it often requires the purchase of specialized software and hardware. • Reliability: Battery storage optimization algorithms rely on data inputs from various sources, including weather

	power in the event of an outage or other disruption. • Increased use of renewable energy: they can help to integrate renewable energy sources, such as solar or wind power, into the grid. • Flexibility: they can also be customized to suit the specific needs of different users, allowing for greater flexibility in how battery storage is used and managed.	forecasts and energy demand data. • Risk of overcharging or undercharging: Battery storage optimization algorithms can lead to overcharging or undercharging of batteries if not properly calibrated.
Power flow control algorithm (Salem et al., 2018) (Mehta et al., 2015) (Deokate, 2022)	• Improved power system stability: These algorithms can improve the stability of the power system by maintaining proper voltage and frequency levels. • Better utilization of existing infrastructure: They can ensure that the existing infrastructure is utilized to its maximum capacity. • Increased efficiency: These algorithms can improve the overall efficiency of the power system by reducing losses due to overloading or congestions. • Increased flexibility: They can increase the flexibility of the power system by enabling power to be directed to where it is needed most. • Enhanced renewable energy integration: These algorithms can facilitate the integration of	• Complexity: Power flow control algorithms are complex and require extensive computing resources to operate. This makes them difficult to implement, especially in large power systems. • Cost: The cost of implementing power flow control algorithms can be prohibitive. • Limited control range: The control range of power flow control algorithms is limited, which can restrict their ability to regulate power flows in certain situations. • Sensitivity to system changes: Power flow control algorithms are sensitive to changes in the power system, such as changes in load demand, power generation, and transmission line outages.

	renewable energy sources into the power system.	• Communication delays: Power flow control algorithms rely on real-time communication between different devices and systems. • Cybersecurity risks: The use of power flow control algorithms can increase the risk of cybersecurity attacks on power systems.
Demand response algorithm (Asgher et al., 2018) (Hadi et al., 2020) (Noor et al., 2023)	• Reduced energy costs: By adjusting energy usage during peak demand periods. • Increased grid reliability: they can help maintain grid stability by reducing demand during peak periods, thereby preventing blackouts or brownouts. • Improved energy efficiency: By optimizing energy usage. • Reduced greenhouse gas emissions: These algorithms can help reduce greenhouse gas emissions, which is beneficial for the environment. • Increased use of renewable energy • Enhanced grid flexibility: they can help make the grid more flexible and responsive to changing energy demand patterns. • Improved customer engagement	• Limited Participation: One of the main drawbacks of demand response algorithms is that they rely on voluntary participation from consumers. • Complexity: Demand response algorithms are complex and require significant resources to implement and maintain. • Lack of Flexibility: Demand response algorithms are often inflexible and can be difficult to adapt to changing energy usage patterns. • Dependence on Communication Networks: Demand response algorithms depend on communication networks to function effectively. • Cost: The cost of implementing and maintaining demand response algorithms can be significant.

2.6. Energy Management System Controls for Hybrid Micro-Grid System

Within a hybrid micro-grid system, the flow of power is managed and controlled by an EMS, which is dependent on software (Mansour et al., 2022). It gathers real-time data from different sensors, which include PV, wind, and energy storage systems, and analyses it to select the ideal operating strategy of the system (Hizam, 2022). The EMS controls determine how to use the energy sources and storage systems most efficiently to satisfy the requirement of the load, reduce the emissions of carbon, and cut down on total operating costs (Thirunavukkarasu et al., 2022). There are several EMS algorithms used in the hybrid micro-grid systems. The most used algorithms include rule-based control, model predictive control, fuzzy logic control, artificial neural network control, and hierarchical control.

2.6.1 Rule-Based Control

This algorithm controls the flow of power in the micro-grid based on the pre-established rules (khelja et al., 2021). It might be preferred to employ RESs such as solar power or wind power when they are available, and when those sources become insufficient, the use of stored energy, such as that provided by batteries or backup generators, may be chosen (Meng, 2020). Although this method is reasonably easy to use, it might not be as effective as more complex ones (Moretti et al., 2021).

2.6.2 Model Predictive Control

This algorithm selects the energy management strategy that will best achieve a set of goals by using a micro-grid model to forecast how various energy management strategies will impact the system in the future (such as minimizing energy costs or maximizing renewable energy usage) (Shahzad et al., 2022). Compared to rule-based control, this method uses more computer resources but has the potential to be more effective and flexible (Babayomi et al., 2020).

2.6.3 Fuzzy Logic Control

This algorithm utilizes fuzzy logic to make decisions about how to manage energy flow in the micro-grid system (Singh et al., 2019). Fuzzy logic, as opposed to conventional Boolean logic, enables more nuanced decision-making, which is advantageous when dealing with complex systems that contain numerous variables and uncertainties (Rahim, 2022). Although very simple to use, this algorithm might not be as accurate as others.

2.6.4 Artificial Neural Network Control

This algorithm uses an artificial neural network (ANN) to learn from data about the micro-grid system and make decisions about how to manage energy flow (Akoubi et al., 2022). Together with real-time input from sensors and other sources, the neural network can be trained using past information about the system. Although it may need more computing power than other algorithms, this algorithm has the potential to be incredibly powerful (Dominka et al., 2021).

2.6.5 Hierarchical Control

This algorithm divides the micro-grid system into smaller subsystems and applies different control strategies to each subsystem while coordinating the overall performance of the system (Li et al., 2022). For instance, it might employ various methods to control energy flow within a single building as opposed to energy transfer between several buildings in the micro-grid (Bera et al., 2022). Despite being difficult to implement, this technique could significantly enhance the micro-grid to operate more effectively (Mingsheng et al., 2018).

The EMS is essential for the hybrid micro-grid system to operate at its best, increasing dependability and lowering operating costs (Nesihath et al., 2023). Table 2.2 presents a summary of previous studies based on EMS using different algorithm. The most suitable EMS algorithm is chosen based on the unique needs and limitations of each system.

Table 2.2: Summary of Previous Studies on EMS using different algorithm

Ref.	System Configuration	Programming Language	EMS Control	Remarks
(Chaouachi et al., 2013)	Standalone PV/wind/microturbine/fuel cell/battery	Linear-programming	Fuzzy logic	The forecasting accuracy of machine learning was evaluated by predicting error in order to validate the neural network ensemble forecasting module. In conjunction with multi-objective optimization based on linear programming, the authors implemented an artificial intelligence technique. The goal of these created strategies was to lower a micro-grid's emission levels and running costs, taking into account pre-operational factors like load needs and the availability of renewable resources in the future.
(Gracia et al., 2013)	Renewable micro-grid	Linear programming via MATLAB/Simulink	Fuzzy logic	The development of the hybrid renewable energy system's enhanced performance was demonstrated by the combination of two distinct energy management techniques, namely optimization and fuzzy logic control. Understanding how to handle uncertainties associated with estimates of load demand and renewable energy generation was the primary goal of this study. These techniques have

				demonstrated how a hybrid renewable energy system should operate.
(Serban et al., 2012)	Autonomous micro-grids with classical and RES-based generators	Hardware-in-the-loop (HIL)	Real-time digital simulator	A novel hardware-in-the-loop (HIL) method was developed to test and optimize the frequency control mechanism in isolated micro-grids in real time. Renewable energy sources and batteries constituted the production system.
(Himabindu & Gopichand, 2020)	Renewable micro-grid connected to a main grid	Linear programming via MATLAB/Simulink	Fuzzy logic	An ideal energy management system was implemented. The primary goals of the research were to meet the load's power requirements and to keep the energy storage systems, which included the battery and the hydrogen charged within a predetermined range. The approach was successful in maximizing both the energy storage systems' lifespan and utilization costs, as evidenced by the findings. The authors recommended using other techniques, such as the grid-connected mode, to assess how well the developed energy management system operates.
				This work proposes an intelligent adjustment of the virtual resistance using a fuzzy logic method to offer appropriate energy storage in BESS and low voltage changes. The proposed

(Beykverdi et al., 2017)	Standalone PV/wind/battery	Linear programming via MATLAB/Simulink	Fuzzy logic and real-time	decentralized technique controls virtual resistance to manage the power supply of DGs to meet load requirements or recharge batteries based on the droop characteristic and SOC level of the BESS. It was found that adding more DG units or batteries to the micro-grid using the recommended fuzzy logic technique can be done without defying or affecting the given generalizations.
(Hu et al., 2021)	Renewable micro-grid connected to a main grid	Linear-programming	Model predictive control	This report reviews the latest research on predictive control in micro-grids. According to this study, MPC is currently used in micro-grids and it is already showing promise as a competitive substitute for well-established power flow, frequency, voltage, and efficiency management strategies.
(Kang et al., 2021)	Renewable hybrid AC/DC micro-grid connected to a main grid	Linear-programming	Artificial Neural Network	This study developed an ANN-based small-scale hybrid AC/DC micro-grid energy management method. To design the implemented EMS, an EMS operating mode was selected, an operation profile was selected for each operation mode, and ANN training was then applied in each mode.

(Andre et al., 2023)	Standalone PV/generator/battery	Linear-programming via MATLAB/Simulink	Model Predictive Control with real-time measurement feedback	The best possible operation of the DC micro-grid has been confirmed in this study by evaluating all control levels, guaranteeing the best possible operation in terms of the utilization of technical resources and economically by obtaining the lowest operating costs and extending the life of the batteries. Following the established SOC limits, the proposed EMS avoids deep discharges and instead offers an optimal operation in which the EMS makes decisions about charging and discharging based on the availability of natural resources and the least expensive DC micro-grid.
(Bilbao et al., 2022)	Renewable hybrid micro-grid	Linear-programming	Machine Learning method of Decision Trees by means of Fuzzy Logic control	The main focus of this article, which is primarily based on mathematical modelling, is on how hybrid micro-grids could operate optimally. This kind of network administration involves a number of alternatives and obstacles to accomplish. The research's primary contribution was the mathematical modelling of several hybrid micro-grid components. This modelling can be used in a variety of network control and management techniques, and three different approaches—one of which is based on the Decision Tree method,

				which is part of the Machine Learning family have demonstrated its viability. The results on a test system with 69 buses shown that its management could be put into practice.
(Wynn et al., 2023)	Renewable micro-grid connected to a main grid	Linear-programming via MATLAB/Simulink	Particle Swarm Optimization (PSO) and Demand Response (DR)	In this research, an energy management system has been proposed to give improved load management techniques and control facilities. Moving the flexible load in the micro-grid system is one way that a decentralized energy management system has been proposed to reduce the system's running costs. The developed approach made use of a demand response (DR) schedule to keep the balance between supply and demand, as well as optimal scheduling of the local generation resources.
(Qu et al., 2022)		Linear-programming via MATLAB/Simulink	Fuzzy Logic	This study outlined the topology of an AC/DC hybrid micro-grid based on solid-state transformers (SSTs). An energy management method was developed in order to solve the issues with the fixed droop coefficient that are now present in conventional droop control systems. Because of this static coefficient, the power distribution remains constant even when the system's operating conditions like the

	Renewable hybrid AC/DC micro-grid connected to a main grid			unpredictable nature of renewable energy sources change. An innovative adaptive droop control method is created for the energy storage system in order to further enhance the financial advantages of power users and prolong the operational life of supercapacitors.
(Reddy et al., 2022)	Standalone PV/wind/battery	Linear-programming via MATLAB/Simulink	Fuzzy Logic	This study presented a novel hybrid battery and PV-wind turbine power system. The recommended model's dynamic behaviour was investigated in a range of operational scenarios. The designed system performed remarkably well, as did its control method. The proposed model provides a helpful instrument for raising the smart grid's efficiency.
(Sayeed et al., 2022)	Hybrid micro-grid PV/fuel cell/battery/supercapacitor connected to main grid	Linear-programming via MATLAB/Simulink	Fuzzy Logic	Fuel cell drawbacks are successfully mitigated by the proposed hybrid energy system, which includes solar panels, fuel cells, batteries, and supercapacitors. It overcomes the shortcomings of the individual source and provides the load with consistent, enough power.
				In this paper, it was proposed that small hybrid DC/AC micro-grids could benefit from an artificial gorilla troop optimizer optimized neural network energy management system. To operate in each

(Troops, 2022)	Renewable hybrid AC/DC micro-grid connected to a main grid	Linear-programming via MATLAB neural network	Artificial Neural Network	mode of the proposed energy management system, a neural network was developed. The performance of neural-network energy management systems optimized using Levenberg-Marquardt, GA, PSO, and cuckoo search was investigated using a synthetic gorilla troop optimizer. Its 99.55 percent efficiency showed that it performed better than the cuckoo search-optimized neural-network energy management systems, GA, PSO, Levenberg-Marquardt, and GA.
(Aviles et al., 2018)	Renewable micro-grid PV/wind/battery connected to the main grid	Linear-programming via MATLAB/Simulink	Fuzzy Logic	Both the load demand and the renewable generation were assumed to be uncontrollable in the proposed energy management system. Maintaining a safe Battery State of Charge while reducing variations in the Grid Power Profile was the main goal of the EMS. Rather of relying solely on forecasts, the implemented system uses both the battery SOC and the micro-grid energy rate-of-change to increase, decrease, or maintain the power delivered to/absorbed by the mains.
				In this work, an energy management in an island micro-grid was studied using model predictive

(Nair & Castello, 2020)	Standalone PV/ dispatchable generators/battery/fuel cell/super capacitor	Linear-programming via MATLAB/Simulink	Model Predictive Control	control. The objective was to lower the rate of storage system degradation, enhance the usage of renewable energy, and improve micro-grid operational efficacy. The benefits of energy scheduling with MPC were emphasized by comparing it with a heuristic-based method such as fuzzy inference. When compared to heuristic methods, it was found that MPC ensures better performance on an islanded micro-grid.
(Sraidi et al., 2022)	Micro-grid PV/wind/battery/EV connected to main grid	Linear-programming via MATLAB/Simulink	Particle Swarm Optimization	This paper proposed a corresponding energy management system. This led to the presentation of an improved particle swarm optimization method with dynamic learning parameters and weights, which enhanced the system's ability to engage in social cognition and self-learning. The results showed that the micro-grid can maximize system operation efficiency and achieve self-sufficiency.

2.7. Future Scope and Challenges

Energy management system (EMS) algorithms and controls play a crucial role in the operation and optimization of hybrid micro-grid systems, which integrate multiple sources of energy generation, storage, and consumption. By looking into the future, there are several areas of potential growth and development, along with associated challenges. The rise of renewable energy sources, like solar and wind, in hybrid micro-grids demands advanced EMS algorithms. These algorithms should adeptly manage the intermittency and variability of renewables. Addressing the unpredictable nature of renewables requires sophisticated forecasting techniques and real-time optimization to ensure grid stability and reliability. Future EMS algorithms must juggle multiple objectives such as cost reduction, grid stability, and sustainability. They need to employ multi-objective optimization techniques to strike a balance among these goals.

Balancing competing objectives while considering factors like energy prices, environmental impact, and grid constraints presents a significant challenge. Energy Storage Systems (ESS) are integral to hybrid micro-grids, offering flexibility and grid support. Future EMS algorithms should optimize ESS operation, including charging/discharging scheduling and state-of-charge management. Managing ESS effectively entails addressing issues like battery degradation, cycle life, and optimal utilization under varying grid conditions. Hybrid micro-grids must seamlessly transition between grid-connected and islanded modes during outages. Future EMS algorithms should facilitate smooth transitions, ensuring grid stability and load balance. Implementing reliable islanding detection, load shedding strategies, and autonomous control mechanisms pose challenges in maintaining grid stability during transitions. With increasing reliance on digital control systems, future EMS algorithms must prioritize cybersecurity measures to safeguard against cyber threats and ensure operational resilience. Developing robust cybersecurity protocols and ensuring resilience against cyberattacks or system failures is a critical challenge.

To foster seamless integration and communication between diverse micro-grid components and EMS platforms, future efforts should focus on standardization and interoperability. Establishing common standards and protocols across different vendors and platforms to ensure compatibility and interoperability presents a significant challenge. Future EMS algorithms should be scalable and adaptable to accommodate the evolving complexity and diversity of hybrid micro-grid systems. Ensuring scalability and flexibility to accommodate changes in system configurations, expansions, and evolving operational requirements is a persistent challenge. In this review, many developed advanced algorithms to improve energy

management in hybrid renewable micro-grids, including model predictive control, fuzzy logic, and artificial neural networks have been listed. These algorithms have shown promising improvements in the sustainability, cost-effectiveness, and energy efficiency of micro-grids. Additionally, a summary of previous studies based on EMS using different algorithm have also been presented in this review.

This complete review revealed that most studies on energy management for hybrid renewable energy systems have been done using Fuzzy Logic control, due to its ability to handle complex, uncertain, and nonlinear systems effectively, and few cases are focused on other methods. Thus, it is important to develop new methods and techniques to control and to manage the power flow in a hybrid renewable micro-grid system. Furthermore, the review emphasizes how crucial it is to continue this kind of research and development to improve the efficiency and scalability of energy management system algorithms for hybrid renewable micro-grids. Global efforts to reduce carbon emissions and combat climate change can be greatly aided by the widespread adoption of these systems in a variety of applications, including remote communities, industrial parks, and smart cities.

2.8. Summary

This chapter discussed a comprehensive literature review, which included not only the concept of hybrid micro-grid, but also considered the energy management systems. Thereafter, the focus was on different micro-grid types. Additionally, some of the EMS algorithms were reviewed and appropriately presented to understand their suitability in hybrid micro-grid system applications.

This study has as its main objective to develop an energy management control to increase the performance and scalability of hybrid renewable micro-grid systems. To understand the operation and configuration of a suitable energy management system, a literature review on different EMS controls for hybrid micro-grid systems like fuzzy logic control, rule-based control, model predictive control, hierarchical control as well as artificial neural network control was presented. The body of research to date has shown that, except for a few examples, most research on EMS for hybrid renewable micro-grids has focused on fuzzy logic control. To regulate and manage the flow of energy in hybrid renewable micro-grids, it is crucial to implement new strategies and methods.

CHAPTER 3: FUNDAMENTAL CIRCUIT MODEL OF VOLTAGE SOURCE CONVERTERS

Article 1: Basic Circuit Model of Voltage Source Converters: Methodology and Modelling

In this chapter fundamental VSC circuit model with an output LC filter is discussed. An AC-DC converter serves as the primary power interface between the hybrid micro-grid and distributed generators. A voltage source converter operates in two modes. When used as a DC bus control, it functions as an active rectifier. When used in the grid-forming mode or grid-feeding mode it functions as an inverter by utilizing various control loops. A comprehensive guide including a range of methods, such as phase lock loop, direct quadrature zero (DQZ) synchronous frame, as well as space vector pulse width modulation (SVPWM) is also introduced.

Additionally, information on fundamental theory and architecture, which enables the VSC to operate in inverter mode by integrating the developed control loops, as well as in rectifier mode using DC bus control are also reviewed. Furthermore, this study provides an in-depth overview of the fundamental circuit model of VSCs, control strategies, and accurate modelling techniques. This paper aims to contribute to the advancement of VSC-based power electronics applications and their integration into contemporary power systems for increased efficiency, reliability, and sustainability by offering insights into the basic ideas and practical considerations related to VSCs.

AppliedMath

MDPI

Article

Basic Circuit Model of Voltage Source Converters: Methodology and Modeling

Christian Bipongo Ndeke *, Marco Adonis and Ali Almaktoof

Department of Electrical, Electronic and Computer Engineering, Cape Peninsula University of Technology, Cape Town 7535, South Africa; adonisma@cput.ac.za (M.A.); almaktoofa@cput.ac.za (A.A.)
* Correspondence: ndekechristian@gmail.com or 219385017@mycput.ac.za; Tel.: +27-62-836-2466

Abstract: Voltage source converters (VSCs) have emerged as the key components in modern power systems, facilitating efficient energy conversion and flexible power flow control. Understanding the fundamental circuit model of VSCs is essential for their accurate modeling and analysis in power system studies. A basic voltage source converter circuit model connected to an LC filter is essential because it lowers the harmonic distortions and enhances the overall power quality of the micro-grid. This guarantees a clean and steady power supply, which is necessary for the integration of multiple renewable energy sources and sensitive loads. A comprehensive methodology for developing a basic circuit model of VSCs, focusing on the key components and principals involved, is presented in this paper. The methodology includes the modeling of space vector pulse-width modulation (SVPWM) as well as the direct quadrature zero synchronous reference frame. Different design controls, including the design of current control loop in the S-domain, the design of the direct current (DC) bus voltage control loop in the S-domain, and the design of the alternating current (AC) voltage control loop in the S-domain, are explored to capture the dynamic behavior and control strategies of VSCs accurately. The proposed methodology provides a systematic framework for modeling VSCs, enabling engineers and researchers to analyze their performance and assess their impact on power system stability and operation. Future studies can be conducted by using case studies and simulation scenarios to show the efficiency and applicability of the developed models in analyzing VSC-based power electronics applications, including high-voltage direct current (HVDC) transmission systems and flexible alternating current transmission systems (FACTS). The significance of this work lies in its potential to advance the understanding and application of VSCs, contributing to more resilient and efficient power systems. By providing a solid foundation for future research and development, this study supports the ongoing integration of renewable energy sources and the advancement of modern electrical infrastructure.

Keywords: voltage source converter; LC filter; current control; DC voltage control; AC voltage control

check for updates

Citation: Ndeke, C.B.; Adonis, M.; Almaktoof, A. Basic Circuit Model of Voltage Source Converters: Methodology and Modeling. *AppliedMath* **2024**, *4*, 889–907. https://doi.org/10.3390/appliedmath4030048

Academic Editor: Jun-Juh Yan

Received: 21 May 2024
Revised: 16 July 2024
Accepted: 18 July 2024
Published: 29 July 2024

Copyright: © 2024 by the authors. Licensee MDPI, Basel, Switzerland. This article is an open access article distributed under the terms and conditions of the Creative Commons Attribution (CC BY) license (https://creativecommons.org/licenses/by/4.0/).

1. Introduction

Voltage source converters (VSCs) have become integral components in modern power systems, playing a crucial role in facilitating efficient energy conversion and enabling flexible power flow control [1]. As the demands for renewable energy integration, grid stabilization, and improved grid reliability continue to grow, the accurate modeling and analysis of VSCs have become paramount [2,3]. The primary power interface connecting distributed generations (DGs) to micro-grids is the AC-DC converter. The voltage source converter functions in two distinct modes, operating as an active rectifier for direct current (DC) bus control and, as depicted in Figure 1, acting as an inverter during grid-feeding and grid-forming operations using distinct control loops [4]. Understanding the basic circuit model of VSCs, along with methodologies for their control and modeling, is essential for engineers and researchers to effectively design, analyze, and optimize VSC-based power electronics applications [5]. The aim of this paper is to present a comprehensive

methodology overview, control strategies, and modeling techniques associated with the basic circuit model of VSCs. This paper delves into the fundamental principles underlying the operation of VSCs, focusing on the key components and their interactions within the circuit. An emphasis is placed on elucidating different methodologies, such as space vector pulse-width modulation (SVPWM), the direct quadrature zero synchronous reference frame, and their integration into VSC circuits.

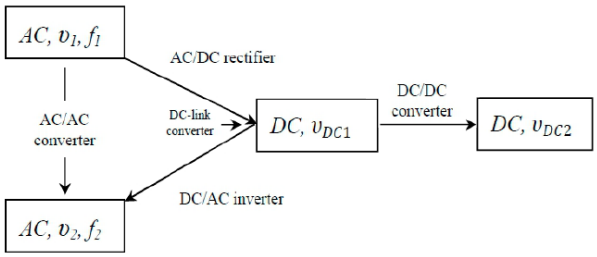


Figure 1. Solid-state power converter groups based on their operating transformation [6].

A fundamental voltage source converter circuit model connected to the LC filter is crucial because it helps in reducing harmonic distortions and improving the overall power quality in the micro-grid. This ensures a stable and clean power supply, which is essential for sensitive loads and the integration of various renewable energy sources. It also plays a key role in converting DC power from renewable sources like solar panels or batteries to AC power, which is required for most loads and for synchronization with the main grid. The LC filter aids in smoothing out the output, making the conversion process more efficient. Understanding the VSC circuit model and its interaction with the LC filter is essential for designing systems that can seamlessly integrate with the main grid or operate in island mode. This ensures that the micro-grid can handle fluctuations in supply and demand without compromising stability. In essence, the significance of introducing the fundamental VSC circuit model connected to the LC filter lies in its ability to address key challenges in energy conversion, stability, integration, and the management of hybrid renewable micro-grid systems.

Furthermore, this paper explores various control strategies employed in VSCs to regulate the voltage, current, and power flow in both grid-connected and standalone applications. Various control techniques using pulse width modulation (PWM) and proportional integral (PI) control are discussed. Moreover, the modeling aspects of the design and control of VSCs are also introduced to develop accurate and dynamic models that capture the transient and steady-state behavior of these devices. To ensure the relevance and applicability of the presented models in real-world scenarios, practical considerations, such as parameter estimation, validation, and implementation challenges, need to be addressed. Case studies and simulations are recommended to be conducted to shown the efficiency and accuracy of the presented methodologies and control strategies in analyzing VSC-based power electronics applications, such as flexible alternating current transmission systems (FACTS), grid-connected renewable energy systems, and high-voltage direct current (HVDC) transmission systems.

The following sections describe the remaining paper parts: In Section 2, two-level grid-connected VSC modeling with an LC filter is presented. The design of the current control loop in the S-domain is introduced in Section 3. Section 4 presents the design of a DC bus voltage control loop in the S-domain. In Section 5, the design of an AC voltage control loop in the S-domain is provided. Section 6 gives a brief discussion, and Section 7 concludes the paper.

2. Two-Level Grid-Connected VSC Modeling with LC Filter

A typical circuit model of a two-level inverter with an LC filter connected to a three-phase load is presented in Figure 2. The signal applied to terminals a, $\grave{a}$, b, $\grave{b}$, c, and $\grave{c}$ regulates the power of the six switches that form the output, denoted as S1 to S6. It is assumed that switches S1 through S6 are complementary [7]. Typically, a voltage source converter with an LCL filter is regulated by a conventional linear controller augmented by a damping loop to ensure the stability of the system [8]. Furthermore, both the three-phase AC system and the DC-side voltage source can directly receive power from the VSC. Consequently, there are two different modes of operation for the VSC, either the inverter (DC/AC) or rectifier (AC/DC) modes.

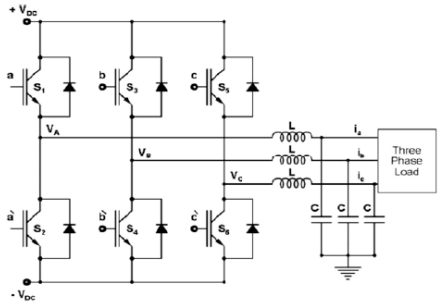


Figure 2. Voltage source converter with three phase-2 levels [7].

To connect the distributed generation systems to the grid, three-phase pulse-width modulation voltage source converters (PWM-VSCs) are commonly employed because of their superior controllability and higher efficiency compared to the other converters [9]. To enable DC-side voltage control and power factor at the point of common coupling (PCC), a two-level PWM-VSC topology is used. However, the implementation of the PWM results in baseband and sideband harmonics appearing in the AC voltage harmonic spectrum, necessitating the use of filters to reduce the harmonics of the grid current [10].

2.1. Space Vector Pulse-Width Modulation (SVPWM) Methodology

Using the triangle comparison strategy simplifies the execution of this procedure. Compared to triangle comparison PWM, it achieves a 15% increase in AC voltage and reduces voltage and current total harmonic distortion (THD). A standard space vector diagram of a two-level voltage source inverter (VSI) with switching states in the six sectors is presented in Figure 3 [11]. Table 1 illustrates that a typical three-phase, two-level voltage source inverter has eight switching states, with six active states producing voltage vectors of either $+V_{dc}$ or $-V_{dc}$, and two null states generating voltage vectors with zero amplitude. In Figure 3, the switch states 000 and 111 represent the null states, while the space vector plane is divided into six equal sectors by the active states. This methodology employs a revolving reference vector, as depicted in Figure 3, sampled once during each sub-cycle, T_s [12]. The main objective is to estimate the vector of the reference voltage V_{ref} utilizing eight switching models.

Figure 3 illustrates that two of the potential output voltage vectors ($\vec{V}_1$ and $\vec{V}_7$) are null or zero vectors, represented by equal values in all three phases (000 or 111). The remaining six vectors ($\vec{V}_1, \ldots, \vec{V}_6$) are non-zero and are all spatially separated by 60°.

The null voltage vector time was arbitrary assumed to be divided equally between t_0 and t_7 for the SVPWM approach, meaning that $T_0 = T_7$.

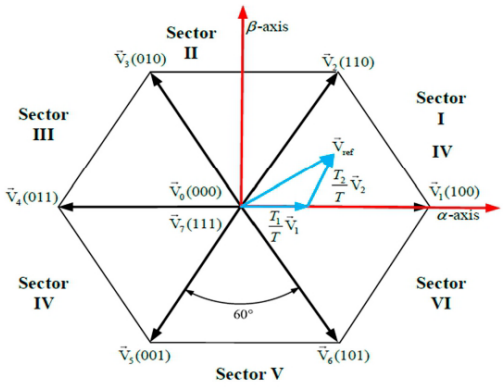


Figure 3. A typical SVPWM diagram for a voltage source inverter with two levels.

Table 1. Phase voltages, output line-to-line voltages, and switching vectors.

Voltage Vectors	Switching Vectors			Line-to-Neutral Voltage			Line-to-Line Voltage		
	S_1	S_2	S_3	V_{an}	V_{bn}	V_{cn}	V_{ab}	V_{bc}	V_{ca}
$\vec{V}_0$	0	0	0	0	0	0	0	0	0
$\vec{V}_1$	1	0	0	$\frac{2}{3}V_{DC}$	$-\frac{1}{3}V_{DC}$	$-\frac{1}{3}V_{DC}$	V_{DC}	0	$-V_{DC}$
$\vec{V}_2$	1	1	0	$\frac{1}{3}V_{DC}$	$\frac{1}{3}V_{DC}$	$-\frac{2}{3}V_{DC}$	0	V_{DC}	$-V_{DC}$
$\vec{V}_3$	0	1	0	$-\frac{1}{3}V_{DC}$	$\frac{2}{3}V_{DC}$	$-\frac{1}{3}V_{DC}$	$-V_{DC}$	V_{DC}	0
$\vec{V}_4$	0	1	1	$-\frac{2}{3}V_{DC}$	$\frac{1}{3}V_{DC}$	$\frac{1}{3}V_{DC}$	$-V_{DC}$	0	V_{DC}
$\vec{V}_5$	0	0	1	$-\frac{1}{3}V_{DC}$	$-\frac{1}{3}V_{DC}$	$\frac{2}{3}V_{DC}$	0	$-V_{DC}$	V_{DC}
$\vec{V}_6$	1	0	1	$\frac{1}{3}V_{DC}$	$-\frac{2}{3}V_{DC}$	$\frac{1}{3}V_{DC}$	V_{DC}	$-V_{DC}$	0
$\vec{V}_7$	1	1	1	0	0	0	0	0	0

The following is used to calculate the sampling interval:

$$T_s = T_0 + T_1 + T_2 \tag{1}$$

or

$$T_S = T_0 + T_{mod} \tag{2}$$

with

$$T_{mod} = T_1 + T_2 \tag{3}$$

where T_{mod} is the modulation time; T_0, T_1, and T_2 are the time intervals; and T_s is the sampling interval. When examining the first sector, the reference voltage vector $\vec{V}_{ref}$ may be presented as function vectors:

$$\vec{V}_{ref} = \frac{T_1}{T_S}\vec{V}_1 + \frac{T_2}{T_S}\vec{V}_2 \tag{4}$$

$$\left|\vec{V}_{ref}\right|\begin{bmatrix}\cos\alpha\\ \sin\alpha\end{bmatrix} = \frac{T_1}{T_S}\left|\vec{V}_1\right|\begin{bmatrix}\cos(0)\\ \sin(0)\end{bmatrix} + \frac{T_2}{T_S}\left|\vec{V}_2\right|\begin{bmatrix}\cos(\pi/3)\\ \sin(\pi/3)\end{bmatrix} \tag{5}$$

Equation (5) can be divided into two parts and expressed as follows:

$$T_S\left|\vec{V}_{ref}\right| \cos\alpha = T_1\left|\vec{V}_1\right|\cos(0) + T_2\left|\vec{V}_2\right|\cos(\pi/3) \tag{6}$$

$$T_S\left|\vec{V}_{ref}\right| \sin\alpha = T_1\left|\vec{V}_1\right|\sin(0) + T_2\left|\vec{V}_2\right|\sin(\pi/3) \tag{7}$$

The sample interval equations are obtained by solving for T_2 using Equation (7), and then substituting the results in Equation (6).

$$T_1 = mT_s\frac{\sin\left(\frac{\pi}{3}-\alpha\right)}{\sin\left(\frac{\pi}{3}\right)} \tag{8}$$

$$T_2 = mT_s\frac{\sin\left(\alpha\right)}{\sin\left(\frac{\pi}{3}\right)} \tag{9}$$

$$T_0 = T_S - T_1 - T_2 \tag{10}$$

The modulation index, $m = \frac{V_{ref}}{V_{dc}}$, is represented as $0 \le \alpha \le 60°$, and T_S is the half-period for switching carriers. The following formulas represent the dwell periods for each sector:

$$T_1 = mT_S\sin\left(\frac{n\pi}{3}-\alpha\right) \tag{11}$$

$$T_2 = mT_s\sin\left(\alpha - \frac{\pi(n-1)}{3}\right) \tag{12}$$

Figure 4 shows the SVPWM output switching sequence in the first sector.

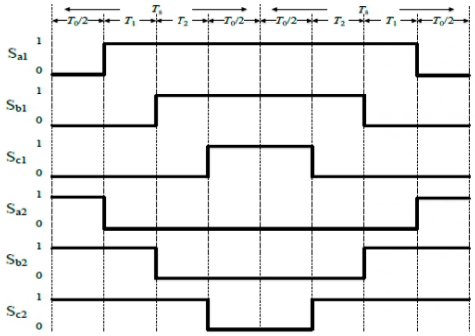


Figure 4. Output switching sequence at the first sector.

The switching periods for the upper and lower switches for each sector are summarized in Table 2 [13].

Table 2. Switching time calculation for every sector.

Sectors	**Upper Switches (S_1,S_3,S_5)**	**Lower Switches (S_4, S_6,S_2)**
Sector 1	$S_1 = T_1 + T_2 + T_0/2$ $S_3 = T_2 + T_0/2$ $S_5 = T_0/2$	$S_4 = T_0/2$ $S_6 = T_1 + T_0/2$ $S_2 = T_1 + T_2 + T_0/2$
Sector 2	$S_1 = T_1 + T_0/2$ $S_3 = T_1 + T_2 + T_0/2$ $S_5 = T_0/2$	$S_4 = T_2 + T_0/2$ $S_6 = T_0/2$ $S_2 = T_1 + T_2 + T_0/2$

Table 2. *Cont.*

Sectors	Upper Switches (S_1,S_3,S_5)	Lower Switches (S_4, S_6,S_2)
Sector 3	$S_1 = T_0/2$ $S_3 = T_1 + T_2 + T_0/2$ $S_5 = T_2 + T_0/2$	$S_4 = T_1 + T_2 + T_0/2$ $S_6 = T_0/2$ $S_2 = T_1 + T_0/2$
Sector 4	$S_1 = T_0/2$ $S_3 = T_1 + T_0/2$ $S_5 = T_1 + T_2 + T_0/2$	$S_4 = T_1 + T_2 + T_0/2$ $S_6 = T_2 + T_0/2$ $S_2 = T_0/2$
Sector 5	$S_1 = T_2 + T_0/2$ $S_3 = T_0/2$ $S_5 = T_1 + T_2 + T_0/2$	$S_4 = T_1 + T_0/2$ $S_6 = T_1 + T_2 + T_0/2$ $S_2 = T_0/2$
Sector 6	$S_1 = T_1 + T_2 + T_0/2$ $S_3 = T_0/2$ $S_5 = T_1 + T_0/2$	$S_4 = T_0/2$ $S_6 = T_1 + T_2 + T_0/2$ $S_2 = T_2 + T_0/2$

2.2. Direct Quadrature Zero Synchronous Reference Frame Methodology

The Direct Quadrature Zero (DQZ) synchronous reference frame methodology is a control technique widely used in power electronics, particularly in VSIs, to achieve the precise and efficient control of three-phase AC systems [14]. This methodology is widely applied in grid-connected renewable energy systems (such as wind and solar inverters), adjustable speed drives for motors, active power filters for harmonic mitigation, and other applications requiring the precise control of the AC voltage and the current waveform [15]. The DQZ synchronous reference frame methodology involves transforming the three-phase AC signals (typically voltages or currents) into a rotating reference frame aligned with the AC frequency of the system. This transformation simplifies the control of the VSIs by decoupling the components of interest (such as active power, reactive power, and harmonic components) from each other.

The three-phase AC signals are transformed from the time domain (a, b, c reference frame) to the rotating DQZ reference frame using Clarke and Park transformations [16]. Park transformation rotates the $\alpha\beta$ components to a stationary DQZ reference frame (d, q, 0), where d and q components represent the direct and quadrature components of the signals, respectively, and 0 represents the zero sequence component [17]. Clarke transformation converts three-phase quantities (a, b, c) into two-phase quantities (α, β), representing the symmetrical components of the AC signals. In the DQZ reference frame, control strategies such as proportional integral (PI) controllers or more advanced algorithms are applied to regulate the d and q components of the reference signals. These controllers adjust the switching patterns of the VSI's semiconductor devices typically insulated gate bipolar transistors (IGBTs) to generate the desired AC output voltage waveform, ensuring the precise control of the voltage magnitude, frequency, and waveform quality [18]. Figure 5 shows a space phasor with the $\alpha\beta0$ reference frame.

The revised three-phase current values (i_a, i_b, i_c) are shown in Figure 5 as projections onto the new reference axis (i_α, i_β). When a three-phase, three-wire system is balanced and the zero axis represents the common mode component, the total phase current is nullified. Thus, the variables α and β can fully characterize a system defined in the ABC reference frame.

The output variables ABC are described in Equation (13) below:

$$i_a = I_M\cos(\omega t);\ i_b = I_M\cos\left(\omega t - \frac{2\pi}{3}\right);\ i_c = I_M\cos\left(\omega t + \frac{2\pi}{3}\right) \tag{13}$$

where t is the amount of time needed to reach steady state and ω is the constant synchronous frequency. Equation (14) expresses the $\alpha\beta0$ transformation in complex form, while Equation (15) expresses it in matrix form.

$$\vec{I_s} = i_\alpha + ji_\beta = \frac{2}{3}\left(i_a + i_b e^{\frac{j2\pi}{3}} + i_c e^{\frac{-j2\pi}{3}}\right) \tag{14}$$

$$\begin{bmatrix} i_\alpha \\ i_\beta \\ i_0 \end{bmatrix} = \frac{2}{3}\begin{bmatrix} 1 & \frac{-1}{2} & \frac{-1}{2} \\ 0 & \frac{\sqrt{3}}{2} & \frac{-\sqrt{3}}{2} \\ \frac{1}{2} & \frac{1}{2} & \frac{1}{2} \end{bmatrix}\begin{bmatrix} i_a \\ i_b \\ i_c \end{bmatrix} \tag{15}$$

The reference axis currents are i_α, i_β, and i_0, while the three-phase currents are i_a, i_b, and i_c.

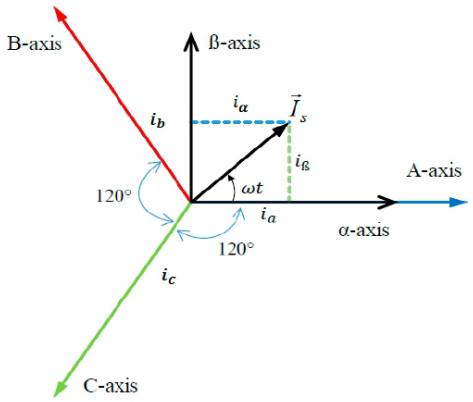


Figure 5. Space phasor and $\alpha\beta 0$ reference frame.

Using Park transformation with a $-90°$ shift, the frame rotates around the 0 axis at the same frequency as the sinusoids defining the phasors, while the system is in the $\alpha\beta 0$ frame. As it can be seen in Figure 6, the component is transformed to Q axis, which is positioned $90°$ at a quadrature angle to the direct component, and the $-\beta$ component is transformed to the d-axis, which is in line with the rotating vector.

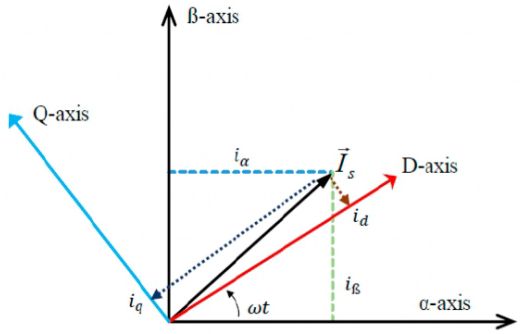


Figure 6. Space phasor and DQ0 reference frame.

Equations (16) and (17) express the DQ0 transformation in complex and matrix representations, respectively.

$$\vec{I}_s = i_d + ji_q = (i_\alpha + ji_\beta)e^{-j(\omega t - \frac{\pi}{2})} \tag{16}$$

$$\begin{bmatrix} i_d \\ i_q \\ i_0 \end{bmatrix} = \begin{bmatrix} \sin(\omega t) & -\cos(\omega t) & 0 \\ \cos(\omega t) & \sin(\omega t) & 0 \\ 0 & 0 & 1 \end{bmatrix} \begin{bmatrix} i_\alpha \\ i_\beta \\ i_0 \end{bmatrix} \tag{17}$$

Consequently, the rotation generates DC values from the periodic signals. Since the spinning frame trails the a-axis by 90 degrees, at $t = 0$, the Q- and A-axes coincide. When I_s is precisely aligned with the reference angle ωt, $i_d = 1$, $i_q = 0$, and $i_0 = 0$ are the DQ0 components. The full transformations from DQ0 to ABC and their corresponding inverses are presented as follow:

$$\begin{bmatrix} i_d \\ i_q \\ i_0 \end{bmatrix} = \begin{bmatrix} \sin(\omega t) & \sin(\omega t - \frac{2\pi}{3}) & \sin(\omega t + \frac{2\pi}{3}) \\ \cos(\omega t) & \cos(\omega t - \frac{2\pi}{3}) & \cos(\omega t + \frac{2\pi}{3}) \\ \frac{1}{2} & \frac{1}{2} & \frac{1}{2} \end{bmatrix} \begin{bmatrix} i_a \\ i_b \\ i_c \end{bmatrix} \tag{18}$$

$$\begin{bmatrix} i_a \\ i_b \\ i_c \end{bmatrix} = \begin{bmatrix} \sin(\omega t) & \cos(\omega t) & 1 \\ \sin(\omega t - \frac{2\pi}{3}) & \cos(\omega t - \frac{2\pi}{3}) & 1 \\ \sin(\omega t + \frac{2\pi}{3}) & \cos(\omega t + \frac{2\pi}{3}) & 1 \end{bmatrix} \begin{bmatrix} i_d \\ i_q \\ i_0 \end{bmatrix} \tag{19}$$

3. Design of the Control Loop for the Current in the S-Domain

The current control loop design in the S-domain for a three-phase two-level VSI is a crucial aspect of ensuring the precise and stable operation of the inverter. This design methodology leverages the classical control theory in the S-domain to achieve the effective regulation of the output currents of the inverter. According to Wencong et al., this control loop modifies the output voltage of the inverter to allow the injection of the necessary current in the utility grid [19]. The three-phase VSI is typically modeled using a set of differential equations that describe the relationship between the input DC voltage, the switching states of the inverter, and the output AC currents. These equations are transformed into the synchronous reference frame (dq-frame) to decouple the three-phase AC currents into two orthogonal components (d-axis and q-axis), simplifying the control design. The system dynamics are represented by transfer functions in the S-domain, which relate the control inputs (reference voltages) to the outputs (actual currents). For a VSI, the transfer function typically includes the LC filter dynamics of the inverter and the influence of the load impedance. Figure 7 illustrates the schematic representation of a three-phase, two-level VSC with an L filter. R_f and L_f represent the resistance and the inductance, respectively, between the converter switches and the PCC.

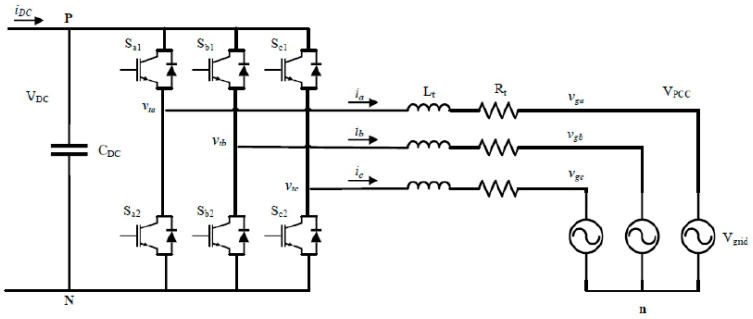


Figure 7. A two-level VSC circuit diagram with an L filter included.

A reduced equivalent per-phase circuit can be produced by applying the voltage law of Kirchhoff to the circuit shown above, as illustrated in Figure 8.

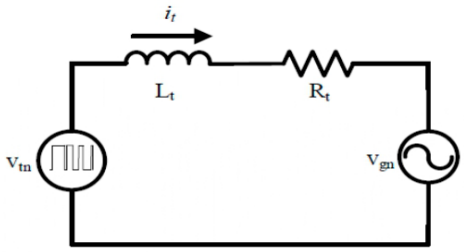


Figure 8. An L filter in a simplified VSC per-phase circuit.

The grid voltage, v_{gn}, is shown in Figure 8 as a relatively fixed component that may be considered disruptive. As a result, the current, i_{tn}, can be regulated by altering the output voltage of the inverter v_{tn}. Consequently, the VSC functions as an energy source that feeds electricity into the grid. The voltage law of Kirchhoff, when applied to the three circuits per phase, yields the following:

$$\begin{aligned} v_{tan} &= L_f \tfrac{di_a}{dt} + R_f i_a + v_{gan} \\ v_{tbn} &= L_f \tfrac{di_b}{dt} + R_f i_b + v_{gbn} \\ v_{tcn} &= L_f \tfrac{di_c}{dt} + R_f i_c + v_{gcn} \end{aligned} \tag{20}$$

The variables v_{tan}, v_{tbn}, and v_{tcn} represent the three per-phase inverter output voltages; L_f and R_f denote the inductance and resistance between the converter switches and the point of common coupling (PCC); v_{gan}, v_{gbn}, and v_{gcn} stand for the three per-phase grid voltages; and i_a, i_b, and i_c represent the three per-phase inverter currents. By consolidating all three equations from (20) into a single equation, we obtain the following:

$$v_{t,abc} = L_f \frac{di_{abc}}{dt} + R_f i_{abc} + v_{g,abc} \tag{21}$$

Equation (15) is used to translate Equation (21) into the reference frame $\alpha\beta 0$, which results in

$$v_{t,\alpha\beta} = L_f \frac{di_{\alpha\beta}}{dt} + R_f i_{\alpha\beta} + v_{g,\alpha\beta} \tag{22}$$

Using the reference frame $dq0$ in (16) and repeating the process for Equation (22), the result is

$$\begin{aligned} v_{t,dq} &= v_{t,\alpha\beta} e^{-j(\omega t - \frac{\pi}{2})} \\ v_{t,dq} L_f \tfrac{di_{dq}}{dt} &+ R_f i_{dq} + v_{g,dq} \end{aligned} \tag{23}$$

The a, b, c frame can be split into the two components, d and q, as was indicated in Section 2.1.

$$L_f \frac{di_d}{dt} = v_{td} + L_f \omega i_q - R_f i_d - v_{gd} \tag{24}$$

$$L_f \frac{di_q}{dt} = v_{tq} + L_f \omega i_q - R_f i_q - v_{gq} \tag{25}$$

with $v_{td} = \frac{V_{DC}}{\sqrt{3}} m_d$ and $v_{tq} = \frac{V_{DC}}{\sqrt{3}} m_q$, where m_{dq} is the index of modulation, and $\frac{V_{DC}}{\sqrt{3}}$ is the SVPWM gain converter.

The i_d and i_q dynamics are related because of the $L_f\omega$ term found in Equations (24) and (25). To decouple the d and q subsystems and account for the grid disruption inputs v_{gd} and v_{gq}, the index of modulation for each must be stated as follows:

$$m_d = \frac{\sqrt{3}}{V_{DC}} \left(u_d - L_f \omega i_q + v_{gd} \right) \tag{26}$$

$$m_q = \frac{\sqrt{3}}{V_{DC}}\left(u_q - L_f\omega i_d + v_{gq}\right) \tag{27}$$

For the d subsystem, the anticipatory term is $-L_f\omega i_q + v_{gd}$, while for the q subsystem, it is $-L_f\omega i_d + v_{gq}$. Equation (26) can be substituted into (24), yielding

$$L_f\frac{di_d}{dt} = u_d - R_f i_d \tag{28}$$

Equation (27) can be substituted into (25) in the same way to obtain

$$L_f\frac{di_q}{dt} = u_q - R_f i_q \tag{29}$$

with u_q as the output of PI compensator.

The control systems of the current control loops are the same in the d and q axes, as seen in (28) and (29). Therefore, the linked compensators can be the same. As a result, only the current control compensator gains in the d-axis will be determined. When Equation (29) is transformed using the Laplace method, the following results are obtained:

$$\begin{gathered} L_f s I_d(s) = u_d(s) - R_f I_d(s) \\ I_d(s) = \frac{u_d(s)}{L_f + R_f} \end{gathered} \tag{30}$$

The control plant can therefore be expressed as follows:

$$G_P(s) = \frac{1}{L_f s + R_f} \tag{31}$$

The following Equation (32) indicates that the compensator is a PI controller:

$$G_c(s) = \frac{k_p s + k_i}{s} \tag{32}$$

Figure 9 illustrates the transfer function of the closed loop in the d-axis:

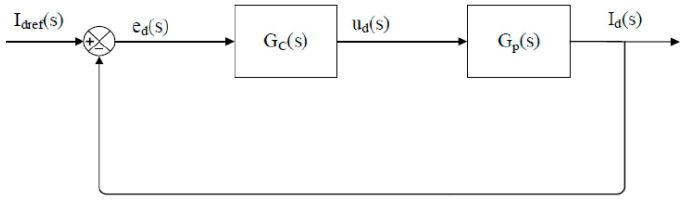


Figure 9. Current-controlled VSC system block diagram in simplified form.

Equation (33) gives the following open loop gain:

$$G_{ol}(s) = G_C(s)G_P(s) \tag{33}$$

By replacing the compensator and control plant Equations by their terms, Equation (33), will be:

$$G_{ol}(s) = \frac{k_p s + k_i}{s} \times \frac{1}{L_f s + R_f} = \frac{k_p s + k_i}{L_f s^2 + R_f s} = \left(\frac{k_p}{L_f s}\right)\frac{s + \frac{k_i}{k_p}}{s + \frac{R_f}{L_f}} \tag{34}$$

Once the terms $\frac{k_i}{k_p} = \frac{R_f}{L_f}$ are equalized by applying the pole cancelation approach, the open-loop gain Equation (34) is reduced from the second to the first order transfer function as follows:

$$G_{ol}(s) = \frac{k_p}{L_f s} \tag{35}$$

Equation (36) represents the current control gain in the closed loop in the d-axis:

$$G_i(s) = G_{cl}(s) = \frac{G_{ol}(s)}{1 + G_{ol}(s)} \tag{36}$$

Equation (35) can be substituted into (36) to obtain the following expression for the closed-look gain:

$$\frac{I_d(s)}{I_{dref}(s)} = G_i(s) = \frac{k_p}{k_p + L_f s} \tag{37}$$

By replacing $k_p = \frac{L_f}{\tau_i}$ and $k_i = \frac{R_f}{\tau_i}$, the closed-look gain will become

$$G_i(s) = \frac{1}{\tau_i s + 1} \tag{38}$$

The resultant closed-loop control constant time is written as τ_i. Therefore, the following formula provides the first-order settling time in the closed-loop system:

$$t_{i,\ settling} = 4.6\tau_i \tag{39}$$

4. Design of the Control Loop for the DC Bus Voltage in the S-Domain

For maintaining balanced power flow, the DC bus voltage control technique is essential. Implementing this control is imperative as it enables the voltage source converter to function as a rectifier, converting AC power to DC power and facilitating control of the DC link capacitor voltage to supply an output load. Moreover, for intermittent DC power sources such as PV systems, this control technique assists in adjusting the current control loop reference to regulate the input of DC power effectively [20]. The circuit from Figure 7 is shown in Figure 10, with a bleeding resistor R_B and extra feedback signals (i_{DC} and i_L) added to simplify DC control modeling.

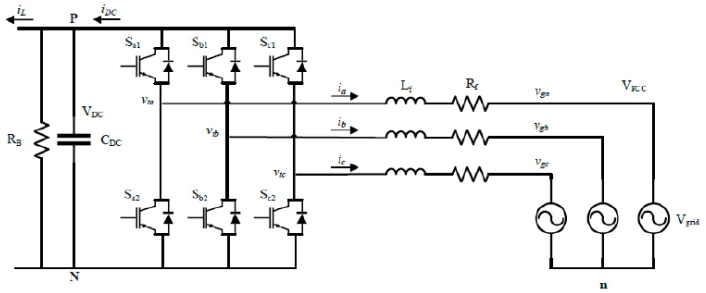


Figure 10. Two-level VSC with an L filter and a DC link circuit bleed resistor.

The resistance and inductance between the PCC and the inverter output are R_f and L_f. The fact that the active power transfer enables to charge and discharge the DC link capacitor, the circuit shown in the DQ synchronous reference frame configuration can only be modeled for the d-axis component. As a result, an instantaneous reactive current is not needed, neither the q-axis component for this procedure, as Figure 11 shows.

The following equations illustrate the voltage dynamic equation of the DC link capacitor:

$$\begin{aligned} i_{DC} &= i_{bus} + i_{RB} + i_L \\ i_{bus} &= i_{DC} - i_{RB} - i_L \\ C_{DC}\frac{dv_{DC}}{dt} &= i_{DC} - \frac{v_{DC}}{R_B} - i_L \end{aligned} \tag{40}$$

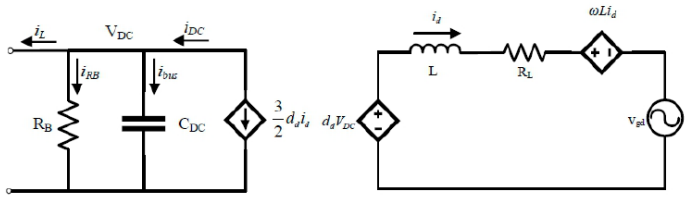


Figure 11. VSC d-axis component configuration with a bleed resistor and a L filter.

Equation (40) can be transformed using the Laplace transform to obtain

$$\begin{gathered}\left[sC_{DC}+\frac{1}{R_B}\right]V_{DC}(s)=I_{DC}(S)-I_L(s)\\ V_{DC}(s)=\frac{1}{\left[sC_{DC}+\frac{1}{R_B}\right]}u_d(s)=\frac{R_B}{sC_{DC}R_B+1}u_d(s)\end{gathered} \tag{41}$$

The formula for calculating the PI compensator output, $u_d(s)$, is $u_d(s) = I_{DC}(s) - I_L(s)$, where $I_L(s)$ is the feedback term. This allows for the controller to avoid making up a measured value. Considering this, the control system is written as follows:

$$G_P=\frac{R_B}{sC_{DC}R_B+1} \tag{42}$$

The relationship between these currents is represented as follows, assuming a converter without losses and the fact that the i_{DC} can only be directly controlled by the current pulled from the grid:

$$P_{3\varnothing}=P_{DC} \tag{43}$$

The active power is given as

$$P_{3\varnothing}=\frac{3}{2}\left(v_{gd}i_d+v_{gq}i_q\right) \tag{44}$$

The DC bus power is obtained by replacing Equation (44) with (43), which yields the following:

$$\frac{3}{2}v_{gd}i_d=-i_{DC}V_{DC} \tag{45}$$

The following Equation describes the relationship between the time constant τ_{DC} of the control loop for the DC bus voltage and the time constant τ_i of the current control loop:

$$\tau_i \ll \tau_{DC} \tag{46}$$

The relationship between these two control loops may be expressed by the following Equation (47) if the condition in Equation (46) is satisfied, $i_d = I_{dref}$, and the two control loops are decoupled.

$$I_{dref}=-\frac{2}{3}\frac{V_{DC}}{v_{gd}}I_{DC} \tag{47}$$

The inner gain coefficient is obtained from the relationship between I_{dref} and I_{DC} and is stated as follows:

$$K_{inner}=\frac{I_{DC}}{I_{dref}}=-\frac{3}{2}\frac{v_{gd}}{V_{DC}} \tag{48}$$

Based on the following, it is presumed that the compensator is a PI controller expressed as

$$G_C(s)=\frac{k_p s+k_i}{s} \tag{49}$$

The selected method for DC voltage control adopts a cascade approach, including an outer loop for the voltage control of the DC bus and an inner loop for the current control. This tactic guarantees that the time reaction of current controller is faster than that for

the controller of the DC voltage in accordance with Equation (46). The DC voltage loop considers the current loop as a constant gain, which permits a gradual shift in the current reference, and hence an error-free response from the current controller. Consequently, the dynamics of the two circuits depicted in Figure 11 are effectively disconnected. Figure 12 shows a DC link voltage loop block diagram of a VSC system in a simplified form.

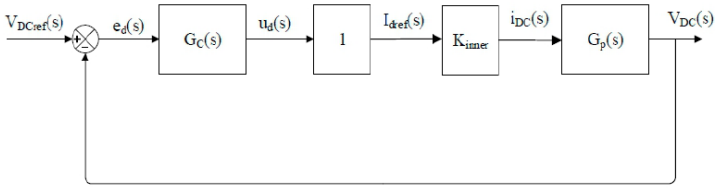


Figure 12. Simplified DC link voltage loop model of the VSC system.

Equation (50) provides the gain in the open loop based on Figure 12.

$$G_{ol}(s) = G_C(S)G_P(S)K_{inner} \tag{50}$$

Equations (42) and (49) can be substituted into (50) to obtain the following:

$$G_{ol}(s) = \frac{k_p s + k_i}{s} \times \frac{R_B}{sC_{DC}R_B + 1} \times K_{inner} = \frac{K_{inner}R_B\left(k_p s + k_i\right)}{s^2 C_{DC}R_B + s} \tag{51}$$

With respect to the current control in d-axis, the closed loop gain is expressed in Equation (52):

$$G_{DC}(S) = G_{cl}(s) = \frac{G_{ol}(s)}{1 + G_{ol}(s)} \tag{52}$$

Equation (51) substituted into (52) will result in

$$G_{DC}(s) = \frac{K_{inner}\left(k_p s + k_i\right)/C_{DC}}{S^2 + \left(\frac{K_{inner}R_B k_p + 1}{C_{DC}R_B}\right)s + \frac{K_{inner}k_i}{C_{DC}}} \tag{53}$$

Seeing that the Equation (53) has a first-order numerator, a pre-filter will be established to eliminate this term, enabling the alignment of (53) with the standard second-order transfer function, which is:

$$G_{PF}(s) = \frac{G_{DC,\,desired}(s)}{G_{DC,old}(s)} = \frac{k_i}{\left(k_p s + k_i\right)} \tag{54}$$

The gain in closed loop of the current control in d-axis can be obtained by multiplying Equations (53) and (54). The result is as follows:

$$G_{DC}(s) = \frac{\frac{K_{inner}k_i}{C_{DC}}}{s^2 + \left(\frac{K_{inner}R_B k_p + 1}{C_{DC}R_B}\right)S + \frac{K_{inner}k_i}{C_{DC}}} \tag{55}$$

The gain in closed loop of the current control in d-axis can be obtained by multiplying Equations (53) and (54). The result is as follows:

$$k_p = \frac{2\xi\omega_n C_{DC}R_B - 1}{K_{inner}R_B} \tag{56}$$

$$k_i = \frac{{\omega_n}^2 C_{DC}}{K_{inner}} \tag{57}$$

Thus, the following is the second closed-loop system settling time:

$$\begin{aligned} \tau_{DC} &= \frac{1}{\xi\omega_n} \\ t_{DC,setting} &= 4.6 \times \tau_{DC} \end{aligned} \tag{58}$$

5. Design of the Control Loop for the AC Voltage in the S-Domain

When a fault or power outage prevents the main grid from supplying power, a VSC system in grid-forming mode creates a grid reference and makes it easier to transfer active or reactive powers during micro-grid operation in isolated mode. This enables the micro-grid to continue operating [21]. The three-phase VSI is modeled using differential equations that describe the relationship between the input DC voltage, the switching states of the inverter, and the output AC voltages. The dynamics of the VSI system, including the LC filter (which is typically used to smooth the inverter output), as presented in Figure 13, are represented in the S-domain by transfer functions [22].

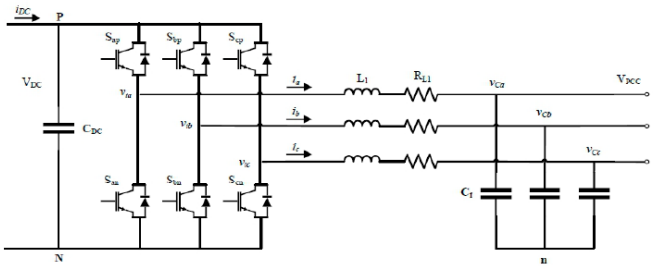


Figure 13. Two level VSC with an LC filter.

The resistances between the converter and the filter capacitor are presented as R_{L1} and L_1. A condensed per-phase equivalent circuit produced by using the voltage law of Kirchhoff is shown in Figure 14.

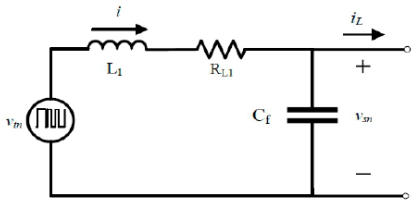


Figure 14. A VSC with an LC filter per-phase circuit in a simplified.

The phase currents for each of the three per-phase circuits can be obtained by using the current law of Kirchhoff as follows:

$$\begin{aligned} i_a &= i_{Cfa} + i_{La} \\ i_b &= i_{Cfb} + i_{Lb} \\ i_c &= i_{Cfc} + i_{Lc} \end{aligned} \tag{59}$$

Combining the three equations from (59) results in the following:

$$i_{abc} = i_{Cf,abc} + i_{L,abc} \tag{60}$$

Using the ABC-$\alpha\beta$0 transform on Equation (60), the following result is obtained:

$$i_{Cf,\alpha\beta} = i_{\alpha\beta} + i_{L,\alpha\beta} \tag{61}$$

Using Equation (16), the $\alpha\beta$0-dq0 transform can be converted to

$$i_{Cf,\,dq} = i_{Cf,\alpha\beta} e^{-j(\omega t - \frac{\pi}{2})} \tag{62}$$

$$i_{C,dq} = i_{dq} - i_{L,dq} \tag{63}$$

Consequently, as described in Section 2.1, the a, b, c frame reference may be divided into d and q components and cascaded via the current control loops in d and q axes, resulting in

$$C_f \frac{dv_{sd}}{dt} = C_f \omega v_{sq} + i_d - i_{Ld} \tag{64}$$

$$C_f \frac{dv_{sq}}{dt} = -C_f \omega v_{sd} + i_q - i_{Lq} \tag{65}$$

The existence of the $C_f\omega$ terms in Equations (64) and (65) causes the v_{sd} and v_{sq} dynamics to be coupled. The feedforward terms $\left(-C_f \omega v_{sq} + i_{Ld}\right)$ for the d-axis component and $\left(C_f \omega v_{sd} + i_{Lq}\right)$ for the q-axis component are introduced in order to decouple them and account for the load disturbance inputs i_{Ld} and i_{Lq}. Furthermore, the control units of the d-axis and q-axis components are the same, as shown in Equations (64) and (65); thus,

$$\frac{dV_{sd}}{dt} = \frac{1}{C_f}[u_d] \tag{66}$$

u_d is the PI compensator output. Equation (66) is solved by applying the Laplace transform, which yields the following:

$$V_{sd}(s) = \frac{u_d(s)}{sC_f} \tag{67}$$

As a result, the following is the control plant:

$$G_P(s) = \frac{1}{sC_f} \tag{68}$$

Furthermore, it is presumed that the control loop time constant of the AC voltage, τ_v, will be five times greater than that of the current control loop, τ_i. If this assumption is met, the two control loops will be decoupled. The circumstance is as follows:

$$\tau_i \ll \tau_v \tag{69}$$

Therefore, the inputs of the current control loops are presented in Equations (70) and (71), and $I_{dq}(s) = I_{dqref}(s)$ for the control loop of AC voltage.

$$I_{dref}(s) = u_d(s) - C_f \omega V_{sq}(s) + I_{Ld}(s) \tag{70}$$

$$I_{qref}(s) = u_q(s) + C_f \omega V_{sd}(s) + I_{Lq}(s) \tag{71}$$

Equation (72) gives the PI controller gain.

$$G_C(s) = \frac{k_p s + k_i}{s} \tag{72}$$

Since the control plants of Equation (68) for the d and q components are the same, the corresponding compensators may also be the same. With reference to Figure 15, the only information that needs to be collected next is the gains of the voltage control compensators in d-axis. The following is the open loop gain:

$$G_{ol}(s) = G_C(s) G_P(s) \tag{73}$$

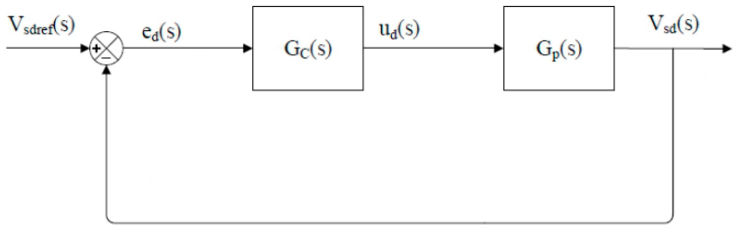


Figure 15. A block diagram for the VSC system AC voltage loop in a simplified form.

$G_C(s)$ and $G_P(s)$ can be substituted with their corresponding values to obtain the following result:

$$G_{ol}(s) = \frac{k_p s + k_i}{s} \times \frac{1}{sC_f} = \frac{k_p s + k_i}{s^2 C_f} \tag{74}$$

The gain of the current control in *d*-axis in closed loop can be represented as follows:

$$G_v(s) = G_{cl}(s) = \frac{G_{ol}(s)}{1 + G_{ol}(s)} \tag{75}$$

When Equation (74) is substituted into (75), this results in

$$G_v(s) = \frac{\frac{(k_p s + k_i)}{C_f}}{s^2 + \left(\frac{k_p}{C_f}\right)s + \frac{k_i}{C_f}} \tag{76}$$

The VSC system AC voltage loop block diagram in a simplified form is shown in Figure 15.

Given that the first-order numerator of Equation (76) must be cancelled, a pre-filter needs to be developed in order to allow for Equation (76) to correspond to the conventional transfer function of the second order. As stated below, a pre-filter is required.

$$G_{PF}(s) = \frac{G_{DC,\,desired}(s)}{G_{DC,\,old}(s)} = \frac{k_i}{k_p s + k_i} \tag{77}$$

The following is the result of multiplying Equations (76) and (77):

$$G_v(s) = \frac{k_i}{s^2 C_f + k_p s + k_i} \tag{78}$$

By resolving the results of the denominator coefficients of Equation (78), the gains of the proportional and integral controllers are solved for

$$k_p = 2\xi\omega_n C_f \tag{79}$$

$$k_i = {\omega_n}^2 C_f \tag{80}$$

As a result, the control loop time constant of the AC voltage is provided as

$$\tau_v = \frac{1}{\xi\omega_n} \tag{81}$$

To decouple the two control loops, the system settling time for this second order in the closed loop is considered to be five times longer than the existing control loop settling time. In other words,

$$t_{v,settling} = \frac{4.6}{\zeta\omega_n} = 4.6 \times 5 \times \tau_i = 5 \times t_{i,settling} \quad (82)$$

6. Discussion

This Discussion section explores the key aspects of the basic circuit model of VSCs. The different methodologies and control strategies employed in VSCs, including the SVPWM methodology, the DQZ synchronous reference frame methodology, the design of the current, the DC bus voltage, and the AC voltage control loops in the S-domain, are presented in Table 3.

Table 3. Summary of the basic circuit model of voltage source converters.

SVPWM methodology	SVPWM is a widely used technique for controlling VSCs because it can produce excellent output waveforms with less harmonic distortion. By effectively synthesizing the desired output voltage vector, SVPWM enables the precise control of the VSC output. However, challenges, such as computational complexity and switching frequency constraints, need to be carefully addressed to ensure an optimal performance.
DQZ synchronous reference frame methodology	The DQ0 synchronous reference frame methodology provides a powerful tool for analyzing and controlling VSCs, particularly in grid-connected applications. By transforming the three-phase system into a two-dimensional space with direct (d) and quadrature (q) axes, this methodology simplifies the control and modeling processes. It allows for the accurate representation of the system dynamics and facilitates the design of control algorithms, enhancing the overall performance and stability of VSC-based systems.
Design of the control loop for the current in the S-domain	Effective current control is crucial for ensuring accurate and dynamic response in VSCs, especially in applications requiring the precise regulation of current flow. By designing current control loops in the S-domain, engineers can leverage advanced control techniques to achieve desired performance objectives, such as fast response, low overshoot, and robust stability. Implementing sophisticated control algorithms, such as proportional integral controllers or model predictive control (MPC), can further improve the current control loops efficiency in VSCs.
Design of the control loop for the DC Bus voltage in the S-domain	The control loop for DC bus voltage plays a critical role in maintaining stable operation and ensuring reliable performance of VSCs. By regulating the DC bus voltage, this control loop enables efficient energy conversion and smooth power transfer between the VSC and the grid or load. Designing the DC bus voltage control loop in the S-domain allows for the precise tuning of controller parameters and dynamic response characteristics, ensuring optimal performance under varying operating conditions and load profiles.
Design of the control loop for the AC voltage in the S-domain	In grid-connected VSC applications, the control loop for the AC voltage is essential for regulating the output voltage to meet grid requirements, such as voltage magnitude and frequency. By designing the control loop for the AC voltage in the S-domain, engineers can develop robust control strategies to maintain grid stability, mitigate voltage harmonics, and ensure the seamless integration of renewable energy sources. Advanced control techniques, such as predictive control and adaptive control, can be employed to enhance the AC voltage control loop efficiency and flexibility in VSCs.

7. Conclusions

The basic VSC circuit model with an output LC filter has been presented in this paper. The main power interface between distributed generators and the micro-grid is the AC-DC converter. Two forms of operation for a voltage source converter have been observed. It acts as an active rectifier when utilized as a DC bus control. It uses a variety of control loops to operate as an inverter when in the grid-feeding and grid-forming modes. A thorough manual that covers a variety of techniques has also been introduced, including the SVPWM, the DQZ synchronous frame, and the phase lock loop. In addition, this paper serves as a comprehensive guide to understanding the basic circuit model of VSCs, methodologies for their control, and techniques for their accurate modeling. By providing insights into the fundamental principles and practical considerations associated with VSCs, this paper aims to contribute to the advancement of VSC-based power electronics applications and their integration into modern power systems for enhanced efficiency,

reliability, and sustainability. Case studies and simulations need to be conducted to illustrate the efficacy and accuracy of the presented methodologies and control strategies in analyzing VSC-based power electronics applications.

Author Contributions: Conceptualization; methodology; formal analysis; writing—original draft preparation, C.B.N.; writing—review and editing; supervision.; project administration, M.A. and A.A. All authors have read and agreed to the published version of the manuscript.

Funding: This research was funded by the National Research Foundation (NRF) grant number PMDS22052313773 And The APC was funded by Cape Peninsula University of Technology.

Institutional Review Board Statement: This research does not involve human or animal subjects; hence, participant consent was not necessary in order to collect data for this project.

Data Availability Statement: Requests for access to the datasets can be made to the corresponding author.

Acknowledgments: As the Corresponding Author, I acknowledge that this paper has been completed as part of doctoral study research under the supervision and support of Marco Adonis, and Ali Almaktoof provided direction, editing, and reviewed the manuscript before publication.

Conflicts of Interest: There are no disclosed conflicts of interest pertaining to this publication.

References

1. Jing, T.; Maklakov, A.S. A Review of Voltage Source Converters for Energy Applications. In Proceedings of the 2018 International Ural Conference on Green Energy (UralCon), Chelyabinsk, Russian Federation, 4–6 October 2018; pp. 275–281.
2. Brodzicki, M.; Klucznik, J.; Czapp, S. Evaluation of VSC Impact on Power System Using Adequate P-Q Capability Curve. *Electronics* **2023**, *12*, 2462. [CrossRef]
3. Ndeke, C.B.; Adonis, M.; Almaktoof, A. Energy management strategy for a hybrid micro-grid system using renewable energy. *Discov. Energy* **2024**, *4*, 1. [CrossRef]
4. Monteiro, V.; Monteiro, L.F.; Franco, F.L.; Mandrioli, R.; Ricco, M.; Grandi, G.; Afonso, J.L. The role of front-end ac/dc converters in hybrid ac/dc smart homes: Analysis and experimental validation. *Electronics* **2021**, *10*, 2601. [CrossRef]
5. Xiong, L.; Liu, X.; Liu, Y.; Zhuo, F. Modeling and Stability Issues of Voltage-source Converter-dominated Power Systems: A Review. *CSEE J. Power Energy Syst.* **2022**, *8*, 1530–1549.
6. Almaktoof, A.M.A. Multilevel Inverters Using Finite Set-Model Predictive Current Control for Renewable Energy Systems Applications. Ph.D. Thesis, Cape Peninsula University, Cape, South Africa, March 2015.
7. Gaballah, M.; El-Bardini, M. Low cost digital signal generation for driving space vector PWM inverter. *Ain Shams Eng. J.* **2013**, *4*, 763–774. [CrossRef]
8. Jeong, M.; Gfrörer, T.; Biela, J. Extending Stable Parameter Range of LCL-filters for Grid-Connected Converters by Inherent Damping of Model Predictive Control (MPC). In Proceedings of the 2022 IEEE 23rd Workshop on Control and Modeling for Power Electronics (COMPEL), Tel Aviv, Israel, 20–23 June 2022.
9. Bernet, D.; Hiller, M. Grid-connected medium-voltage converters with parallel voltage-source active filters. *IET Electr. Power Appl.* **2019**, *13*, 1507–1513. [CrossRef]
10. Kouchaki, A.; Nymand, M. Analytical Design of Passive LCL Filter for Three-Phase Two-Level Power Factor Correction Rectifiers. *IEEE Trans. Power Electron.* **2018**, *33*, 3012–3022. [CrossRef]
11. Kumar Peddapelli, S. 2. Space vector pulse width modulation technique. In *Pulse Width Modulation: Analysis and Performance in Multilevel Inverters*; De Gruyter Oldenbourg: Berlin, Germany; Boston, MA, USA, 2017; pp. 13–22. [CrossRef]
12. Lewicki, A.; Odeh, C.I.; Kondratenko, D.; Morawiec, M. Hybridized Space-Vector Pulsewidth Modulation for Multiphase Two-Level Voltage Source Inverter. *IEEE Trans. Power Electron.* **2022**, *37*, 7663–7674. [CrossRef]
13. Doan, N.S.; Tsvetkov, A.N.; Nguyen, T.H. Study and implementation of space vector pulse width modulation inverter on an Arduino. *E3S Web Conf.* **2021**, *288*, 4–9. [CrossRef]
14. Waqas, M.; Ahmed, T.; Elavarasan, R.M.; Waqar, A.; Leong, K.; Pugazhendhi, R.; Das, N.; Jeelani, M.W. DQ Transformation Based Control of Single-Phase Grid-Tied Inverter. In Proceedings of the 2021 31st Australasian Universities Power Engineering Conference (AUPEC), Virtual, 26–30 September 2021.
15. Venkatramanan, D.; Singh, M.K.; Ajala, O.; Dominguez-Garcia, A.; Dhople, S. Integrated System Models for Networks with Generators & Inverters. *arXiv* **2022**, arXiv:2203.08253.
16. Altahir, A.A.R. Park and Clark Transformations: A Short Review. April 2020, pp. 2–5. Available online: https://www.researchgate.net/profile/Ali-Altahir/publication/340681625_Park_and_Clark_Transformations_Park_and_Clark_Transformations_A_Short_Review/links/5e98bb8a4585150839e3768b/Park-and-Clark-Transformations-Park-and-Clark-Transformations-A-Short-Review.pdf (accessed on 27 May 2024).

17. Casado-Machado, F.; Martinez-Ramos, J.L.; Barragan-Villarejo, M.; Maza-Ortega, J.M.; Rosendo-Macias, J.A. Reduced Reference Frame Transform: Deconstructing Three-Phase Four-Wire Systems. *IEEE Access* **2020**, *8*, 143021–143032. [CrossRef]
18. O'Rourke, C.J.; Qasim, M.M.; Overlin, M.R.; Kirtley, J.L. A Geometric Interpretation of Reference Frames and Transformations: Dq0, Clarke, and Park. *IEEE Trans. Energy Convers.* **2019**, *34*, 2070–2083. [CrossRef]
19. Hollweg, G.V.; Khan, S.A.; Chaturvedi, S.; Fan, Y.; Wang, M.; Su, W. Grid-Connected Converters: A Brief Survey of Topologies, Output Filters, Current Control, and Weak Grids Operation. *Energies* **2023**, *16*, 3611. [CrossRef]
20. Ali, M.; Yaqoob, M.; Cao, L.; Loo, K.H. Enhancement of DC-bus voltage regulation in cascaded converter system by a new sensorless load current feedforward control scheme. *IET Power Electron.* **2021**, *14*, 1457–1467. [CrossRef]
21. Wu, H.; Wang, X. Control of Grid-Forming VSCs: A Perspective of Adaptive Fast/Slow Internal Voltage Source. *IEEE Trans. Power Electron.* **2023**, *38*, 10151–10169. [CrossRef]
22. Sadeque, F.; Fateh, F. On Control Schemes for Grid-Forming Inverters. In Proceedings of the 2022 IEEE Kansas Power and Energy Conference (KPEC), Manhattan, KS, USA, 25–26 April 2022.

Disclaimer/Publisher's Note: The statements, opinions and data contained in all publications are solely those of the individual author(s) and contributor(s) and not of MDPI and/or the editor(s). MDPI and/or the editor(s) disclaim responsibility for any injury to people or property resulting from any ideas, methods, instructions or products referred to in the content.

CHAPTER 4: ENERGY MANAGEMENT STRATEGY FOR DC MICROGRID SYSTEM

Article 2: Energy Management Strategy for DC Micro-Grid System with the Important Penetration of Renewable Energy

The objective of this article is to finally preserve the appropriate operation of the DC micro-grid system by concentrating on its energy management system (EMS) control. Various loads, including commercial, industrial, and residential loads, are taken into consideration when developing this DC micro-grid model. The Stateflow logical programming environment in MATLAB/Simulink software is utilized in the design and development of this EMS algorithm. The energy management system algorithm demonstrates its ability to guarantee the dependability, resilience, robustness, and correct functioning of the system based on all of the developed circumstances.

The results show that the energy management technique performs well in a variety of scenarios, successfully balancing energy generation and consumption while maintaining the dependability of the micro-grid system. The technique exhibits adaptability and resilience, ensuring stable operation and minimal disruptions despite fluctuations in renewable energy generation and load demand. Moreover, the robustness study emphasizes how adaptable the energy management plan is to uncertainties and changes in the micro-grid environment.

applied sciences

MDPI

Article

Energy Management Strategy for DC Micro-Grid System with the Important Penetration of Renewable Energy

Christian Bipongo Ndeke *, Marco Adonis and Ali Almaktoof

Department of Electrical, Electronic and Computer Engineering, Cape Peninsula University of Technology, Cape Town 7535, South Africa; adonisma@cput.ac.za (M.A.); almaktoofa@cput.ac.za (A.A.)
* Correspondence: ndekechristian@gmail.com; Tel.: +27-628362466

Abstract: This paper presents an energy management strategy using a Stateflow controller related to DC microgrids with the important penetration of renewable energy. The increase in world electricity demand is one of the principal drivers of the exhaustion of fossil fuels and increased greenhouse gas emissions. To solve these problems, several countries have adopted actions for widespread renewable energy deployment, which includes wind energy, solar power, biomass power, tidal, and hydropower. These sources are considered as significant in delivering clean energy and reducing greenhouse gas emissions for sustainable improvement. As these sources play an increasingly vital role in the global energy landscape, the efficient management of these intermittent sources is essential for grid stability and sustainability. This paper aimed to develop an energy management strategy for DC microgrids to supply power to a DC microgrid system. The main objective of this paper was to implement an energy management system to ensure the proper operation of DC microgrid systems utilizing Simulink blocks available in MATLAB/Simulink 2020b software. The simulation results demonstrated that the developed energy management algorithm was unconditionally reliable, ensuring the proper operation of the microgrid systems. Additionally, the results demonstrated that the energy management strategy exhibited robust performance across different scenarios, effectively balancing energy generation and consumption while ensuring the reliable operation of the microgrid system. Moreover, the developed algorithm model presents another advantage, as it enables users to access and to change any control parameters within the DC microgrid. By comparing these results with the literature, the developed energy management algorithm provides safety and the automatic control of the microgrid.

Keywords: energy management system; DC microgrid; renewable energy; distributed generation

check for updates

Citation: Ndeke, C.B.; Adonis, M.; Almaktoof, A. Energy Management Strategy for DC Micro-Grid System with the Important Penetration of Renewable Energy. *Appl. Sci.* **2024**, *14*, 2659. https://doi.org/10.3390/app14062659

Academic Editor: Subhas Mukhopadhyay

Received: 12 February 2024
Revised: 8 March 2024
Accepted: 18 March 2024
Published: 21 March 2024

Copyright: © 2024 by the authors. Licensee MDPI, Basel, Switzerland. This article is an open access article distributed under the terms and conditions of the Creative Commons Attribution (CC BY) license (https://creativecommons.org/licenses/by/4.0/).

1. Introduction

The augmentation of world electricity requirements is one of the principal drivers of the exhaustion of fossil fuels and expanded greenhouse gas emissions. To solve these problems, several countries have adopted actions for the widespread deployment of renewable energy sources, which include wind energy, solar power, biomass energy, and tidal and hydropower [1]. These sources are considered as significant in delivering clean energy and reducing greenhouse gas emissions for sustainable development [2]. Topić et al. reported that in 2016, a total of 921 GW was achieved from the deployment of renewable energy resources, excluding hydropower, which resulted in increased awareness of climate change. These renewable energy sources are often connected to the conventional power system through the distribution network near the loads; thus, no transmission system is needed. In such a case, these are referred to as distributed generation systems [3]. Distributed generation can negatively impact the performance of the distribution network as the distribution network will no longer operate with a unidirectional power flow pattern [4].

The issues related to a bidirectional power flow pattern are intensified by increasing the levels of the distributed generation systems in the distribution network. Some of the known

issues affect power quality and desensitized relays, cause increased fault currents, and the increased maintenance of the equipment utilized, and even affect a large portion of the distribution grid [5]. To address these issues, microgrids are used as platforms to integrate distributed generation systems, as they provide significant benefits to end-users and to the distribution network. A microgrid can minimize disruption, lower costs, and optimize the size of the system components, thereby reducing operation costs and ensuring access to affordable, reliable, and sustainable forms of energy [6]. Besides distributed generation systems, a typical microgrid consists of a controllable load and an energy storage system. An energy storage system refers to a device that converts energy from one form (usually electrical energy) to a storable form, and then, the stored energy can be converted back into electricity when required. The utilization of energy storage systems, especially in renewable microgrids, has a significant impact on the reliability of the electric power as it can smooth the power fluctuation, reduce power quality problems, control the microgrid frequency and voltage, deliver initial energy when there is a transition between grid connection and islanded mode operation of microgrids, provide ride-through capability in the case of dynamic variations in intermittent energy sources, and enable distributed generations to operate as dispatchable units [7,8].

Three different types of microgrids exist, namely, the AC microgrid, the DC microgrid, and the hybrid microgrid [9]. This paper considers a DC microgrid. The rapid increase in renewable energy sources requires a robust energy management system to connect these renewable energy sources, including energy storage systems. Based on the inexact models, deterministic estimations, and balance conditions, different researchers have reported findings which focus on enhancing the efficient action and operation of EMS, which requires much more improvement. Thus, new research needs to be performed to improve the reliability of microgrid systems. The aim of this paper was to develop an energy management system for DC microgrids, which contributes to an increase in the deployment of renewable energy sources (RESs). The principal contribution of this research was the implementation of an energy management strategy that attempts to ensure the proper operation of a DC microgrid system with the deep penetration of renewable energy sources. The developed DC microgrid model was created using MATLAB/Simulink software. The rest of the paper is presented as follows. The concept of microgrid systems is presented in Section 2. Section 3 discusses the mathematical modeling of the system components. In Section 4, the developed energy management system is presented. Section 5 explores and evaluates the simulation results of the developed method, and finally, Section 6 presents the conclusion of the paper.

2. Concept of Micro-Grid Systems

A typical microgrid refers to a set of distributed generation (DG) systems based on renewable and/or nonrenewable sources, incorporating an energy storage system (ESS) and local controllable loads, generally connected to the distribution system [10]. It may operate in both grid connection as well as isolated mode depending on the load condition. Microgrids can be grouped into diverse categories depending on the location (such as campus, military, residential, commercial, and industrial), size (such as small, medium, and large scale), and application (such as premium power, resilience-oriented, and loss mitigation) [11].

A microgrid involves the integration of several distributed energy sources; the power from these sources is collected, converted, and distributed according to the load requirements. A control system is needed to ensure the proper operation of the microgrid when the power electronics interface with it to form a single unit. The control system is essential; besides providing flexibility, it also preserves the specific energy production and the power quality [12]. Each of these three sorts of microgrid presents advantages and disadvantages. The following Figure 1 presents the different types of microgrids.

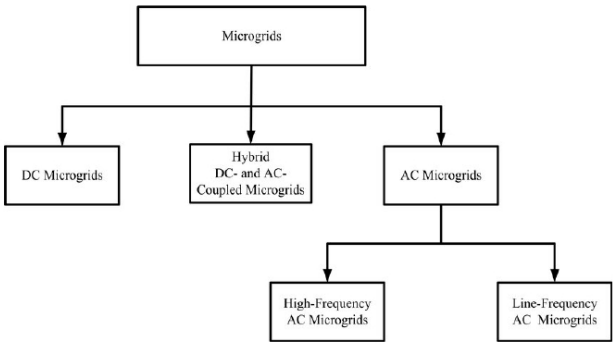


Figure 1. Classification of the microgrids based on power type [9].

DC microgrids have recently received much attention, especially for commercial and residential small-scale applications, as they provide increased efficiency and controllability with additional power conversion stages being eliminated, and the synchronization and compensation of reactive power is no longer needed [13]. In a typical microgrid, the common bus is DC; hence, AC generators are connected to the DC bus via rectifiers, while inverters are used to supply AC loads (see Figure 2).

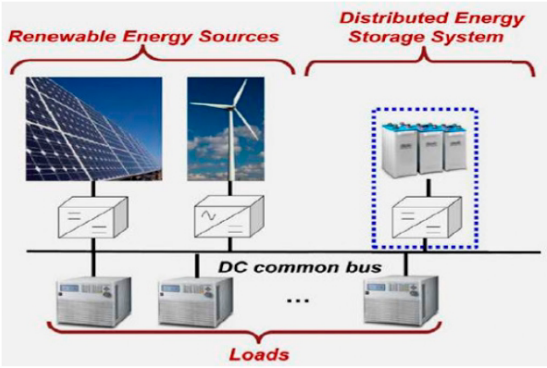


Figure 2. Islanded DC microgrid structure [14].

The DC microgrid can operate connected to the grid or isolated from it. It gives various operational advantages [14]. Many of the devices which are connected to a DC microgrid are generally electronic devices. As they are directly connected to a DC microgrid, no power systems like AC-to-DC, DC-to- AC, or AC-to-DC-to-DC are needed, which could be needed for an AC microgrid. No transformer is used in a DC microgrid; this characteristic makes it more efficient, reduces its size, and makes it more reliable in a DC power system [15]. However, a DC microgrid still presents various problems that must be surmounted. There are no good practices implemented to manage fault situations and a basic protective element such as circuit breakers, fuses, and protection relays is lacking, as in the case of AC microgrids [16].

The hybrid microgrids result from the combination of AC and DC microgrids; they include both AC and DC types of buses [17]. The type of connection to each bus depends on the proximity of the distributed generation unit and the load on the bus. The following steps in the electricity improvement distribution system are the AC microgrid systems.

They can operate in a grid-connected or island mode. Based on the tasks that they have been designed to accomplish, their grid-connected or island modes can possess many suboperational states and or topological configurations [18]. DC-AC converters are used to connect DC generators and energy storage systems to AC buses, while rectifiers are used to supply DC loads.

To optimize the components of a microgrid system, an energy management system is used, which resolves decision-making strategies. These strategies consider increased system energy efficiency, increased reliability, reduced power consumption, the reduced operating cost of distributed energy resources, reduced system losses, and mitigated greenhouse gas emissions for sustainable improvement [9].

2.1. Distributed Generation Sources

A distributed generation system is composed of different sources, both renewable and nonrenewable. Renewable sources are generators that utilize renewable energy technologies such as photovoltaic, solar thermal power, wind power, biomass, tidal power, and geothermal power as the primary energy to generate power [19], whereas nonrenewable sources utilize natural resources that are not naturally replenished to produce power [20].

(A) Solar Power: Solar power can produce power through two different forms, which include solar thermal generation and photovoltaic conversion. The first method, which is the solar thermal process, is a process of converting solar power into heat, and that heat runs a steam turbine which produces power, and photovoltaic conversion converts sunlight into electricity using photoelectric phenomena [21]. A solar cell is a basic component of a PV system. Solar cells can be grouped in series and parallel to constitute modules, which are also connected in series to form strings, and the strings are finally connected in parallel to form arrays. Different from the photovoltaic system, solar thermal generation utilizes solar collectors to collect heat, and the most widely used include parabolic, concentrated solar collectors, etc. [22].

(B) Wind Power: The wind turbine operating mode is focused on two methods. Firstly, the kinetic energy of the moving air is converted into mechanical energy. This conversion is obtained by using aerodynamic rotor blades and a mechanical power controller. Secondly, the electromechanical energy is converted into electric power via a generator [23]. According to the wind turbine topology, they can be classified into two categories (horizontal axis and vertical axis); however, the most used topology is the horizontal axis wind turbine [24,25]. Various generator topologies are utilized to convert the electro-mechanical energy into electricity.

(C) Geothermal Power: A geothermal power system converts the energy contained in the hot rock into electricity by injecting water into the rock to absorb heat from the rock and transport that heat to the surface of the Earth, where it can be converted into electrical power through a turbine generator. High-temperature water (>240 °C) is vaporized into steam, and that heat is transferred to a low-pressure steam turbine, which converts the steam into mechanical energy [26]. Usually, exploitable geothermal reservoirs are mostly located close to young volcanic rock areas [27].

(D) Hydropower: Hydropower is a process that produces electricity from water flowing in the river or the oceans. The purpose of hydropower production is to generate clean energy [28]. A hydropower plant is generally composed of a generator, a turbine, a penstock, and a wicket gate. Mainly, two types of turbines are utilized, which include a pulse turbine (a Pelton Wheel turbine) and a reaction turbine like Francis and Kaplan turbines. Generally, the generator and turbine are directly linked to the same vertical shaft [29].

(E) Biomass Power: A biomass power system utilizes biomass to produce biogas, which is utilized as fuel for a biomass generator [30]. The utilized biomass includes both energy crops and wastes, such as forest residues and a range of other agricultural and industrial compounds. Actually, the use of biomass is a fundamental part of global

renewable energy and contributes to an ever-increasing share of global electricity capacity [31].

(F) Micro-Turbines: Micro-turbines are energy generators, which have a range of capacity between 15 and 500 kW. They operate under the open cycle gas turbine principle, and they have shown many different characteristics and operate easily and at high speed. Some of their benefits include having variable speeds, being easy to install, having compact sizes, being low maintenance, having air bearings, having low NOx emissions, and being mostly recuperators [32]. Micro-turbine generators have demonstrated strong improvements in distributed small-scale power production. However, the results have shown that these generators are not able to supply power during peak periods, but they may meet peak demand and improve the power generation reliability, as they can provide standby capabilities when the power grid fails [33].

(G) Diesel Generators: A diesel generator (also known as a genset) is composed of an internal combustion engine and a synchronous generator connected to the same shaft. Diesel generators are generally utilized as backup or emergency power systems in commercial and industrial installations. They are also widely utilized in new areas where connection to the distribution grid is unfeasible or expensive to perform [34]. Their principal disadvantage is the negative impact that they can have on the environment due to their high NOx.

2.2. Power Electronics Converter Control

The hierarchical control architecture of a microgrid system includes the primary, secondary, and tertiary controllers. A primary controller consists of the preliminary power sharing and regulation of current/voltage, whereas a secondary controller is higher than the primary controller and helps to compensate for the voltage and improve the performance sharing. Finally, a tertiary controller focuses on power management, energy management, and economic dispatch [35].

2.2.1. Primary Controller

A primary controller consists of an inner loop (current/voltage regulation) and droop control (preliminary power sharing) based on the control of the power converters. The response time of the primary controller is very short, and there is no need for communication when it is utilized in the decentralized system [36]. But when it is used in centralized control, distributed control, and master–slave control, there is a need for communication. This controller is mostly used for regulating the frequency and voltage of the inner loop of control.

2.2.2. Secondary Controller

A secondary controller has a longer operating time than a primary controller because it minimizes the frequency and voltage deflections that persevere even after primary control is performed, and it can also be utilized for centralized and decentralized controls [37]. The secondary controller is performed by a central controller of the microgrid in centralized control and in decentralized control; it is implemented by local controllers.

2.2.3. Tertiary Controller

The principal goal of a tertiary controller is to regulate power flow and load sharing between converters and between several hybrid microgrid systems if they are connected in a group and finally synchronize individual incremental costs. Additionally, a tertiary controller is utilized to update the set point for the secondary controller depending on the production cost preferences by updating the loading ratio of each converter [38]. Compared to the secondary controller, the tertiary controller is able to suppress voltage fluctuations and change voltage operating points to attain the optimal dispatch of power production.

2.3. Description of the Developed System

The developed DC microgrid system includes different loads such as a commercial load, industrial load, and residential load. The capacity of the power produced by all DG sources are 150 kWp for solar, 150 kW for wind energy, and 345 kWh for battery banks. Power generation from the PV and battery is DC, but for wind, it is AC; therefore, the power generation from the AC source is converted to DC by using a rectifier. To reduce the voltage fluctuation, each DG source is equipped with a converter. A battery is used to ensure power supply to consumers without any interruption. The DC microgrid supplies the loads directly by 380 Vdc. The total produced power, which includes PV and wind, are connected in parallel. The battery bank will be used as back-up power during peak demand and to decrease variations in the power produced by renewable sources. Thus, the total power required to supply the loads is 280 kW. Figure 3 illustrates the block diagram of the developed DC microgrid system.

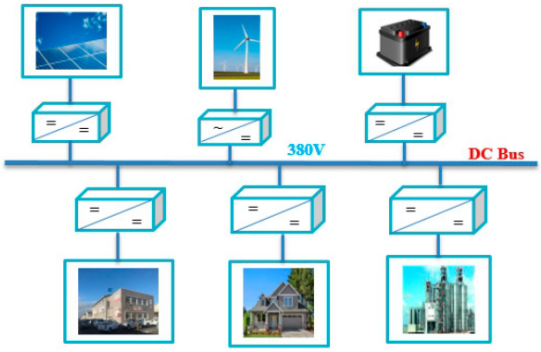


Figure 3. Block diagram of the developed system.

3. Mathematical Modeling of the System Components

The concern at this point was to design a dynamic model of the developed DC microgrid, which helped to verify the efficacy of the designed controller. The MATLAB/Simulink mathematical modules were used to build the DC microgrid model, including the battery systems, which used the component-equivalent circuits. Three different power supplies were considered in this model, which include PV, wind, and battery bank.

3.1. Photovoltaic Module Modelling

The output characteristic of a photovoltaic array is determined by cell temperature, solar irradiation, and output voltage. The operation mode of a PV or solar cell refers to the PN junction diode operation, which converts light energy into electricity by the photovoltaic effect [39]. Figure 4 represents the configuration of a single PV cell.

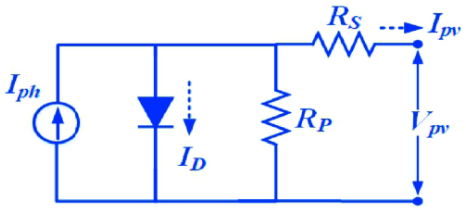


Figure 4. A single equivalent circuit model of a PV cell [40].

According to this circuit, the solar irradiance is described through a current source I_{ph}, and diode current I_D, output current I_{pv}, series resistance R_s, parallel resistance R_p, and output voltage V_{pv} represent the remaining circuit parameters of the configuration. The output current is determined by the following formula:

$$I = \mathrm{N_p}\left[I_{ph} - \mathrm{I_{rs}}\left(exp\frac{\mathrm{q(V} + IR_S)}{\mathrm{akTN_s}} - 1\right)\right] \quad (1)$$

$$\mathrm{I_{rs}} = \mathrm{I_{rr}}\left(\frac{\mathrm{T}}{\mathrm{T_{ref}}}\right)^3 \mathrm{e}^{\frac{\mathrm{E_g}}{\mathrm{k}}\left(\frac{1}{\mathrm{T_{ref}}} - \frac{1}{\mathrm{T}}\right)} \quad (2)$$

where $\mathrm{N_p}$ and $\mathrm{N_s}$ are the numbers of cells connected in parallel and series, k is Boltzmann's constant, 1.380658×10^{-23} J/K, q is the charge of an electron equal to 1.6×10^{-19} (C), a is the ideal diode factor between 1 and 5, $\mathrm{I_{rs}}$ represents the reverse saturation current of the cell, $\mathrm{I_{rr}}$ represents the reverse saturation current at $\mathrm{T_r}$, $\mathrm{T_{ref}}$ is the reference temperature (K), Eg is the energy in eV ($1.602176634 \times 10^{-19}$J), and T is the absolute temperature of the junction.

$$I_{ph} = \left[\mathrm{I_{scr}} + \mathrm{K_i(T - T_r)}\frac{\mathrm{S}}{100}\right] \quad (3)$$

where $\mathrm{I_{scr}}$ represents the short-circuit current at a reference temperature of the cell, $\mathrm{K_i}$ is the coefficient of the short-circuit temperature ($\mathrm{A/m^2K}$),$\mathrm{T_r}$ refers to cell temperature, and S/100 represents the solar radiation in $\mathrm{W/cm^2}$ [41]. According to this configuration, the shunt resistance in parallel with the ideal shunt diode and the I–V characteristics are described by the following equation:

$$I_{pv} = I_{ph} - I_D \quad (4)$$

The PV output power is a function of the solar irradiation and the area of PV module, as shown in the following equation:

$$\mathrm{P_{solar}} = \eta_g \mathrm{i_r A}. \quad (5)$$

where η_g is the production efficiency, $\mathrm{i_r}$ is the radiation of solar in $\mathrm{W/m^2}$, and A is the area.

3.2. Modeling of Wind Power

The wind model is characterized by the variation in wind velocity with gust and wind speed.

$$\mathrm{W_v} = \mathrm{V_w} + \mathrm{V_g} + \mathrm{V_{wr}} \quad (6)$$

With the following parameters:

- $\mathrm{V_w}$ is the base wind velocity;
- $\mathrm{V_g}$ is the gust wind velocity;
- $\mathrm{V_{wr}}$ is the ramp wind component.

Wind power is given by the following expression:

$$\mathrm{P_w} = \frac{\mathrm{dW_w}}{\mathrm{dt}} \quad (7)$$

The energy drawn by the wind turbine is expressed by the formula below:

$$\left.\begin{aligned}\mathrm{W_w} &= \mathrm{V_a} \times \tfrac{1}{2}\rho\left(\mathrm{V_1}^2 - \mathrm{V_3}^2\right)\\ \mathrm{P_w} &= \mathrm{d}\frac{\mathrm{V_a} \times \frac{1}{2}\rho\left(\mathrm{V_1}^2 - \mathrm{V_3}^2\right)}{\mathrm{dt}}\end{aligned}\right\} \quad (8)$$

where W_w is the energy drawn by the wind turbine and ρ is the air density. Based on Betz, the maximum output power of a wind turbine is given by the following:

$$P_M = \frac{16}{27}\rho A\frac{3}{2}V^3 \tag{9}$$

where, A is the area, ρ is the air density, and V is the wind velocity.

The substitution of the value for V_1, and V_3 enable us to obtain the following equation:

$$V_2 = \frac{2}{3}V_1 \tag{10}$$

$$V_3 = \frac{1}{3}V_1 \tag{11}$$

where V_1, V_2, and V_3 are wind velocities in different areas.

The modeling of a wind turbine helps to describe the captured output power of the turbine [42]. The wind power according to a given area is calculated as follows:

$$P_w = \frac{1}{2}\rho A{W_v}^3 \tag{12}$$

$$P_M = P_w C_p \tag{13}$$

$$C_p = \frac{1}{2}\left[\delta - 0.22\beta^2 - 5.6\right]e^{-0.17\delta} \tag{14}$$

where β is the pitch angle of the blade (deg, °), δ is the tip speed ratio of the turbine, and C_p is the power coefficient.

The maximum produced power by a wind turbine is calculated by the following equation:

$$P_G = V_G I_G \tag{15}$$

3.3. Modeling of the Battery

The principal focusing parameters of the battery mathematical model are the voltage and current. The current can be determined by the change in the terminal voltage of the battery. The current production is driven by the transmission of electrons from one electrode to another [43]. The potential difference between the positive and negative electrodes determines the open circuit voltage of the battery [44]. The following equations present the charging and discharging voltages of the battery:

$$V_{discharge} = E_0 - {V_{op}}^+ - V_{op} - IR_{pol} \tag{16}$$

$$V_{charge} = E_0 + {V_{op}}^+ + V_{op} + IR_{pol} \tag{17}$$

$$= E_0 - K\left[\frac{Q}{Q - it}\right]i - R_0 I \tag{18}$$

$$V_{battery} = E_0 - \left(\frac{K}{SOC}\right)i - R_0 I. \tag{19}$$

$$V_{discharge} = E_0 - K_{dr}\frac{Q}{Q - it}i_1 - R_0 i - K_{dv}\frac{Q}{Q - it}it + e(t) \tag{20}$$

$$V_{charge} = E_0 - Kc_r\frac{Q}{it + \lambda Q}i_1 - R_0 i - Kc_v\frac{Q}{Q - it}it + e(t) \tag{21}$$

$$e(t) = Bi\left[e(t) + Au(t)\right] \tag{22}$$

$$V_{discharge} = E_0 - K_{dr}\left(\frac{K}{SOC}\right)I - R_0 I - K_V\left(\frac{K}{SOC} - 1\right) + e(t) \tag{23}$$

The composed relation model allows us to modify Equations (18) and (19). V_{op} is the open circuit voltage at the battery and $V_{op}{}^{+}$ is the open circuit voltage at the positive electrode of the battery. E_0 represents the open circuit voltage of the battery expressed in Volt, I is the battery current, *i.t* is the discharged capacity (Ah), K is the polarization coefficient (Ω), Q represents the battery capacity (Ah), R is the internal resistance, A is the exponential voltage coefficient in V, B is the exponential capacity in $(Ah)^{-1}$, R_0 is the ohmic resistance in Ω, and SOC is the battery state of charge in %.

Equations (18) and (19) present some limitations such as (i) battery aging and self-discharge, (ii) the current amplitude not having an impact on the battery capacity, and (iii) no consideration of the temperature coefficient. To surmount these limitations, it is crucial to consider the aspects that have an impact on the life of the battery [45]. The analysis of the SOC condition is conducted at each instant and is calculated with the threshold capacity using Equation (24).

The following equation determines the net power produced by a DC microgrid structure:

$$P_{net} = P_{PV} + P_{wind} + P_{bio} \tag{24}$$

4. Developed Management System

Generally, the energy management system is used to control power production and schedule programs for a group of power grid applications. However, it may be considered as another way to control the electrical loads in microgrids. The present system is designed to meet the loads. As renewable resources are intermittent sources, the battery is used as a back-up system, and this is also designed to meet the load as well. The developed system includes three different types of loads (industrial, residential, and commercial loads), and in the developed model, the industrial load is assumed to be a priority load. The system comprises two renewable sources and a storage system. The net power generated P_G and the load power P_L are calculated as follows:

$$P_G = P_{pv} + P_{wind} \tag{25}$$

$$P_L = P_{Ind} + P_{Res} + P_{Com} \tag{26}$$

where P_G is the power generated from the renewable energy sources; P_{pv} is the power produced from PV; P_{wind} is the power produced from wind; P_L is the load power; P_{Ind} is the industrial load power; P_{Res} is the residential load power; and P_{Com} is the commercial load power.

The battery bank will charge when there is excess production and will discharge when the power generated is not able to handle the load demands. Based on this architecture, the power generation will supply the load through four conditions and by the support of the battery bank.

- ✔ Firstly, when the power generation is equal to the load demands, in this case, the loads are supplied by the power generation from PV and wind without any disruption.
- ✔ Secondly, when the power generation exceeds the load demands, in this case, the power generation is more than the demand of the loads; thus, the loads are supplied by the power generation and the surplus of the production is used to charge the battery. When the battery is fully charged, the remaining excess of production is located to an auxiliary load.
- ✔ When the power generation becomes less than the demand of the loads, then the loads are supplied with the help of the battery bank. The battery is discharged until its SOC reaches its minimum value.

$$SOC_{min} < SOC_{batt} < SOC_{max} = 20\% < SOC_{batt} < 100\%$$

- ✔ When the $SOC_{batt} < 20\%$, the battery is disconnected from the system, and at this time, the priority load, which is the industrial load, is supplied by the power generation

from the renewable energy sources. If the power production exceeds the industrial load, in this case, the excess of the production is used to charge the battery. When the power production falls below the priority load, then the power generated from the renewable energy sources is used to charge the battery. The system will permanently verify the power generation and the battery SOC until the power generation meets the loads or the battery becomes able to handle the loads.

5. Simulation Results and Discussion of the Developed Model

The following section presents the description of the developed energy management control and diverse specified simulation procedures and simulation results. The developed model was implemented in the MATLAB/SIMULINK 2020b software and the block diagram of the developed system and EMS algorithm is shown in Appendix A. All circuit elements and machines are represented by their respective model blocks available in the software. Different parameters of the simulation are presented in Table 1. The developed EMS strategy controls the PV, wind, battery, and loads. The load is subdivided into three categories: industrial load (which is the high-priority load), residential load, and commercial load [46].

Table 1. Simulation parameters.

Unit	Specification
Photovoltaic	150 kW, 380 V
Wind power	150 kW, 380 V
Battery	900 Ah, 380 V
DC bus voltage	380 V
DC-DC converter	380 V
Load demands	280 kW

Figure 5 illustrates the PV outputs voltage and power as a function of the simulation time.

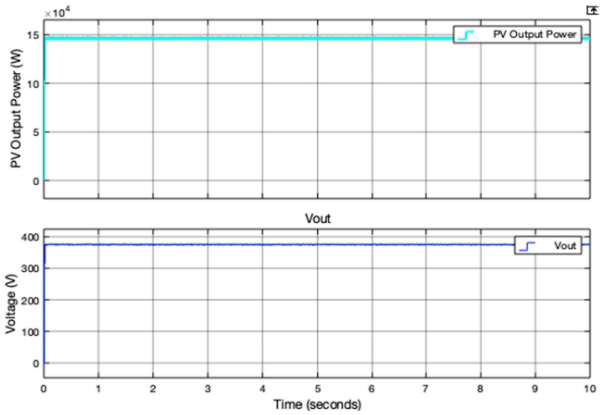


Figure 5. PV output power and voltage from the developed DC microgrid model.

The output voltage remains constant at 380 V_{dc} with very small ripples; the designed model allows a ripple with 0.9% variation from the steady state. The power generation stays constant at 149.68 kW.

Figure 6 presents the universal bridge rectifier output voltage and output power of the wind model as a function of the simulation time. The steady states of the outputs are

attained at approximately 2.2 s and remain constant after, with very small ripples. The output voltage is 380 V_{dc}, and the average value of the power generation is 148.78 kW.

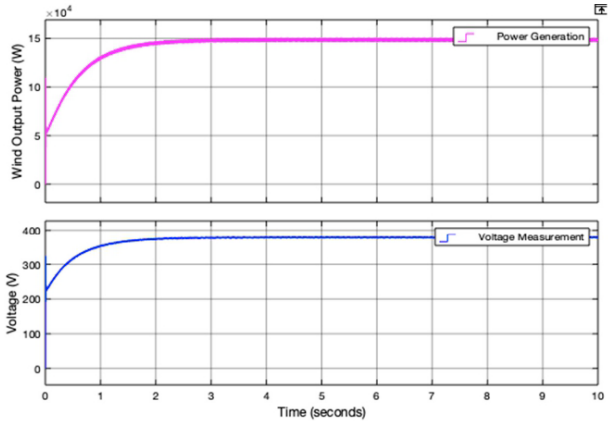


Figure 6. Wind output power and voltage from the developed DC microgrid model.

The developed EMS algorithm is designed in the Stateflow logical programming environment. In this section, different cases are considered. Table 2 summarizes the different operating modes of these cases. In this study, Load 1 is considered as the priority load, which is the industrial load.

Table 2. Action table for the energy management system.

Operation	Descriptions	Actions
1	Loads connected	A1: Loads = ON;
2	Load connected and battery charging	A2: Loads and battery = ON;
3	Battery charging	A3: Battery = ON;
4	Auxiliary load connected	A4: Damp load = ON; battery = OFF; loads = ON;
5	Battery connected	A5: Battery = ON; Damp load = OFF;
6	Battery discharging	A6: Battery = ON;
7	Battery disconnected	A7: Battery = OFF;
8	$Load_1$ and $Load_3$ connected	A8: $Load_1$ and $Load_3$ = ON; $Load_2$ = OFF; battery = ON;
9	$Load_1$ and battery connected	A9: $Load_2$ and $Load_3$ = OFF; $Load_1$ = ON; battery = ON;
10	$Load_2$ and battery connected	A10: $Load_1$ and $Load_3$ = OFF; $Load_2$ = ON; battery = ON;
11	Loads disconnected and battery connected	A11: Load = OFF; battery = ON;

The operating mode of the Stateflow environment corresponds to that of a logical system; it is either 0 or 1. When the system is in operation mode, the output indicates 1, and when the output indicates 0, this means that the system is not in operation.

Case 1: In this first case, the power supply is equal to the demand of the loads, as shown in Figure 7. The battery and the auxiliary load are disconnected from the system. The power is supplied to the loads and the battery SOC is assumed to be below its maximum capacity (100%). In this case, the battery SOC is kept at 50%.

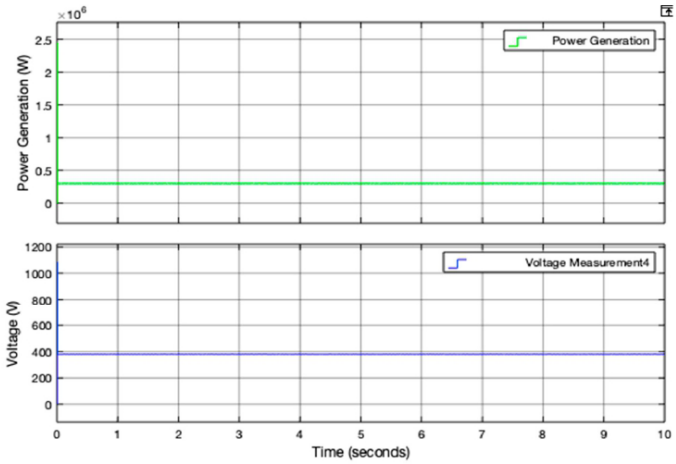


Figure 7. Power and voltage generation.

The demand of the loads is fixed at 280 kW, and the power production from the RES is 281 kW. Therefore, the loads are supplied by the power generation without any interruption. Figure 8 presents the Stateflow transition state of this scenario. The battery in this case is not charging or discharging.

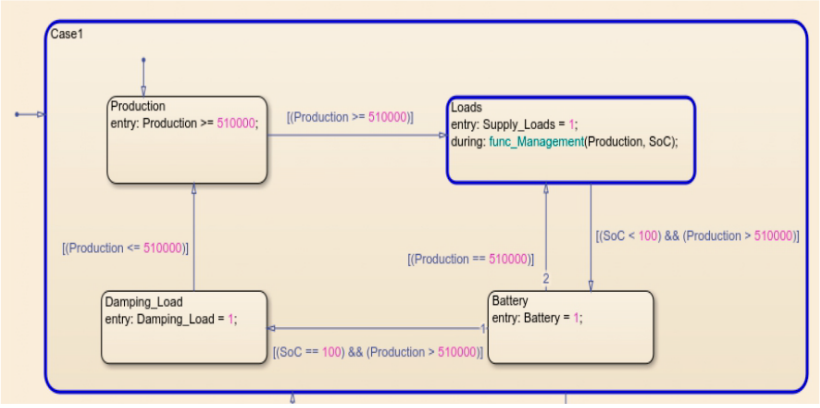


Figure 8. Transition state from the Stateflow chart for the first scenario.

As shown in Figure 9, the output result from the EMS algorithm shows that all the loads are supplied without any interruption because the power produced meets the demand of the loads. In this case, the battery bank and the damp load are 0, which means that they are disconnected.

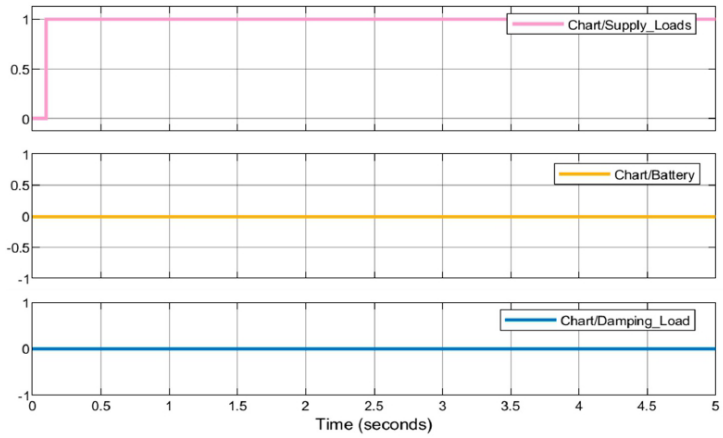


Figure 9. EMS control output results for the first scenario.

Case 2: Here, the power generation becomes higher compared to the load requirements, as shown in Figure 10. Thus, the EMS checks if the battery is fully charged or not. If the SOC is less than 100%, as shown in Figure 11, the loads are supplied by the power produced, and at the same time, the battery is connected to be charged by the excess of production until it reaches its charge limit, which is 100%.

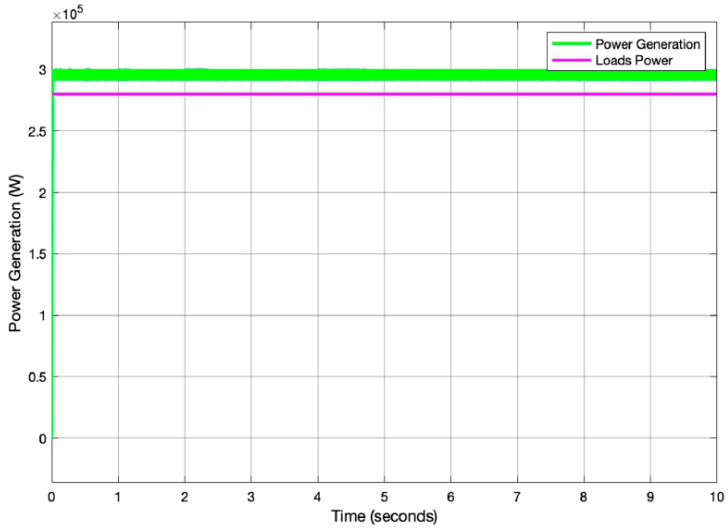


Figure 10. Power generation.

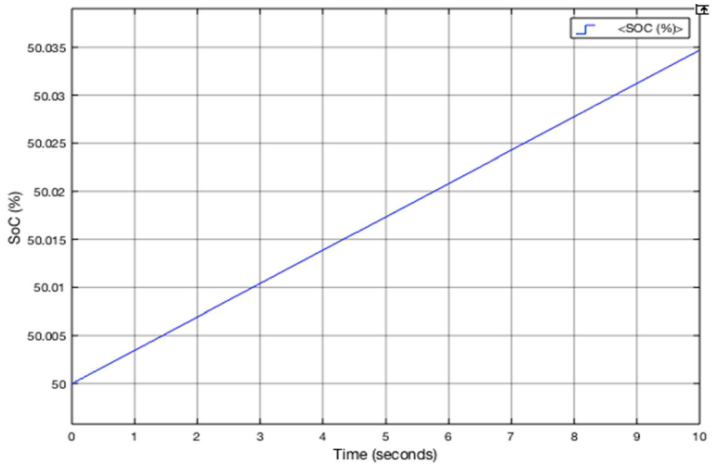


Figure 11. Charging mode of the battery.

Figure 11 presents the battery graph in which it shows the battery charging.

When the battery reaches its maximum charge value (100%), it is disconnected from the system to wait for the discharge phase. Figure 12 shows that the loads and battery outputs are 1, while the damp load output is 0. This means that the loads are supplied, and at the same time, the battery is also charging.

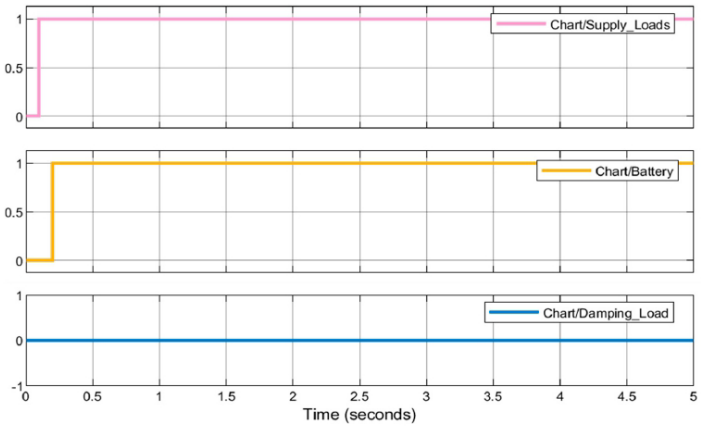


Figure 12. EMS control output results for the second scenario.

Figure 13 shows the transition from the Stateflow chart. Power supplied from the RESs is 298 kW, and the demand of the loads is 280 kW. Thus, the excess of production (18 kW) is stored in the battery, as shown in Figure 13.

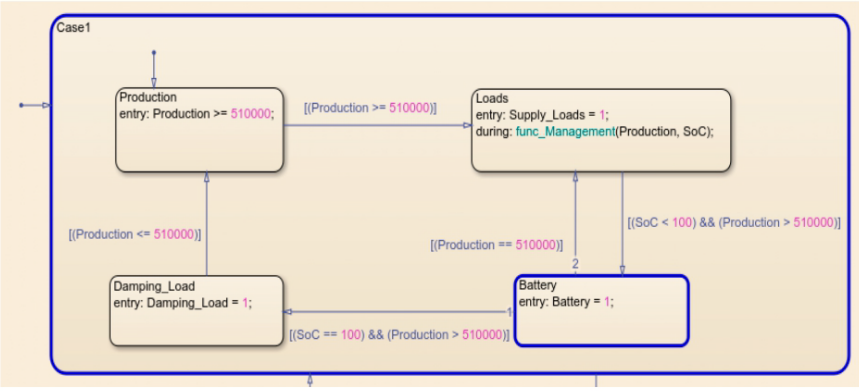


Figure 13. Transition state from Stateflow chart for the second scenario.

When the battery is fully charged (100%), the surplus of production is transferred to the auxiliary load, as shown in Figure 14, until the power generation meets the demand of the loads or the condition changes.

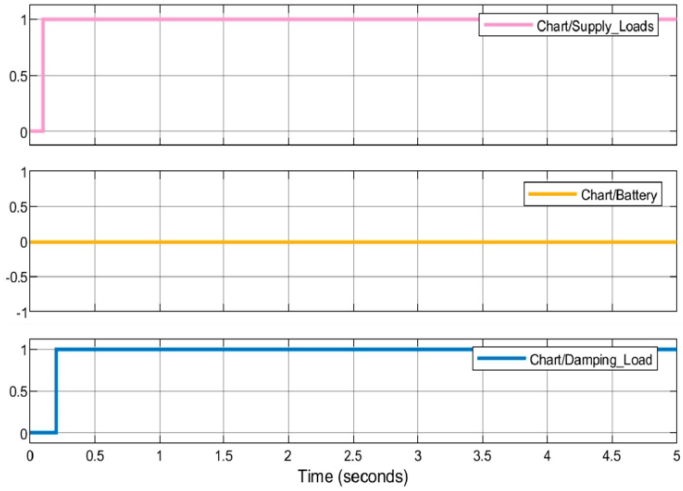


Figure 14. EMS control output results for the second scenario: battery fully charged.

Case 3: The power generation becomes lower than the load requirements, as shown in Figure 15. Based on the EMS control, the loads are supplied by the help of the battery. Firstly, the SOC of the battery is measured. If the it is more than 20%, then the battery is connected to be discharged. The condition is that, when the SOC becomes equal to or less than 20%, automatically, the battery must be disconnected from the system.

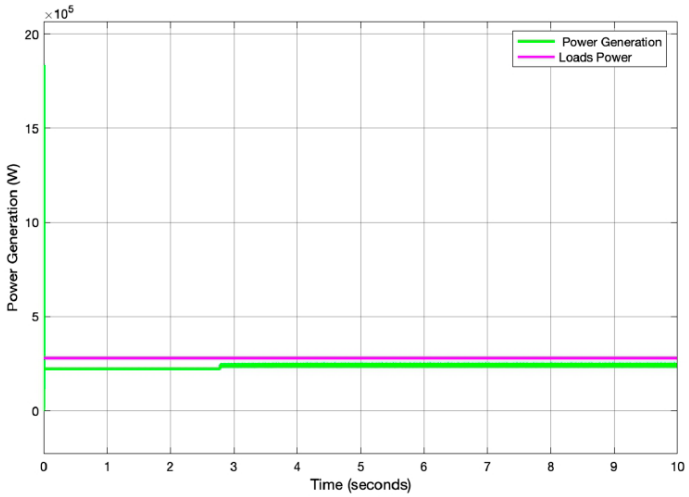


Figure 15. Power generation.

In Figure 16, the battery is charging. When the minimum value of the SOC is reached, then the battery stops discharging to avoid deep discharge.

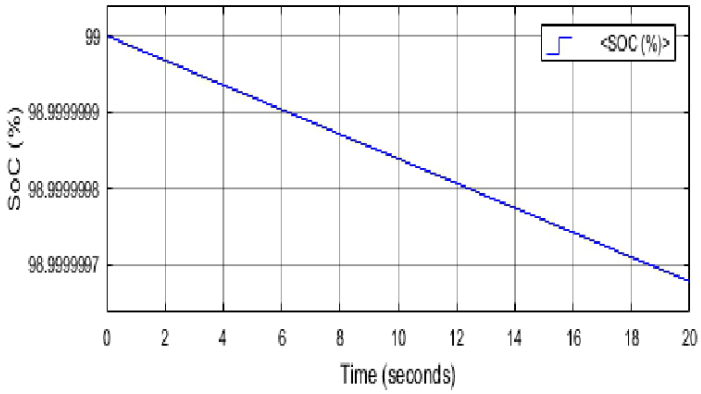


Figure 16. Discharging mode of the battery.

Figure 17 presents the results from the Stateflow chart, where the battery is connected to be discharged.

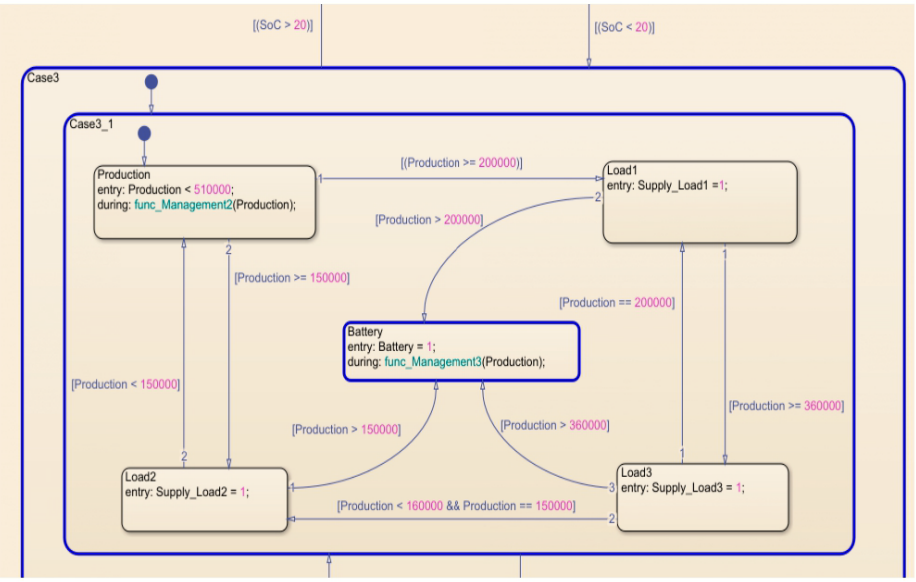


Figure 17. Transition state from Stateflow chart for the third scenario.

Once the SOC of the battery becomes 20%, the battery is disconnected. The EMS control allows power to be supplied to the priority load, which is the industrial load (Load 1). Before that, the EMS measures the power generation to check if it is able to provide power to the priority load and charge the battery at the same time; if the condition is approved, then the battery is charged as well. Figure 18 presents the simulation results, showing that the priority load is supplied by the power generation, and Figure 19 illustrates the transition state.

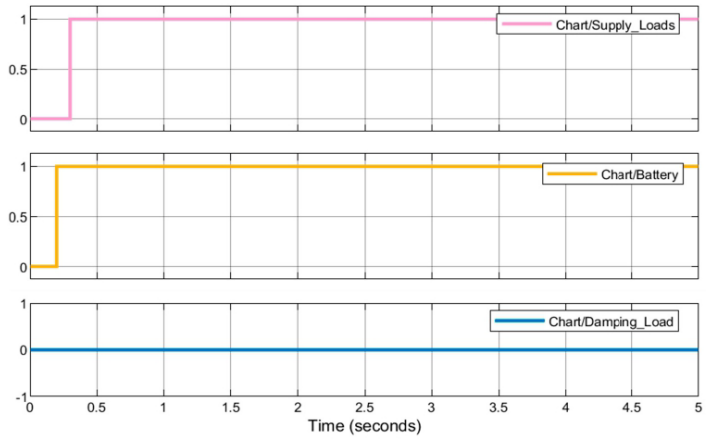


Figure 18. EMS control output results.

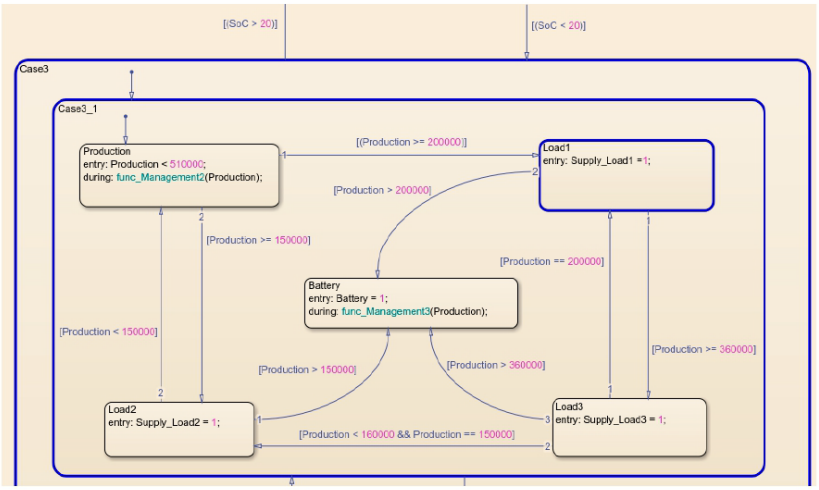


Figure 19. Transition state from Stateflow chart.

When the power generation is not able to simultaneously supply the priority load and charge the battery, the EMS control checks if the power generation can handle the priority load. If the condition is met, then the priority load is supplied by the available power produced, as presented in Figure 20.

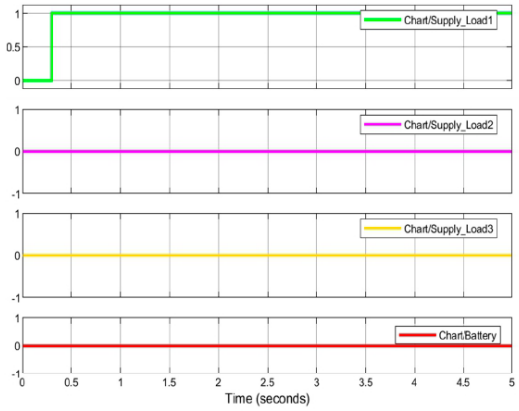


Figure 20. EMS control output results when priority is supplied.

When the power generation becomes lower than the priority load, the EMS control checks if the power generated is able to supply the residential load (Load 2) or both supply the residential load and charge the battery at the same time. If the condition is approved, the residential load and the battery are supplied by the power generation, and if not, only the residential load is supplied. When the power generation falls below the residential load, the EMS control automatically disconnects all the loads (shut-down loads). In this case, no load is supplied. The loads are momentarily disconnected and the available power

generation is used to charge the battery until its SOC meets the requirement or the power generation becomes active. The result of this scenario is shown in Figure 21.

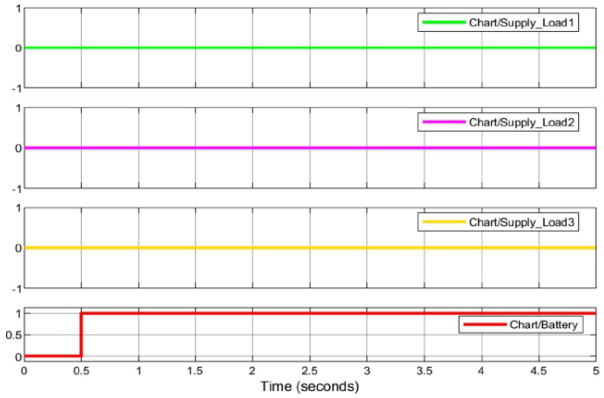


Figure 21. EMS control output results.

The simulation results of the developed DC microgrid and energy management algorithm model are presented in this section. The model was designed and developed using MATLAB/Simulink software. In this paper, it was a question of focusing on the energy management control of the DC microgrid system to finally maintain its proper operation. The method used to design and develop this energy management system algorithm was the Stateflow logical programming environment in MATLAB/Simulink software. Based on all these scenarios, the developed energy management system algorithm has shown the ability to ensure the reliability, resiliency, robustness, and proper operation of the system.

The developed controllers reveal a promising approach towards effectively integrating renewable energy sources into DC microgrid systems. One notable aspect of the results is the robustness analysis conducted to assess the performance of the developed energy management strategy under various scenarios and conditions. During the robustness analysis, the energy management strategy was evaluated against a range of factors, including changes in renewable energy availability, and variations in load demand. This analysis provided valuable insights into the resilience and stability of the developed strategy in real-world operating conditions.

The results demonstrate that the energy management strategy exhibits robust performance across different scenarios, effectively balancing energy generation and consumption while ensuring the reliable operation of the microgrid system. Despite fluctuations in renewable energy generation and load demand, the strategy demonstrates adaptability and resilience, maintaining stable operation and minimizing disruptions. Furthermore, the robustness analysis highlights the flexibility of the energy management strategy in accommodating changes and uncertainties in the microgrid environment. By optimizing energy flow, the strategy enhances the overall efficiency and reliability of the microgrid system, while maximizing the integration of renewable energy sources.

6. Conclusions

This paper presents an energy management strategy using a Stateflow controller related to DC microgrids with the important penetration of renewable energy. The energy management system model was developed on MATLAB/Simulink. This developed DC microgrid model considered different loads such as commercial, industrial, and residential loads. The simulation was conducted to show the interaction between different components of the system and to demonstrate the operation of the developed energy management

strategy model. Different results of the scenarios of the developed energy management system algorithm successfully show that this developed algorithm is capable of ensuring the reliability, the resiliency, the robustness, and the proper operation of the entire system, including the battery bank. The main advantage of this developed algorithm is that it ensures a proper relation between the charge/discharge rate of battery energy storage systems on their operating conditions and allows their SOC to be kept in the admissible limits (between 20% and 100%), according to the input power conditions from the EMS flow chart, to avoid the deep charge/discharge of the battery bank, which in return will significantly impact its lifespan and the reliability in a DC microgrid. The results demonstrated that the battery is able to handle the load demands for the different scenarios studied. Additionally, this analysis provides confidence in the practical implementation of the strategy, offering valuable guidance for designing and operating resilient and sustainable microgrid systems in the face of dynamic and uncertain operating conditions.

Author Contributions: C.B.N. is listed as the first author; he provided the most significant contributions to the project, including data acquisition, analysis, and the conceptualization of a practical energy management strategy testing model. M.A. and A.A., listed as the second and third authors, respectively, played vital roles in guiding the project, providing revisions, and ensuring quality control throughout its development. All authors have read and agreed to the published version of the manuscript.

Funding: This research received no external funding.

Institutional Review Board Statement: Not applicable.

Informed Consent Statement: Not applicable.

Data Availability Statement: Access to the datasets utilized in this study is available upon request from the corresponding author.

Acknowledgments: This paper is based on the thesis work and results of author C. Ndeke Bipongo. This paper is a summary of the most important aspects of his thesis entitled "Energy management of a battery energy storage system for renewable energy DC microgrid".

Conflicts of Interest: The authors declare no conflict of interest.

Nomenclature

I_{ph}	Solar irradiance described through a current source (Ampere)
I_d	Diode current (Ampere)
I_{pv}	PV output current (Ampere)
R_s	Series resistance (Ω)
R_p	Parallel resistance (Ω)
V_{pv}	PV output voltage (Volt)
N_p and N_s	Number of cells connected in parallel and series
k	Boltzmann's coefficient (1.380658×10^{-23} J/K)
a	Ideal diode factor between 1 and 5
I_{RS}	Reverse saturation current of cell at T (Ampere)
I_{rr}	Reverse saturation current at T_r (Ampere)
I_{scr}	Short-circuit current at a reference temperature of the cell (Ampere)
K_i	Coefficient of the short-circuit temperature (A/m^2K)
T	Absolute temperature of the junction (K)
T_r	Cell temperature (K)
T_{ref}	Reference temperature (K)
P_{solar}	PV output power (Watt-peak)
η_g	PV production efficiency
i_r	Radiation of solar (kWh/m^2)
A	Area (m^2)
V_w	Base wind velocity (m/s)
V_g	Gust wind velocity (m/s)

V_{wr}	Ramp wind component (m/s)
W_v	Wind speed (m/s)
P_w	Wind turbine output power (Watt)
W_w	Energy drawn by the wind turbine (Joule)
ρ	Air density (kg/m^3)
P_M	Maximum wind turbine output power (Watt)
B	Pitch angle of the blade (deg, °)
Δ	Tip speed ratio of the turbine
C_P	Power coefficient
P_G	Maximum wind turbine produced power (Watt)
V_G	Maximum wind turbine produced voltage (Volt)
I_G	Maximum wind turbine produced current (Ampere)
E_0	Open circuit voltage of the battery (Volt)
K	Polarization coefficient (Ω)
Q	Battery capacity (Ah)
q	Charge of an electron equal to 1.6×10^{-19} (C)
R	Battery internal resistance (Ω)
P_G	Generated power from the renewable energy resources (Watt)
P_{pv}	Power produced by PV (Watt-peak)
P_{wind}	Power produced by wind (Watt)
SOC	State of charge (%)

Appendix A. Block Diagram of the Developed EMS for DC Micro-Grid System Model

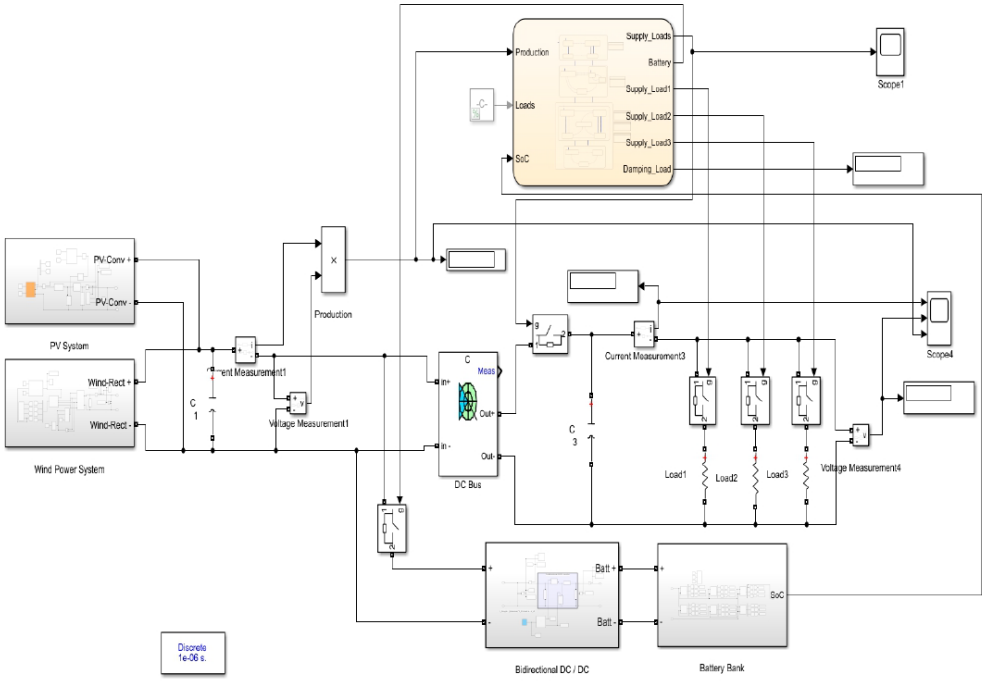


Figure A1. Block diagram of the developed DC microgrid system and EMS algorithm.

References

1. Lu, X.; Sun, K.; Guerrero, J.M.; Vasquez, J.C.; Huang, L.; Teodorescu, R. SoC-based droop method for distributed energy *Storage* in DC microgrid applications. In Proceedings of the IEEE International Symposium on Industrial Electronics, Hangzhou, China, 28–31 May 2012; pp. 1640–1645. [CrossRef]
2. Lasseter, R.H.; Paigi, P. Microgrid: A conceptual solution. In Proceedings of the IEEE 35th Annual Power Electronics Specialists Conference, Aachen, Germany, 20–25 June 2004; Volume 6, pp. 4285–4290. [CrossRef]
3. Topić, D.; Knežević, G.; Perko, J.; Kosić, D. Simplified model for optimal sizing of the off-grid PV system regarding value of loss of load probability. *Teh. Vjesn.* **2018**, *25*, 420–426. [CrossRef]
4. Takele, H. Distributed generation adverse impact on the distribution networks protection and its mitigation. *Heliyon* **2022**, *8*, e09624. [CrossRef]
5. Maor, T.T.; El-Kishky, H. *Impacts of Power System-Tied Distributed Generation on the Performance of Protection Systems*; University of Texas at Tyler: Tyler, TX, USA, 2017. Available online: https://scholarworks.uttyler.edu/ee_grad (accessed on 1 December 2017).
6. Morstyn, T.; Hredzak, B.; Agelidis, V.G. Control Strategies for Microgrids with Distributed Energy Storage Systems: An Overview. *IEEE Trans. Smart Grid* **2018**, *9*, 3652–3666. [CrossRef]
7. Faisal, M.; Hannan, M.A.; Ker, P.J.; Hussain, A.; Mansor, M.B.; Blaabjerg, F. Review of energy storage system technologies in microgrid applications: Issues and challenges. *IEEE Access* **2018**, *6*, 35143–35164. [CrossRef]
8. Nadeem, F.; Hussain SM, S.; Tiwari, P.K.; Goswami, A.K.; Ustun, T.S. Comparative review of energy storage systems, their roles, and impacts on future power systems. *IEEE Access* **2019**, *7*, 4555–4585. [CrossRef]
9. Wang, C.; Yu, Y.; Niu, J.; Liu, Y.; Bridges, D.; Liu, X.; Pooran, J.; Zhang, Y.; Hu, A. Recent Progress of Metal–Air Batteries—A Mini Review. *Appl. Sci.* **2019**, *9*, 2787. [CrossRef]
10. Agrawal, M.; Mittal, A. Micro Grid Technological Activities across the Globe: A review. *Int. J. Res. Rev. Appl. Sci.* **2011**, *7*, 147–152. Available online: http://www.arpapress.com/Volumes/Vol7Issue2/IJRRAS_7_2_07.pdf (accessed on 1 January 2011).
11. Lotfi, H.; Khodaei, A. AC versus DC microgrid planning. *IEEE Trans. Smart Grid* **2017**, *8*, 296–304. [CrossRef]
12. Wu, X.; Shi, S.; Wang, Z. Micro-grid planning considering the supply adequacy of critical loads under the uncertain formation of sub-micro-grids. *Sustainability* **2019**, *11*, 4683. [CrossRef]
13. Hirsch, A.; Parag, Y.; Guerrero, J. Microgrids: A review of technologies, key drivers, and outstanding issues. *Renew. Sustain. Energy Rev.* **2018**, *90*, 402–411. [CrossRef]
14. Beykverdi, M.; Jalilvand, A.; Ehsan, M. Intelligent Power Management of Islanded DC Microgrid based on Droop Fuzzy Control. *Am. J. Sci.* **2017**, *1*, 1–11.
15. Yadav, A.K.; Ray, A.; Lokhande, M.M. Low-voltage DC microgrid network: A case study for Standalone system. *Int. J. Renew. Energy Res.* **2017**, *7*, 1186–1194.
16. Lago, J.; Heldwein, M.L. Operation and control-oriented modeling of a power converter for current balancing and stability improvement of DC active distribution networks. *IEEE Trans. Power Electron.* **2011**, *26*, 877–885. [CrossRef]
17. Kishore, P.M.; Ravikumar, B. Refined Hybrid Microgrid Architecture for the Improvement of Voltage Profile. *Energy Procedia* **2016**, *90*, 645–654. [CrossRef]
18. Vegunta, S.C.; Higginson, M.J.; Kenarangui, Y.E.; Li, G.T.; Zabel, D.W.; Tasdighi, M.; Shadman, A. AC microgrid protection system design challenges—A practical experience. *Energies* **2021**, *14*, 2016. [CrossRef]
19. Ustun, T.S.; Ozansoy, C.; Zayegh, A. Recent developments in microgrids and example cases around the world—A review. *Renew. Sustain. Energy Rev.* **2011**, *15*, 4030–4041. [CrossRef]
20. Muthuvel, P.; Arul Daniel, S.; Paul, S.K. Sizing of PV array in a DC nano-grid for isolated households after alteration in time of consumption. *Eng. Sci. Technol. Int. J.* **2017**, *20*, 1632–1641. [CrossRef]
21. Maghami, M.R.; Hizam, H.; Gomes, C.; Radzi, M.A.; Rezadad, M.I.; Hajighorbani, S. Power loss due to soiling on solar panel: A review. *Renew. Sustain. Energy Rev.* **2016**, *59*, 1307–1316. [CrossRef]
22. Wang, R. Research on Solar Power Generation Technology of Power Plant. In Proceedings of the Conference of Russian Young Researchers in Electrical and Electronic Engineering, ElConRus, Saint Petersburg, Russia, 25–28 January 2022; Volume 2022, pp. 1295–1301. [CrossRef]
23. Das, S.; Mazumder, D.; Mia, N.; Rahman, S. A review on power generation from wind power created by fast moving train perspective Bangladesh. In Proceedings of the IEEE International Conference on Technology, Engineering, Management for Societal Impact Using Marketing, Entrepreneurship and Talent, TEMSMET, Bengaluru, India, 10 December 2020. [CrossRef]
24. Camm, E.H.; Behnke, M.R.; Bolado, O.; Bollen, M.; Bradt, M.; Brooks, C.; Dilling, W.; Edds, M.; Hejdak, W.J.; Haouseman, D.; et al. Characteristics of wind turbine generators for wind power plants. In Proceedings of the IEEE Power and Energy Society General Meeting, PES '09, Calgary, AB, Canada, 26–30 July 2009; pp. 1–5. [CrossRef]
25. Sharif, Y.A.; Rahman, M.; Soloiu, V.; Kiernan, M.; Grall, D.; Hossain, M.S. Wind Power Generation from Multiple Array Configuration and Efficient Power Integration to Grid. In Proceedings of the North American Power Symposium, NAPS, College Station, TX, USA, 14–16 November 2021. [CrossRef]
26. Schastlivtsev, A.I.; Borzenko, V.I.; Dunikov, D.O. Improvement of efficiency of geothermal power plants by using hydrogen combustion technologies. In Proceedings of the International Science and Technology Conference "EastConf", EastConf, Vladivostok, Russia, 1–2 March 2019; pp. 1–6. [CrossRef]

27. Jolie, E.; Scott, S.; Faulds, J.; Chambefort, I.; Axelsson, G.; Gutiérrez-Negrín, L.C.; Zemedkun, M.T. Geological controls on geothermal resources for power generation. *Nat. Rev. Earth Environ.* **2021**, *2*, 324–339. [CrossRef]
28. Ahlfors, C.; Amelin, M. Weekly planning of hydropower in systems with large volumes and varying power generation: A literature review. In Proceedings of the IEEE Madrid PowerTech, PowerTech 2021—Conference Proceedings, Madrid, Spain, 28 June–2 July 2021. [CrossRef]
29. Sysoev, A.A.; Lazareva, N.V.; Proskurina, A.A. Modeling complex hydropower systems for research and training. In Proceedings of the International Conference on Industrial Engineering, Applications and Manufacturing, ICIEAM 2021, Sochi, Russia, 17–21 May 2021; pp. 152–157. [CrossRef]
30. Ali, G.; El-Hawary, M. Generating Heat and Power from Biomass—An Overview. In Proceedings of the IEEE Canadian Conference of Electrical and Computer Engineering, (CCECE), Edmonton, AB, Canada, 5–8 May 2019; pp. 8–13. [CrossRef]
31. Tumiran; Na'iem, M.; Sarjiya; Putranto, L.M.; Listyanto, T.; Priyanto, A.; Muthahhari, A.A.; Budi, R.F.S. Potential of Biomass as RE Source for Sustainable Electricity Supply in Eastern Indonesia. In Proceedings of the 3rd International Conference on High Voltage Engineering and Power Systems, ICHVEPS, Bandung, Indonesia, 5–6 October 2021; pp. 22–27. [CrossRef]
32. Aslanidou, I.; Rahman, M.; Zaccaria, V.; Kyprianidis, K.G. Micro Gas Turbines in the Future Smart Energy System: Fleet Monitoring, Diagnostics, and System Level Requirements. *Front. Mech. Eng.* **2021**, *7*, 676853. [CrossRef]
33. Asgharian, P.; Noroozian, R. Modeling and simulation of microturbine generation system for simultaneous grid connected/islanding operation. In Proceedings of the 24th Iranian Conference on Electrical Engineering, ICEE, Shiraz, Iran, 10–12 May 2016; pp. 1528–1533. [CrossRef]
34. Premadasa, P.N.D.; Silva, C.M.M.R.S.; Chandima, D.P. An optimal configuration of diesel generator and battery storage system for off-grid residential applications. In Proceedings of the IEEE Electrical Power and Energy Conference, EPEC, Toronto, ON, Canada, 22–31 October 2021; pp. 486–491. [CrossRef]
35. Bidram, A.; Davoudi, A. Hierarchical structure of microgrids control system. *IEEE Trans. Smart Grid* **2012**, *3*, 1963–1976. [CrossRef]
36. Beerten, J.; Belmans, R. Analysis of power sharing and voltage deviations in droop-controlled DC grids. *IEEE Trans. Power Syst.* **2013**, *28*, 4588–4597. [CrossRef]
37. Dragicevic, T.; Guerrero, J.M.; Vasquez, J.C.; Skrlec, D. Supervisory control of an adaptive-droop regulated DC microgrid with battery management capability. *IEEE Trans. Power Electron.* **2014**, *29*, 695–706. [CrossRef]
38. Abhishek, A.; Ranjan, A.; Devassy, S.; Kumar Verma, B.; Ram, S.K.; Dhakar, A.K. Review of hierarchical control strategies for DC microgrid. *IET Renew. Power Gener.* **2020**, *14*, 1631–1640. [CrossRef]
39. Mandelli, S.; Barbieri, J.; Mereu, R.; Colombo, E. Off-grid systems for rural electrification in developing countries: Definitions, classification and a comprehensive literature review. *Renew. Sustain. Energy Rev.* **2016**, *58*, 1621–1646. [CrossRef]
40. Azzollini, I.A.; Felice VDi Fraboni, F.; Cavallucci, L.; Breschi, M.; Rosa, A.D.; Zini, G. Lead-acid battery modeling over full state of charge and discharge range. *IEEE Trans. Power Syst.* **2018**, *33*, 6422–6429. [CrossRef]
41. Gunasekaran, M.; Ismail, H.M.; Chokkalingam, B.; Mihet-Popa, L.; Padmanaban, S. Energy management strategy for rural communities' DC micro grid power system structure with maximum penetration of renewable energy sources. *Appl. Sci.* **2018**, *8*, 585. [CrossRef]
42. Bhayo, M.A.; Yatim AH, M.; Khokhar, S.; Aziz MJ, A.; Idris, N.R.N. Modeling of Wind Turbine Simulator for analysis of the wind energy conversion system using MATLAB/Simulink. In Proceedings of the IEEE Conference on Energy Conversion, CENCON, Johor Bahru, Malaysia, 19–20 October 2015; pp. 122–127. [CrossRef]
43. Yu, S.Y.; Kim, H.J.; Kim, J.H.; Han, B.M. SoC-based output voltage control for BESS with a lithium-ion battery in a stand-alone DC microgrid. *Energies* **2016**, *9*, 924. [CrossRef]
44. Camacho, O.M.F.; Mihet-Popa, L. Tests de recharge rapide et intelligente de batteries pour voitures électriques utilisant des énergies renouvelables. *Oil Gas Sci. Technol.* **2016**, *71*, 13. [CrossRef]
45. Zhou, N.; Liu, N.; Zhang, J.; Lei, J. Multi-objective optimal sizing for battery storage of PV-based microgrid with demand response. *Energies* **2016**, *9*, 591. [CrossRef]
46. Ndeke, C.; Marco, A. Energy Management of a Battery Energy Storage System for Renewable Energy DC Microgrid. Master's Thesis, Cape Peninsula University of Technology, Cape Town, South Africa, 2021.

Disclaimer/Publisher's Note: The statements, opinions and data contained in all publications are solely those of the individual author(s) and contributor(s) and not of MDPI and/or the editor(s). MDPI and/or the editor(s) disclaim responsibility for any injury to people or property resulting from any ideas, methods, instructions or products referred to in the content.

CHAPTER 5: HYBRID MICROGRID LOCAL CONTROLLER

Article 3: Implementation of Local Controller for Micro-Grid System

The principal controller implementation for various hybrid micro-grid applications is covered in this chapter. Low-level variables including the injection of voltage, current, and frequency into the VSC are locally regulated by the primary controller are also discussed. It has been seen that zero-level micro-grid control is another term for the management of these variables, which pertain to different power converter control operations based on how they function in the AC micro-grid. Moreover, the definition and application of various primary control operations for distinct micro-grid cases that utilize a DC source and PV array are examined. DC voltage regulation is an essential part of the system because solar panels provide DC power that requires regulation to guarantee consistent as well as dependable operation. Since the inverter is directly connected to PV arrays, thus the PQ method is utilized because this PQ controller handled the AC power injection. The PQ method regulates the power flow between a power source and a load by controlling the real and reactive powers independently. The PV voltage and current are adjusted to match those of the load. To achieve the control, PI controller are used to receive input signals from measured load voltage and current values. The output voltage is adjusted to regulate the reactive power, while the output current is adjusted to control the real power used in the simulation. These two outputs (voltage and current) are adjusted to reach the required power flow while maintaining synchronization with the load.

Implementation of Local Controller for Microgrid System

Christian Ndeke Bipongo*, Marco Adonis, Ali-Almaktoof

Department of Electrical, Electronic and Computer Engineering, Cape Peninsula University of Technology, Cape Town 7535, South Africa
* Corresponding author. Tel.: +27-62-836-2466., *E-mail address:* ndekechristian@gmail.com / 219385017@mycput.ac.za

Abstract

This paper focuses on a comprehensive overview of the design, implementation, and optimization of local controller for microgrid systems. The implementation of local controller contributes significantly to improve the performance, stability, and reliability of microgrid systems. The local controller, situated at distributed energy resources (DERs) or specific points within the microgrid, enables autonomous operation, seamless grid integration, and effective management of generation, storage, and load resources. The aim of this study is to develop a local microgrid controller that improves distribution-level microgrid voltage regulation for stable and consistent operation. This paper has as principal objective to implement control techniques like voltage and current controls to achieve the desired power flow while maintaining synchronization with the load in different microgrid system applications using MATLAB/Simulink software. Additionally, the use of advanced technologies like artificial intelligence (AI), blockchain technology (BT), and predictive control, is explored to enhance the intelligence, adaptability, and resilience of local controller in dynamic microgrid environments. The results of the simulation show the efficiency and performance of local controller in improving microgrid stability, power quality, and energy efficiency. Additionally, this paper contributes to provide valuable insights into the implementation of local controller for microgrid systems, offering guidance for researchers, engineers, and practitioners involved in microgrid design, operation, and optimization.

Highlights

- A local controller design for microgrid systems, ensuring stability and reliability in the operation of distributed energy resources (DERs) within the microgrid.
- The controller design offers scalability and flexibility to accommodate varying microgrid configurations and operational requirements, making it suitable for a wide range of microgrid applications, from small-scale community systems to larger industrial installations.
- Through coordinated control of distributed energy resources (DERs) like solar photovoltaics (PV), the local controller enhances grid stability by regulating voltage, current, and power flow within the microgrid.
- The local controller optimizes energy management techniquees, maximizing the utilization of renewable energy sources while ensuring seamless transition between grid-connected and islanded modes of operation.

Keywords: Local Controller; Micro-Grid System; Distributed Energy Resources; DC Control; Grid-following

1. Introduction

In recent years, microgrid system has become a viable remedy for enhancing energy efficiency, reliability, as well as resilience in both grid-connected and isolated environments [1]. These distributed energy systems incorporate diverse renewable energy sources (RESs), energy storage devices, as well as variable loads to form a localized power network capable of operating independently or in coordination with the main grid [2]. A critical component of microgrid systems is the local controller, which governs the individual distributed energy resources (DERs) operation and coordinates their actions to optimize system performance [3]. The implementation of local controller is essential for enabling autonomous operation, maintaining the grid stable and enabling the smooth incorporation of renewable energy sources within microgrid systems. This controller, situated at DERs or specific points within the microgrid, regulate voltage, current, and power flow to ensure reliable and efficient operation. By

leveraging advanced control strategies, communication protocols, and coordination mechanisms, local controller enables dynamic response to changing system conditions, grid disturbances, and load variations [4].

This study aims to provide a comprehensive investigation of the design, implementation, and optimization of local controller for microgrid systems. The study explores various control strategies, including the regulation of both voltage and current to manage their injection into the voltage source converters (VSCs). The motivation of this research is to exhibit the efficacy and performance of local controller in improving microgrid stability, power quality, and energy efficiency. It also provides insights into emerging trends, issues and potential paths forward for local controller implementation in microgrid systems. This paper serves as a comprehensive guide for researchers, engineers, and practitioners involved in the design, operation, and optimization of microgrid systems. By understanding the role and capabilities of local controller, researchers can develop innovative solutions to address the growing demand for sustainable and resilient energy infrastructure. The implemented local control is developed utilizing MATLAB / Simulink software.

The following is the reminded paper organization: in Section 2, the local controller role is discussed. Local control in grid-following mode is discussed in Section 3. Section 4 provides a short discussion. Section 5 brings the paper to a final conclusion.

1. Role of Local Controller

The role of a local controller in a microgrid system is multifaceted and crucial for the overall performance and stability of the system. The local controller regulates the levels of voltage and frequency within the microgrid to guarantee that they remain within acceptable limits. This is essential for maintaining power quality and grid stability [5]. To manage the flow of power between DERs, energy storage devices, as well as the loads to minimize losses and maximize the energy utilization, a local controller is very important. The local controller serves as the intelligence hub of the microgrid, ensuring efficient and reliable operation while enabling seamless RESs incorporation, enhancing system resilience and flexibility [6]. A local controller is responsible for managing load sharing among distributed energy resources in the microgrid, which prevents undesired circulating currents [7].

1.1. Integration of Advanced Technologies

The integration of advanced technologies into the local controller of a microgrid system enhances its intelligence, adaptability, and performance. Several advanced technologies can be leveraged to augment the capabilities of local controllers. Fig. 1 presents different advanced technologies in the local controller of microgrid systems.

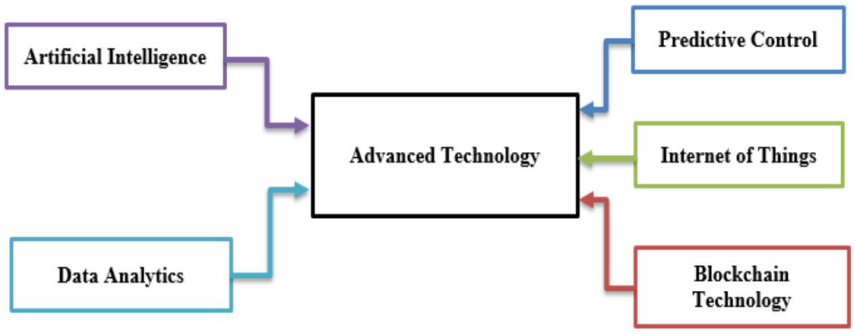


Fig. 1. Advanced technologies in local controller.

By integrating these advanced technologies into the local controller, microgrid systems can achieve higher levels of automation, optimization, and resilience. This enables more efficient energy management, greater grid stability,

and improved integration of renewable energy sources, ultimately advancing the sustainability and reliability of microgrid operations. The summary of different advanced technologies is presented in Table 1.

Table 1. An example of a table.

Artificial Intelligence (AI)	AI methods like machine learning (ML) and neural networks enable local controllers to get knowledge of historical data and adjust their control strategies according to the real-time conditions. AI algorithms can improve energy efficiency, forecast load patterns, and anticipate system faults, thereby improving efficiency and reliability of the entire system [8].
Data Analytics	Advanced data analytics techniques allow local controllers to analyse large volumes of data from sensors, meters, and additional resources to determine patterns, trends, and anomalies [9]. This enables proactive maintenance, fault detection, and optimization of system performance.
Predictive Control	Predictive control algorithms utilize mathematical models of the microgrid system to forecast system behaviour in the future and adjust control measures accordingly. By anticipating changes in load demand, weather conditions, or grid disturbances, predictive control enhances the responsiveness and stability of the microgrid [10].
Internet of Things (IoT)	IoT components like smart meters, sensors, and actuators provide data in real time about grid conditions, production, and consumption of energy. By integrating IoT technology, local controllers can gather comprehensive data for decision-making, optimize energy usage, and improve system reliability [11].
Block-chain Technology	Block-chain technology offers secure, transparent, and decentralized data management for microgrid transactions, energy trading, and grid coordination. Local controllers can use block-chain-based systems to validate transactions, enforce contracts, and maintain an auditable record of energy transactions within the microgrid [12].

2. Local Control in Grid-Following Operation

In order to function in the grid-supporting mode, the grid-following converter incorporates voltage droop regulators and a higher-level frequency [13]. Fig. 2 shows a traditional grid-following inverter (GFLI) block schematic. The interaction between the grid and the inverter-based resource (IBR) is facilitated through its filter. The filter is represented by the series resistance, R_f, and the inductor, L_f. The grid, together with the inductance (L_g) and the resistance (R_g) connected in series, constitute the ideal voltage source. The GFLI model has as main goal to control the exchange of electricity between the inverter and the grid. It is often accomplished through a vector current controller, to which external power control loops supply the references, or $I_{dq,ref}$, and the grid phase-angle is used to enable the conversion of the inverter current to a d_q frame [14].

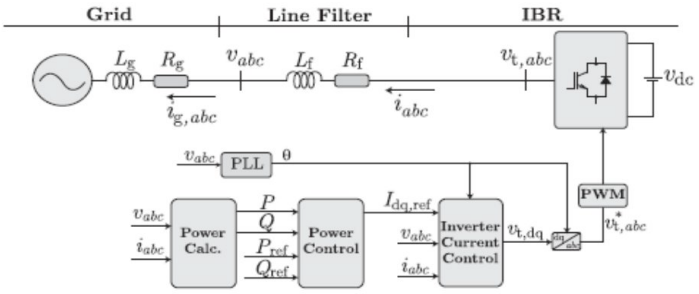


Fig. 2. A traditional GFLI control block schematics [14]

A phase-locked control (PLL) at the point of connection (POC) in GFLIs provides the phase-angle of the grid voltage. The outputs of reactive and active powers are regulated by the GFL mode. To successfully share real and reactive powers and regulate their transmitted amount with the grid. The grid voltage and the GFLI have to be correctly synchronized at the point of common coupling (PCC) [15]. To achieve this, the PCC frequency and phase angle must be estimated using a grid [16]. Both are accomplished with the PLL. During the GFL mode control, the successful synchronization process is followed by the conversion of DC quantity into AC quantity by a grid-connected inverter, which also regulates the active power and reactive power injection. The frequency and voltage of PCC are maintained by the main grid in this mode [17]. Fig. 3 presents a GFLI architecture, which also includes parts for power reference and measurement. Power and current control loops are shown sequentially.

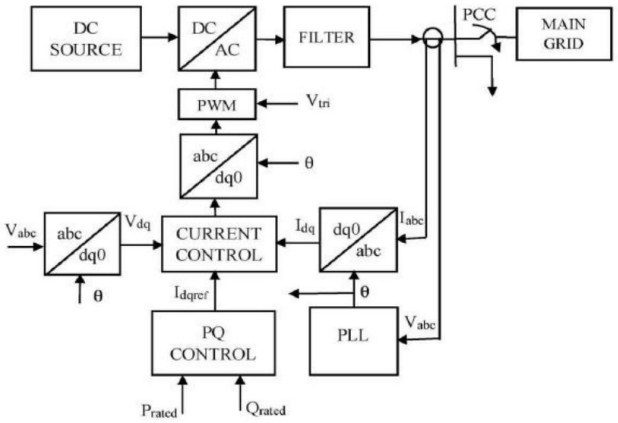


Fig. 3. Grid-following inverter diagram [17]

Similar to a constant power inverter, the grid-following inverter tracks the needed power reference with its output power. The active power and reactive power in this control mode are adjusted by adjusting I_d and I_q, respectively.

2.1. PQ Control

By independently adjusting real and reactive powers, the flow of the energy between the power source and the load is regulated by the real and active power (PQ) control [18]. In grid-following mode, the power electronics system has to stay in synchronization with the grid frequency and voltage. For this to be achieved, the voltage and current of the power electronics system are adjusted to match the grid's [19]. This objective is achieved by using the PQ control strategy. PI controllers are used to receive input signals from measured grid voltage and current levels in order to achieve control [20]. The PI controllers then generate the control signals needed to modify the outputs voltage and current of the power electronics system.

The output voltage is adjusted to regulate the reactive power, while the output current is adjusted to control the real power [21]. The PI controllers integrate proportional and integral control to achieve precise and consistent power flow regulation [22]. To keep the power electronics system in sync with the grid, a synchronization algorithm is also incorporated into the control algorithm. To do this, a PLL is used, which regulates the power electronics system output voltage and current according to the frequency and phase measurements of the grid [23]. Fig. 4 displays the PQ control diagram.

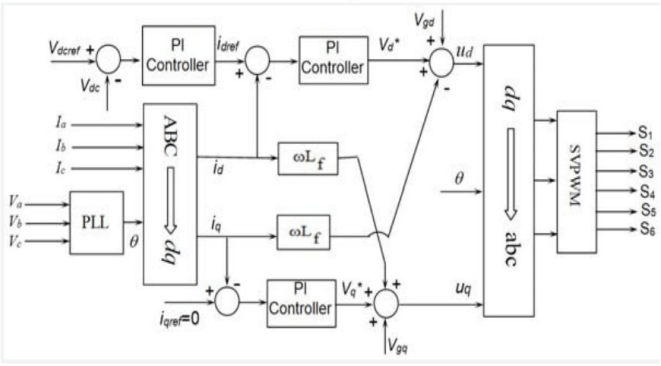


Fig. 4. Diagram of PQ grid-following control [23]

The intended power flow is shown in this block diagram as inputs to the PQ control algorithm. Two PI controllers receive the error signals after the desired and measured grid voltage and current are compared. According to Jayalakshmi et al. (2019), one PI controller controls the actual power (P) by modifying the power electronics system output current, while the other PI controller controls the reactive power (Q) by modifying the output voltage [23]. Using a PLL, the synchronization algorithm analyses the grid phase and frequency and modifies the power electronics system output voltage and current to keep it in sync with the grid [24].

To achieve the intended power flow while keeping synchronization with the grid, the output voltage and current are adjusted [25]. Following that, during the Space Vector Pulse Width Modulation (SVPWM) phase, the pertinent pulses are produced and transferred to the VSC transistor gates. Figure 5 illustrates the simulated model utilized for the validation of the control model presented in Figure 4. The parameters for the LCL filter's computation components are listed in table 2. These specifications are designed to manage power levels of about 1MVA.

Table 2: Parameters of the LCL filter design

Parameters	Symbols	Values
Line to line voltage	V_{LL}	380 V
Nominal power	P_n	1 MW
DC-link voltage	V_{dc}	800 V
Inverter configuration	3φ	Three phase system
Power factor	pf	1
Grid frequency	f_g	50 Hz
Switching frequency	f_{sw}	30 kHz

It is possible to determine various LCL filter parameters by utilizing the values listed in Table 2. Equations (1) and (2) are used to calculate the base capacitance and base impedance:

$$Z_b = \frac{{V_{LL}}^2}{P_n} \tag{1}$$

$$Z_b = \frac{380^2}{1000000} = 0.1444\ \Omega$$

$$C_b = \frac{1}{\omega_n Z_b} \tag{2}$$

$$C_b = \frac{1}{2 \times \pi \times 50 \times 0.1444} = 22.1\ mf$$

The inductor on the inverter side can be found by replacing L_i in Equation (3), provided that the inverter-side inductor is chosen to be 5% of the base impedance as allowable current ripple, which meets the 10% of nominal current value limit criteria:

$$X_{Lpu} = \frac{\omega_n L_i}{Z_b} \tag{3}$$

$$L_i = \frac{X_{Lpu} Z_b}{\omega_n} = \frac{0.05 \times 0.1444}{2 \times \pi \times 50} = 22.99\ \mu H$$

Based on the L_i calculation above, the LCL filter should reduce the likely current ripple below 10%. When the grid-side inductor is added, the ripple should be further reduced by 2%, as calculated below. The primary goal of the inductance at the grid side, the ripple attenuation, is established by the constant "r," which describes the relationship between the inverter-side and grid-side inductors and is calculated using Equation (4).

$$L_g = rL_i \tag{4}$$

Since the inductive reactance is determined by Equation (5), the LCL filter total inductance is assumed to be 0.09 per unit.

$$L_{TOTAL} = \frac{X_{L-TOTALpu} Z_b}{\omega_n} \tag{5}$$

$$L_{TOTAL} = \frac{0.09 \times 0.1444}{2 \times \pi \times 50} = 41.39\ \mu H$$

The total inductance and the inverter side inductance can be utilized to calculate the grid side inductance using the inverter side inductance.

$$L_g = L_{TOTAL} - L_i = 41.39\ \mu H - 22.99\ \mu H$$

$$L_g = 18.4\ \mu H$$

The maximum power factor fluctuation, or 5% multiplied by the base capacitance value of the system, can be used to calculate the filter capacitance. Equation (6) is used to determine the filter capacitance C_f, which acts as a sink for high-frequency harmonics.

$$C_f = \beta \times C_b \tag{6}$$

$$C_f = 0.05 \times 22.1\ mf = 1.11\ mF$$

When the results for a range of values of "r" are displayed, the filter transfer function for a particular resonant frequency can be calculated by using the nominal grid impedance. Resonance can be avoided by reducing the ripple on the switching frequency and connecting the capacitor and the dampening resistor R_f in series. The filter

resonance is calculated using Equation (7). The resistor value selected should be one-third of the filter capacitor impedance at the resonant frequency.

$$f_{res} = \frac{1}{2\pi}\sqrt{\frac{L_i + L_g}{L_i L_g C_f}} \tag{7}$$

$$f_{res} = \frac{1}{2\pi}\sqrt{\frac{22.99\ \mu H + 18.4\ \mu H}{22.99\ \mu H \times 18.4\ \mu H \times 1.11\ mF}} = 47.29\ Hz$$

$$\omega_{res} = 2 \times \pi \times f_{res} = 2 \times 3.14 \times 47.29\ kHz = 296.98\ \ rad/sec$$

By connecting the filter capacitor C_f in series with the resistor R_f, which functions as a damping resistor, passive damping is produced. The VSI control system stabilization depends on the passive damping. The damping effect increases with the damping value of the resistor; yet, this can have an undesirable negative impact on efficiency. Equation (8) can be used to calculate the damping resistor.

$$R_f = \frac{1}{3 \times \omega_{res} \times C_f} \tag{8}$$

$$R_f = \frac{1}{3 \times 296.98 \times 1.11\ 10^{-3}} = 1.011\ \Omega$$

The control flowchart in Figure 4 is validated using the model presented in Fig 5. Table 3 presents the parameters for the component parts of the simulation.

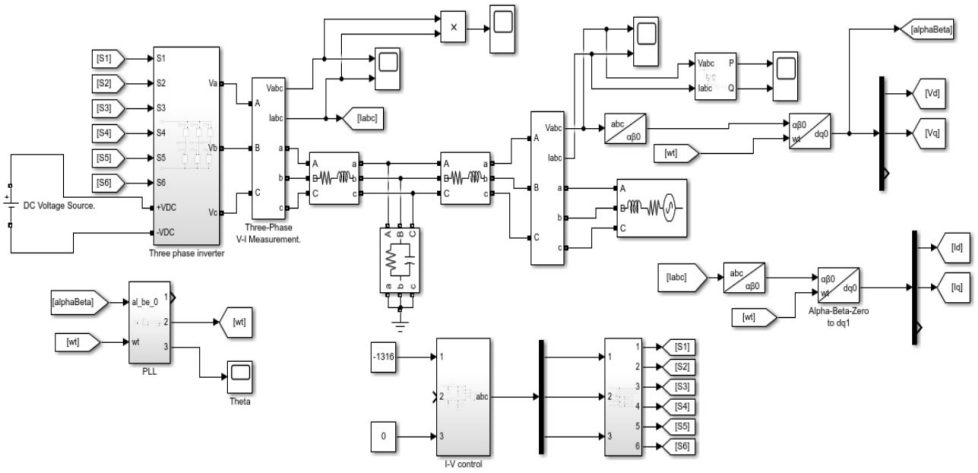


Fig. 5. PQ grid-following Simulink model

Table 3: Simulation parameters for the PQ control

Parameter	Symbol	Value
Rated output voltage of the inverter	V_o	380 V

DC Link voltage	V_{dc}	800 V
Rated power of the inverter	S_B	1 MVA
Grid frequency	f_g	50 Hz
Switching frequency	f_{sw}	30 kHz
DC Link capacitor	C_{DC}	0.1 μH
Grid side inductor	L_g	18.4 μH
Inverter side inductor	L_i	22.99 μH
Filter capacitance	C_f	1.11 mF
Damping resistance	R_f	3.123 mΩ
Resonance frequency	f_{res}	47.29 Hz
Approximated total inductor resistance	R_T	0.1
PLL settling time	$T_{S\,PLL}$	2.25 ms
Active reference power	P_{ref}	1 MW
Reactive reference power	Q_{ref}	0 VAR

The PQ grid-following test results are presented in Fig. 6, where the necessary amount of power is received by the grid and its output results of the voltage and current display sinusoidal waveforms with little harmonic content.

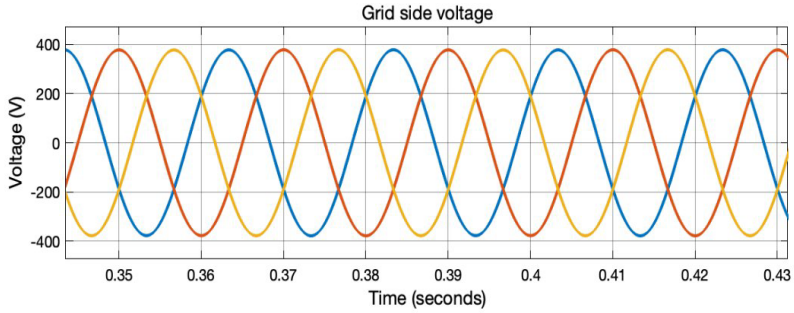


Fig. 6a. Grid output voltage

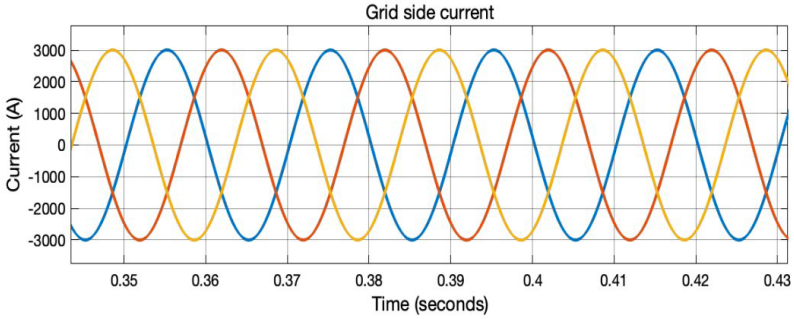


Fig. 6b. Grid output current

Fig. 7 present the output results of the active power and reactive power from the grid side. From the simulations it is seen that the right quantity of generated power is fed into the grid.

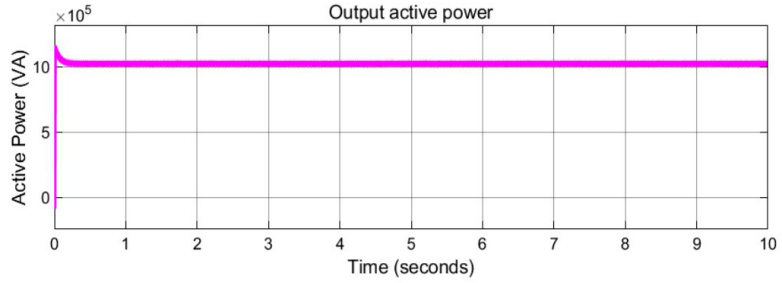


Fig. 7a. Grid-side active output power

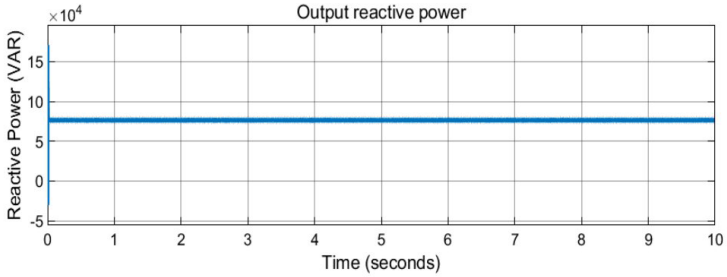


Fig. 7b. Grid-side reactive output power

Fig. 8 shows the PQ grid-following test results, in which the inverter output voltage is presented.

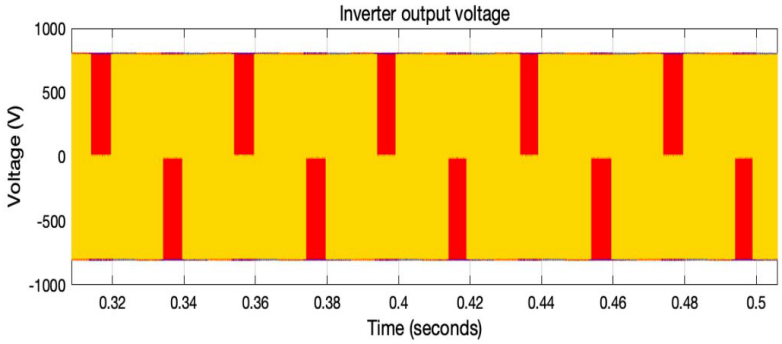


Fig. 8. Inverter output voltage

The inverter output current display sinusoidal waveforms and there is a very minimal harmonic content. The grid is supplied with the necessary power quantity as illustrated in Fig. 9.

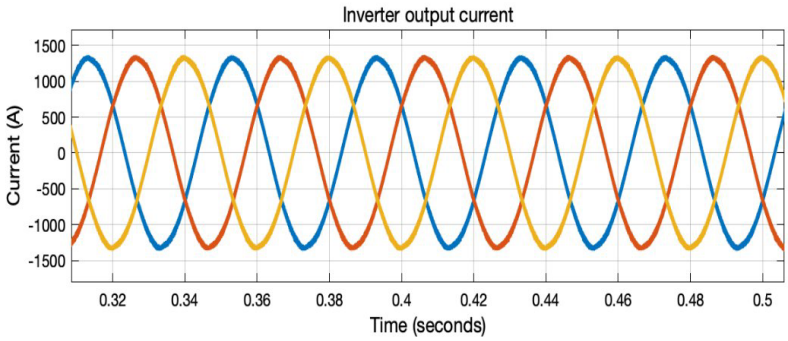


Fig. 9. Output voltage from the inverter

2.2. Regulation of the DC Voltage

The injection of an AC power is handled by a PQ controller and do not consider the DC link voltage regulation, this is managed by a stiff DC supply, which is not always available for distributed renewable energy sources; the DC link voltage needs to be regulated by a power converter like a DC/DC converter [26]. This technique is used when inverters are indirectly connected to a wind turbine via another converter which regulates its generator; or when they are directly connected to an intermittent power supply, like PV source [27].

The cell temperature and radiation levels of the sun affect the current and voltage fluctuations in photovoltaic arrays. As a result, DC regulators are required to change the voltage levels of these energy sources according to the situation at diverse periods to maximize the power of PV. The reference of the DC voltage, which provides the voltage of the maximum power point (MPP) at a specific moment, is determined by a maximum power point tracking (MPPT) algorithm [28]. The MPPT in PV systems is commonly achieved by the Perturb and Observe (P&O) algorithm. Finding the operating point at which the PV array generates the most electricity is the objective of the algorithm [29].

PV systems commonly employ this algorithm to boost their efficiency and performance [30]. It could be applied to both software and hardware. Regrettably, the method is prone to oscillations and slow convergence, particularly in settings where environmental changes occur often. To solve these issues, several P&O algorithm variations have been developed, including the perturb and observe with adaptive step size (P&O-AS) algorithm and the incremental conductance algorithm, which offer improved stability and performance under particular operating conditions [31].

DC voltage regulation is an essential part of renewable energy systems since most of renewable energy sources, including PV and wind plants, produces DC power that needs to be regulated to maintain consistent and dependable functioning [32]. Since wind turbines generate AC power, a rectifier is utilized to change its AC power into DC power so that it may be used in a battery. An output voltage of the wind turbine can be controlled with a DC-DC converter circuit, and its output power might be maximized by varying its pitch angle and the speed of the rotor with MPPT controllers [33]. Alternatively, in the event of a generator, the same process can be followed. Fig. 10 shows the DC voltage regulator implementation.

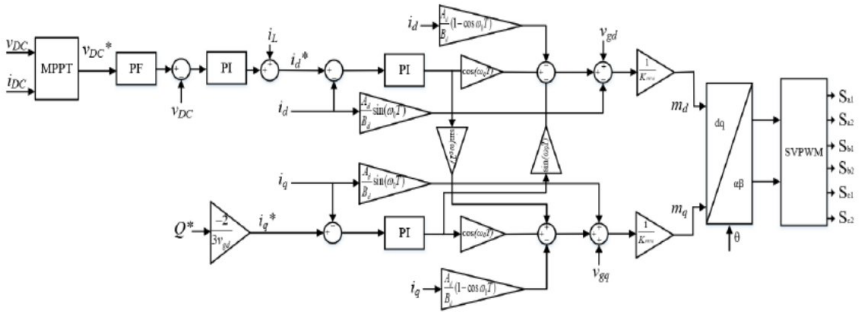


Fig. 10. The control diagram of a DC voltage regulator

Fig. 10 presents the four main stages of this control scheme: the voltage control and current control loops of the DC bus, the MPPT algorithm, which supplies the voltage reference of a DC bus, and the SVPWM phase that generates the matching pulses supplied to the VSC transistor gates [34]. The main difference between the represented model in Figure 5 and Fig. 11 refers to the fact that the DC source is replaced by the PV. Table 4 lists each parameter used in the simulation.

Table 4: Simulation parameters

Parameter	Symbol	Value
Rated output voltage of the inverter	V_o	380 V
MPPT voltage	V_{MPPT}	800 V
Cell temperature	T	25°C
Sun irradiance	I_r	500, 1000 W/m^2
Max power of the PV	P_{PV_max}	500 kW_p
Rated power of the inverter	S_B	1 MVA
Grid frequency	f_g	50 Hz
Switching frequency	f_{sw}	30 kHz
DC Link capacitor	C_{DC}	0.1 μH
Grid side inductor	L_g	18.4 μH
Inverter side inductor	L_i	22.99 μH
Filter capacitance	C_f	1.11 mF
Damping resistance	R_f	3.123 mΩ
Resonance frequency	f_{res}	47.29 Hz
Approximated total inductor resistance	R_T	0.1
PLL settling time	$T_{S\,PLL}$	2.25 ms
Active reference power	P_{ref}	1 MW
Reactive reference power	Q_{ref}	0 VAR

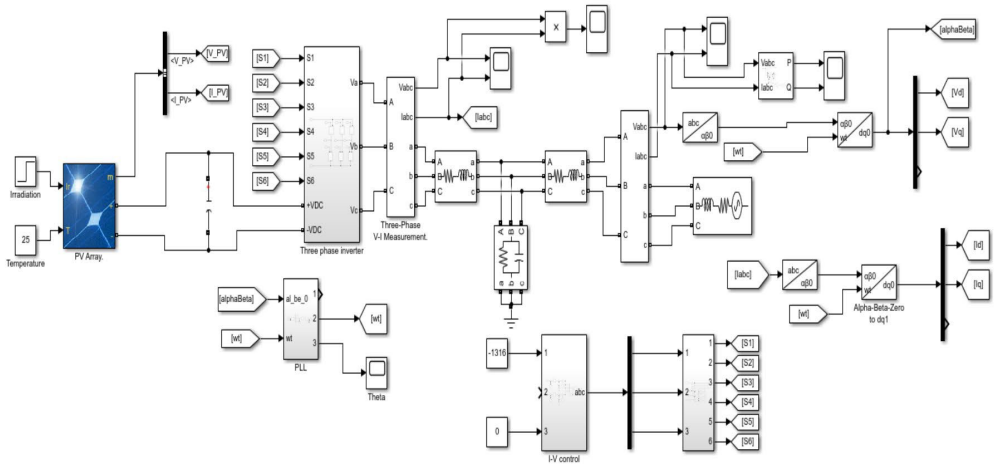


Fig. 11. Simulink model of the DC regulator for the GFL

The PV system consists of 19 parallel strings, having each 186 modules connected in series. This setup yields a DC voltage of about 800V and a power rating of 1 MW, which is in line with the specification of the inverter, as Table listed 4. Fig. 12 presents the test results conducted on the inverter output voltage and current. The output voltages are essentially the same as they were in the previous simulation that used a DC source; they show sinusoidal waveforms with very little harmonic content, and the grid receives the necessary amount of power. As the output current increases, the results in Fig. 12 demonstrate a step rise in irradiance at 1.

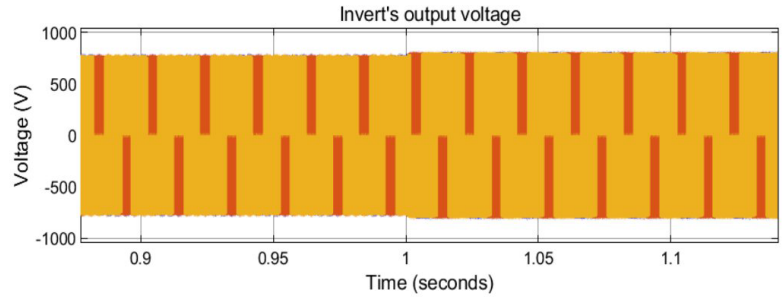


Fig. 12a. Inverter output voltage

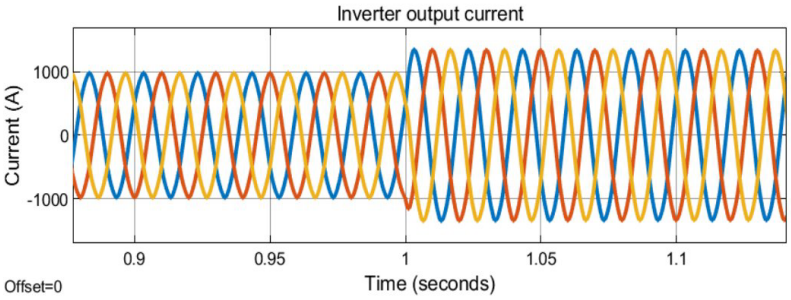


Fig. 12b. Inverter output current

Fig. 13 present the grid side outputs voltage and current test results. These voltages show sinusoidal waveforms with very minimal harmonic content, and the grid receives the necessary quantity of power.

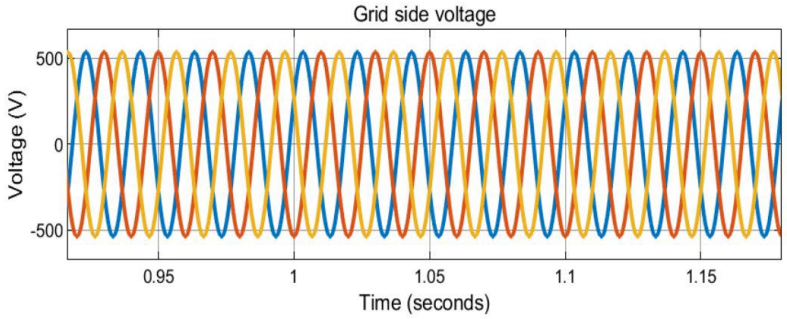


Fig. 13a. Output voltage from the grid-side

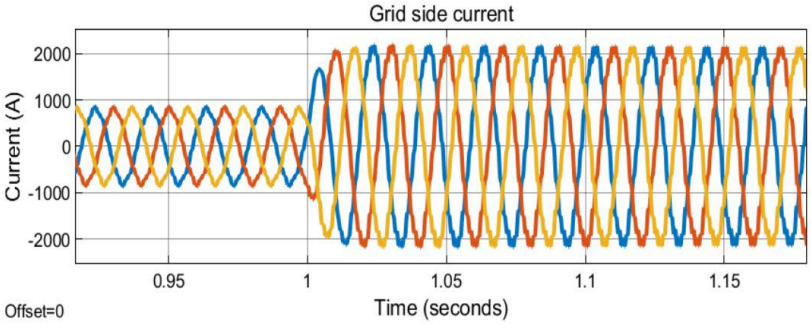


Fig. 13b. Output current from the grid-side

Fig. 14 presents the grid side active output power and reactive output power results. There is a step rise in irradiation, as indicated by the results in Fig. 14, which is consistent with a rise in power output.

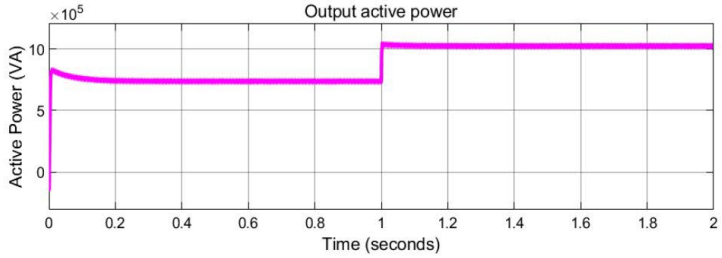


Fig. 14. Active and reactive output powers from the grid-side

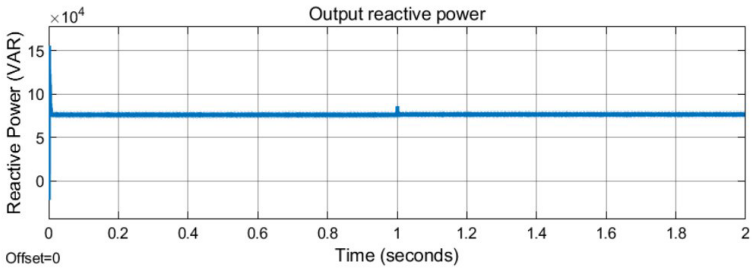


Fig. 14b. Reactive output power from the grid-side

3. Discussion

A local controller technique is designed and developed to demonstrate the voltage regulation operation within a micro-grid at the distribution level. The simulation is conducted in two ways. Firstly, DC source is used and secondly a PV array is utilized. The regulation of the DC voltage system is crucial since solar panels generate DC power, which must be regulated to guarantee steady and dependable operation. Since the PQ controller handled the AC power injection, the PQ controller is chosen because the inverter is directly connected to the PV arrays. By controlling real power and reactive power independently, the PQ control mode is an approach that controls the flow of power between the power source and the load. The voltage and current of the PV arrays are regulated to correspond with the load. A PI controller is used to receive input signals from measured load voltage and current levels to satisfy the control. Figure 14 illustrated that the output voltage is regulated for reactive power control, and the output current is adjusted to control real power. To maintain synchronization with the load and get the desired power flow, the output voltage and current are adjusted.

4. Conclusion

The implementation of local controllers is integral for an effective and reliable microgrid systems operation, facilitating seamless incorporation of distributed energy resources, optimization of energy management, and maintenance of grid stability. This paper presents the local controller implementation for different microgrid applications. The local controller controls low-level factors like frequency, and the injection of voltage and current into the VSCs locally. It is observed that the control of these variables, which relate to the different control modes of power converters depending on how they operate in the AC micro-grid, sometimes referred to as control of micro-grid at zero level. The definition and application of different local control models for diverse microgrid implementations that use a DC source and PV array are examined. The results of the simulation show how well the local controller operates and is effective in improving microgrid stability, power quality, and energy efficiency. The future of local controller implementation in microgrid systems resides in integrating advanced methods like artificial intelligence, machine learning, and predictive control. These technologies enable autonomous decision-making, adaptive control, and optimization of microgrid operations in real time.

Acknowledgements

As the Corresponding Author, I thus declare that this work was completed as a part of doctoral study under the guidance, direction, and editorial support of Drs. Marco Adonis and Ali Almaktoof, who also reviewed and edited the text prior to publication. I also acknowledge the financial support I received from the National Research Foundation (NRF).

Ethical Approval

As neither humans nor animals are the subjects of the research, participant consent was not required for the collecting of data for this project.

Contribution of Authors

As the Corresponding Author, I attest that each of the listed authors has reviewed the work and given their approval for submission. Christian Ndeke Bipongo is the first author named since it is anticipated that he will contribute most to the project's data collecting, analysis, and conception of the testing model. Drs. Marco Adonis and Ali Almktoof are the second and third co-authors of this work, respectively, as they played a crucial role in providing direction, editing, and quality assurance.

Competing Interests

This publication does not have any known conflicts of interest.

Availability of data

Requests for access to the datasets can be made to the corresponding author.

References

[1] Ndeke C. B., Adonis M., and Almaktoof. A., "Energy Management Strategy for DC Micro-Grid System with the Important Penetration of Renewable Energy," applied sciences (MDPI) 2024.

[2] Ndeke C. B., Adonis M., and Almaktoof A., "Energy management strategy for a hybrid micro - grid system using renewable energy," *Discov. Energy*, 2024.

[3] Sharma R., Zakerian A., and Karimi G. M., "Local Controller for an Autonomous Grid-Supportive Battery Energy Storage System," *IEEE Trans. Power Electron.*, vol. 37, no. 2, pp. 2191–2202, 2022.

[4] Abhishek A., Ranjan A., Devassy S., Kumar V. B., Ram S. K., and Dhakar A. K., "Review of hierarchical control strategies for DC microgrid," *IET Renew. Power Gener.*, vol. 14, no. 10, pp. 1631–1640, 2020.

[5] Abbasi M., Abbasi E., Li L., Aguilera R. P., Lu D., and Wang F., "Review on the Microgrid Concept, Structures, Components, Communication Systems, and Control Methods," *Energies*, vol. 16, no. 1, 2023.

[6] Ahmed K., Seyedmahmoudian M., Mekhilef S., Mubarak N. M., and Stojcevski A., "A Review on Primary and Secondary Controls of Inverter-interfaced Microgrid," *J. Mod. Power Syst. Clean Energy*, vol. 9, no. 5, pp. 969–985, 2021.

[7] Ashok K. A. and Amutha P. N., "A comprehensive review of DC microgrid in market segments and control technique," *Heliyon*, vol. 8, no. 11, p. e11694, 2022.

[8] Mohammadi E., Alizadeh M., Asgarimoghaddam M., Wang X., and Simoes M. G., "A Review on Application of Artificial Intelligence Techniques in Microgrids," *IEEE J. Emerg. Sel. Top. Ind. Electron.*, vol. 3, no. 4, pp. 878–890, 2022.

[9] Zhang Y., Huang T., and Bompard E. F., "Big data analytics in smart grids: a review," *Energy Informatics*, vol. 1, no. 1, pp. 1–24, 2018.

[10] Shahzad S., Abbasi M. A., Chaudhry M. A., and Hussain M. M., "Model Predictive Control Strategies in Microgrids: A Concise Revisit," *IEEE Access*, vol. 10, no. October, pp. 122211–122225, 2022.

[11] Li S., Patnaik S., and Li J., "IoT-Based Technologies for Wind Energy Microgrids Management and Control," *Electron.*, vol. 12, no. 7, pp. 1–7, 2023.

[12] Khubrani M. M. and Alam S., "Blockchain-Based Microgrid for Safe and Reliable Power Generation and Distribution: A Case Study of Saudi Arabia," *Energies*, vol. 16, no. 16, 2023.

[13] Zuo Y., Yuan Z., Sossan F., Zecchino A., Cherkaoui R., and Paolone M., "Performance assessment of grid-forming and grid-following converter-interfaced battery energy storage systems on frequency regulation in low-inertia power grids," *Sustain. Energy, Grids Networks*, vol. 27, p. 100496, 2021.

[14] Bahrani B., "Power-synchronized grid-following inverter without a phase-locked loop," *IEEE Access*, vol. 9, pp. 112163–112176, 2021.

[15] Anttila S., Döhler J. S., Oliveira J. G., and Boström C., "Grid Forming Inverters: A Review of the State of the Art of Key Elements for Microgrid Operation," *Energies*, vol. 15, no. 15, pp. 1–30, 2022.

[16] Yusuf S. S. and Abubakar A. S., "A Comprehensive Review on Grid-forming Inverter : Potential and Future Trends," vol. 17, no. 1, pp. 1–27, 2023.

[17] Rani P., Murugesan S., and Singh A. K., "Modeling and Implementation of Grid Following and Grid Forming Inverters."

[18] Chen M. R., Wang H., Zeng G. Q., Dai Y. X., and Bi D. Q., "Optimal P-Q control of grid-connected inverters in a microgrid based on adaptive population extremal optimization," *Energies*, vol. 11, no. 8, 2018.

[19] She B., *et al.*, "Inverter PQ Control with Trajectory Tracking Capability for Microgrids Based on Physics-informed Reinforcement Learning," *IEEE Trans. Smart Grid*, vol. PP, p. 1, 2023.

[20] Hossen T. and Mirafzal B., "On Stability of PQ-Controlled Grid-Following and Droop-Control Grid-Forming Inverters," *2022 IEEE Energy Convers. Congr. Expo. ECCE 2022*, pp. 1–7, 2022.

[21] Gao X., Zhou D., Anvari M. A., and Blaabjerg F., "Grid-Following and Grid-Forming Control in Power Electronic Based Power Systems: A Comparative Study," *IECON Proc. (Industrial Electron. Conf.*, vol. 2021-Octob, pp. 1–6, 2021.

[22] Ahmad S., Mekhilef S., and Mokhlis H., "DQ-axis Synchronous Reference Frame based P-Q Control of Grid Connected AC Microgrid," *2020 IEEE Int. Conf. Comput. Power Commun. Technol. GUCON 2020*, pp. 842–847, 2020.

[23] Jayalakshmi N. S., Gaonkar D. N., and Jain S. K., "Power smoothing method of PMSG based grid integrated wind energy conversion system using BESS/DSTATCOM," *Int. J. Power Electron. Drive Syst.*, vol. 10, no. 4, pp. 1969–1976, 2019.

[24] Khan A., Easley M., Hosseinzadehtaher M., Shadmand M. B., Abu R. H., and Fajri P., "PLL-less Active and Reactive Power Controller for Grid-Following Inverter," *ECCE 2020 - IEEE Energy Convers. Congr. Expo.*, pp. 4322–4328, 2020.

[25] Zamee M. A., Han D., and Won D., "Integrated grid forming-grid following inverter fractional order controller based on Monte Carlo Artificial Bee Colony Optimization," *Energy Reports*, vol. 9, pp. 57–72, 2023.

[26] Avdeev B. A., Vyngra A. V., and Sobolev V. S., "Integration of Renewable Energy Sources into Smart Grids Using Converters Based on Solid-State Transformers," *2022 5th Int. Youth Sci. Tech. Conf. Relay Prot. Autom. RPA 2022*, pp. 1–10, 2022.

[27] Korompili A. and Monti A., "Review of Modern Control Technologies for Voltage Regulation in DC/DC Converters of DC Microgrids," *Energies*, vol. 16, no. 12, p. 4563, 2023.

[28] Zhou X., Liu Q., Ma Y., Li W., and Xie B., "A modified ladrc-based dc-link voltage controller for photovoltaic grid-connected inverters," *Electron.*, vol. 10, no. 8, 2021.

[29] AL W. I. *et al.*, "Maximum power extraction and DC-Bus voltage regulation in grid-connected PV/BES system using modified incremental inductance with a novel inverter control," *Sci. Rep.*, vol. 12, no. 1, pp. 1–21, 2022.

[30] Liu H. D., Lin C. H., Der L. S., and Ahmad J., "A Novel VFVDC Optimized Full Bridge Inverter Control Strategy for Independent Solar Power Systems," *IEEE Access*, vol. 10, pp. 44231–44247, 2022.

[31] Manuel N. L. and İnanç N., "Sliding Mode Control-Based MPPT and Output Voltage Regulation of a Stand-alone PV System," *Power Electron. Drives*, vol. 7, no. 1, pp. 159–173, 2022.

[32] U. Distributed and E. Storage, "Using Distributed Energy Storage Systems," 2022.

[33] Mumtaz F., Zaihar Y. N., Tanzim M. S., Singh B., Kannan R., and Ibrahim O., "Review on non-isolated DC-DC converters and their control techniques for renewable energy applications," *Ain Shams Eng. J.*, vol. 12, no. 4, pp. 3747–3763, 2021.

[34] Jamal I., Elmorshedy M. F., Dabour S. M., Rashad E. M., Xu W., and Almakhles D. J., "A Comprehensive Review of Grid-Connected PV Systems Based on Impedance Source Inverter," *IEEE Access*, vol. 10, pp. 89101–89123, 2022.

CHAPTER 6: ENERGY MANAGEMENT SYSTEM FOR A HYBRID RENEWABLE AC MICRO-GRID SYSTEM

Article 4: Energy Management Strategy for a Hybrid Micro-Grid System Using Renewable Energy

An energy management system for a hybrid micro-grid system using renewable energy sources is provided in this chapter. For a hybrid renewable micro-grid system to operate efficiently, it needs a sophisticated energy management plan that can handle the intricate relationships between various energy sources and loads. Certain aspects, such as variations in demand and weather patterns, must be taken into account in this method. It is important to accomplish the main goals of these systems, which are to maximize the use of renewable energy, lower greenhouse gas emissions, encourage energy independence, and maintain grid resilience.

This article aims to maximize the deployment of renewable energy resources and increase their integration in the power system by developing an energy management system for a hybrid renewable micro-grid system. Thus, the main objective of this work is to implement an energy management strategy that regulates the energy flow between the hybrid micro-grid system and the load as well as the utility grid using MATLAB/Simulink software. The second goal is to control the battery charge and discharge. According to the energy management strategy, the battery could only be charged if the amount of power produced from renewable sources accounted for at least 20% of the overall amount produced.

The results demonstrate that the developed algorithm is able to maintain a proper relationship between the battery charging and discharging rates based on its operating conditions, control the energy flow between the hybrid micro-grid system and the variable AC load, which is directly connected to micro-grid and connected to the utility grid. Finally, battery SOC is maintained within allowable bounds because of the charging conditions that use higher charging power.

Discover Energy

Research

Energy management strategy for a hybrid micro-grid system using renewable energy

Christian Bipongo Ndeke[1] · **Marco Adonis**[1] · **Ali Almaktoof**[1]

Received: 16 October 2023 / Accepted: 1 February 2024
Published online: 08 February 2024
© The Author(s) 2024 OPEN

Abstract
This paper introduces an energy management strategy for a hybrid renewable micro-grid system. The efficient operation of a hybrid renewable micro-grid system requires an advanced energy management strategy able to coordinate the complex interactions between different energy sources and loads. This strategy must consider some factors such as weather fluctuations and demand variations. Its significance lies in achieving the overarching objectives of these systems, including optimizing renewable energy utilization, reducing greenhouse gas emissions, promoting energy independence, and ensuring grid resilience. The intermittent nature of renewable sources necessitates a predictive approach that anticipates the energy availability and adjusts the system operation. The aim of this study was to develop an energy management system for a hybrid renewable micro-grid system to optimize the deployment of renewable energy resources and increase their integration in the power system. Therefore, the main objective of this work was to develop an energy management strategy that controls the flow of energy between the hybrid micro-grid system and the load connected directly as well as the load connected to the utility grid using MATLAB/Simulink software. The second objective was to control the charging and discharging of the battery. The results show that the developed algorithm was able to control the energy flow between the hybrid micro-grid system and the utility grid and also to ensure a proper relation between the charging /discharging rate of the battery based on their operating conditions. In this application, the battery was charged at higher power. It was seen that a higher charging power enables to fully recharge the battery in a shorter amount of time than usual. The results have shown that it is possible to maximize the charging time by using a greater power and this algorithm ensures the state of charge (SOC) of battery to remain in the admissible limits (between 20 and 100%).

Keywords Energy management strategy · Hybrid micro-grid · Renewable energy sources · Battery energy storage · Distributed generation

Abbreviations

AC	Alternating current
DC	Direct current
DER	Distributed energy resources
DG	Distributed generation
EMS	Energy management system
ESS	Energy storage system
Kv	Kilo volt

✉ Christian Bipongo Ndeke, ndekechristian@gmail.com; Marco Adonis, AdonisMA@cput.ac.za; Ali Almaktoof, ALMAKTOOFA@cput.ac.za | [1]Department of Electrical, Electronic and Computer Engineering, Cape Peninsula University of Technology, Cape Town 7535, South Africa.

KWh Kilowatt hour
KWp Kilowatt peak
MW Mega watt
PCC Point of common coupling
PV Photovoltaic
SOC State of charge

1 Introduction

The global energy landscape is undergoing a paradigm shift, marked by a heightened focus on sustainability and a transition towards renewable energy sources [1]. Micro-grid systems, characterized by their localized generation and distribution capabilities, have gained prominence as a means to enhance energy resilience and efficiency [2]. Hybrid micro-grid systems combine multiple sources of energy, often integrating conventional and renewable sources, to create a robust and adaptive energy infrastructure. This integration necessitates sophisticated energy management strategies to harness the full potential of diverse energy resources and ensure a reliable power supply. While the integration of renewable energy into micro-grid systems offers many benefits, it introduces challenges that must be addressed for effective implementation. The intermittent nature of renewable sources, variability in energy production, and the mismatch between energy supply and demand pose significant hurdles [3].

Additionally, the integration of diverse energy storage technologies and the seamless coordination of multiple energy sources require advanced control strategies. Addressing these challenges is essential for realizing the full economic and environmental potential of hybrid micro-grid systems [4]. A thorough examination of the existing literature reveals a growing body of research dedicated to the optimization of hybrid micro-grid systems. Studies have explored various aspects, including energy management algorithms, control strategies, and the integration of different renewable energy sources [5]. Different contributions have been made in the areas of predictive modeling, real-time monitoring, and economic dispatch strategies. However, there remains a need for more comprehensive approaches that address the unique challenges of hybrid micro-grid systems, considering both technical and economic factors [6, 7].

This research aimed to contribute to the existing body of knowledge by developing an advanced energy management strategy for hybrid micro-grid systems using renewable energy sources. The study explored the integration of solar, wind, and diesel generator, coupled with a battery energy storage, to create a resilient and efficient energy network. The focus was on addressing challenges related to intermittency, optimizing energy dispatch, and ensuring grid stability. The motivation behind this research lied in the imperative to accelerate the adoption of sustainable energy solutions. By developing a robust energy management strategy for hybrid micro-grid systems, this study provides practical insights for engineers, policymakers, and stakeholders involved in the planning and implementation of renewable energy projects. The potential impact extends beyond theoretical advancements, offering tangible contributions to the transition towards a cleaner and more sustainable energy future.

The primary contribution of this study included an advanced energy management algorithm. Developing an algorithm to optimize the coordination of renewable energy sources and battery energy storage within a hybrid micro-grid. Moreover, the research had the objective to provide practical guidelines for the design and operation of hybrid micro-grid systems, fostering a more widespread adoption of sustainable energy practices. The developed hybrid renewable micro-grid model and energy management system algorithm were performed using the Stateflow logical language in the MATLAB/Simulink environment. This paper is organized as follows. Section 2 presents the concept of hybrid micro-grid. In Sect. 3, the energy management strategy is presented. Section 4 presents and evaluates the simulation results of the developed algorithm and finally, Sect. 5 gives the conclusion of the paper.

1.1 Critic on literature

Hybrid micro-grid systems are becoming more prevalent and are finding more interesting applications in different fields. A hybrid micro-grid system is composed of different generation resources including fossil fuel-based (e.g., diesel) and renewable energy-based resources such as solar PV, micro-hydro, wind and biomass. The role of a hybrid micro-grid system is of paramount importance in the current complex energy transition. Hybrid micro-grids are increasingly being adopted worldwide. They can operate in grid connected and island mode. Except for the distributed generation units, a hybrid micro-grid is composed of controllable load and energy storage systems. An energy management system is

important to optimize its performance. The energy management system of a micro-grid includes both generation and demand side management by providing satisfaction of the system constraints, to realize an economical, sustainable, and reliable operation of the micro-grid. An energy management system offers many benefits from production dispatch to energy savings, reactive power support to the regulation of frequency, reliability to loss cost-reduction, energy balance to mitigate greenhouse gas emissions, and customer participation to customer privacy. As the level of the renewable energy sources penetration raises, the requirement of a real-time and robust energy management strategy becomes necessary to connect the distribution generation resources as well as the energy storage systems.

1.2 Existing works related to energy management system of hybrid micro-grid system

A brief overview on the energy management system of hybrid micro-grid system using renewable energy sources is outlined below:

1. Himabindu et al. have developed an optimal energy management strategy. The main objective of the research was to satisfy the power demand by the load and to maintain the state of the charge of the energy storage systems, which included the battery and the hydrogen in a certain range. The results have shown that the method was able to optimize the utilization costs and the lifespan of the energy storage systems. The authors suggested the utilization of other methods to check the performance of the proposed energy management system and also include the grid-connected mode [8].
2. Kang et al. [9] have proposed a small-scale hybrid AC/DC microgrid energy management technique based on Artificial Neural Network control. An EMS operation mode was chosen, an operation profile was chosen in each operation mode, and then ANN training was implemented in each operation mode in order to develop the proposed EMS.
3. Elkazaz et al. [10] have implemented a new energy management system (EMS) that can minimize the micro-grid daily operating cost and maximize the renewable energy source self-consumption by determining the optimal configuration for a central battery energy storage system (BESS) based on a defined cost function was proposed. This EMS had a two-layer structure. Firstly, the upper layer. In this structure a Convex Optimization Technique was used to solve the optimization issue and to determine the reference values for the power that should be drawn by the micro-grid from the main grid utilizing a 15 min sample time. The reference values were then fed to a lower control layer, which uses a 1 min sample time, to determine the settings for the BESS which then ensured that the micro-grid accurately follows these references.
4. Bilbao et al. [11] focused on the optimal operation of hybrid microgrids, based generally on the mathematical modelling. To implement the management of this type of networks requires several challenges and various options. The main contribution of the research was the mathematical modelling of many hybrid microgrid components. This modelling can be utilized in various control and management methods of the network, and its feasibility has been shown in three methods, which include one based on the Decision Tree method, which belongs to the Machine Learning family. The results on a test system of 69 buses showed that it is possible to implement its management.
5. A new hybrid battery and PV-wind turbine power system was proposed by Reddy et al. [12] using Fuzzy Logic control. The dynamic behaviour of the recommended model was examined under various operating conditions. The developed system and its control strategy displayed exceptional performance. The proposed model offers a useful tool for enhancing the efficiency of the smart grid.

However, the study done by Lanre Olatomiwa et al. [13] provided a review on energy management system in hybrid renewable energy systems. In this research, particular consideration was focused on smart grids energy management systems. The methods using fuzzy logic techniques are also presented to develop the energy management systems. The study pointed out that the requirement for a real-time and effective energy management strategies has become very vital to connect the hybrid renewable resources associated with the energy storage systems. This complete review revealed that most of studies on the energy management for a hybrid renewable energy systems have been done in islanded mode, and only a few cases are focused on grid connected. Thus, it is important to develop new strategies and techniques to control and to manage the power flow in a hybrid renewable micro-grid system operating in grid connected mode.

2 Concept of hybrid micro-grid

A typical hybrid micro-grid system refers to a group of distributed generation (DG) systems based on renewable and/or non-renewable resources, including an energy storage system (ESS) as well as local controllable loads, usually connected to the distribution system [14]. It can either operate in grid connected mode or island mode according to the load condition. Hybrid micro-grid systems can be classified in different categories based on the location, size, application, and connectivity [15]. Three types of hybrid micro-grid configurations exist in general, which are remote, grid-connected and networked. Hybrid micro-grid systems can be principally classified into three categories according to the system architecture and voltage characteristics, AC micro-grid, DC micro-grid, and Hybrid AC/DC micro-grid [16].

A hybrid micro-grid is composed of different distributed generation sources; the power from these DGs is collected, converted and distributed based on the load demands. To assure an effective operation of the system, a control strategy is required and it is important when power electronics interface with the system to constitute a single unit. The control system is very important because it also enables to conserve the specific energy supply and the power quality [17]. Figure 1 gives a typical representation of a hybrid micro-grid system, where it can be seen that a micro-grid could also be interconnected with the main grid and includes a diversity of assets and power sources, which provide different services to a range of facilities.

According to the environmental concerns (like atmospheric, ground and water pollution, climate change), the use of fossil fuels, the finite and limited quantities of conventional fuels, the increase in the cost of electrical energy, the need of energy security and the independence of certain nations, increase the necessity to embrace and develop renewable energy resources [18]. The decentralization of electricity supply brings production closer to the point of consumption, increasing system reliability, because when a fault occurs somewhere and as a part of the network is insulated, this will not affect the other branches. Additionally, it increases the efficiency of the entire system because the transmission losses are reduced [19].

Hybrid micro-grid systems are getting more attentions due to the increase in energy needs around the world, with a variable rate between nations and continents. For practical and scientific advantages, important incentives are established to promote the integration of hybrid micro-grid projects for electrification in remote areas and developing nations [20]. To improve the power generating system overall, the hybrid micro-grid depends on the interconnect converter. It also enhances the quality of the power and facilitates the AC or DC power supply between each micro-grid [21].

2.1 Architecture of a hybrid micro-grid system

In the pursuit of a resilient, sustainable, and decentralized energy system, hybrid micro-grid architectures have emerged as a cutting-edge solution that integrates the benefits of diverse distributed energy resources, storage technologies, and intelligent control systems. Figure 2 shows the structure of a hybrid micro-grid. The basic architecture includes a variety of

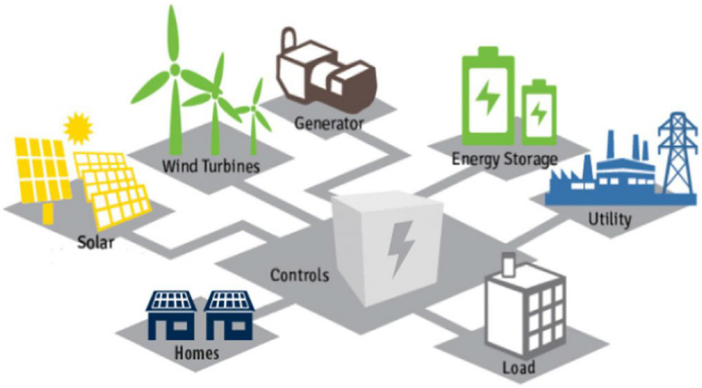


Fig. 1 Hybrid micro-grid concept [17]

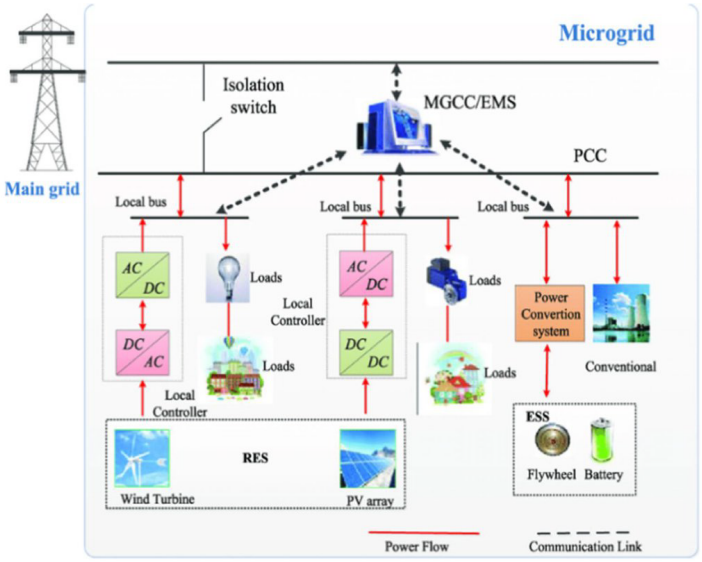


Fig. 2 Micro-grid architecture [24]

renewable energy sources, a conventional generator and different types of loads as well as energy storage devices, which interface with the power electronic systems [22]. For a proper system harmonization and control, the Point of Common Coupling (PCC) defines the operating mode, which can be either grid connected mode or islanded mode. It also allows to connect the micro-grid with the main grid. The PCC has as role to connect or disconnect the hybrid micro-grid system from, or to the main grid. To ensure overall system stability, different levels of control, utilizing micro-sources and central controllers support and coordinate the micro-grid [23].

A hybrid micro-grid architecture represents an innovative approach to energy distribution and management that harmonizes renewable and conventional energy sources, storage technologies, and advanced control systems [25]. Hybrid micro-grids are at the forefront of the global movement to change the energy landscape because they promote the local energy production, improve grid resilience, and contribute to environmental sustainability [26]. Hybrid micro-grids have a compelling potential to shape a more efficient and sustainable energy future as technology advances and the understanding of energy dynamics expands [27]. An energy management system (EMS), which is software-based, manages and controls the flow of energy in a hybrid micro-grid system. It collects real-time data from multiple sensors, such as solar panels, wind turbines, and energy storage devices, and evaluates it to determine the best way to operate the system.

2.2 Energy management controls for hybrid micro-grid

For reliable, sustainable, and efficient energy systems, hybrid micro-grids have emerged as a transformative solution that uses the cooperation of diverse energy sources and storage technologies [28]. For a successful operation of hybrid micro-grids, it is important to implement sophisticated energy management controls [29]. These controls serve as the brains behind the system, coordinating the complex interaction of renewable and conventional energy resources, storage systems, and load demands to optimize the performance, resilience, and environmental impact [30].

Energy management controls for hybrid micro-grids are dynamic, adaptive systems that include a range of hardware and software components designed to monitor, analyze, and direct the flow of energy within the micro-grid. At their core, these controls aim to achieve several key objectives. Different control strategies of the energy management are presented below.

2.2.1 Optimal resource allocation

Hybrid micro-grids often consist of diverse energy sources, including solar PV, wind turbines, fossil fuel generators, and energy storage. The energy management controls determine the most efficient combination of these resources to meet the current energy demand while considering factors such as availability, cost, and environmental impact [31].

2.2.2 Load balancing

The controls actively balance the energy supply and demand by adjusting the distribution of power from different sources. This ensures that the micro-grid operates smoothly, avoiding overloading or underutilization of any particular component [32].

2.2.3 Islanding and grid connection

One of the unique features of hybrid micro-grids is their ability to switch between grid-connected and islanded modes. The energy management controls monitor grid conditions and initiate a seamless transition between these modes as needed, ensuring continuity of power supply and maintaining stability [33].

2.2.4 Storage management

Energy storage systems, such as batteries, play a pivotal role in hybrid micro-grids by storing excess energy and releasing it when demand exceeds supply. The controls determine the optimal times for charging and discharging these storage systems to maximize their lifespan and efficiency [34].

2.2.5 Predictive analytics

Advanced energy management controls use predictive algorithms that anticipate the energy generation, consumption patterns, and storage needs based on historical data, weather predictions, and load profiles [35]. This enables proactive decision-making and enhances the ability of micro-grid to adapt to changing conditions [36].

2.2.6 Demand response

The controls can also facilitate demand response strategies by intelligently adjusting energy consumption in response to grid conditions or pricing signals [37]. This not only benefits the micro-grid but also contributes to overall grid stability during peak demand periods [38].

2.2.7 Environmental considerations

Energy management controls can factor in environmental considerations, such as reducing carbon emissions, when making operational decisions. This ensures that the operation of micro-grid aligns with sustainability goals [39].

The complexity of hybrid micro-grid systems demands a multidisciplinary approach to energy management controls [40]. This involves a fusion of control theory, power electronics, data analytics, communication protocols, and real-time monitoring. As technology continues to advance, artificial intelligence and machine learning techniques are increasingly being integrated into energy management systems to enhance their adaptability and decision-making capabilities [41].

2.3 Description of the developed hybrid microgrid system

The developed hybrid micro-grid architecture was applied to supply a variable AC load. The power generation capacity of each distributed generation source was 500 kWp for solar, 500 kW for wind energy, 900 kWh for the battery and 1.5 MW for the diesel generator. The power generated from the PV and battery are DC, but for wind is AC, therefore,

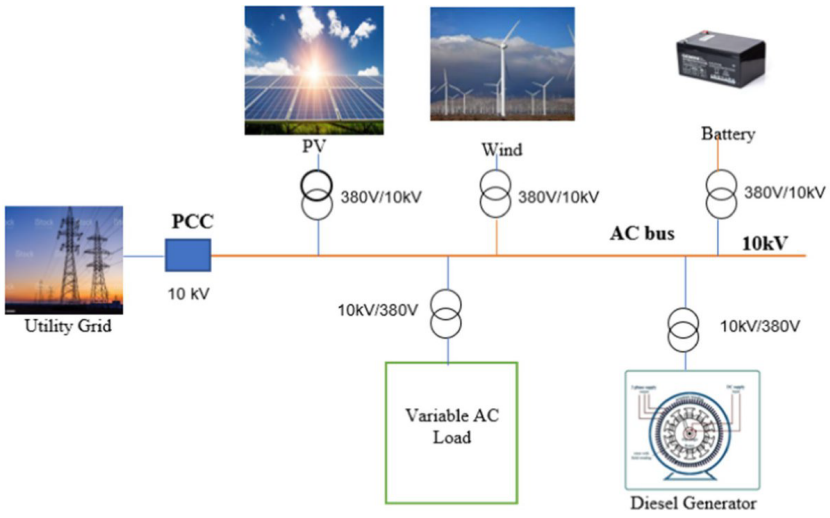


Fig. 3 Block diagram of the developed system

Table 1 Required values for the developed system

System	Capacity	Number of unit	Total
PV power plant	500 kW_p	1	500 kW_p
Wind power plant	500 kW	1	500 kW
Battery	900 kWh	1	900 kWh
Diesel generator	1.5 MW	1	1.5 MW
AC Load	800 kW	1	800 kW

the power generated from the DC sources were converted in AC by using an inverter. The line to line voltage from PCC was 10 kV and a transformer was used to set the AC bus voltage for the system to 380 Vac. The battery was utilized to assure power supply to the variable load without any interruption. It supplied power when the available power from the distributed generation was not sufficient to satisfy the load.

2.3.1 Load profile

The developed hybrid micro-grid supplied the load directly by 380Vac through a transformer. The power system grid included generation, transmission, and distribution. According to the generation system, the total generated power, such as PV and Wind, were connected in parallel. The battery was used as a back-up system during peak demand and fluctuations in the power generated from renewable energy sources. Figure 3 illustrates the block diagram of the developed system and Table 1 presents the summary of all the variables for the developed hybrid micro-grid.

3 Energy management strategy for the developed hybrid micro-grid

The system consisted of two renewable energy sources (wind and PV power plants), an energy storage system, and a generator that supplied electricity to the load demand when the utility grid was unavailable. The following formula in Eq. (1) was used to determine the net power generation:

$$P_G = P_{pv} + P_{wind} + P_{batt} \quad (1)$$

where, P_G the power generation; P_{pv} the power produced from PV; P_{wind} the power produced from Wind; P_{batt} the power produced from Battery.

When there was an excess of power generation, the battery was charged; when there was not enough power generation to meet the load demand, the battery was discharged. According to the developed energy management system (EMS), the power generation was supplied the load demand through four scenarios and with the help

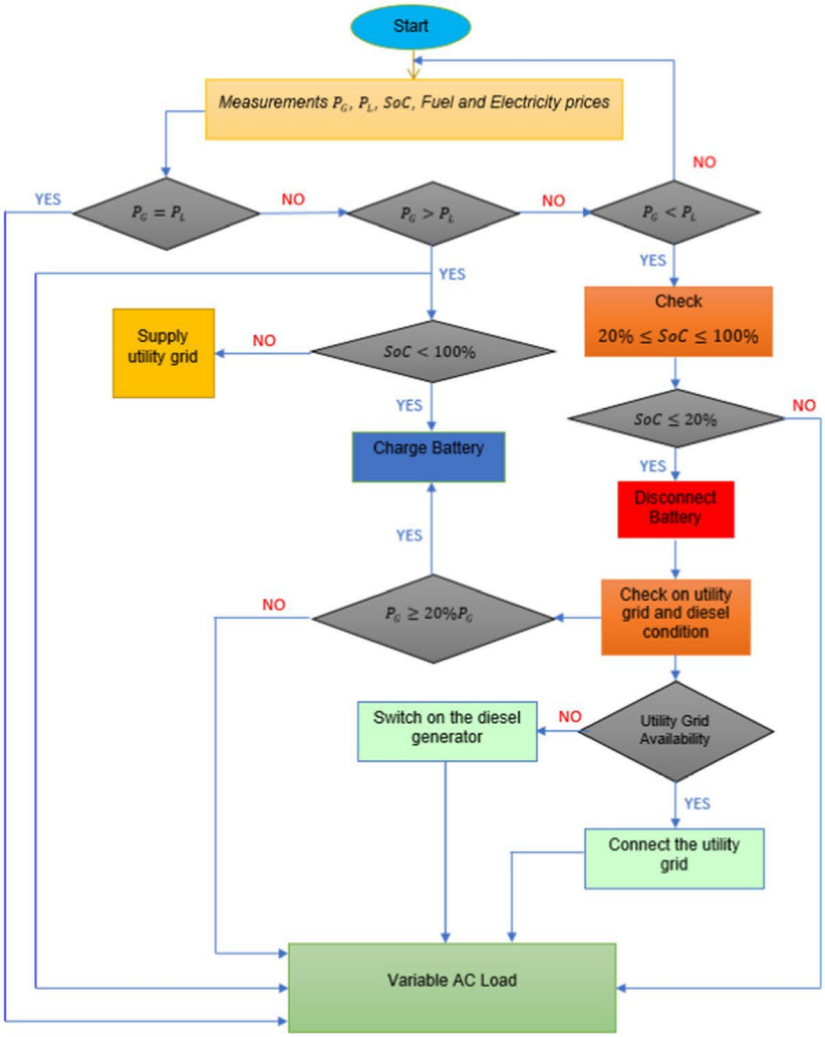


Fig. 4 Flowchart of the energy management strategy for the hybrid microgrid

of the battery, a diesel generator, and the utility grid. Figure 4. shows the architecture of the energy management algorithm flow chart. First, the power generated by various sources and the load demand was measured using the scenarios listed below.

Case 1: When the load demand is met by the power generated.

$$P_L = P_{pv} + P_{wind} \tag{2}$$

According to this scenario, the load was continuously supplied by the power generated from wind power plant and PV power plant sources as illustrated in Eq. (2).

Case 2: When the power generation was greater than the load demand.

$$P_{pv} + P_{wind} > P_G \tag{3}$$

In this case, the power generation exceeded the load demand as presented in Eq. (3); as a result, the load demand was satisfied by the power generation, and the surplus was used to charge the battery. The SOC of the battery was firstly measured and see if it fell below the maximum value, which was 100%. When the condition was satisfied, the load was supplied and the battery was also connected to be charged until its SOC reached the maximum value. When the battery was fully charged, it was disconnected and waited the discharge phase as presented in Eqs. (4), (5), which show the charging condition. The excess of production was supplied to the utility grid. The conditions were formulated as below:

$$SOC_{min} < SOC_{batt} < SOC_{max} = 20\% < SOC_{batt} < 100\% \tag{4}$$

$$P_G > P_L = \text{Charging} \tag{5}$$

Case 3: when the power generation is not enough to meet load demand as presented in Eq. (6).

$$P_{pv} + P_{wind} < P_G \tag{6}$$

The battery was used to supply the load, in this case because the power generation was less than what was required to meet the load demand as shown in Eqs. (6), (7) give the condition of discharge. The energy management system (EMS) calculated and checked the difference between the available power generation from the renewable energy sources and load. It also measured the SOC of the battery at the same time. When the power from the battery was sufficient to meet the demand of the load, when the condition was satisfied, then the battery was discharged until its SOC reached the minimum point. In Eq. (8), the supply power formula is given where the battery is used to support the load. Equations (9), (10) and (11) presents the operating modes of the battery.

$$P_G < P_L = \text{Battery Discharging} \tag{7}$$

$$P_L = P_{PV} + P_{wind} + P_{batt} \tag{8}$$

$$SOC_{batt} = 20\% = \text{Battery Disconnected} \tag{9}$$

$$SOC \leq 20\% = \textit{Charge battery} \tag{10}$$

$$SOC > 20\% = \textit{Discharge battery} \tag{11}$$

Case 4: When the battery reached its minimum value and the generated power was less than the load demand.

$$P_{PV} + P_{wind} + P_{batt} < P_L \tag{12}$$

In this case, the SOC of the battery reached its minimum value, which was 20% thus, the battery was disconnected and Eq. (12) presents the formula of the power supplied with the support of the battery when this total amount becomes less than the demand of the load. At this stage, the load demand was provided by the help of the generator or the utility grid based on the availability of the utility grid. When the utility grid was available, then the utility grid

supplied the load and when the utility grid was not available, then the diesel generator was switched on to supply the load. The EMS checked the availability of the generated power from the renewable energy sources to see if it was ≥ 20% of the total power produces from the renewable energy sources. When the condition was approved, then the battery was connected to be charged by the available power generation. In contrary, when the condition was not satisfied, then the available generated power from the renewable energy sources was added to the utility grid or generator to supply the load. For this study, it was specified that the battery could be charged when the available power was ≥ 20% of the total production, when it reached its minimum value. Charging a battery with a greater power input, compared to a smaller one, offers several advantages in terms of efficiency, charging time, and overall battery performance. The flow chart architecture of the EMS is presented in the Fig. 4 below.

4 Simulation results

The developed energy management system algorithm was designed and built on MATLAB/SIMULINK environment by physical modelling. The Stateflow logical programming environment was used to design the energy management system algorithm. All the components of the model were represented by their respective model blocks available in Stateflow logical programming environment. This section is focused on the different simulation results of the developed energy management system algorithm and considers various scenarios. Adopting scenarios allows to position with a neutral and objective point of view while also better understanding the real environment. Scenarios are essential for providing a clear technique and strategy. As a result, considering the scenarios in chronological order offers a very helpful direction. The Stateflow logical programming environment is used in the implementation of the developed energy management system algorithm. The operational mode of Stateflow environment refers to a logical system that can be either 0 or 1. When the output of the flow chart reads 1, it signifies the system is operational (ON), and when it reads 0, it means the system is OFF. The test parameters for each component used in the simulation are presented in the Table 2.

Table 2 Test parameters used for the MATLAB simulation

Parameter	Symbol	Value
Inverter rated output voltage	V_o	380 V
MPPT voltage	V_{MPPT}	800 V
Cell temperature	T	25 °C
Sun irradiance	I_r	250, 500, 1000 W/m^2
PV max power	P_{PV_max}	500 kW_p
Wind turbine speed	N_s	13 rad/s
Wind max power	P_{wind_max}	500 kW
Wind turbine torque	T_r	13,000 Nm
Wind voltage	V_{conv}	800 V
Nominal battery voltage	V_{nom_batt}	1000 V
Nominal battery capacity	BAh	900 Ah
Inverter rated power	S_B	1 MVA
Diesel generator rated power	S_G	1.5 MVA
Grid frequency	f_g	50 Hz
Switching frequency	f_{sw}	30 kHz
DC Link capacitor	C_{DC}	0.1 μH
Grid side inductor	L_g	18.4μH
Inverter side inductor	L_i	22.99μH
Filter capacitance	C_f	1.11mF
Damping resistance	R_f	3.123 mΩ
Resonance frequency	f_{res}	47.29 Hz
Approximated total inductor resistance	R_T	0.1
PLL settling time	T_{SPLL}	2.25 ms
Load reference power	P_{ref}	800 kW

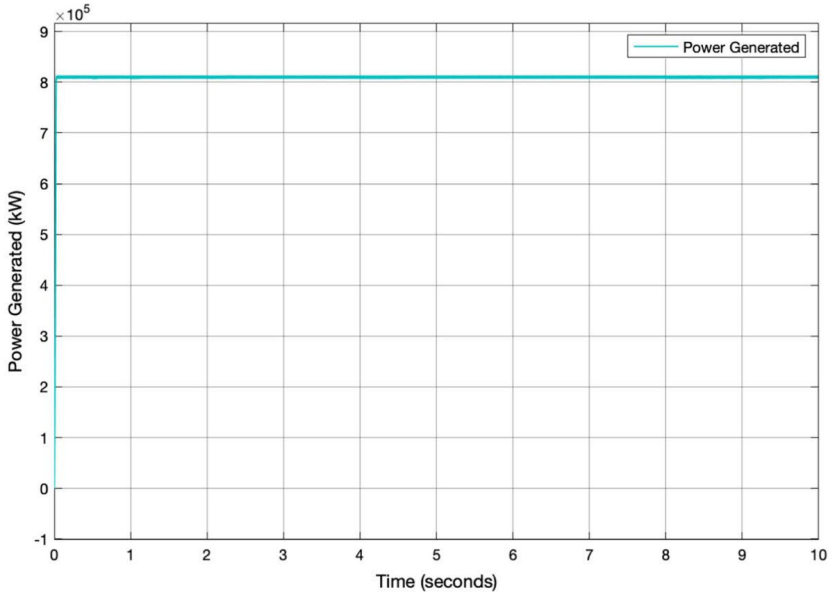


Fig. 5 Power generated by renewable energy sources

Scenario 1: In this first case, the power production from the renewable energy sources was equal to the total load power demand. As shown in Table 1, the load power was fixed at 800 kW. Thus, the total power generated from the renewable energy sources was supplied to the load without any interruption and in this stage, the battery, utility

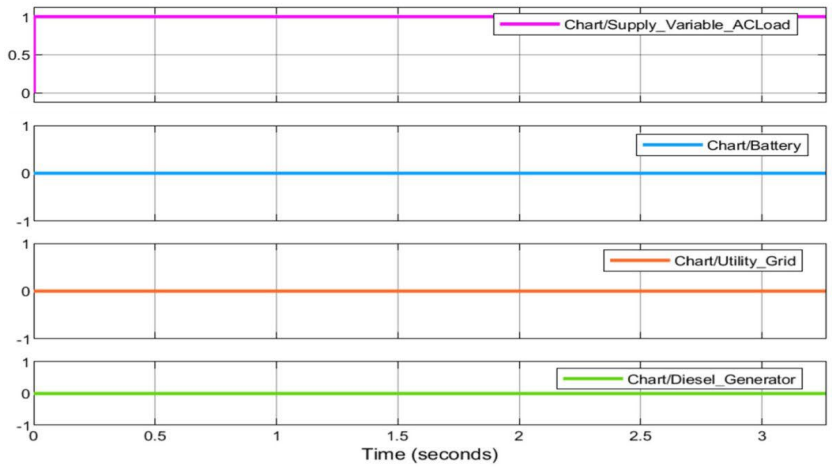


Fig. 6 Stateflow output results chart

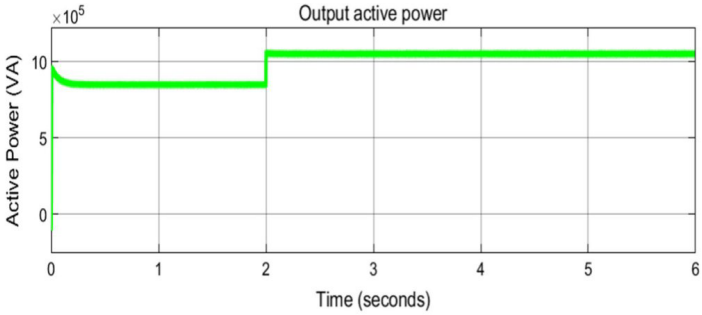


Fig. 7 Power generated by renewable energy sources

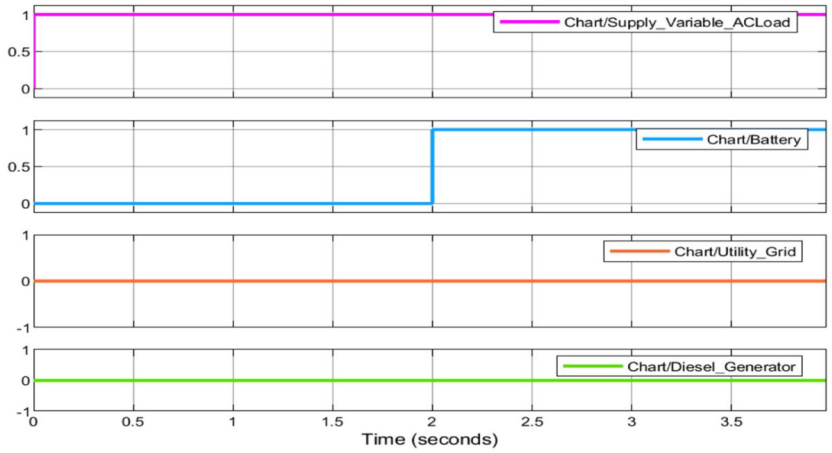


Fig. 8 Stateflow output results chart

grid and diesel generator were disconnected from the system. Figure 5 below illustrates the power generation from the renewable sources, which are PV and wind.

As it can be seen in Fig. 5, the power generated is equal to the load demand power. Figure 6 presents the chart of the output results for this first scenario, in which all the results are displayed graphically. It is shown that only the load is supplied and other outputs, which include the battery, utility and diesel generator are not operational.

Scenario 2 In this second case, the total power generation from the renewable energy sources became higher than the load demand power. As shown in Fig. 7, the power produced from the renewable energy sources is more than the expected load demand power. Thus, the battery is charging according to the charge / discharge condition and when the maximum value was reached then it was automatically disconnected from the system and the excess of production was directed to the utility grid.

Figure 8 presents the graphical output results from the block diagram, showing the operating mode of the system. The result shown that the battery is charging and at the same time the load is being supplied.

In Fig. 9 below, the battery is fully charged. Therefore, it was disconnected and the surplus of production was directed to the utility grid. In this case, the load demand and utility grid were completely supplied until the production condition change.

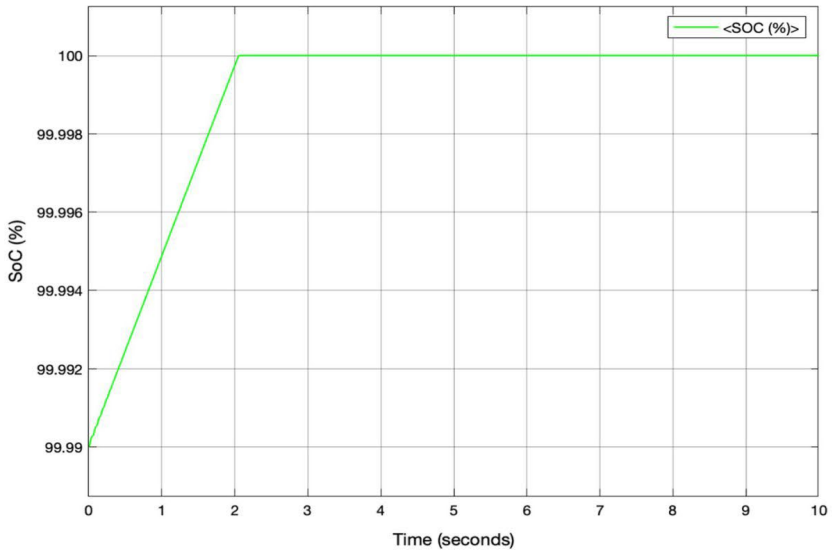


Fig. 9 Battery fully charged

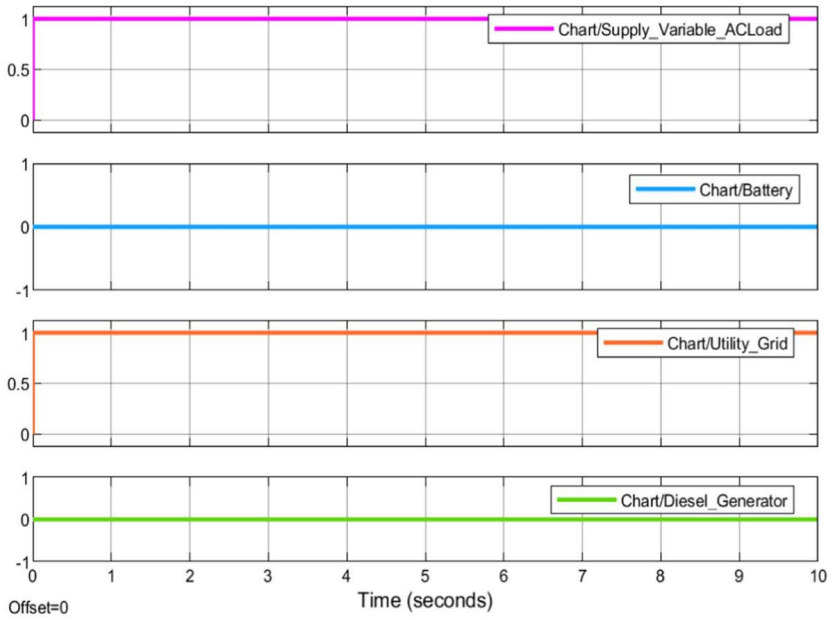


Fig. 10 Stateflow output results chart

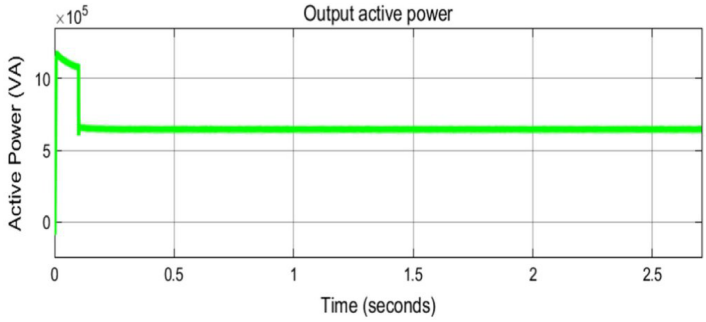


Fig. 11 Power generated by renewable energy sources

Figure 10 also shows the output results from the Stateflow chart in which all the outputs (variable AC load, battery, utility grid and diesel generator) are presented. It is shown that the two outputs are operational, the load demand and the utility grid. This shows that the battery is fully charged and waiting for the discharging phase.

Scenario 3 In this third case, the power generated from the renewable energy sources became less than the load demand power as illustrated in Fig. 11, thus, the load demand was met by the assistance of the battery energy storage.

In Fig. 12, it is shown that the battery was at its maximum value (100%) and it is discharging according to the stated condition. In this case, the battery was discharged until it reached its minimum value (20%) or the condition changed.

Figure 13 shows the stateflow chart, where the output results are displayed. The first and second graphs show that the load and the battery are in operating mode and the two other outputs, which are the utility grid and diesel generator are disconnected. In Fig. 14, the state of charge of the battery is presented. It shows that the battery has reached its minimum value (20%) and was automatically disconnected from the system. In this stage, according to the developed energy management system, the load demand was met by the help of the utility grid or diesel generator based on the utility grid availability.

When the battery reached its minimum value, the condition was that, if the utility grid was available, then the load was supplied by the utility grid and if not, the diesel generator was switched on to supply the load. Additionally, the

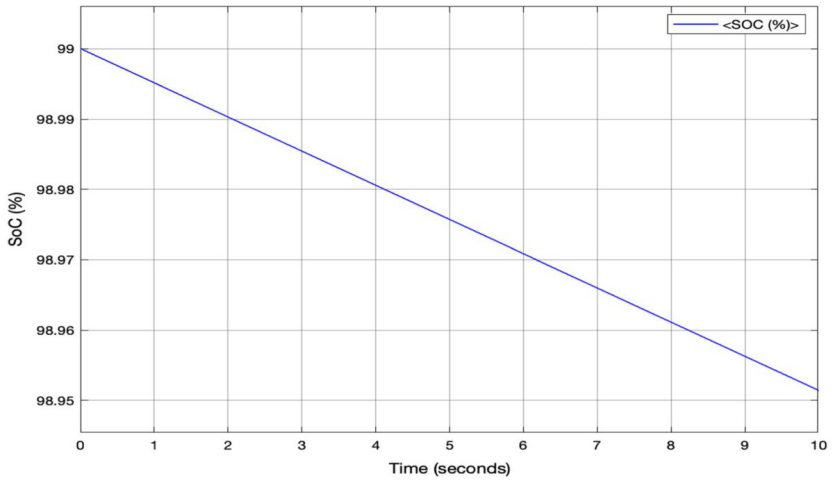


Fig. 12 Battery discharging

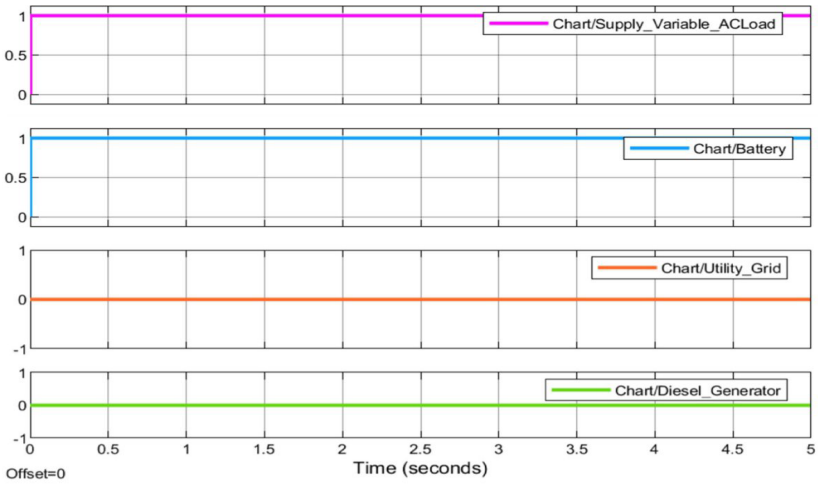


Fig. 13 Stateflow output results chart

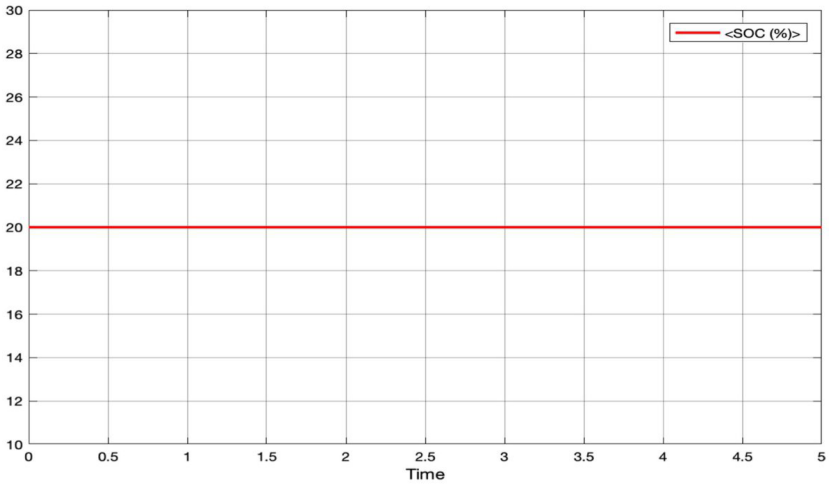


Fig. 14 Battery discharged and disconnected from the system

developed energy management strategy stated that the battery could only be charged if the power generated from the renewable energy sources was more or equal to 20% of the total produced power from these sources. The total power produced from the renewable energy sources was 1 MW and 20% of this production was 200 kW, thus, the battery could only be charged when the power generation was $\geq$ 200 kW. This condition of charging a battery with a higher power input, compared to a smaller one, offers several advantages in terms of efficiency, charging time, and overall battery performance.

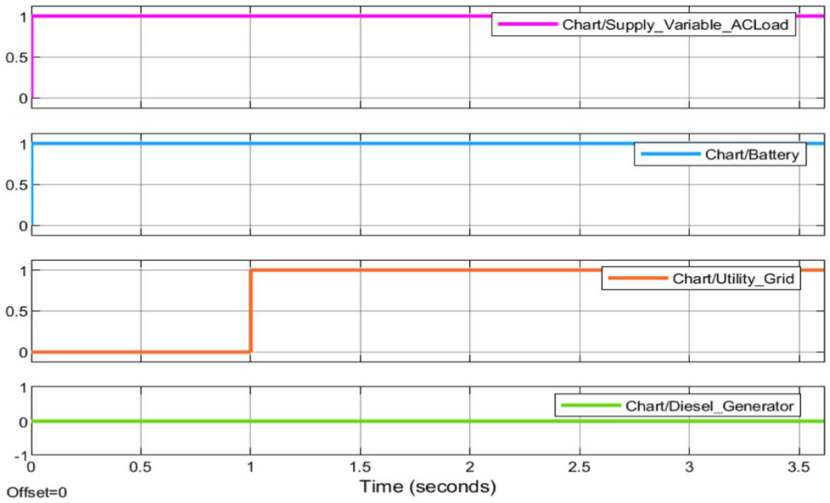


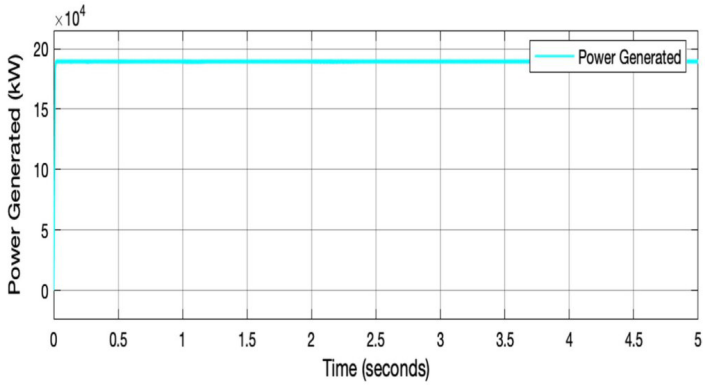
Fig. 15 Stateflow output results chart

The Stateflow chart is shown in Fig. 15, where the output results are displayed. The load was supplied by the assistance of the utility grid and the available power supplied from the renewable sources. The battery was charging through the power generated from the renewable energy sources because the power generated from the renewable energy source exceeded 20% of the total power produced in this case. When the power generated from the renewable energy sources dropped below 20% of the total power generated, which means below 200 kW as illustrated in Fig. 16, the battery was assumed to be automatically disconnected from the system as defined from the algorithm and it is shown in Fig. 17.

Figure 17 shows the Stateflow chart, where the output results of this case are presented. It is seen that the system is operating on grid connected mode and the battery is disconnected from the system.

When the utility grid became unavailable, the diesel generator was switched on to supply the load as shown in Fig. 18. The load was supplied through the diesel generator and the available power produced from the renewable energy sources. The battery was charging at the same time because the generated power from the renewable energy sources was more or equal to 20% of the total power generated (≥ 200 kW).

Fig. 16 Power generation by renewable energy sources



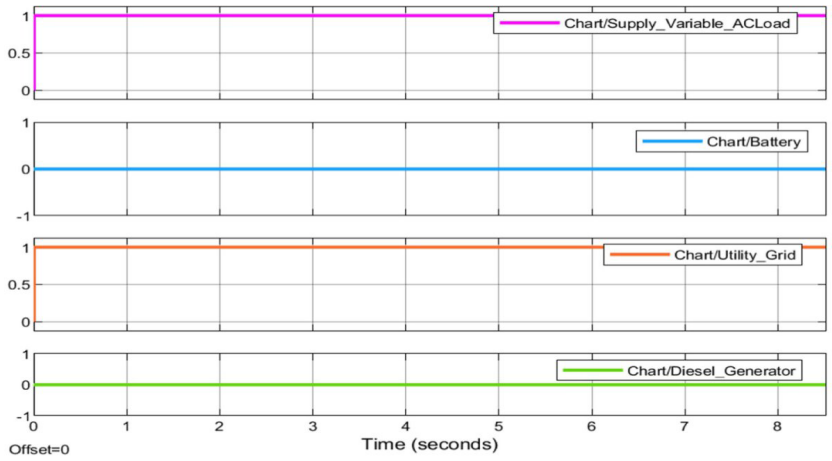


Fig. 17 Output results from the developed energy management system chart

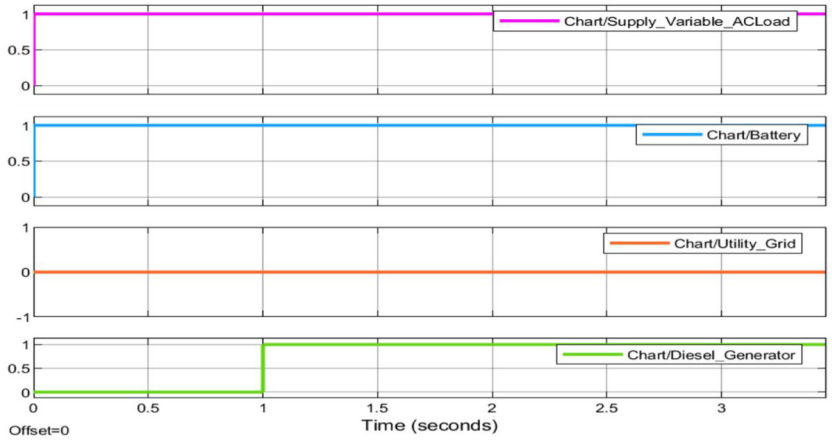


Fig. 18 Stateflow output results chart

The output results from the Stateflow chart is presented in the Fig. 18 above. The results show that the load, battery and diesel generator graphs are in operating mode (1) and the utility grid graph is (0), which shows that the utility grid is unavailable. As discussed for the utility grid availability case, when the power generated from the renewable energy sources became less than 20% of the total power generated, which means below 200 kW as illustrated in Fig. 19, then the battery was automatically disconnected from the system and only the load demand was supplied from the available power produced and diesel generator.

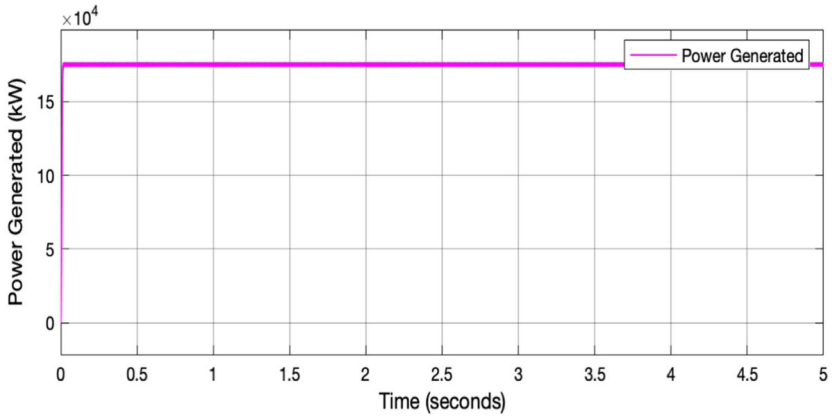


Fig. 19 Power generation by renewable energy sources

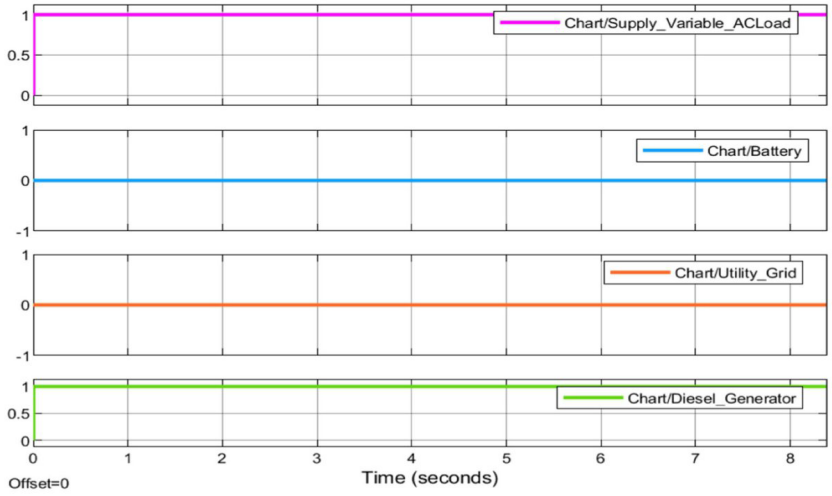


Fig. 20 Stateflow output results chart

Figure 20 shows the Stateflow chart, where the output results of the presented case are shown. It is seen that the load is supplied through the diesel generator and the battery is disconnected from the system because the power generated is less than 20% of the total power produced from the renewable energy sources.

The demand was supplied via the diesel generator, and the developed energy management strategy was continuously checking the power produced from the renewable energy sources and the utility grid availability. Once the power generated was enough to provide power to the load demand or the utility grid became available, then the diesel generator was switched off. This developed algorithm enabled to provide the variable AC load with uninterrupted power and to keep

the SOC of the battery in the admissible limits by charging the battery at higher power. In this application, because of the intermittent nature of the renewable resources, a higher charging power is required to fully recharge the battery in a shorter amount of time than usual. The results have shown that it is possible to maximize the charging time by using a greater power. Moreover, a higher power charging of a battery has presented a better energy density utilization. By utilizing the developed control rules for the hybrid renewable microgrid, the system achieved power balance and the battery SOC maintained the required value for extending the battery life.

5 Conclusion

This paper presented an energy management strategy for hybrid microgrid system using renewable energy. Different scenarios were used during the simulation to show the robustness and the effectiveness of the developed energy management system control to handle the load in both islanded mode and grid connected mode and ensure the proper operation of the battery energy storage system in hybrid microgrid system. The variable AC load for the developed hybrid microgrid system was fixed to 800 kW and the total generation power from the renewable energy sources was 1 MW. To achieve the aim and objectives of the research, a hybrid microgrid model was implemented and developed using MATLAB/Simulink software software and an energy management system algorithm was developed using Stateflow logical programming environment in MATLAB/Simulink software. The energy management strategy dictated that the battery can only charge if the generated power from renewable sources is equal to or greater than 20% of the total production. The overall power supply from renewable sources is 1 MW, and 20% of this amount is 200 kW. Hence, the battery can only charge when the power production is ≥ 200 kW. This condition of charging the battery with a higher power input, offers various advantages in terms of efficiency, charging time, and overall battery performance compared to a scenario with a smaller input. The results show that this developed algorithm was able to control the energy flow between the hybrid micro-grid system and the variable AC load directly connected as well as connected to the utility grid and also to ensure a proper relation between the charging/discharging rate of the battery energy storage system based on their operating conditions and finally, it allowed to keep the SOC of battery in the admissible limits. To improve the overall reliability of the system, more research in this area is necessary. In this study, excess energy was stored in the battery and then sent to the utility grid because renewable sources sometimes produce more energy than the load demands. Developing an energy management plan that maximizes the use of this extra energy is advised. Examples of such loads include water pumping, ambient heating or air conditioning, and water heating with storage tanks.

Author contributions As Corresponding Author, I confirm that the manuscript has been read and approved for submission by all the named authors. The first author listed is CBN, since it is expected of him to make the greatest contribution to the project data acquisition, analysis thereof and conceptualization of a practical working energy management strategy testing model. Second and third authors are Dr MA and Dr AA, since they are an integral part of guidance, revision, and quality control during this project.

Funding There has been no significant financial support for this work that could have influenced its outcome.

Data availability The datasets used can be accessed by request from the corresponding author.

Declarations

Ethical approval and consent to participate The data collection for this project did not require the consent of participants since humans or animals are not the subject of research.

Competing interests We know of no competing of interests associated with this publication.

Open Access This article is licensed under a Creative Commons Attribution 4.0 International License, which permits use, sharing, adaptation, distribution and reproduction in any medium or format, as long as you give appropriate credit to the original author(s) and the source, provide a link to the Creative Commons licence, and indicate if changes were made. The images or other third party material in this article are included in the article's Creative Commons licence, unless indicated otherwise in a credit line to the material. If material is not included in the article's Creative Commons licence and your intended use is not permitted by statutory regulation or exceeds the permitted use, you will need to obtain permission directly from the copyright holder. To view a copy of this licence, visit http://creativecommons.org/licenses/by/4.0/.

Appendix 1

Energy management system condition table

Descriptions	Conditions	1	2	3	4	5	6	7
Scenario 1 ($P_G = P_L$)								
Supply variable AC Load	$P_G = P_L$	**1**	0	0	0	0	0	0
Scenario 2 ($P_G > P_L$)								
Supply variable AC Load and Charge Battery	SOC < 100%	0	**1**	0	0	0	0	0
Supply variable AC Load and Utility grid	SOC = 100%	0	0	**1**	0	0	0	0
Scenario 3 ($P_G < P_L$)								
Discharge battery	SOC > 20%	0	0	0	**1**	0	0	0
Disconnect battery	SOC ≤ 20%	0	0	0	0	**1**	0	0
Connect the utility grid if it is available	Utility grid availability = 1	0	0	0	0	0	**1**	0
Switch on the diesel generator if the utility grid it is unavailable	Utility grid availability = 0	0	0	0	0	0	0	**1**

Bold values represent active state of the system

Appendix 2

Energy management system action table

N*	Descriptions	Actions
1	Variable AC Load supplied	**A1:** AC Load = **ON**;
2	Variable AC Load supplied & Battery charging	**A2:** AC Load & Battery = **ON**;
3	Variable AC Load & Utility grid supplied	**A3:** AC Load = **ON**; Battery = **OFF**; Utility grid = **ON**;
4	Battery discharging	**A4:** AC Load = **ON**; Battery = **ON**;
5	Battery disconnected	**A5:** Battery = **OFF**;
6	Utility grid connected	**A6:** AC Load = **ON**; Utility grid = **ON**;
7	Diesel generator switched on	**A7:** AC Load = **ON**; Diesel generator = **ON**;

Bold values represent active state of the system

References

1. Aljohani TM, Ebrahim AF, Mohammed O. Hybrid microgrid energy management and control based on metaheuristic—driven vector-decoupled algorithm considering intermittent renewable sources and electric vehicles charging lot. Energies. 2020;13(13):3423.
2. Sayeed F, et al. A novel and comprehensive mechanism for the energy management of a hybrid micro-grid system. Energy Rep. 2022;8:847–62.
3. Liu X, Zhao T, Deng H, Wang P, Liu J, Blaabjerg F. microgrid energy management with energy storage systems: a review. CSEE J Power Energy Syst. 2023;9(2):483–504.
4. Kumar GVB, Palanisamy K. Energy management of renewable energy-based microgrid system with HESS for various operation modes. Front Energy Res. 2022;10(October):1–21.
5. Zia MF, Elbouchikhi E, Benbouzid MEH. An energy management system for hybrid energy sources-based stand-alone marine microgrid. IOP Conf Ser Earth Environ Sci. 2019;322(1):012001.
6. Arunkumar AP, Kuppusamy S, Muthusamy S, Pandiyan S, Panchal H, Nagaiyan P. "An extensive review on energy management system for microgrids. Energy Sourc Part A Recover Util Environ Eff. 2022;44(2):4203–28.
7. Helal SA, Najee RJ, Hanna MO, Shaaban MF, Osman AH, Hassan MS. An energy management system for hybrid microgrids in remote communities. Can. Conf. Electr. Comput. Eng., pp. 1–4, 2017.
8. Himabindu E and Gopichand NM. "Energy Management System for grid integrated microgrid using Fuzzy Logic Controller."2020 IEEE 7th Uttar Pradesh Section International Conference on Electrical, Electronics and Computer Engineering, 2020.
9. Kang KM, et al. Energy management method of hybrid ac/dc microgrid using artificial neural network. Electron. 2021;10(16):1939.

10. Elkazaz M, Sumner M, Thomas D. Energy management system for hybrid PV-wind-battery microgrid using convex programming, model predictive and rolling horizon predictive control with experimental validation. Int J Electr Power Energy Syst. 2020;115:105483.
11. Bilbao J, Bravo E, García O, Rebollar C, Varela C. Optimising energy management in hybrid microgrids. Mathematics. 2022;10(2):214.
12. Reddy CR, Rani BG, Kondalu M, Sekhar OC, Venu G, Kalyan CNS. "Energy Management System for Hybrid Renewable Energy-Based Microgrid. INDICON 2022 - 2022 IEEE 19th India Counc. Int. Conf., 2022.
13. Olatomiwa L, Mekhilef S, Ismail MS, Moghavvemi M. Energy management strategies in hybrid renewable energy systems: a review. Renew Sustain Energy Rev. 2016;62:821–35. https://doi.org/10.1016/j.rser.2016.05.040.
14. Agrawal M, Mittal A. Micro grid technological activities across the globe: A review. Int J Res Rev Appl Sci. 2011;7(May):147–52.
15. Lotfi H, Khodaei A. AC versus DC microgrid planning. IEEE Trans Smart Grid. 2017;8(1):296–304.
16. Ahmed M, Meegahapola L, Vahidnia A, Datta M. Stability and control aspects of microgrid architectures-a comprehensive review. IEEE Access. 2020;8:144730–66.
17. Totem E. Microgrids and First Nations. 2019.
18. Chowdhury S, Chowdhury SP, Crossley P. Microgrids and active distribution networks. 2009.
19. Jones GW, Chowdhury BH. "Distribution system operation and planning in the presence of distributed generation technology. Transm. Distrib. Expo. Conf. 2008 IEEE PES Powering Towar. Futur. PIMS 2008, no. June, 2008.
20. Hirsch A, Parag Y, Guerrero J. Microgrids: a review of technologies, key drivers, and outstanding issues. Renew Sustain Energy. 2018;90:402–11.
21. Carpintero-Rentería M, Santos-Martín D, Guerrero JM. Microgrids literature review through a layers structure. Energies. 2019;12(22):1–22.
22. Bhavaraju V, Yang Y, Buck EF. Distributed energy resource control and utility interconnection management. Industry Appl Magazine. 2022;28(5):38.
23. Altaf MW, Member GS. Microgrid protection challenges and mitigation approaches — a comprehensive review. IEEE Access. 2022;10:38895–922.
24. Han Y, Zhang K, Li H, Coelho EAA, Guerrero JM. MAS-based distributed coordinated control and optimization in microgrid and microgrid clusters: a comprehensive overview. IEEE Trans Power Electron. 2018;33(8):6488–508.
25. Kishore PM, Ravikumar B. Refined hybrid microgrid architecture for the improvement of voltage profile. Energy Procedia. 2016;90:645–54.
26. Choudhary MSMK. IRJET-Architectures and overview of hybrid micro-grid. Irjet. 2021;8(3):2275–81.
27. Azeem O, et al. A comprehensive review on integration challenges, optimization techniques and control strategies of hybrid ac/dc microgrid. Appl Sci. 2021;11(14):6242.
28. Elmouatamid A, Ouladsine R, Bakhouya M, Kamoun NEl, Khaidar M, Zine K. Review of control and energy management approaches in micro-grid systems. Energies. 2021;14(1):168.
29. Ahmad S, Shafiullah M, Ahmed CB, Alowaifeer M. A review of microgrid energy management and control strategies. IEEE Access. 2023;11:21729–57.
30. Allwyn RG, Al-Hinai A, Margaret V. A comprehensive review on energy management strategy of microgrids. Energy Rep. 2023;9:5565–91.
31. Kreishan MZ, Zobaa AF. Optimal allocation and operation of droop-controlled islanded microgrids: a review. Energies. 14: 15. 2021.
32. Ortiz L, Orizondo R, Águila A, González JW, López GL, Isaac I. Hybrid AC/DC microgrid test system simulation: grid-connected mode. Heliyon. 2019. https://doi.org/10.1016/j.heliyon.2019.e02862.
33. Antalem DT, Muneer V, Bhattacharya A. Decentralized control of islanding/grid-connected hybrid DC/AC microgrid using interlinking converters. Sci Technol Energy Transit. 2022;77:7.
34. Bharatee A, Ray PK, Subudhi B, Ghosh A. Power management strategies in a hybrid energy storage system integrated AC/DC microgrid: a review. Energies. 2022;15(19):7176.
35. Abadi SAGK, Habibi SI, Khalili T, Bidram A. A model predictive control strategy for performance improvement of hybrid energy storage systems in DC microgrids. IEEE Access. 2022;10:25400–21.
36. Joshal KS, Gupta N. Microgrids with model predictive control: a critical review. Energies. 2023;16(13):4851.
37. Saxena A, Kumar S, Shankar R, Parida SK. "Demand response strategy in a multi-microgrid integrating renewable sources for improved frequency regulation", 2022 IEEE IAS Glob. Conf Emerg Technol GlobConET. 2022;2022:77–83.
38. Mina-Casaran JD, Echeverry DF, Lozano CA. Demand response integration in microgrid planning as a strategy for energy transition in power systems. IET Renew Power Gener. 2021;15(4):889–902.
39. Ahmad A, Shafiullah M, Ahmed CB, Alowaifeer M. A review of microgrid energy management and control strategies. IEEE Access. 2023;11(January):21729–57.
40. Murty VVSN, Kumar A. Ti Multi-objective energy management in microgrids with hybrid energy sources and battery energy storage systems. Rev Afr Political Econom. 2018. https://doi.org/10.1080/03056244.2018.1546429.
41. Bihari SP, et al. A Comprehensive review of microgrid control mechanism and impact assessment for hybrid renewable energy integration. IEEE Access. 2021;9:88942–58.

Publisher's Note Springer Nature remains neutral with regard to jurisdictional claims in published maps and institutional affiliations.

CHAPTER 7: REAL–TIME ENERGY MANAGEMENT SYSTEM FOR A HYBRID RENEWABLE AC MICRO-GRID SYSTEM

Article 5: Real-Time Energy Management System for a Hybrid Renewable Micro-Grid System

This chapter provides a thorough analysis of the real-time software-based design and implementation of an energy management system (EMS) for a hybrid renewable micro-grid system. Micro-grids have difficulties in preserving stability and dependability despite their capacity to include renewable energy sources. The aim and objective of this article are accomplished through the implementation and development of a hybrid micro-grid model using the virtual environment of the Typhoon Hardware-in-loop (HIL) simulation program with HIL402 configuration. The results show that the developed control is able to regulate the energy flow between the load and the renewable energy resources including the utility grid. Moreover, it guarantees the best possible correlation between the rates of battery charge and discharge. Furthermore, the results show that utilizing a higher charging power instead of a small one, optimize the charging time. The battery therefore obtained a full charge more quickly than usual.

Real-Time Energy Management System for a Hybrid Renewable Micro-Grid System

Christian Ndeke Bipongo*, Marco Adonis, Ali-Almaktoof

Department of Electrical, Electronic and Computer Engineering, Cape Peninsula University of Technology, Cape Town 7535, South Africa
* Corresponding author. Tel.: +27-62-836-2466., *E-mail address:* ndekechristian@gmail.com / 219385017@mycput.ac.za

Abstract

This paper gives a detailed study for the design and implementation of an energy management system (EMS) for a hybrid renewable micro-grid system using real-time software. Micro-grids, with their ability to integrate renewable energy sources, face challenges in maintaining stability and reliability. The implemented EMS aimed to maximize the renewable energy sources utilization, including PV and wind power, in conjunction with a battery energy storage system. The objectives of this research included the implementation of an EMS that ensures a reliable and stable operation between the micro-grid system and the main grid including the control of charge and discharge of the battery using Typhoon Hardware-in-the-Loop (HIL) software. The simulation results and case studies demonstrated the effectiveness and performance of the developed EMS in managing a hybrid renewable micro-grid system. The results also demonstrated that the time of charging was maximized by utilizing a higher power. By doing so, the battery was fully charged in a shorter timeframe. The battery state of charge (SOC) was maintained between the fixed values (20% and 100%) as stated by the algorithm.

Keywords: Real-time Energy Management System; Hybrid Renewable Micro-Grid; Renewable Energy Sources; battery energy storage; Distributed generation

For Review Only

1. Introduction

The use of renewable energy sources has significantly increased in recent years as a means to address environmental concerns and achieve energy sustainability [1]. Micro-grid systems constituted by distributed generations and diverse energy sources, have become an effective remedy to incorporate renewable energy into the existing power infrastructure. However, renewable energy sources (RESs) such as solar and wind power are erratic, which makes micro-grid systems less stable and reliable [2]. Real-time energy management becomes crucial to guarantee the effective use of RESs while maintaining grid stability [3].

The motivation behind this study stemmed from the augmentation of demand for sustainable energy solutions and the necessity to address the limitations of traditional power grids. Micro-grid systems offer a decentralized approach to energy generation and distribution, allowing communities and industries to minimize emissions of greenhouse gas and decrease their dependence on fossil fuels [4]. By harnessing the potential of RESs, micro-grids contribute to the energy transition infrastructure to a clean and more resilient. However, effective management of hybrid renewable micro-grid systems requires sophisticated control algorithms and real-time monitoring capabilities [5].

The implemented energy management system (EMS) aimed to optimize the energy generation, storage, and distribution in real-time. This study had as primary objective the design and development of a real-time EMS adapted for hybrid renewable micro-grid systems.

The implemented system was developed utilizing Typhoon Hardware-in-the-loop (HIL) simulation package with HIL402 configuration in the virtual environment. The organization of the remaining parts of the paper include, Section 2, the architecture of micro-grid systems is presented. Real time energy management system is presented in Section 3. Section 4 presents the developed EMS control flowchart. The results of the simulation are provided in

Section 5. The conclusion of the paper is provided in Section 6.

1. Nomenclature

AC	Alternative Current
DC	Direct Current
DER	Distributed Energy Resource
DG	Distributed Generation
EMS	Energy Management System
ESS	Energy Storage System
HIL	Hardware-in-loop
Kv	Kilo Volt
KWh	Kilowatt hour
KWp	Kilowatt Peak
MW	Mega Watt
PCC	Point of Common Coupling
PV	Photovoltaic
SOC	State of Charge

2. Hybrid Renewable Micro-Grid System Architecture

Hybrid renewable micro-grid systems have attracted a lot of interest lately because of their capacity to handle energy sustainability challenges while enhancing grid resilience and reliability [6]. Fig. 1 presents the illustration of the renewable micro-grid architecture. Hybrid renewable micro-grid systems incorporate RES like photovoltaic (PV) arrays and wind turbines, which are the primary RESs in hybrid micro-grid configurations [7]. These sources provide clean and sustainable energy but are intermittent in nature, requiring effective management and integration strategies. Besides the RES, a hybrid micro-grid also includes energy storage systems, inverters and power electronics, control and monitoring systems as well as grid interconnection. Hybrid micro-grid systems may operate connected to the main grid utility or operate in isolation (i.e., islanded mode) [8]. Grid interconnection enables bi-directional power flow, allowing excess energy to be exported to the main grid or imported during periods of low generation.

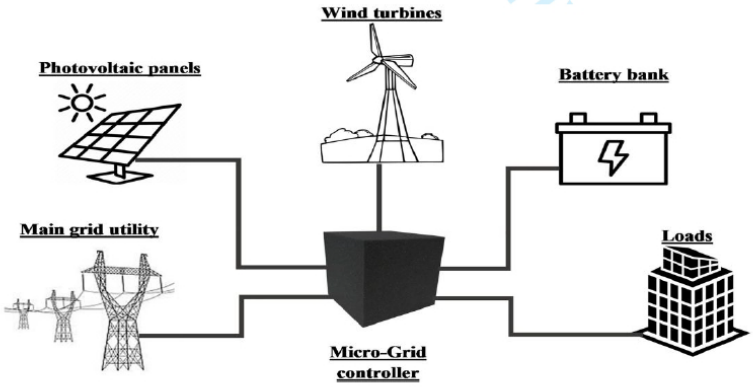


Fig. 1. Micro-grid architecture [9].

For Peer Review Only

Hybrid renewable micro-grid systems offer a promising solution for enhancing energy sustainability and resilience in distributed power generation networks [10]. However, to fully utilize hybrid micro-grid systems in the transition to a cleaner and more sustainable energy future, intermittency, system integration, and optimization issues must be resolved.

3. Real-Time Energy Management System

A Real-Time EMS is a critical component of modern power systems, enabling efficient utilization and optimization of energy resources in real-time [11]. Due to the expansion of the RESs incorporation into the grid, the need for effective energy management systems has become more pronounced [12]. Real-time EMS facilitates dynamic control and power production monitoring, distribution, including consumption, to finally ensure grid stability, reliability, and cost-effectiveness. There are different components of real-time energy management system, which include:

- Control Algorithms and Optimization Techniques: Real-time EMS utilizes sophisticated control algorithms and optimization strategies to regulate energy flow and maintain supply and demand equilibrium [13]. These algorithms dynamically adjust generation schedules, dispatch power from renewable and conventional sources, and optimize energy storage usage to meet system requirements while minimizing operating costs and environmental impacts [14].
- Forecasting and Predictive Analytics: Real-time EMS integrates weather forecasting, load forecasting, and predictive analytics to anticipate changes in energy generation and consumption patterns [15]. By accurately predicting future conditions, EMS can proactively adjust system parameters and optimize energy management methods to mitigate the variability and uncertainty impact [16].
- Energy Storage Integration: Energy storage systems (ESSs), which include batteries, flywheels, and pumped hydro storage, have vital functions in real-time EMS as they provide flexibility and resilience to the grid [17]. EMS algorithms optimize the schedules of ESSs charge/discharge to mitigate variations in the production of renewable energy, stabilize grid frequency, and provide backup power during outages.
- Grid Connectivity and Communication: Real-time EMS relies on robust communication networks and grid connectivity to exchange data and control signals between various grid components [18]. Smart grid technologies like distributed energy resources management systems (DERMS) and demand response systems, enable bi-directional communication and coordination among grid stakeholders, enhancing grid reliability and efficiency.

For Review Only

4

4. Energy Management Control for the Implemented System

The developed system included two supply power sources (PV and wind power systems), along with a battery and a diesel generator. The generator provided power to satisfy the demand of the load in the absence of the utility grid. The implemented hybrid micro-grid and EMS were physically built using Typhoon HIL software, which was also utilized to test, validate, and improve its performance. Every component of the circuit is represented by matching model blocks that are included in the software. Fig. 2 presents the developed energy management control flowchart.

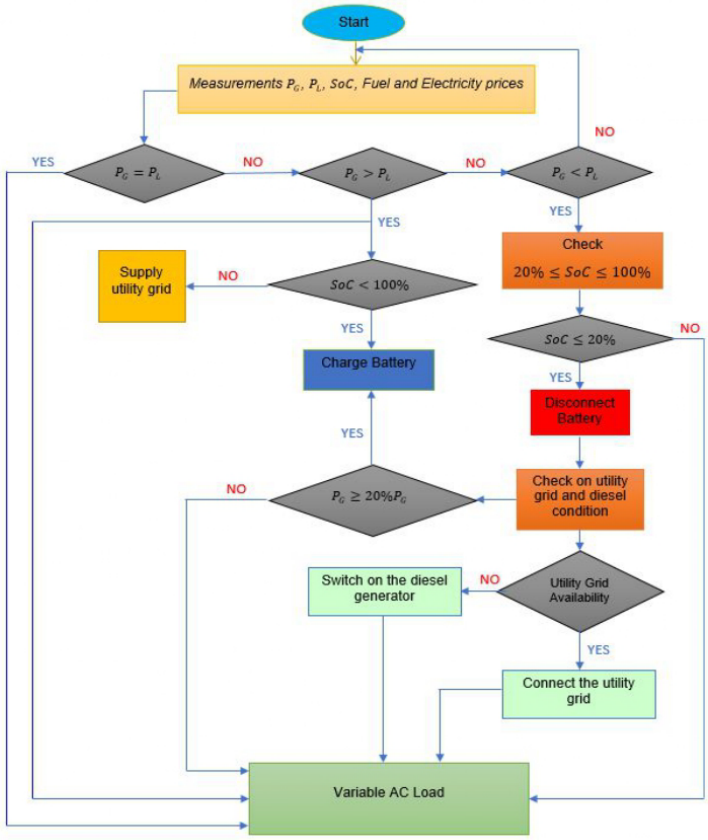


Fig. 2. Energy management algorithm flowchart

Fig. 3 presents the developed Typhoon HIL model.

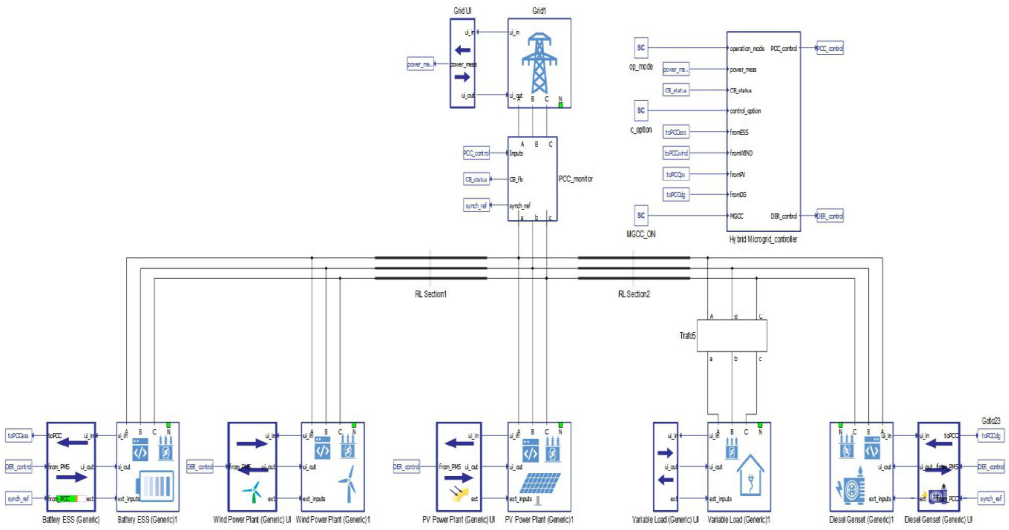


Fig. 3. Hybrid micro-grid mode

The developed EMS ensured that the power supply provides the requirement of the load based on four scenarios, assisted by the battery, the diesel generator, and the utility grid.

Scenario 1: When the requirement of the load and the supplied power are equal.

Scenario 2: When the power generated become higher than the load requirement.

Scenario 3: When the supplied power is insufficient to satisfy the load requirement.

Scenario 4: When the battery attained its minimum limit (20%) and the requirement of the load still high than the power generated.

5. Simulation Results and Discussion

This section presents the results of the simulation for the implemented EMS control and consider different scenarios. Using scenarios helps to understand the real world more fully. Using scenarios is essential since it can give a specific plan and method. Thus, it is a very useful guideline to use the situations in chronological order. Table 1 provides the summary of the diverse modes of operation for these scenarios.

Table 1: Energy management system Table condition

Conditions	Variable AC Load	Battery	Utility Grid	Generator
$\mathbf{P_G = P_L}$	supply load	-	-	-
$\mathbf{P_G > P_L}$	supply load	charge battery	-	-
$\mathbf{SOC < 100\%}$	supply load	charge battery	-	-
$\mathbf{SOC = 100\%}$	supply load	disconnect batt	connect grid	-
$\mathbf{SOC \geq 20\%}$	supply load	-	-	-
		$\boldsymbol{SOC \leq 20\%}$		
Grid available	supply load	-	connect grid	-
Grid unavailable	supply load	-	-	Connect gen
$\mathbf{P_G \geq 20\% P_G}$ **Check grid availability, if yes**	supply load	charge battery	Connect grid	-
$\mathbf{P_G \geq 20\% P_G}$ **Check grid availability, if no**	supply load	charge battery	-	Connect generator

Table 2 presents the component test variables for the simulation utilization.

Table 2: Test variables component

Variable	Symbol	Value
Nominal grid line voltage	V_{PCC}	10 kV
Nominal converter line voltage	V_{nom_LL}	380 V
Nominal battery voltage	V_{nom_batt}	1000 V

For Review Only

7

Nominal capacity of the battery	BAh	900 Ah
Rated power	S_B	1MW
Load active and reactive power	P_L, Q_L	800 kW, 0 VAR
Wind power	P_{wd}	500 kW
PV power	P_{pv}	500 kW
Rated power of the diesel generator	S_G	1.5 MVA
Nominal frequency	f_B	50 Hz
Current Loop Proportional Gain	k_p	0.5
Current Loop Integral Gain	k_i	3.0
Transformer equivalent series inductance1	Tr_{L1}	0.0034 H
Transformer equivalent series resistance1	Tr_{R1}	0.0862 Ω
Transformer equivalent series inductance2	Tr_{L2}	5.0817 μH
Transformer equivalent series resistance2	Tr_{R2}	1.2272 10^{-4} Ω
Faster execution rate	T_{s1}	1 μs
Slower execution rate	T_{s2}	5 μs

Scenario 1: The load demand and the supplied power from the RESs in the first scenario are equal. Table 2 shows that an 800 kW load demand is assumed. As result, all of the generation power is supplied to the load directly and uninterrupted. Fig. 4 illustrates the power graph from the load supplied by the generated power.



Fig. 4. Load demand power graph

Fig. 5 presents the HIL SCADA panel interface, as it can be seen, the utility grid, the diesel generator as well as the battery, are isolated. In this instance, the entire production power is continuously provided to the load, as the HIL interface shows. As can be seen on the HIL interface, the diesel generator and utility grid are off, the battery is in red, and the LED indicators for PV power and wind power are displayed in green to signify their functioning states. The highlighted circles illustrate different values and operation of the system on HIL SCADA panel based on each scenario in which battery, wind plant, PV plant, diesel genset, variable load and utility grid interfaces and the micro-grid controller are presented.

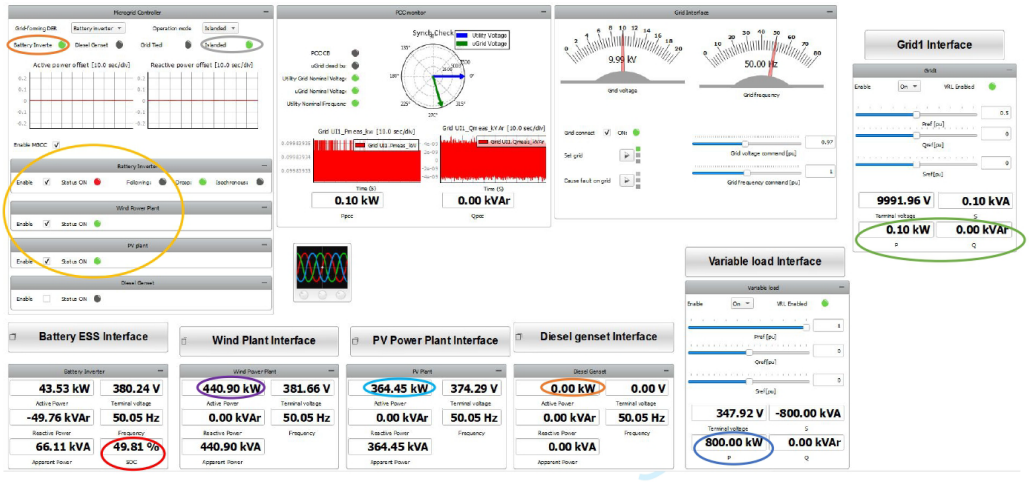


Fig. 5. HIL SCADA panel interface for scenario 1

Scenario 2: The production power exceeds the load requirement. In this situation, the production surplus is either used to supply the utility grid or recharge the battery, based on the battery state of charge (SOC). The battery will be recharged if its SOC is in the minimal range (≤ 20%), and the excess of production will be fed into the utility grid if it is in the maximum range (100%). The charging mode of the battery is shown in Fig. 6.



Fig. 6. Battery SOC on the charging mode

Fig. 7 presents the load demand power. At this point, the production power supplied the load and charges the battery concurrently.



Fig. 7. Graph of the required power from the load

Fig. 8 provides the HIL SCADA panel interface for this second case. The panel shows that the generated power exceeds the load demand power. The panel interface shows that the production surplus is utilized to recharge the battery because the battery SOC was below its maximum value. The battery will be recharged until it attained its maximum value (100%), and when this limit is attained then the production surplus will be supplied to the utility grid until the condition changed. At this time the diesel generator is turned off as shown in the HIL SCADA panel.

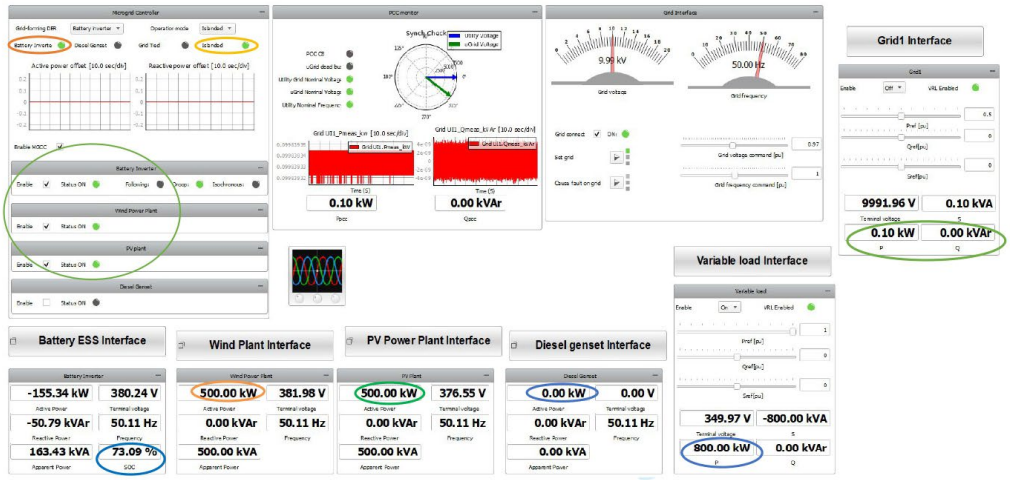


Fig. 8. HIL SCADA panel interface for scenario 2

Looking at Fig. 9, the battery has reached its maximum capacity and is now removed from the system in order to await the discharge mode when necessary.

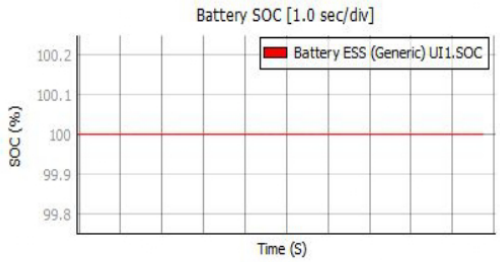


Fig. 9. Maximum charge of the battery

Fig. 10 shows how the excess production supplies the utility grid, as it can be seen, the utility grid is currently connected to receive supplies from the production excess.

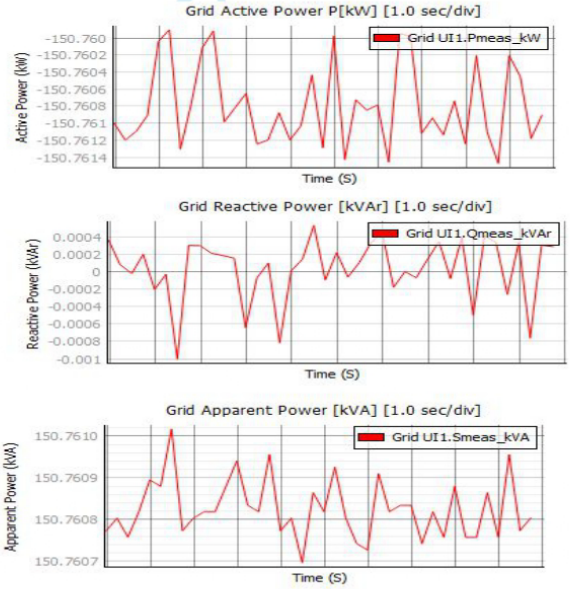


Fig. 10. Utility grid power (supplied by the production excess)

Fig. 11 provides the HIL SCADA panel interface when the maximum charge limit of the battery is attained.

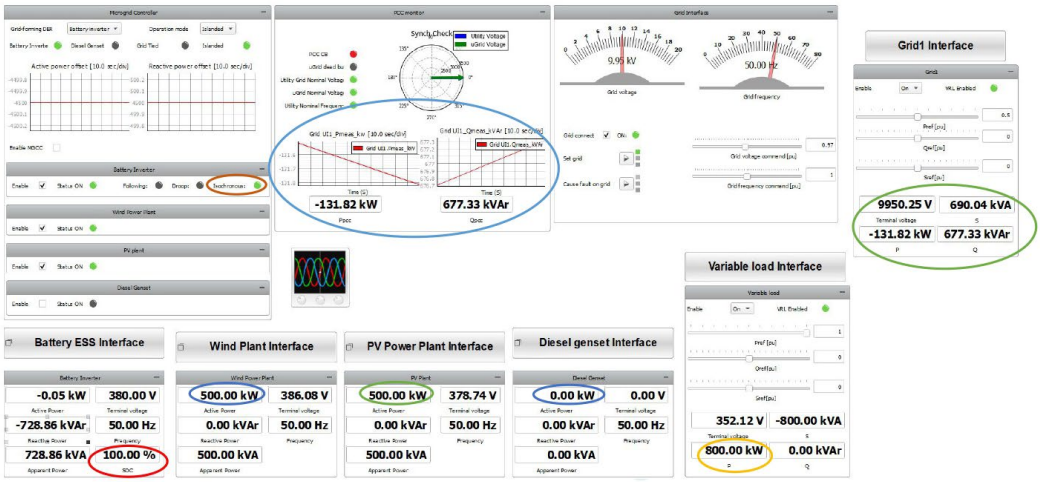


Fig. 11. HIL SCADA panel interface for grid-connected mode

When the maximum battery charge limit is attained, the production excess is sent to the utility grid and the demand of the load is simultaneously satisfied as illustrated from Fig. 11. The battery is immediately disconnected when its maximum value is reached, as indicated in the HIL panel interface. Fig. 12 shows the load demand power graph.



Fig. 12. Load demand power graph

Scenario 3: The requirement of the load exceeds the generation power in this case, thus, the battery will help to satisfy the load demand. The requirement is that the implemented EMS first verifies the maximum and lowest values of the battery storage to determine how much power is available. When the SOC exceeds 20%, the battery is connected for discharge; if the SOC falls below 20%, the battery is unplugged from the system. The battery was previously completely charged, as seen in Fig. 13. In this case, the battery discharges in accordance with the given condition and keeps going until it hits 20% SOC, the minimum value, or the conditions change.

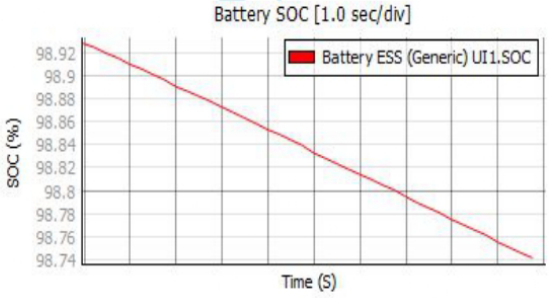


Fig. 13. Battery SOC on the discharging mode

The HIL SCADA panel interface is displayed in Fig. 14 when the generated power falls short of the load requirement. The results show that the battery is discharging and the utility grid as well as the diesel generator are isolated. Once the minimum limit value will be attained, the battery will stop to discharge and the demand of the load will be satisfied by the grid or the diesel generator.

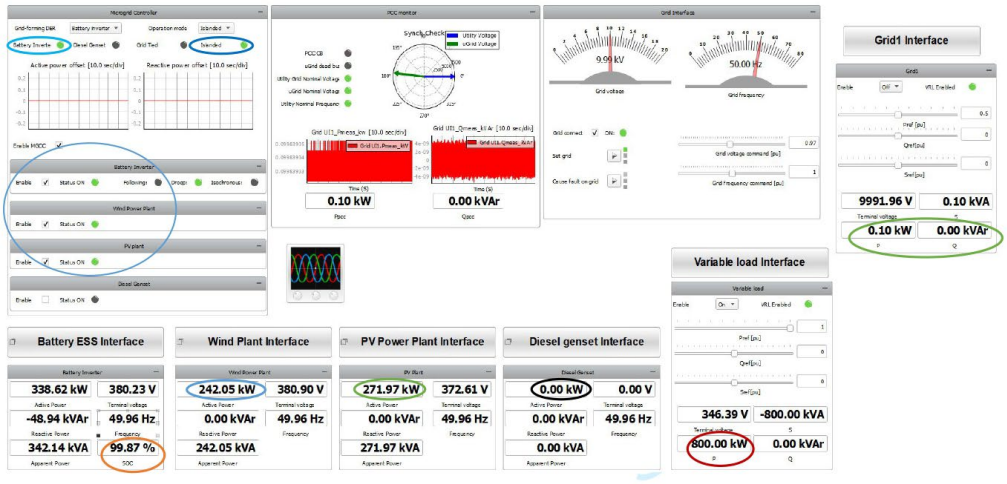


Fig. 14. HIL SCADA panel interface for the third scenario

When the minimum battery SOC limit is attained and the supplied power is below the amount required to meet load demands. In this instance, depending on the utility grid accessibility, the demand of the load is satisfied either by the utility grid or the diesel generator assistance. The battery is automatically unplugged to prevent a deep discharge when the minimum value is achieved, as shown by the battery SOC graph in Fig. 15.

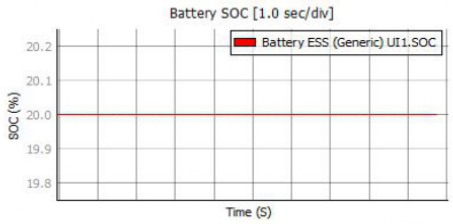


Fig. 15. Battery SOC on its minimum value

Fig. 16 shows the power supplied from the utility grid.

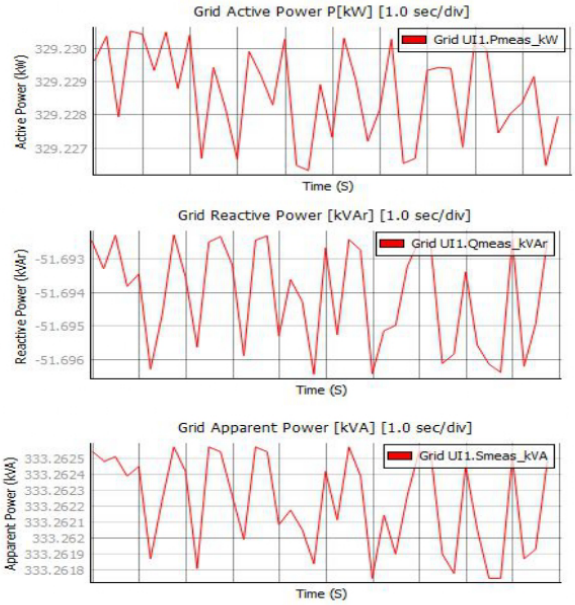


Fig. 16. Utility grid supplied power (grid connected mode)

Fig. 17 shows the HIL SCADA panel interface for the third scenario in which the battery reaches its minimal value.

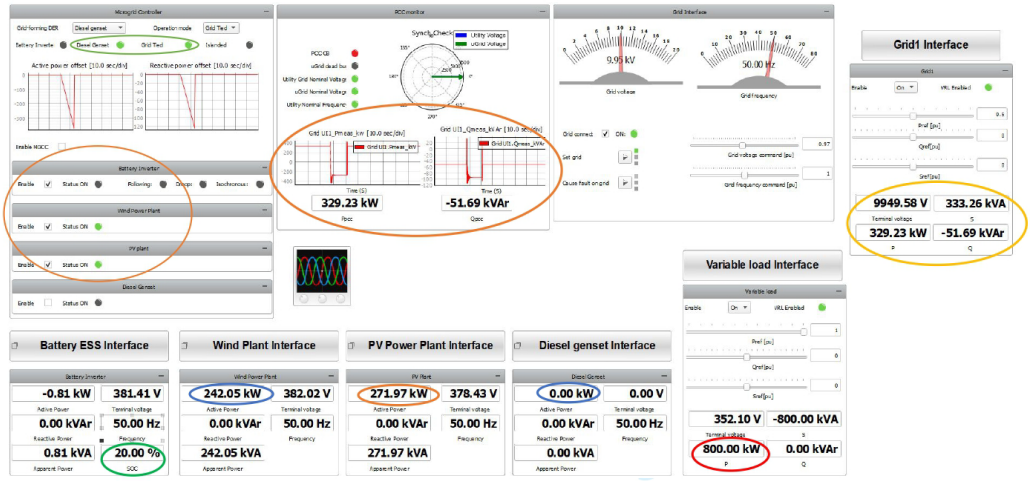


Fig. 17. HIL SCADA panel interface when the battery attained its minimum value

Fig. 18 presents the utility grid HIL SCADA panel interface, the remaining power is provided according to the accessibility of the utility grid. Here, the grid is providing power to the load.

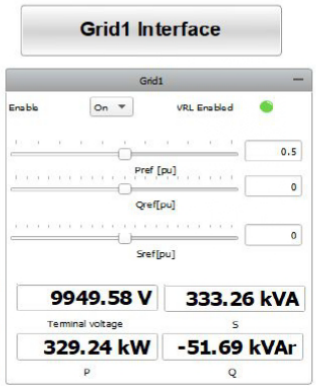


Fig. 18. Utility grid SCADA panel interface

Fig. 19 shows the load demand power graph. The utility grid and RESs assist to satisfy the requirement of the load.



Fig. 19. Load demand power graph

Fig. 20 presents the HIL SCADA panel interface for the third scenario in which the utility grid is not operational. Thus, the diesel generator is activated to satisfy the requirement of the load. The diesel generator LED indicator is turned on, while the LED indicators of the utility grid and the battery are turned off, as shown on the HIL panel interface in Fig. 20.

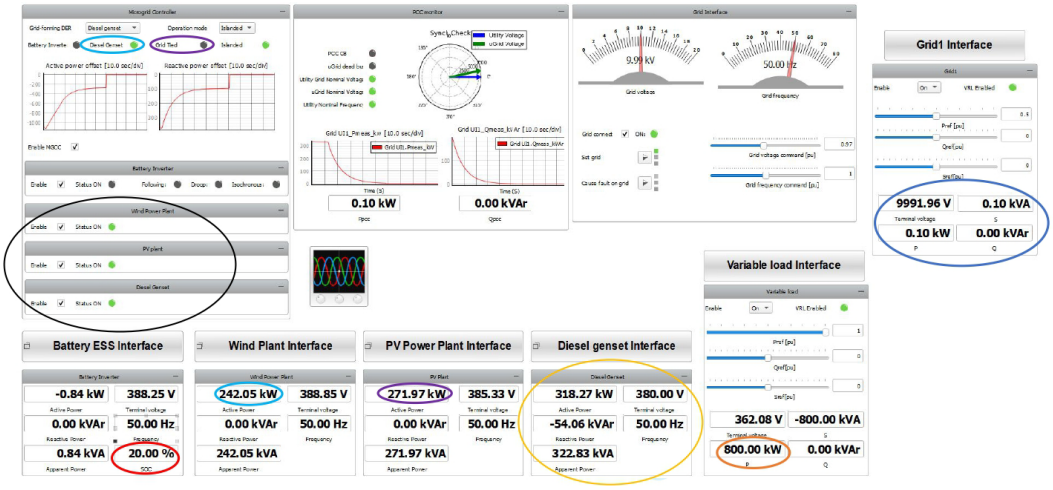


Fig. 20. HIL SCADA panel interface when diesel generator switched on

Fig. 21 shows the diesel generator output power graphs. As it can be seen for this case, the diesel generator is activated to assist the demand by providing power to the load in the absence of the utility grid.

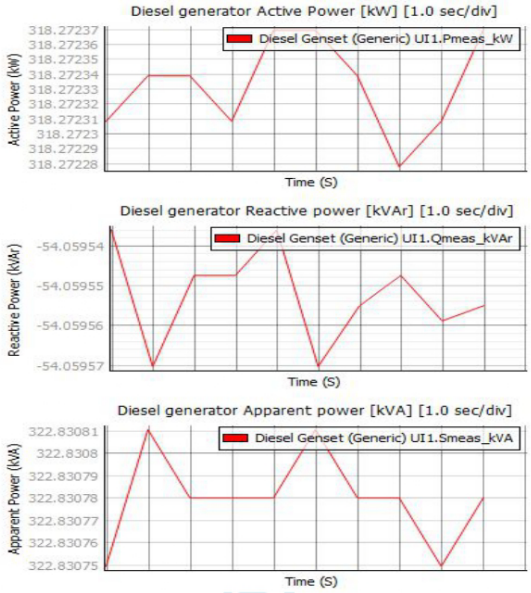


Fig. 21. Diesel generator output power graph

Fig. 22 shows the load demand graph. The diesel generator and renewable energy sources help to meet the demand.



Fig. 22. Load demand power graph

The Typhoon HIL software test shows how effective the implemented EMS is. The developed EMS facilitates the efficient use of RESs and enhances their incorporation within the electrical system. Additionally, it fulfils every scenario that is illustrated and regulates the energy flow between the load demand, and the micro-grid as well as the utility grid. Furthermore, the developed EMS prevents the battery from rapid charge and deep discharge by keeping its SOC in admissible limits.

6. Conclusion

In this paper, a real-time EMS for hybrid renewable micro-grid system was provided. During the simulation, a variety of scenarios were used to demonstrate the resilience and efficacy of the implemented algorithm to manage the load in both isolated and grid-connected modes and guarantee an optimal battery operation as intended. The hybrid micro-grid system that was designed had a fixed variable AC load of 800kW and a total generation power of 1 MW from renewable sources.

The aim and objective of this research were achieved by implementing and developing a hybrid micro-grid model utilizing the virtual environment of Typhoon Hardware-in-loop (HIL) simulation package with HIL402 configuration. The results demonstrate the ability of the implemented control to manage the energy flow between the RESs and the load, which are both operating in conjunction with the utility grid. It also ensures an optimal relationship between the battery charge and discharge rates. Additionally, the results showed that using a higher charging power rather than a reduced one maximized the charging time. As a result, the battery received a full charge faster than usual. The algorithm had defined the permissible limits between 20% and 100%, and it was discovered that the battery SOC remained within those ranges. In order to increase the entire system dependability, further research based on EMS of cost-effective for smart micro-grids network is necessary.

Acknowledgements

As the Corresponding Author, I thus declare that this work was produced as a component of a PhD project, with the supervision, direction, and editorial support of Drs. Marco Adonis and Ali Almaktoof. They also edited and revised the text before the publication. I also acknowledge the financial assistance provided by the National Research Foundation (NRF).

Ethical Approval

Since neither humans nor animals are the focus of the study, participant consent was not required in order to collect data for this project.

Competing interests

There are no known conflicts of interest pertaining to this publication.

Contribution of Authors

As the Corresponding Author, I attest that each of the listed authors reviewed the work and gave their submission approval. Christian Ndeke Bipongo is the first author named since it is anticipated that he contributed most to the analysis and conception of the implemented control, model testing as well as validation. Drs. Marco Adonis and Ali Almaktoof are the second and third authors of this work, respectively, as they played a crucial role in providing direction, editing, and quality assurance of this work, respectively, as they played a crucial role in providing direction, editing, and quality assurance.

Availability of data and materials

Requests for access to the datasets can be made to the corresponding author.

References

[1] C. Kalaivani, M. V. Subramanyam, G. Singaram, A. Udhaya Kumar, K. Mohanraj, and R. Saravanakumar, "Review of Hybrid Microgrid Power Management Using Renewable Energy Sources," 2023 9th Int. Conf. Adv. Comput. Commun. Syst. ICACCS 2023, vol. 1, pp. 1491–1496, 2023.

[2] F. Sayeed *et al.*, "A novel and comprehensive mechanism for the energy management of a Hybrid Micro-grid System," *Energy Reports*, vol. 8, pp. 847–862, 2022.

[3] A. Satapathy, N. Nayak, and T. Parida, "Real-Time Power Quality Enhancement in a Hybrid Micro-Grid Using Nonlinear Autoregressive Neural Network," *Energies*, vol. 15, no. 23, 2022.

[4] R. G. Allwyn, A. Al-Hinai, and V. Margaret, "A comprehensive review on energy management strategy of microgrids," *Energy Reports*, vol. 9, pp. 5565–5591, 2023.

[5] S. Ahmad, M. Shafiullah, C. B. Ahmed, and M. Alowaifeer, "A Review of Microgrid Energy Management and Control Strategies," *IEEE Access*, vol. 11, pp. 21729–21757, 2023.

[6] M. M. Iqbal, S. Kumar, C. Lal, and C. Kumar, "Energy management system for a small-scale microgrid," *J. Electr. Syst. Inf. Technol.*, vol. 9, no. 1, pp. 1–17, 2022.

[7] A. Aghmadi, H. Hussein, K. H. Polara, and O. Mohammed, "A Comprehensive Review of Architecture, Communication, and Cybersecurity in Networked Microgrid Systems," *Inventions*, vol. 8, no. 4, 2023.

[8] F. Nejabatkhah, "Optimal Design and Operation of a Remote Hybrid Microgrid," *CPSS Trans. Power Electron. Appl.*, vol. 3, no. 1, pp. 3–13, 2018.

[9] D. El Bourakadi, A. Yahyaouy, and J. Boumhidi, "Multi-agent system based sequential energy management strategy for Micro-Grid using optimal weighted regularized extreme learning machine and decision tree," *Intell. Decis. Technol.*, vol. 13, no. 4, pp. 479–494, 2019.

[10] A. Bandara, K. Hemapala, and N. C. Ekanayake, "A survey on hybrid renewable energy systems for microgrid application," *PIICON 2020 - 9th IEEE Power India Int. Conf.*, 2020.

For Review Only

[11] S. Zeinal-Kheiri, S. Ghassem-Zadeh, A. M. Shotorbani, and B. Mohammadi-Ivatloo, "Real-time energy management in a microgrid with renewable generation, energy storages, flexible loads and combined heat and power units using Lyapunov optimisation," *IET Renew. Power Gener.*, vol. 14, no. 4, pp. 526–538, 2020.

[12] Q. Hassan, S. Algburi, A. Z. Sameen, H. M. Salman, and M. Jaszczur, "A review of hybrid renewable energy systems: Solar and wind-powered solutions: Challenges, opportunities, and policy implications," *Results Eng.*, vol. 20, no. September, p. 101621, 2023.

[13] S. Yu, L. You, and S. Zhou, "A review of optimization modeling and solution methods in renewable energy systems," *Front. Eng. Manag.*, vol. 10, no. 4, pp. 640–671, 2023.

[14] S. Basnet, K. Deschinkel, L. Le Moyne, and M. Cécile Péra, "A review on recent standalone and grid integrated hybrid renewable energy systems: System optimization and energy management strategies," *Renew. Energy Focus* , vol. 46, pp. 103–125, 2023.

[15] M. Amir, Zaheeruddin, and A. Haque, "Intelligent based hybrid renewable energy resources forecasting and real time power demand management system for resilient energy systems," *Sci. Prog.*, vol. 105, no. 4, pp. 1–33, 2022.

[16] A. Elmouatamid, R. Ouladsine, M. Bakhouya, N. El Kamoun, M. Khaidar, and K. Zine-Dine, "Review of control and energy management approaches in micro-grid systems," *Energies*, vol. 14, no. 1, 2021.

[17] S. Choudhury, "Review of energy storage system technologies integration to microgrid: Types, control strategies, issues, and future prospects," *J. Energy Storage*, vol. 48, no. July 2021, p. 103966, 2022.

[18] J. Ugwu, K. C. Odo, C. P. Ohanu, J. García, and R. Georgious, "Comprehensive Review of Renewable Energy Communication Modeling for Smart Systems," *Energies*, vol. 16, no. 1, pp. 1–28, 2023.

For Review Only

CHAPTER 8: GENERAL DISCUSSION AND CONCLUSION

8.1. Introduction

In this chapter, a general discussion of the developed EMS for the hybrid micro-grid using MATLAB/Simulink software and Typhoon HIL404 blocks available in the Typhoon HIL software is discussed. The discussion of the simulation results is involved in this chapter since it presents many specified simulation processes and describes the model structure. Simulink blocks from the MATLAB/Simulink software were used to design and develop the hybrid micro-grid simulation model and hardware and software solutions for real-time simulation were utilized to conduct the testing, validation and optimization performance of the developed EMS. The blocks used include photovoltaic, wind power, generator, battery, inverter and converters, transformer, a variable load and a utility grid. Additionally, blocks for load, circuit breakers, display devices and measuring were also utilized.

The organization of this chapter is as follows: Section 8.2 provides the fundamental VSC circuit model connected to the LC filter discussion. Section 8.3 introduces the discussion of the implementation of energy management strategy for DC micro-grid system with the important penetration of renewable energy. Section 8.4 discusses the principal controller implementation for different hybrid micro-grid applications. Section 8.5 discusses the energy management strategy for a hybrid micro-grid system using renewable energy using MATLAB/Simulink and Section 8.6 covers the EMS control simulations using Typhoon HIL software. Section 8.7 provides the conclusion of the research.

8.2. Fundamental VSC Circuit Model Connected to the LC Filter Discussion (Article 1)

Chapter Three presented the fundamental VSC circuit model connected to the LC filter. The literature revealed that the primary power interface between the hybrid micro-grid system and distributed generators is an AC-DC converter. The operating modes of a voltage source converter were discussed as well in this article. It was seen that when the VSC is used as a DC bus control, it functions as an active rectifier. When used in the grid-forming mode and grid-feeding mode it functions as an inverter by utilizing various control loops. Finally, a comprehensive guide including a range of methods, such as phase lock loop, direct quadrature zero synchronous frame, as well as space vector pulse width modulation was also introduced.

The fundamental voltage source converter circuit model connected to the LC filter is crucial because it helps in reducing harmonic distortions and improving the overall power quality in the micro-grid. This ensures stable and clean power supply, which is essential for sensitive

loads and the integration of various renewable energy sources. It also plays a key role in converting DC power from renewable sources like solar panels or batteries to AC power, which is required for most loads and for synchronization with the main grid. The LC filter aids in smoothing out the output, making the conversion process more efficient. Understanding the VSC circuit model and its interaction with the LC filter is essential for designing systems that can seamlessly integrate with the main grid or operate in island mode. This ensures that the micro-grid can handle fluctuations in supply and demand without compromising stability. In essence, the significance of introducing the fundamental VSC circuit model connected to the LC filter lies in its ability to address key challenges in energy conversion, stability, integration, management of hybrid renewable micro-grid systems.

8.3. Discussion of the Implementation of Energy Management Strategy for DC Micro-Grid System with the Important Penetration of Renewable Energy (Article 2)

Chapter Four introduced the implementation of energy management strategy for DC micro-grid system with the important penetration of renewable energy. The objective of the article was to finally preserve the proper operation of the DC micro-grid system by focussing on EMS control. Different loads, including commercial, industrial, and residential loads, were considered when implementing this DC micro-grid model. The Stateflow logical programming environment in MATLAB/Simulink software was used to design and develop the EMS algorithm. This chapter demonstrates how the EMS effectively manages the load in isolated mode, ensuring the proper functioning of the battery within the micro-grid system. This algorithm demonstrated its capability to assure the dependability, resilience, robustness, and correct operation of the system based on all of the developed circumstances. The results shown that this control performed well in a variety of scenarios, successfully balancing power production and consumption while maintaining the dependability of the micro-grid system. The technique exhibited adaptability and resilience, ensuring stable operation and minimal disruptions despite fluctuations in renewable energy generation and load demand. Moreover, the robustness study emphasized how adaptable the energy management plan was to uncertainties and changes in the micro-grid environment.

8.4. Discussion of the Principal Controller Implementation for Different Hybrid Micro-Grid Applications (Article 3)

Chapter Five covered the principal controller implementation for different hybrid micro-grid applications. This article discussed the injection of current and voltage into the VSC, which are locally regulated by the primary controller. It has been seen that zero-level micro-grid control is another term for the control of these variables, which relates to different power converter

control modes based on how they function in the AC micro-grid. Moreover, diverse local control applications for micro-grid systems that utilize a DC source and PV array have been examined. The DC voltage regulation was an essential part of the system because solar panels provide DC power that requires regulation to guarantee consistent and dependable operation. Since the inverter was directly connected to the PV arrays, the PQ control was used because it handles the AC power injection. The PQ control mode regulates the power flow between a power source and a load by controlling the real and reactive powers independently. The PV voltage and current were adjusted to match those of the load. To achieve the control, PI controllers were used to receive input signals from the load voltage and current measured values. The output voltage was adjusted to regulate the reactive power, while the output current was adjusted to control the real power used in the simulation. To obtain the required power flow, the output voltage and current were adjusted while maintaining synchronization with the load.

The significance of implementing local controllers in hybrid renewable micro-grid systems lies in their ability to enhance the efficiency, reliability, and sustainability of energy management, ensuring that each resource is used optimally based on availability and demand. They enable the seamless integration of various renewable energy sources, making the system more resilient to fluctuations in energy supply and demand. Local controllers help maintain the stability and reliability of the micro-grid by balancing supply and demand in real-time, preventing issues such as power outages or overloading. The PQ control was developed to regulate the power flow between the DC power source and the load by controlling the real and reactive powers independently. This regulated power was used in the simulation developed in article 4.

8.5. Discussion of the Energy Management Strategy for a Hybrid Micro-Grid System Using Renewable Energy using MATLAB/Simulink (Article 4)

Chapter Six presented the results of the simulation of the developed energy management strategy. To achieve the aim and objectives of the study, MATLAB/Simulink software was used in Chapter Seven to implement and develop the hybrid micro-grid model, as well as to develop the control system scheme and the EMS algorithm. The Stateflow logical programming environment in MATLAB/Simulink software was also utilized in the development of the control system schemes. A comprehensive discussion on the resilience and efficacy of the implemented Energy Management System control in managing the load is presented.

This chapter demonstrates how the EMS effectively manages the load in both isolated and grid-connected modes, ensuring the proper functioning of the battery within the hybrid micro-

grid system in comparison to Article 2, which focused only in isolated mode. The discussion is supported by four conducted case studies, which illustrate the system's performance and reliability. Firstly, the robustness of the algorithm when the power produced was equal to the requirement of the load was presented. The results showed that the demand of the load was met by the power generated from the RESs (PV and wind) without any interruption. Secondly, the effectiveness of the control was presented when the power generated exceeded the requirement of the load. The results have demonstrated that the requirement of the load was met by the supplied power. The production excess was stored in the battery. When the battery was fully charged, any surplus of the power generated was sent to the utility grid. Thirdly, when the requirement of the load exceeds the power produced was also assessed. The results have demonstrated the robustness of the control by automatically connecting the battery to meet the requirement of the load.

The developed algorithm calculated and evaluated the difference between the production power and the required power of the load, while simultaneously monitoring the battery SOC. Thus, the load was met by the assistance of the battery. Finally, the performance of the developed control was demonstrated when the battery attained the minimum limit (20%). The requirement of the load in this situation was met either by the utility grid or diesel generator, according to the grid accessibility. When the grid was available, it supplied the power to the load. In the case where it was inaccessible, the diesel generator was activated to supply the required power to the load. The developed energy management strategy in this study has shown the control effectiveness in comparison to the other controls found in the literature. This technique ensures an uninterrupted power supply to the AC variable load and maintains the battery SOC within permissible limits by employing high charging power.

This study indicated that the battery could be recharged when the generated power exceeds 20% of the power produced from the renewable energy sources. The threshold of 20% excess power generation is set to ensure that the battery charging process starts only when there is a significant surplus, thus avoiding frequent, small charge cycles that can reduce battery lifespan. Due to the RESs intermittent nature, in this application, a higher charging power was necessary to rapidly charge the battery. The results indicated the feasibility of maximizing charging time using higher power, leading to improved energy density utilization.

The fast charging model is designed to charge the batteries quickly up to a certain level of SOC and then slow down the charging rate to prevent damage to the battery and extend its lifespan. At the beginning of the charging process, a high power input was used to quickly charge the battery up to approximately 70% SOC. This phase used a higher current to rapidly

increase the charge level. The value of this higher power can vary depending on the battery specifications and system requirements, but typical values for the charging power in the initial phase can range from 0.5C to 1C (where C is the battery's capacity in ampere-hours). For this research, a 900 Ah battery was charged at 0.5C which received 450 A of current.

Once the battery reaches around 70% SOC, the charging rate was reduced to prevent overheating and overcharging, which can damage the battery cells and reduce their lifespan. The charging power was gradually reduced as the battery approaches full capacity. This slower charging rate helps maintain the battery's health and ensures a longer operational life. The initial fast charging power was 0.5C of the battery capacity from 0% to 70% SOC. For the 900 Ah battery, 450 A of charging current were considered and as the battery approached full charge, the charging power was reduced, less than 0.5C from 70% to 100% SOC.

This implemented control algorithm contributes to achieve a power balance, with the battery SOC consistently meeting the specified values to extend battery life. The operating point, the battery charging/discharging relationship, overcurrent, overvoltage, and unbalanced conditions, which may generally affect the battery lifetime and the hybrid micro-grid reliability have been improved by this novel approach. The study illustrated that a battery charged at higher power can be more versatile in terms of charging options. By being compatible with different charging environments, this control demonstrated that greater flexibility and adaptation to a variety of charging scenarios are provided by batteries with higher charging power. Due to the intermittent behaviour of the RESs, a higher charging power was adopted to charge the battery within a smaller charging time-window.

By using a higher power, most of the available charging duration can be made. Additionally, the energy density utilization was improved by charging the battery with higher power. The results also showed that it is a possible to maximize the rate at which the energy is transferred into the battery by charging it at higher power, and it ensures efficient utilization of its energy storage capacity. It was realized that when the battery was charged at lower power levels, the charging process was very slow and in real life, this can produce heat, and heat may be harmful to the lifespan of batteries. Increasing the power input during charging can shorten the charging period, minimize the total heat production, and possibly increase the longevity of batteries.

8.6. Discussion of the Energy Management Strategy for a Hybrid Micro-Grid System Using Renewable Energy using Typhoon HIL402/404 System/Platform (Article 5)

To achieve the aim and objectives of the study, the developed EMS control was tested, validated and optimized utilizing real-time digital simulator of Typhoon HIL. The simulation results of the developed energy management strategy were presented in Chapter Seven.

Scenario 1: The battery, grid and diesel generator are not connected in this case as illustrated in the HIL SCADA panel interface in Figure 8.1. The system operates in isolated mode; this can also be seen from the HIL panel showing the LED indicator of islanded operation mode in green. The highlighted circles illustrate different values and operation of the system on HIL SCADA panel based on each scenario in which battery, wind plant, PV plant, diesel genset, variable load and utility grid interfaces and the micro-grid controller are presented.

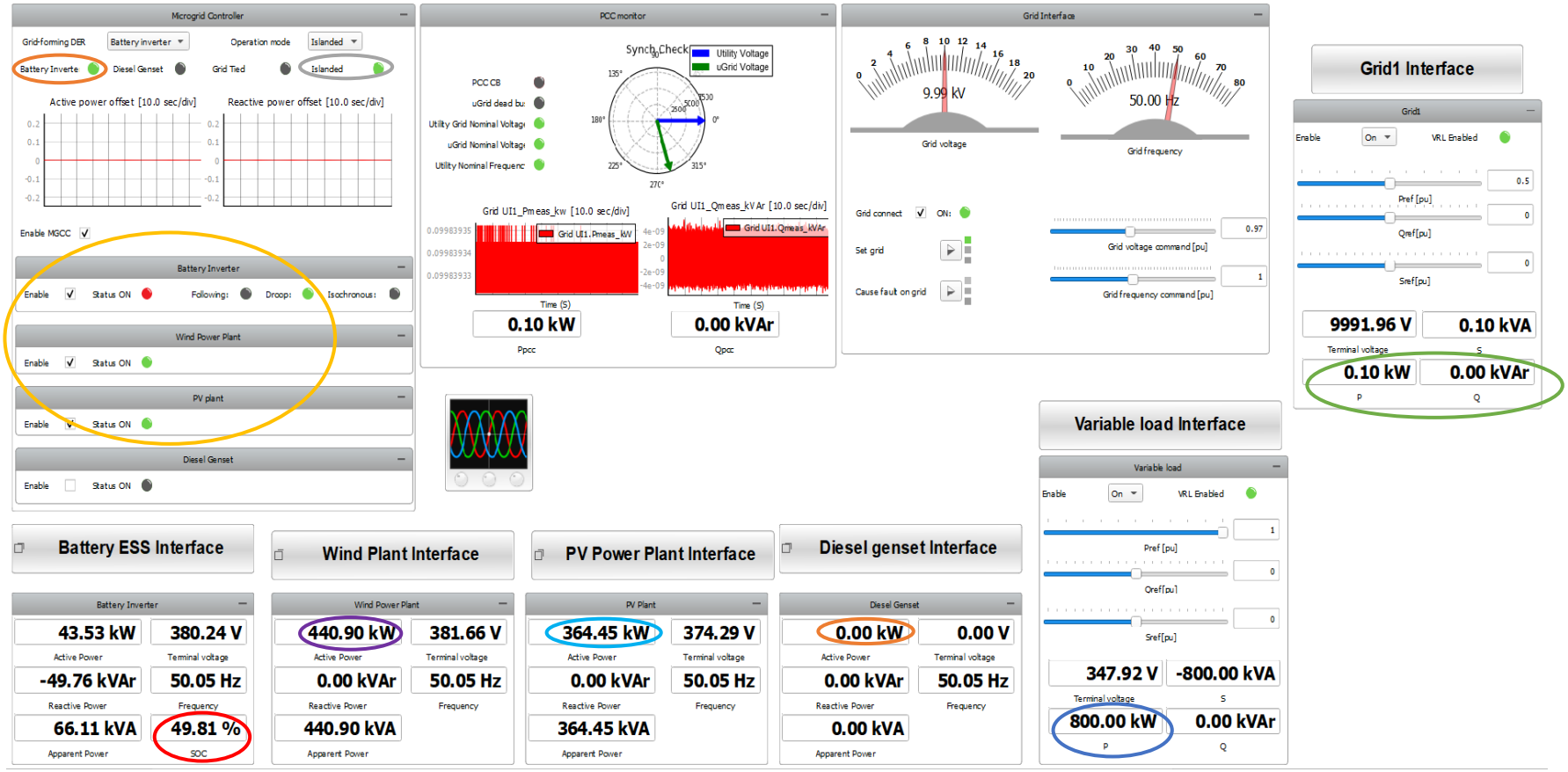


Figure 8.1: HIL SCADA panel interface for scenario 1.

Scenario 2: Based on this scenario, the produced power becomes more than the requirement of the load as illustrated in the HIL SCADA panel interface Figure 8.2.

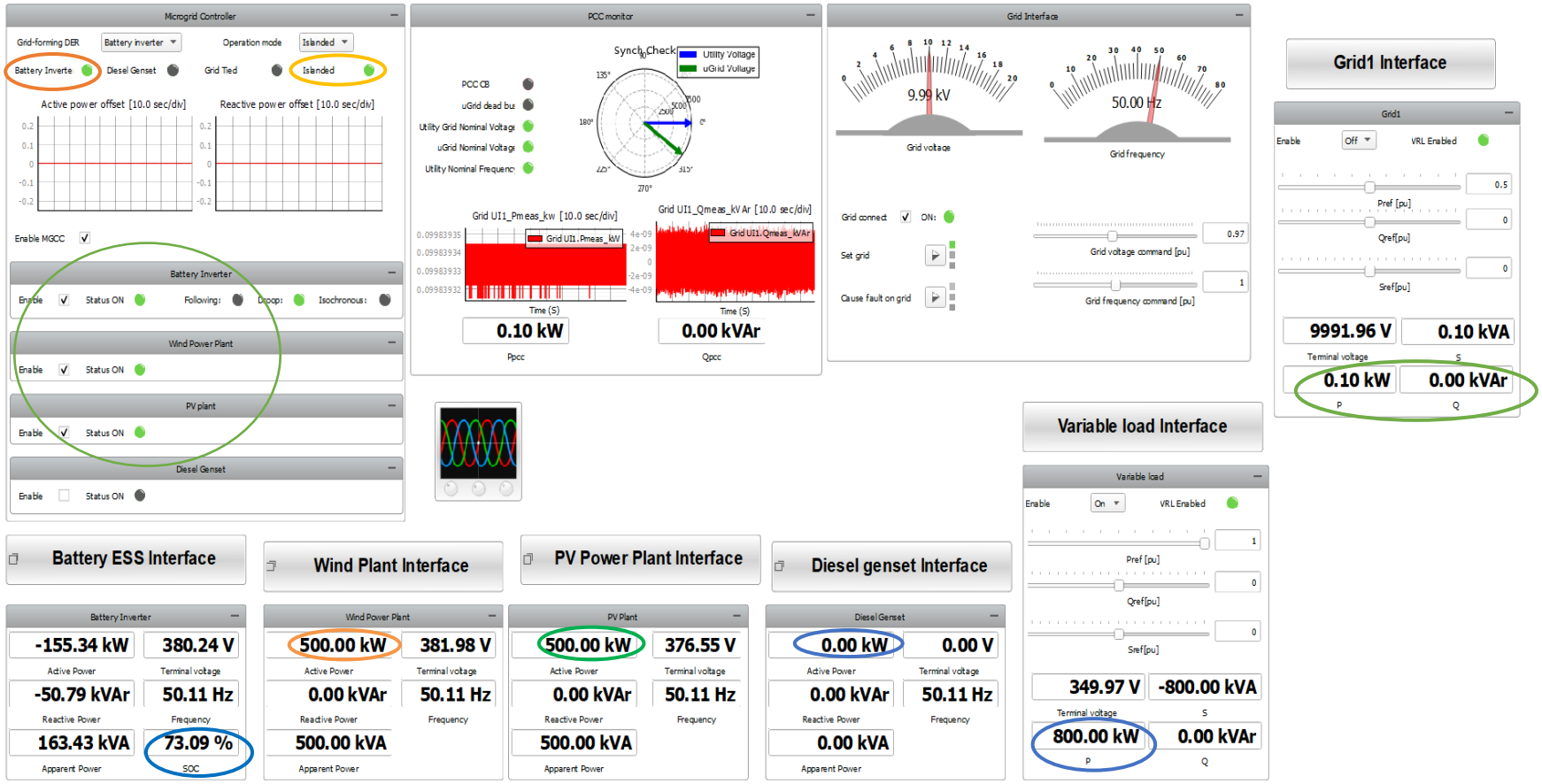


Figure 8.2: HIL SCADA panel interface for scenario 2.

Figure 8.3 shows the HIL panel interface when the battery is fully charged and the utility grid is connected to the system to be supplied by the excess of production.

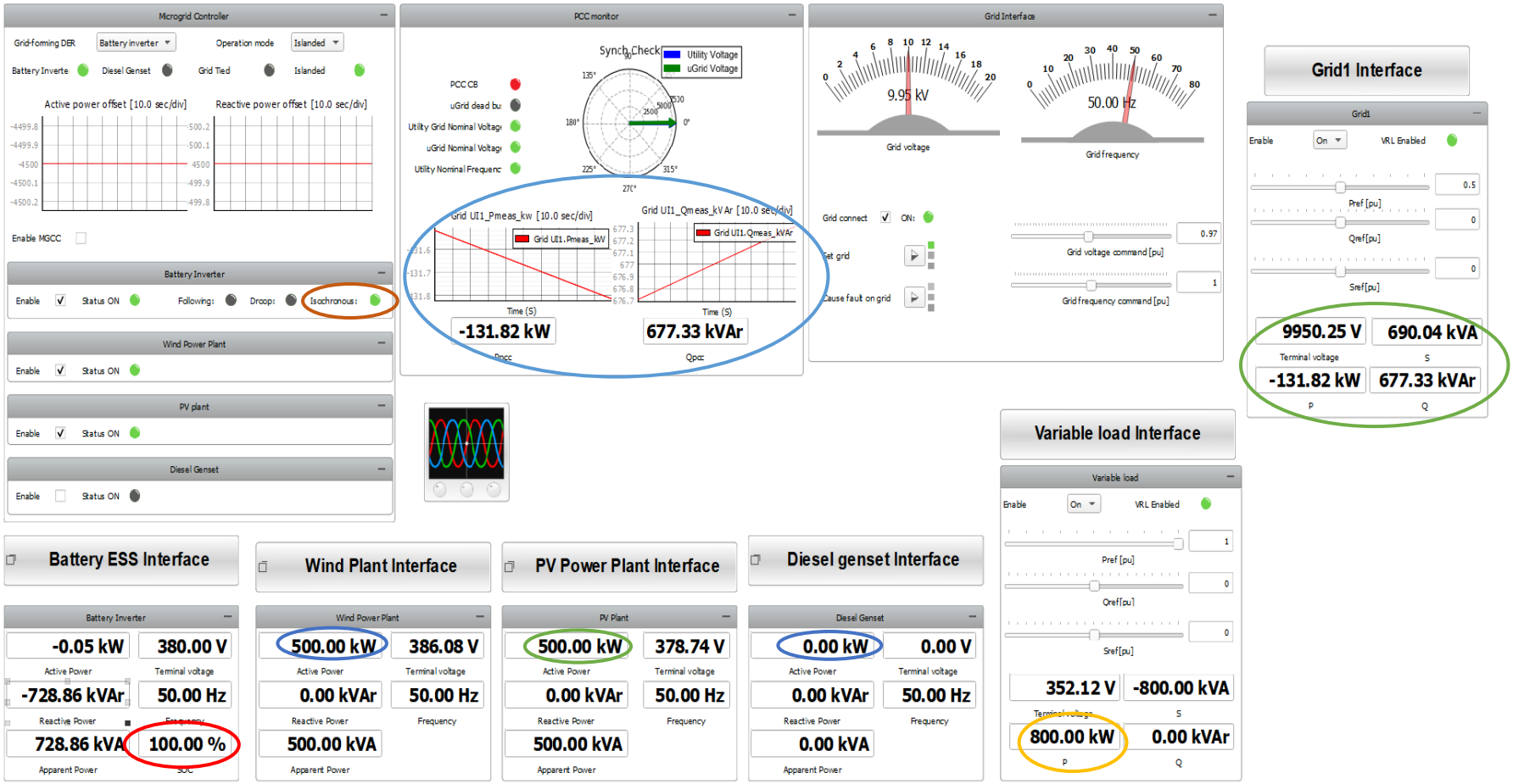


Figure 8.3: HIL SCADA panel interface for grid connected mode.

Scenario 3: This Figure 8.4 shows the HIL SCADA panel interface when the load demand exceeds the power generation.

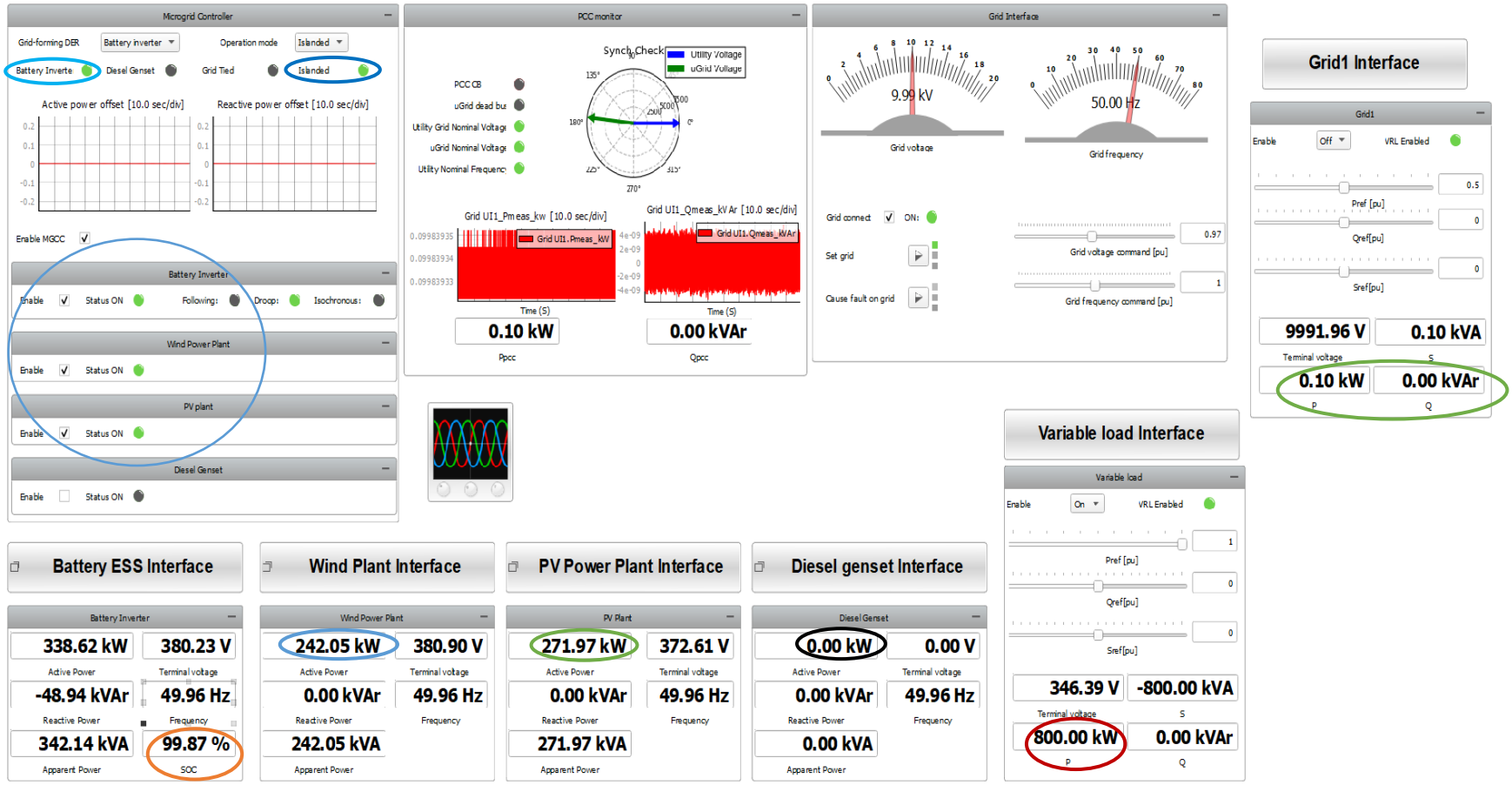


Figure 8.4: HIL SCADA panel interface for scenario 3.

When the battery reaches its minimum limit, it is disconnected. Figure 8.5 presents the HIL SCADA panel interface for the third scenario.

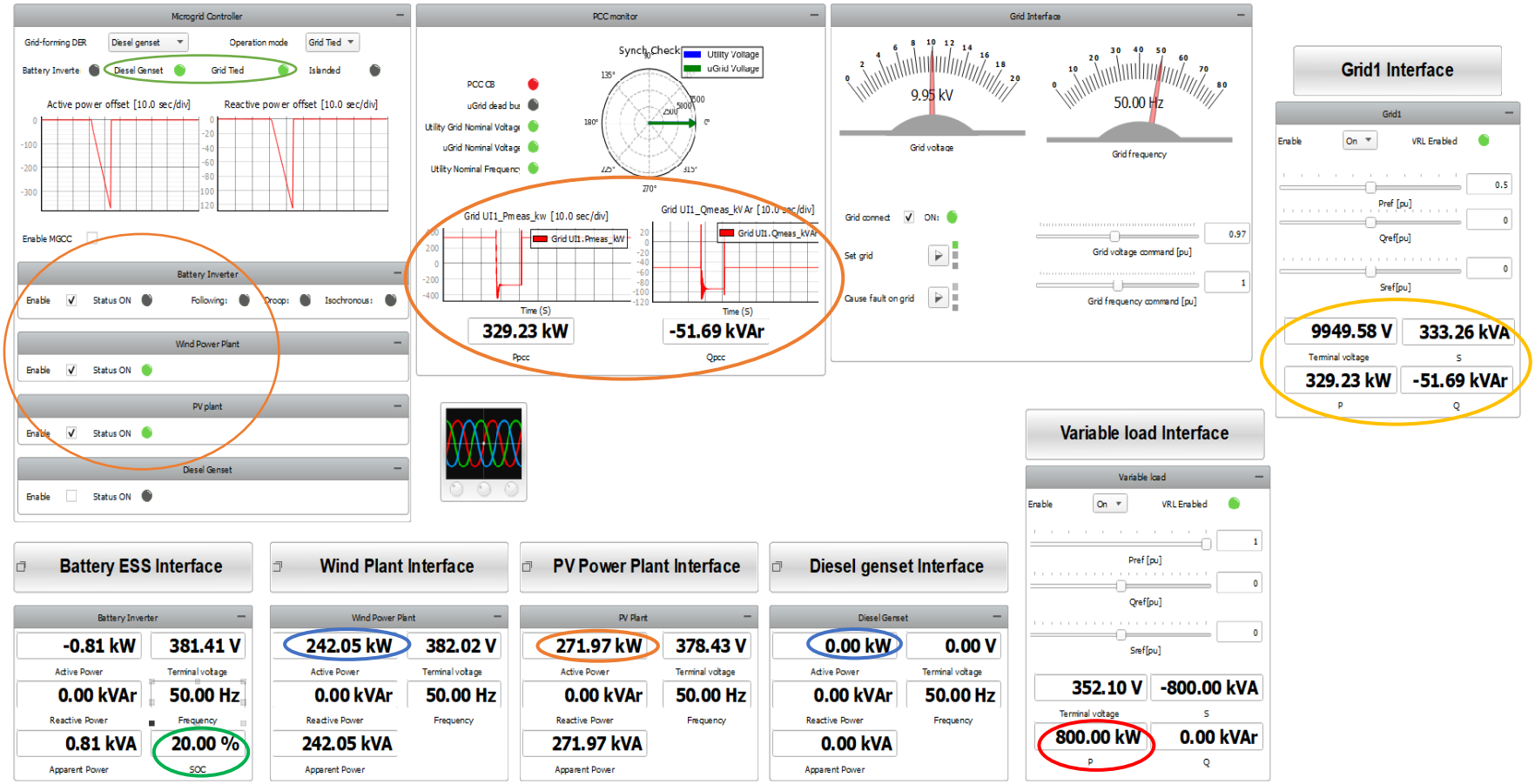


Figure 8.5: HIL SCADA panel interface when the battery attained its minimum value.

The HIL SCADA panel interface for scenario 3 when the utility grid is not available, is illustrated in Figure 8.6.

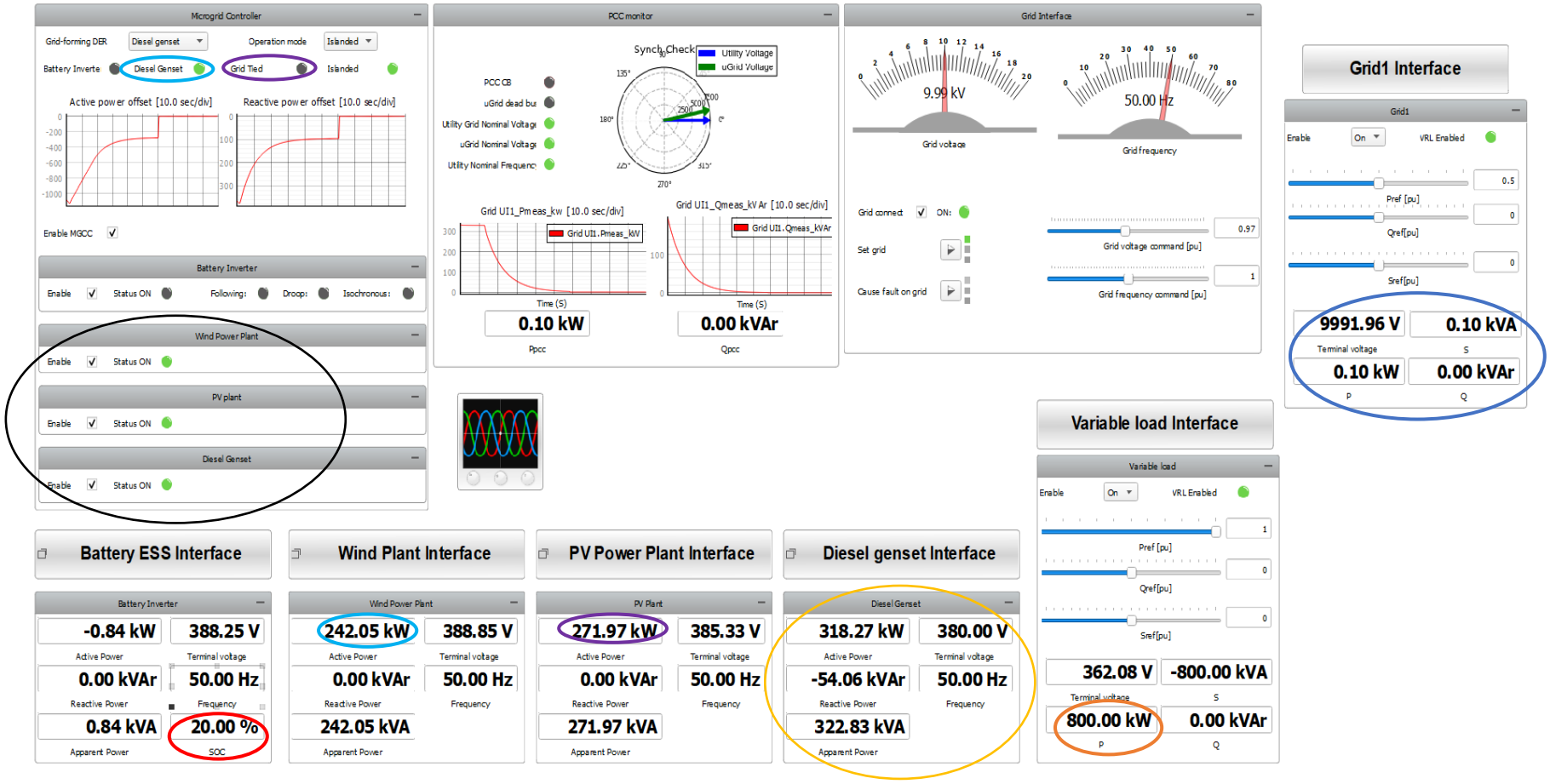


Figure 8.6: HIL SCADA panel interface when diesel generator switched on.

Two different software platforms have been used in this research. Simulink blocks from the MATLAB / Simulink software were used in the design and development of the hybrid micro-grid simulation model and Stateflow logical programming environment was employed to implement the EMS algorithm model. Hardware and software solutions for real-time simulation from Typhoon HIL software was utilized to test, validate and optimize the developed energy management control performance. Through the development of an advanced EMS control for hybrid micro-grid systems integrating RESs, this research contributes to the body of knowledge already in existence. In order to build a robust and effective energy network, the study integrates solar, wind, and diesel generator with a battery. Intermittency related issues were the main focus, along with energy dispatch optimization and system stability.

Developing an algorithm to optimize the coordination of RESs and battery energy storage inside a hybrid micro-grid was the motivation behind this study, which aimed to expedite the adoption of sustainable energy solutions. This work offers useful insights for engineers, policymakers, and stakeholders engaged in the planning and execution of renewable energy projects by creating reliable EMS control for hybrid micro-grid systems. Beyond just theoretical developments, the potential impact offers real help in the shift to cleaner, more sustainable energy sources in the future. Furthermore, by offering useful instructions for the development and management of hybrid micro-grid systems, this research encourages a wider adoption of sustainable energy practices. Additionally, the implemented algorithm control is adaptable, allowing users to access and modify any control parameter.

The test from the Typhoon HIL software demonstrates the effectiveness of the implemented EMS control. The results found in the Typhoon HIL software are coherent with those found in the MATLAB/Simulink software. The developed EMS algorithm enhances the integration of RESs into the power grid and facilitates their optimal deployment. It also satisfies all scenarios illustrated and regulates the energy transfer between the utility grid, the load demand, and the hybrid micro-grid system. Additionally, the developed energy management system controls the battery’s state of charge and discharge and allows the battery to avoid rapid charge and deep discharge by maintaining its SOC into admissible conditions. The results comparison from MATLAB/Simulink software and Typhoon HIL software is presented in Table 8.1.

Table 8.1: Results Comparison

Conditions	MATLAB / Simulink	Typhoon HIL
Scenario 1 (P_G = P_L)		
P_G = P_L	For this scenario, the generated power from the renewable energy sources is equal to the demand of the load, then, the load is provided without any interruption.	The real–time simulation demonstrated that the load demand was perfectly supplied by the power generated from the RESs and supplied without any interruption.
Scenario 2 (P_G > P_L)		
SOC < 100%	When the power generated becomes more than the load demand, the surplus of the production was used to charge the battery based on the charging conditions.	The real–time simulation showed that the condition was respected. The battery was charged until its reached its maximum value and at the same time the load was also supplied.
SOC = 100%	When the battery was fully charged, it was disconnected from the system and the remaining excess of production was sent to the utility grid and at the same time, the load was supplied without interruption.	The simulation in real–time confirmed that the condition was successfully respected. The battery was automatically disconnected and the surplus of production was supplied to the utility grid and the load was supplied.
Scenario 3 (P_G < P_L)		
SOC > 20%	The third scenario was when the generated power was not able to handle the load demand. The requirement of the load was met by the help of the battery according to its SOC state. The load was supplied by the available power generated from the renewable energy sources and the battery. When the battery discharge limit was reached, it was disconnected from the system.	The real–time simulations have shown that the conditions were reached. The power generated from the renewable energy sources and battery supplied the load. When the minimum value of the SOC was attained, the battery was automatically disconnected from the system.

$SOC \leq 20\%$	The third scenario was when the battery reached its minimum value and the generated power was not able to handle the load demand. For this case, the load demand was met by the utility grid or the diesel generator assistance according to the utility grid accessibility.	The simulation on the real–time demonstrated that the load demand was supplied by the help of the utility grid or diesel generator based on the utility grid availability and the power generated from the renewable energy sources.
Utility grid availability = 1	For the first case when the utility grid was available, the load demand was supplied by the available produced power and the utility grid.	The real–time simulation showed that the condition was satisfied and the load demand was supplied by the available power generated and the utility grid.
Utility grid availability = 0	For the second case when the utility grid was not available, the load demand was supplied by the available power generated RESs and the diesel generator.	The simulation in real–time showed that the condition was met and the load demand was met by the available generated power and the diesel generator.

8.7. Conclusions

The transition towards a more sustainable and resilient energy future has led to increased interest in hybrid renewable micro-grid systems. These systems combine different renewable energy sources, energy storage technologies, and advanced control strategies to create a localized energy network, which can operate in both connected to and independently from a utility grid. An energy storage system is an essential component of hybrid renewable micro-grid systems, offering a wide range of benefits that improve energy reliability, efficiency, cost-effectiveness, and environmental sustainability. The most popular energy storage devices in renewable micro-grids is batteries. They store and manage energy, which effectively addresses the inherent challenges of intermittent RESs.

This research implemented and developed an energy management system for a hybrid renewable micro-grid system. MATLAB/Simulink software was used to develop the hybrid micro-grid model and the EMS algorithm control, and Typhoon HIL's real - time digital simulator was used to test, validate and optimize their performance. This research aimed to implement an EMS control for hybrid renewable micro-grid systems in order to maximize the use of RESs and improve their integration into the power grid. Thus, the primary objective of this research

was to implement an EMS control that regulates the energy transfer between the hybrid micro-grid system and both directly connected to the load and the utility grid. The battery charge / discharge control was the second objective of this study. Various sequences were employed to conduct these objectives, including designing a model of the components of a hybrid micro-grid that was used in the simulation, developing a simulation of a hybrid micro-grid, developing a control scheme for the hybrid micro-grid, and developing an EMS algorithm for the hybrid micro-grid system.

In order to achieve the aim and objectives of the study, MATLAB/Simulink software was used to implement and develop a micro-grid model, as well as to develop a control system scheme and an energy management system algorithm. Firstly, a DC micro-grid system operating in isolated mode was developed and secondly, a hybrid AC micro-grid system operating in both isolated and connected to the utility grid was also developed. The Stateflow logical programming environment method in MATLAB/Simulink software was utilized in the development of the control system scheme. The developed EMS control was tested, validated and optimized utilizing Typhoon HIL's real - time digital simulator. During the simulation, a variety of scenarios were utilized to demonstrate the resilience and efficacy of the developed EMS control to support the load in both isolated and grid-connected modes and guarantee the battery in the hybrid micro-grid system operates as intended.

The objective of the work presented in Chapter Four was to implement an energy management system and control system methods for the DC micro-grid using MATLAB/Simulink software. This algorithm demonstrated its capability to assure the dependability, resilience, robustness, and correct operation of the system based on all of the developed circumstances. The results show that the battery could manage the load requirements for each of the scenarios that were taken into consideration. Furthermore, compared to previous comparable works, this developed method had a 20% lower total cost and a lower battery degrading impact. The results also demonstrated that the economic analysis in terms of levelized cost of energy (LCOE) could drop and that the initial investment cost could be relatively lower.

The work presented in Chapter Six and Chapter Seven demonstrated how the developed EMS effectively manages the load in both isolated and grid-connected modes, ensuring the proper functioning of the battery within the hybrid AC micro-grid system. To achieve the aim and objectives of the study, MATLAB/Simulink software was used in Chapter Six to implement and develop the hybrid AC micro-grid model, as well as to develop the control system scheme and the EMS algorithm. The Stateflow logical programming environment in MATLAB/Simulink software was also utilized in the development of the control system schemes. The developed

EMS control was tested, validated and optimized utilizing real-time digital simulator of Typhoon HIL in Chapter Seven.

Compare to the work presented in Chapter Four, the EMS algorithm developed in this study allowed the battery to charge when the production power from RESs is greater or equal to 20% of the generated power. The total power produced by RESs was 1 MW, and 20% is equivalent to 200 kW. Thus, the battery could only be recharged when ≥ 200 kW of power are produced. At the beginning of the charging process, a high power input was used to quickly charge the battery up to approximately 70% SOC. This phase used a higher current to rapidly increase the charge level. The value of this higher power can vary depending on the battery specifications and system requirements, but typical values for the charging power in the initial phase can range from 0.5C to 1C (where C is the battery's capacity in ampere-hours). For this research, a 900 Ah battery was charged at 0.5C which received 450 A of current. Once the battery reaches around 70% SOC, the charging rate was reduced to prevent overheating and overcharging, which can damage the battery cells and reduce their lifespan. In comparison to a situation when the input is smaller, the results show that charging the battery under these conditions with a higher power input has several benefits in terms of efficiency, charging time, and batteries overall performance.

The main advantage of this implemented algorithm is that the transfer of energy between the micro-grid system and the variable AC load, both directly connected and connected to the utility grid, is regulated. It also maintains a proper relationship between the battery charging and discharging rates according to their operating conditions and allows the battery to maintain its state of charge within acceptable bounds, which range from 20% to 100% and increases the lifespan of batteries. Additionally, the real-time experimental results obtained using the Typhoon HIL software demonstrated a good performance in comparison with those achieved utilizing the Stateflow logical language in the MATLAB/Simulink environment. The developed EMS control was tested according to different scenarios and showed to be extremely effective. Both results were similar and were based on the RESs production, utility grid, diesel generator, variable AC load demand and battery SOC. In discharge mode, the battery responded instantly, and during high production, it was perfectly recharged. Both the utility grid and the hybrid micro-grid system were able to successfully operate since the power was shared between them according to the defined conditions.

These implemented control rules of the hybrid renewable micro-grid contribute to achieving power balance, with the battery SOC consistently meeting the specified values to extend battery life. It is seen that a battery charged at higher power can be more versatile in terms of

charging options. By being compatible with different charging environments, the results show that greater flexibility and adaptation to a variety of charging scenarios are provided by batteries with higher charging power. In this research, due to the intermittent behavior of the renewable resources a higher charging power was adopted to refill the energy of the battery within a shorter charging time-window. By using a higher power, most of the available charging duration can be made. Moreover, the energy density utilization can be improved by charging the battery with greater power. It is also seen that there is a possibility to maximize the rate at which the energy is transferred into the battery by charging at higher power, and it ensures an efficient utilization of its energy storage capacity. It was realized that when the battery was charged at lower power levels, the charging process was very slow and in real life, this can produce heat, and heat may be harmful to the lifespan of batteries. Increasing the power input during charging can shorten the charging period, minimize the total heat production, and possibly increase the longevity of batteries.

CHAPTER 9: RECOMMENDATIONS FOR FUTURE WORK

Further investigation is warranted in this domain to improve the system's overall reliability. The following are recommended:

- As generally the power produced by RESs exceeds the requirements of the load, in this research, the production excess was stored in the battery and subsequently supplied to the grid. It is recommended to implement an EMS control that optimizes the utilization of this power excess by supplying it toward a specific load like water heating with storage tanks, ambient heating or air-conditioning, and water pumping.
- More exploration into cost-effective energy management techniques for a smart micro-grid network needs to be undertaken.
- In this research project, an EMS algorithm control utilizing Stateflow logical method was developed to guarantee an effective operation of the hybrid renewable micro-grid and battery storage systems. Consequently, alternative methods like Fuzzy logic can also be employed to assess the efficacy of this approach.
- In this study, a battery was used as a backup. It is important to note that different storage systems provide distinct advantages, thus it is recommended to explore other energy storage options, such as supercapacitors, flywheels or pump hydro storage and this will help to identify the most suitable technical and financial options across various timeframes.

REFERENCES

A. Farret, F., & A. Vieira, E. (2020). Recovery of Photovoltaic Module Heat Using Thermoelectric Effect. *Renewable Energy - Resources, Challenges and Applications*, 0–17. https://doi.org/10.5772/intechopen.87989

Abbasi, M., Abbasi, E., Li, L., Aguilera, R. P., Lu, D., & Wang, F. (2023). Review on the Microgrid Concept, Structures, Components, Communication Systems, and Control Methods. *Energies*, *16*(1). https://doi.org/10.3390/en16010484

Abhishek, A., Ranjan, A., Devassy, S., Verma, K. B., Ram, S. K., and Dhakar, A. K., "Review of hierarchical control strategies for DC microgrid," IET Renew. Power Gener., vol. 14, no. 10, pp. 1631–1640, 2020.

Adajah, Y. Y., Thomas, S., Haruna, M. S., & Anaza, S. O. (2021). Distributed Generation (DG): A Review. *2021 1st International Conference on Multidisciplinary Engineering and Applied Science, ICMEAS 2021*. https://doi.org/10.1109/ICMEAS52683.2021.9692353

Agrawal, M., & Mittal, A. (2011). Micro grid technological activities across the globe: A review. *Int. J. Res. Rev. Applied Sci*, *7*(May), 147–152. Retrieved from http://www.arpapress.com/Volumes/Vol7Issue2/IJRRAS_7_2_07.pdf

Ahmad, S., Mekhilef, S., & Mokhlis, H. (2020). DQ-axis Synchronous Reference Frame based P-Q Control of Grid Connected AC Microgrid. *2020 IEEE International Conference on Computing, Power and Communication Technologies, GUCON 2020*, 842–847. https://doi.org/10.1109/GUCON48875.2020.9231080

Ahmed, K., Seyedmahmoudian, M., Mekhilef, S., Mubarak, N. M., & Stojcevski, A. (2021). A Review on Primary and Secondary Controls of Inverter-interfaced Microgrid. *Journal of Modern Power Systems and Clean Energy*, *9*(5), 969–985. https://doi.org/10.35833/MPCE.2020.000068

Ahmed, M., Meegahapola, L., Vahidnia, A., & Datta, M. (2020). Stability and Control Aspects of Microgrid Architectures-A Comprehensive Review. *IEEE Access*, *8*, 144730–144766. https://doi.org/10.1109/ACCESS.2020.3014977

Akoubi, N., Salem, J. Ben, & El Amraoui, L. (2022). Contribution on the Combination of Artificial Neural Network and Incremental Conductance Method to MPPT Control Approach. *Proceedings of the 2022 5th International Conference on Advanced Systems and Emergent Technologies, IC_ASET 2022*, 109–114. https://doi.org/10.1109/IC_ASET53395.2022.9765914

Al-Ismail, F. S. (2021). DC Microgrid Planning, Operation, and Control: A Comprehensive Review. *IEEE Access*, *9*, 36154–36172. https://doi.org/10.1109/ACCESS.2021.3062840

AL-Wesabi, I., Zhijian, F., Hussein Farh, H. M., A. Al-Shamma'a, A., Dong, H., M. Al-Shaalan, A., & Kandil, T. (2022). Maximum power extraction and DC-Bus voltage regulation in grid-connected PV/BES system using modified incremental inductance with a novel inverter control. *Scientific Reports*, *12*(1), 1–21. https://doi.org/10.1038/s41598-022-22952-0

Al Tahtawi, A. R., Yahya, S., & Ferdian, A. (2021). Fuzzy Integral Control Design for Boost Converter Based on State-Space Average Model Approach. *2021 8th International Conference on Information Technology, Computer and Electrical Engineering, ICITACEE 2021*, 24–29. https://doi.org/10.1109/ICITACEE53184.2021.9617507

Ali-Almaktoof, A. M., Kahn, M., T., E., Raji., A., K., Multilevel inverters using finite set-model predictive current control for renewable energy systems applications. (2015). *Cape Peninsula University of Technology*, (March)

Ali, M., Yaqoob, M., Cao, L., & Loo, K. H. (2021). Enhancement of DC-bus voltage regulation in cascaded converter system by a new sensorless load current feedforward control scheme. *IET Power Electronics*, *14*(8), 1457–1467. https://doi.org/10.1049/pel2.12123

Ali, S., et al., "Demand Response Program for Efficient Demand-Side Management in Smart Grid Considering Renewable Energy Sources," IEEE Access, vol. 10, pp. 53832–53853, 2022.

Altaf, M. W., & Member, G. S. (2022). Microgrid Protection Challenges and Mitigation Approaches — A Comprehensive Review. *IEEE Access*, *10*, 38895–38922. https://doi.org/10.1109/ACCESS.2022.3165011

Altahir, A. A. R. (2020). Park and Clark Transformations: A Short Review. *No. April*, (April), 2–5. https://doi.org/10.13140/RG.2.2.20287.46241

Andre, J., Estefan, D., and Llanos, J. R., "Energy Management System (EMS) Based on Model Predictive Control (MPC) for an Isolated DC Microgrid," Energies, pp. 1–22, 2023.

Anttila, S., Döhler, J. S., Oliveira, J. G., & Boström, C. (2022). Grid Forming Inverters: A Review of the State of the Art of Key Elements for Microgrid Operation. *Energies*, *15*(15), 1–30. https://doi.org/10.3390/en15155517

Asgher, U., Rasheed, M. B., and Awais, M., "Demand Response Benefits for Load Management Through Heuristic Algorithm in Smart Grid," 2018 International Symposium on Recent Advances in Electrical Engineering (RAEE), pp. 1–6, 2018.

Ashagire, A. A., Adjallah, K. H., & Bekele, G. (2021). A New Design Approach of Hybrid AC/DC Microgrid System Based on Resilience Index and Lifecycle Cost Evaluation. *International Conference on Electrical, Computer, and Energy Technologies, ICECET 2021*, (December), 9–10. https://doi.org/10.1109/ICECET52533.2021.9698602

Ashok Kumar, A., & Amutha Prabha, N. (2022). A comprehensive review of DC microgrid in market segments and control technique. *Heliyon*, *8*(11), e11694. https://doi.org/10.1016/j.heliyon.2022.e11694

Avdeev, B. A., Vyngra, A. V., & Sobolev, V. S. (2022). Integration of Renewable Energy Sources into Smart Grids Using Converters Based on Solid-State Transformers. *2022 5th International Youth Scientific and Technical Conference Relay Protection and Automation, RPA 2022*, 1–10. https://doi.org/10.1109/RPA57581.2022.9951082

Avendano, A. (2022). Microgrid Controller Evaluation Using Real-Time Digital Simulation. *2022 IEEE Power and Energy Society Innovative Smart Grid Technologies Conference, ISGT 2022*, 5–9. https://doi.org/10.1109/ISGT50606.2022.9817558

Aviles, A. D., Pascual, J., Marroyo, L., Sanchis, P., and Guinjoan, F., "Fuzzy logic-based energy management system design for residential grid-connected microgrids," IEEE Trans. Smart Grid, vol. 9, no. 2, pp. 530–543, 2018.

Ayenew Haile, E., Biru Worku, G., Mulatu Beyene, A., & Berhanu Tuka, M. (2021). Upwind Horizontal Axis Wind Turbine Output Power Optimization via Artificial Intelligent Control System. *Automation, Control and Intelligent Systems*, *9*(1), 6. https://doi.org/10.11648/j.acis.20210901.13

Babayomi, O., Li, Z., Zhang, Z., Sun, Y., Dragicevic, T., & Rodriguez, J. (2020). The Role of Model Predictive Control in Microgrid Power Quality-A Survey. *2020 IEEE 11th International Symposium on Power Electronics for Distributed Generation Systems, PEDG 2020*, 340–345. https://doi.org/10.1109/PEDG48541.2020.9244364

Bahrani, B. (2021). Power-synchronized grid-following inverter without a phase-locked loop. *IEEE Access*, *9*, 112163–112176. https://doi.org/10.1109/ACCESS.2021.3102631

Balamurugan, S., "Real Power Flow Control in a Transmission Line by Varying the Turns Ratio of the Injection Transformer," 2019 Innovations in Power and Advanced Computing Technologies (i-PACT), pp. 1–5, 2019.

Barasa Kabeyi, M. J., & Olanrewaju, O. A. (2022). Geothermal wellhead technology power plants in grid electricity generation: A review. *Energy Strategy Reviews*, *39*, 100735. https://doi.org/10.1016/j.esr.2021.100735

Bateman, M., “Measurement of elastic parameters of anisotropic medium Experimental sample Experimental sample Observation system Observation system Measurement of transmitted wave field in Ti medium Fixed (smaller) offset experimental results” Rev. Afr. Polit. Econ., vol. 0, no. 0, pp. 1–6, 2018.

Baziar, A., & Kavousi-Fard, A. (2013). Considering uncertainty in the optimal energy management of renewable micro-grids including storage devices. *Renewable Energy*, *59*, 158–166. https://doi.org/10.1016/j.renene.2013.03.026

Beerten, J., and Belmans, R., “Analysis of power sharing and voltage deviations in droop-controlled DC grids,” IEEE Trans. Power Syst., vol. 28, no. 4, pp. 4588–4597, 2013.

Ben Mansour, H., Chaarabi, L., Jelassi, K., & Guerrero, J. M. (2022). Supervisory control for Energy Management of Islanded Hybrid AC/DCMicrogrid. *International Journal of Computer Science and Network Security*, *22*(3), 355–363. https://doi.org/10.22937/IJCSNS.2022.22.3.1

Bera, S., Chakraborty, S., Kar, S., & Samantaray, S. R. (2022). Hierarchical Control for Voltage Unbalance Mitigation Considering Load Management in Stand-Alone Microgrid. *IEEE Transactions on Smart Grid*. https://doi.org/10.1109/TSG.2022.3222490

Bernet, D., & Hiller, M. (2019). Grid-connected medium-voltage converters with parallel voltage-source active filters. *IET Electric Power Applications*, *13*(10), 1507–1513. https://doi.org/10.1049/iet-epa.2019.0021

Beykverdi, M., Jalilvand, A., and Ehsan, M., “Intelligent Power Management of Islanded DC Microgrid based on Droop Fuzzy Control,” International journal of Engineering, Business and Management (IJEBM), Am. J. Sci., vol. 1, no. 1, pp. 1–11, 2017.

Bhavaraju, V., Yang, Y., & Buck, E. F. (2022). *Distributed Energy Resource Control and Utility Interconnection Management*.

Bidram, A., and Davoudi, A., “Hierarchical structure of microgrids control system,” IEEE Trans. Smart Grid, vol. 3, no. 4, pp. 1963–1976, 2012.

Bilbao, J., Bravo, E., García, O., Rebollar, C., and Varela, C., “Optimising Energy Management in Hybrid Microgrids,” Mathematics, vol. 10, no. 2, 2022.

Bompard, E., Mazza, A., and Toma, L., “Classical grid control: Frequency and voltage stability,” Convert. Dyn. Control Mod. Power Syst., pp. 31–65, 2021.

Bradbury, K. (2010). Energy Storage Technology Review. *A Brief Introduction to Batteries*, (September), 1–33.

Carpintero-Rentería, M., Santos-Martín, D., & Guerrero, J. M. (2019). Microgrids literature review through a layers structure. *Energies*, *12*(22), 1–22. https://doi.org/10.3390/en12224381

Casado-Machado, F., Martinez-Ramos, J. L., Barragan-Villarejo, M., Maza-Ortega, J. M., & Rosendo-Macias, J. A. (2020). Reduced Reference Frame Transform: Deconstructing Three-Phase Four-Wire Systems. *IEEE Access*, *8*, 143021–143032. https://doi.org/10.1109/ACCESS.2020.3012510

Chaouachi, A., Kamel, R. M., Andoulsi, R., & Nagasaka, K. (2013). Multiobjective intelligent energy management for a microgrid. *IEEE Transactions on Industrial Electronics*, *60*(4), 1688–1699. https://doi.org/10.1109/TIE.2012.2188873

Chaturvedi, S., Fan, Y., & Wang, M. (2023). *Output Filters , Current Control , and Weak Grids Operation*.

Chen, M. R., Wang, H., Zeng, G. Q., Dai, Y. X., & Bi, D. Q. (2018). Optimal P-Q control of grid-connected inverters in a microgrid based on adaptive population extremal optimization. *Energies*, *11*(8). https://doi.org/10.3390/en11082107

Chowdhury, S., Chowdhury, S. P., & Crossley, P. (2009). Microgrids and active distribution networks. In *Microgrids and Active Distribution Networks*. https://doi.org/10.1049/pbrn006e

Come Zebra, E. I., van der Windt, H. J., Nhumaio, G., & Faaij, A. P. C. (2021). A review of hybrid renewable energy systems in mini-grids for off-grid electrification in developing countries. *Renewable and Sustainable Energy Reviews*, *144*(March). https://doi.org/10.1016/j.rser.2021.111036

Dadi, R., Meenakshy, K., & Damodaran, S. K. (2023). A Review on Secondary Control Methods in DC Microgrid. *Journal of Operation and Automation in Power Engineering*, *11*(2), 105–112. https://doi.org/10.22098/JOAPE.2022.9157.1636

Dagdougui, H., Minciardi, R., Ouammi, A., Robba, M., & Sacile, R. (2010). Modelling and control of a hybrid renewable energy system to supply demand of a green-building. *Modelling for Environment's Sake: Proceedings of the 5th Biennial Conference of the International Environmental Modelling and Software Society, IEMSs 2010*, *2*, 972–979.

Deokate, M. B., "Distributed Optimal Power Flow Control Topology," 2022 International Conference on Electronics and Renewable Systems (ICEARS), pp. 198–204, 2022.

Ding, W., & Bauer, T. (2021). Progress in Research and Development of Molten Chloride Salt Technology for Next Generation Concentrated Solar Power Plants. *Engineering*, *7*(3), 334–347. https://doi.org/10.1016/j.eng.2020.06.027

Distributed, U., & Storage, E. (2022). *Using Distributed Energy Storage Systems*.

Doan, N. S., Tsvetkov, A. N., & Nguyen, T. H. (2021). Study and implementation of space vector pulse width modulation inverter on an arduino. *E3S Web of Conferences*, *288*, 4–9. https://doi.org/10.1051/e3sconf/202128801059

Dolara, A., Grimaccia, F., Magistrati, G., and Marchegiani, G., "Optimal management algorithm for battery energy storage system included in an islanded Microgrid," EEEIC 2016 - Int. Conf. Environ. Electr. Eng., 2016.

Dominka, S., Smith, H., & Hartmann, B. (2021). Artificial Neural Networks for (Automotive) Embedded Control - A Comparative Study. *2021 IEEE 11th Annual Computing and Communication Workshop and Conference, CCWC 2021*, 1489–1494. https://doi.org/10.1109/CCWC51732.2021.9376085.

Dragicevic, T., Guerrero, J. M., Vasquez, J. C., and Skrlec, D., "Supervisory control of an adaptive-droop regulated DC microgrid with battery management capability," IEEE Trans. Power Electron., vol. 29, no. 2, pp. 695–706, 2014.

El Haj Assad, M., Almallahi, M. N., Alshabi, M., & Delnava, H. (2022). Heating and Cooling By Geothermal Energy. *2022 Advances in Science and Engineering Technology International Conferences, ASET 2022*. https://doi.org/10.1109/ASET53988.2022.9734943

Faisal, M., Hannan, M. A., Ker, P. J., Hussain, A., Mansor, M. Bin, & Blaabjerg, F. (2018). Review of energy storage system technologies in microgrid applications: Issues and challenges. *IEEE Access*, *6*, 35143–35164. https://doi.org/10.1109/ACCESS.2018.2841407

Fazeli, A., Sumner, M., Christopher, E., and Johnson, M., "Power Flow Control for Power and Voltage Management in Future Smart Energy Communities," 3rd Renewable Power Generation Conference (RPG 2014), pp. 1–6, 2014.

Feng, W., Jin, M., Liu, X., Bao, Y., Marnay, C., Yao, C., & Yu, J. (2018). A review of microgrid development in the United States – A decade of progress on policies, demonstrations, controls, and software tools. *Applied Energy*, *228*(July), 1656–1668. https://doi.org/10.1016/j.apenergy.2018.06.096

Feng, J., Li, Q., and Lee, F. C., "Load Detection and Power Flow Control Algorithm For an Omnidirectional Wireless Power Transfer System," IEEE Transactions on Industrial Electronics, vol. 69, no. 2, pp. 1422–1431, 2022.

Fuxing, Z., Yonghua, G., Honglei, M., Juan, L., Pan, C., & Zhaoyu, Z. (2021). Analysis of AC / DC Hybrid Microgrid System Architecture and Typical Operation Conditions. *2021 4th International Conference on Energy, Electrical and Power Engineering, CEEPE 2021*, 807–

812. https://doi.org/10.1109/CEEPE51765.2021.9475635

Gaballah, M., & El-Bardini, M. (2013). Low cost digital signal generation for driving space vector PWM inverter. *Ain Shams Engineering Journal*, *4*(4), 763–774. https://doi.org/10.1016/j.asej.2013.02.004

Gao, X., Zhou, D., Anvari-Moghaddam, A., & Blaabjerg, F. (2021). Grid-Following and Grid-Forming Control in Power Electronic Based Power Systems: A Comparative Study. *IECON Proceedings (Industrial Electronics Conference)*, *2021-Octob*, 1–6. https://doi.org/10.1109/IECON48115.2021.9589432

García, P., Torreglosa, J. P., Fernández, L. M., & Jurado, F. (2013). Optimal energy management system for stand-alone wind turbine/photovoltaic/ hydrogen/battery hybrid system with supervisory control based on fuzzy logic. *International Journal of Hydrogen Energy*, *38*(33), 14146–14158. https://doi.org/10.1016/j.ijhydene.2013.08.106

Ghorashi Khalil Abadi, S. A., Habibi, S. I., Khalili, T., & Bidram, A. (2022). A Model Predictive Control Strategy for Performance Improvement of Hybrid Energy Storage Systems in DC Microgrids. *IEEE Access*, *10*, 25400–25421. https://doi.org/10.1109/ACCESS.2022.3155668

Guerrero J. M., Chandorkar, M., Lee, T. L., and Loh, P. C., “Advanced control architectures for intelligent microgridspart i: Decentralized and hierarchical control,” IEEE Trans. Ind. Electron., vol. 60, no. 4, pp. 1254–1262, 2013.

Gulipalli, S. C., Gude, S., & Chu, C. C. (2021). A Novel In-Loop Filtered Dual Synchronous Reference Frame Phase Locked Loop under Practical Grid Conditions. *Proceedings of 2021 IEEE 2nd International Conference on Smart Technologies for Power, Energy and Control, STPEC 2021*. https://doi.org/10.1109/STPEC52385.2021.9718661

Hadi, A. A. L., Silva, C. A. S., Hossain, E., and Challoo, R., “Algorithm for Demand Response to Maximize the Penetration of Renewable Energy,” IEEE Access, vol. 8, pp. 55279–55288, 2020.

Haider, S., Member, G. S., and Moghadam, S. H., “Algorithm and Optimization Model for Energy Storage Using Vertically Stacked Blocks,” vol. 8, IEEE, pp. 217688-217700, 2020.

Halifa, M. O. K., and Rikiez, M. O. A., “a Lgorithms for E Nergy M Anagement in M Icro - Grids,” no. December, pp. 70–80, 2016.

Han, Y., Li, H., Shen, P., Coelho, E. A. A., & Guerrero, J. M. (2017). Review of Active and Reactive Power Sharing Strategies in Hierarchical Controlled Microgrids. *IEEE Transactions on Power Electronics*, *32*(3), 2427–2451. https://doi.org/10.1109/TPEL.2016.2569597

Han, Y., Zhang, K., Li, H., Coelho, E. A. A., & Guerrero, J. M. (2018). MAS-Based Distributed Coordinated Control and Optimization in Microgrid and Microgrid Clusters: A Comprehensive Overview. *IEEE Transactions on Power Electronics*, *33*(8), 6488–6508. https://doi.org/10.1109/TPEL.2017.2761438

Hasan, M. A., & Parida, S. K. (2019). Modeling and Design of a Synchronous Reference Frame Enhanced Phase Locked Loop. *Proceedings of 2019 IEEE PES Innovative Smart Grid Technologies Europe, ISGT-Europe 2019*, (2), 1–4. https://doi.org/10.1109/ISGTEurope.2019.8905493

Himabindu, E., and Naik, G. M., "Energy Management System for grid integrated microgrid using Fuzzy Logic Controller."2020 IEEE 7th Uttar Pradesh Section International Conference on Electrical, Electronics and Computer Engineering, 2020.

Hirsch, A., Parag, Y., & Guerrero, J. (2018). Microgrids: A review of technologies, key drivers, and outstanding issues. *Renewable and Sustainable Energy Reviews*, *90*(September 2017), 402–411. https://doi.org/10.1016/j.rser.2018.03.040

Hong, P., & Qin, Z. (2022). Distributed Active Power Optimal Dispatching of Wind Farm Cluster Considering Wind Power Uncertainty. *Energies*, *15*(7). https://doi.org/10.3390/en15072706

Hossen, T., & Mirafzal, B. (2022). On Stability of PQ-Controlled Grid-Following and Droop-Control Grid-Forming Inverters. *2022 IEEE Energy Conversion Congress and Exposition, ECCE 2022*, 1–7. https://doi.org/10.1109/ECCE50734.2022.9947923

Hu, J., Shan, Y., Guerrero, J. M., Ioinovici, A., Chan, K. W., and Rodriguez, J., "Model predictive control of microgrids – An overview," Renew. Sustain. Energy Rev., vol. 136, no. October, 2021.

Ishaq, S., Khan, I., Rahman, S., Hussain, T., Iqbal, A., & Elavarasan, R. M. (2022). A review on recent developments in control and optimization of micro grids. *Energy Reports*, *8*, 4085–4103. https://doi.org/10.1016/j.egyr.2022.01.080

Islam, M. A., Hasanuzzaman, M., Rahim, N. A., Nahar, A., & Hosenuzzaman, M. (2014). Global renewable energy-based electricity generation and smart grid system for energy security. *Scientific World Journal*, *2014*(November). https://doi.org/10.1155/2014/197136

Jamal, I., Elmorshedy, M. F., Dabour, S. M., Rashad, E. M., Xu, W., & Almakhles, D. J. (2022). A Comprehensive Review of Grid-Connected PV Systems Based on Impedance Source Inverter. *IEEE Access*, *10*, 89101–89123. https://doi.org/10.1109/ACCESS.2022.3200681

Jayalakshmi, N. S., Gaonkar, D. N., & Jain, S. K. (2019). Power smoothing method of PMSG based grid integrated wind energy conversion system using BESS/DSTATCOM. *International Journal of Power Electronics and Drive Systems*, *10*(4), 1969–1976. https://doi.org/10.11591/ijpeds.v10.i4.pp1969-1976

Jeong, M., Gfrorer, T., & Biela, J. (2022). Extending Stable Parameter Range of LCL- filters for Grid-Connected Converters by Inherent Damping of Model Predictive Control (MPC). *Proceedings of the IEEE Workshop on Computers in Power Electronics, COMPEL*, *2022-June*. https://doi.org/10.1109/COMPEL53829.2022.9829978

Jones, G. W., & Chowdhury, B. H. (2008). Distribution system operation and planning in the presence of distributed generation technology. *Transmission and Distribution Exposition Conference: 2008 IEEE PES Powering Toward the Future, PIMS 2008*, (June). https://doi.org/10.1109/TDC.2008.4517274

Julian David Gutierrez, T., Paola Catalina Sanchez, C., & Diana Marcela Ovalle, M. (2019). Design and simulation of controllers for a horizontal axis wind turbine. *4th IEEE Colombian Conference on Automatic Control: Automatic Control as Key Support of Industrial Productivity, CCAC 2019 - Proceedings*, (7). https://doi.org/10.1109/CCAC.2019.8921083

Kang, K. M., et al., “Energy management method of hybrid ac/dc microgrid using artificial neural network,” Electron., vol. 10, no. 16, 2021.

Kathiresan, A. C., PandiaRajan, J., Sivaprakash, A., Babu, T. S., & Islam, M. R. (2020). An adaptive feed-forward phase locked loop for grid synchronization of renewable energy systems under wide frequency deviations. *Sustainability (Switzerland)*, *12*(17). https://doi.org/10.3390/su12177048

Kawasaki Heavy Industries. (2016). Battery Energy Storage System -GIGACELL-. *Kawasaki.Com*, (Cict), Characteristics, FAQs. Retrieved from http://global.kawasaki.com/en/energy/solutions/battery_energy/

Khan, A., Easley, M., Hosseinzadehtaher, M., Shadmand, M. B., Abu-Rub, H., & Fajri, P. (2020). PLL-less Active and Reactive Power Controller for Grid-Following Inverter. *ECCE 2020 - IEEE Energy Conversion Congress and Exposition*, 4322–4328. https://doi.org/10.1109/ECCE44975.2020.9236408

Korompili, A., & Monti, A. (2023). Review of Modern Control Technologies for Voltage Regulation in DC/DC Converters of DC Microgrids. *Energies*, *16*(12), 4563. https://doi.org/10.3390/en16124563

Kouchaki, A., & Nymand, M. (2018). Analytical Design of Passive LCL Filter for Three-Phase

Two-Level Power Factor Correction Rectifiers. *IEEE Transactions on Power Electronics*, *33*(4), 3012–3022. https://doi.org/10.1109/TPEL.2017.2705288

Kumar, D., Zare, F., & Ghosh, A. (2017). DC Microgrid Technology: System Architectures, AC Grid Interfaces, Grounding Schemes, Power Quality, Communication Networks, Applications, and Standardizations Aspects. *IEEE Access*, *5*, 12230–12256. https://doi.org/10.1109/ACCESS.2017.2705914

Kumar Peddapelli, S. (2016). 2. Space vector pulse width modulation technique. *Pulse Width Modulation*, (May), 13–22. https://doi.org/10.1515/9783110470420-002

Kumar, S., Kumar, R., & Singh, N. (2017). Performance of closed loop SEPIC converter with DC-DC converter for solar energy system. *2017 4th International Conference on Power, Control and Embedded Systems, ICPCES 2017*, *2017-Janua*(November), 1–6. https://doi.org/10.1109/ICPCES.2017.8117668

Lewicki, A., Odeh, C. I., Kondratenko, D., & Morawiec, M. (2022). Hybridized Space-Vector Pulsewidth Modulation for Multiphase Two-Level Voltage Source Inverter. *IEEE Transactions on Power Electronics*, *37*(7), 7663–7674. https://doi.org/10.1109/TPEL.2022.3145161

Li, Z., Cheng, Z., Si, J., & Li, S. (2022). Distributed Event-Triggered Hierarchical Control to Improve Economic Operation of Hybrid AC/DC Microgrids. *IEEE Transactions on Power Systems*, *37*(5), 3653–3668. https://doi.org/10.1109/TPWRS.2021.3133487

Liu, H. D., Lin, C. H., Lu, S. Der, & Ahmad, J. (2022). A Novel VFVDC Optimized Full Bridge Inverter Control Strategy for Independent Solar Power Systems. *IEEE Access*, *10*, 44231–44247. https://doi.org/10.1109/ACCESS.2022.3169516

Lotfi, H., & Khodaei, A. (2017). AC versus DC microgrid planning. *IEEE Transactions on Smart Grid*, *8*(1), 296–304. https://doi.org/10.1109/TSG.2015.2457910

Mahmoud, G. M., ElRefaie, H. B., Elsayed, M. E., & Abo-Elkhair, E. (2022). *Novel Photovoltaic Modules and Wind Turbine Performance Modeling Techniques Based on Artificial Intelligence and Deep-Learning*. 1–7. https://doi.org/10.1109/itc-egypt55520.2022.9855721

Mahmoudian, A., Garmabdari, R., Bai, F., Stegen, S., & Lu, J. (2022). Secondary Controller for Voltage and Frequency Regulation in an Islanded Microgrid System Based on Anti-Windup Loop. *Asia-Pacific Power and Energy Engineering Conference, APPEEC*, *2022-Novem*, 1–5. https://doi.org/10.1109/APPEEC53445.2022.10072287

Malik, S., Modi, B., & Mangrolia, D. (2022). Grid Integration of Distributed Generation: Issues

and Challenges. *2022 International Conference for Advancement in Technology, ICONAT 2022*, 1–6. https://doi.org/10.1109/ICONAT53423.2022.9725826

Manuel, N. L., & İnanç, N. (2022). Sliding Mode Control-Based MPPT and Output Voltage Regulation of a Stand-alone PV System. *Power Electronics and Drives*, *7*(1), 159–173. https://doi.org/10.2478/pead-2022-0012

Mehta, D., Ravindran, A., Joshi, B., and Kamalasadan, S., "Graph Theory Based Online Optimal Power Flow Control of Power Grid With Distributed Flexible AC Transmission Systems (D-FACTS) Devices." 2015 North American Power Symposium (NAPS), 2015.

Mingsheng, Z., Peilei, F., Hesong, W., Wenkui, W., & Pengcheng, C. (2018). Hierarchical Control Strategy for Microgrid. *Proceedings of 2018 2nd IEEE Advanced Information Management, Communicates, Electronic and Automation Control Conference, IMCEC 2018*, (Imcec), 1528–1532. https://doi.org/10.1109/IMCEC.2018.8469405

Moghimi, M., Garmabdari, R., Stegen, S., Lu, J., "Battery Energy Storage Cost and Capacity Optimization for University Research," Conference: 2018 IEEE/IAS 54th Industrial and Commercial Power Systems Technical Conference (I&CPS), pp. 1–8, 2018.

Mohamed, I. S., Rovetta, S., Do, T. D., Dragicevic, T., & Diab, A. A. Z. (2019). A neural-network-based model predictive control of three-phase inverter with an output LC Filter. *IEEE Access*, *7*, 124737–124749. https://doi.org/10.1109/ACCESS.2019.2938220

Mohamadi, B., and Noshahr, J. B., "Optimal Battery Energy Storage Sizing in Microgrids by using Artificial Flora Algorithm." 2020 IEEE International Conference on Environment and Electrical Engineering and 2020 IEEE Industrial and Commercial Power Systems Europe (EEEIC / I&CPS Europe), 2020.

Monteiro, V., Monteiro, L. F. C., Lo Franco, F., Mandrioli, R., Ricco, M., Grandi, G., & Afonso, J. L. (2021). The role of front-end ac/dc converters in hybrid ac/dc smart homes: Analysis and experimental validation. *Electronics (Switzerland)*, *10*(21). https://doi.org/10.3390/electronics10212601

Moretti, L., Meraldi, L., Niccolai, A., Manzolini, G., & Leva, S. (2021). An innovative tunable rule-based strategy for the predictive management of hybrid microgrids. *Electronics (Switzerland)*, *10*(10), 1–16. https://doi.org/10.3390/electronics10101162

Morstyn, T., Hredzak, B., & Agelidis, V. G. (2018). Control Strategies for Microgrids with Distributed Energy Storage Systems: An Overview. *IEEE Transactions on Smart Grid*, *9*(4), 3652–3666. https://doi.org/10.1109/TSG.2016.2637958

Mumtaz, F., Zaihar Yahaya, N., Tanzim Meraj, S., Singh, B., Kannan, R., & Ibrahim, O.

(2021). Review on non-isolated DC-DC converters and their control techniques for renewable energy applications. *Ain Shams Engineering Journal*, *12*(4), 3747–3763. https://doi.org/10.1016/j.asej.2021.03.022

Naeinian, B., “Seamless Operation of a Microgrid Using BESS During Transition Between Grid-connected and Stand-alone Modes.” http://repository.tudelft.nl/, 2016

Nair, U. R., and Castello, R. C., “A Model Predictive Control-Based Energy Management Scheme for Hybrid Storage System in Islanded Microgrids,” IEEE Access, vol. 8, pp. 97809–97822, 2020.

Ndeke, C.B.; Adonis, M.; Almaktoof, A. Basic Circuit Model of Voltage Source Converters: Methodology and Modeling. AppliedMath 2024, 4, 889-907. https://doi.org/10.3390/appliedmath4030048

Ndeke, C. B., Adonis, M., & Almaktoof, A. M., (2024). Energy management strategy for a hybrid micro - grid system using renewable energy. *Discover Energy*. https://doi.org/10.1007/s43937-024-00025-9.

Ndeke, C.B.; Adonis, M.; Almaktoof, A. Energy Management Strategy for DC Micro-Grid System with the Important Penetration of Renewable Energy. Appl. Sci. 2024, 14, 2659. https://doi.org/10.3390/app14062659

Nesihath, M. K., Muraleedharan, V, Nafeesa, K., and Sreedharan, S., “Optimal Energy Management System for Hybrid Residential Microgrids.” Cost-Effective and Intelligent Controller Based Design for Wind and Photovoltaic Power Generation Systems), 2023.

Noor, A., et al., “Artificial Intelligence Application in Demand Response : Advantages , Issues , Status , and Challenges,” IEEE Access, vol. 11, no. January, pp. 16907–16922, 2023.

O’Rourke, C. J., Qasim, M. M., Overlin, M. R., & Kirtley, J. L. (2019). A Geometric Interpretation of Reference Frames and Transformations: Dq0, Clarke, and Park. *IEEE Transactions on Energy Conversion*, *34*(4), 2070–2083. https://doi.org/10.1109/TEC.2019.2941175

Olatomiwa, L., Mekhilef, S., Ismail, M. S., & Moghavvemi, M. (2016). Energy management strategies in hybrid renewable energy systems: A review. *Renewable and Sustainable Energy Reviews*, *62*, 821–835. https://doi.org/10.1016/j.rser.2016.05.040

Olivares, D., E., et al., “Trends in microgrid control,” IEEE Trans. Smart Grid, vol. 5, no. 4, pp. 1905–1919, 2014.

Oymak, A., Altun, M., Cakmak, F., Atic, S., Tur, M. R., & Bayindir, R. (2022). *Distributed*

generation system planning based on renewable energy source. 368–373. https://doi.org/10.1109/icsmartgrid55722.2022.9848727

Parhizi, S., Lotfi, H., Khodaei, A., & Bahramirad, S. (2015). State of the art in research on microgrids: A review. *IEEE Access*, *3*, 890–925. https://doi.org/10.1109/ACCESS.2015.2443119

Pi, Z., Li, X., Ding, Y., Zhao, M., and Liu, Z., "Residential energy demand response management algorithm considering consumer usage patterns," 2021 33rd Chinese Control and Decision Conference (CCDC), pp. 2768–2775, 2021.

Pohl, O., Dalhues, S., Rewald, F., and Jörke, P., "Advancements in Distributed Power Flow Control," 53rd International Universities Power Engineering Conference (UPEC), 2018.

Pragya, & Thakur, R. (2022). *A Review of Architecture and Control Strategies of Hybrid AC/DC Microgrid*. 1–5. https://doi.org/10.1109/iciccsp53532.2022.9862386

Prince, S. K., Kumar, D., Affijulla, S., & Panda, G. (2022). Electric Faults Detection Technique for DC Microgrids. *PESGRE 2022 - IEEE International Conference on "Power Electronics, Smart Grid, and Renewable Energy,"* 0–5. https://doi.org/10.1109/PESGRE52268.2022.9715884

Priya, L., "A Distributed Demand Response Management Algorithm for Multi-Utility Environment in Smart Grid," 2020 International Conference on Mathematics and Computers in Science and Engineering (MACISE), pp. 229–235, 2020.

Qu, Z., Shi, Z., Wang, Y., Siada, A. A, Chong, Z., and Dong, H., "Energy Management Strategy of AC/DC Hybrid Microgrid Based on Solid-State Transformer," IEEE Access, vol. 10, pp. 20633–20642, 2022.

Rahim, A. H. M. A. (2022). Fuzzy Logic Control of Supercapacitor Energy Storage System in a Microgrid. *2022 International Conference on Innovations in Science, Engineering and Technology, ICISET 2022*, (February), 516–521. https://doi.org/10.1109/ICISET54810.2022.9775843

Rahman, S. (2018). *Power management and control of hybrid AC/DC microgrids integrated with renewable energy sources and electric vehicles*.

Rani, P., Murugesan, S., & Singh, A. K. (n.d.). *Modeling and Implementation of Grid Following and Grid Forming Inverters*.

Raya-Armenta, J. M., Bazmohammadi, N., Avina-Cervantes, J. G., Sáez, D., Vasquez, J. C., & Guerrero, J. M. (2021). Energy management system optimization in islanded microgrids:

An overview and future trends. *Renewable and Sustainable Energy Reviews*, Vol. 149. https://doi.org/10.1016/j.rser.2021.111327

Reddy, C. R., Rani, B. G., Kondalu, M., Sekhar, O. C., Venu, G., and Kalyan, C. N. S., "Energy Management System for Hybrid Renewable Energy-Based Microgrid," INDICON 2022 - 2022 IEEE 19th India Counc. Int. Conf., 2022.

Richter, A., Van Der Laan, E., Ketter, W., & Valogianni, K. (2012). Transitioning from the traditional to the smart grid: Lessons learned from closed-loop supply chains. *2012 International Conference on Smart Grid Technology, Economics and Policies, SG-TEP 2012*. https://doi.org/10.1109/SG-TEP.2012.6642382

Rodriguez-Martinez, O. F., Andrade, F., Vega-Penagos, C. A., & Luna, A. C. (2023). A Review of Distributed Secondary Control Architectures in Islanded-Inverter-Based Microgrids. *Energies*, *16*(2). https://doi.org/10.3390/en16020878

Rokrok, E., Shafie-khah, M., & Catalão, J. P. S. (2018). Review of primary voltage and frequency control methods for inverter-based islanded microgrids with distributed generation. *Renewable and Sustainable Energy Reviews*, *82*(September 2017), 3225–3235. https://doi.org/10.1016/j.rser.2017.10.022

Sadeque, F., & Fateh, F. (2022). On Control Schemes for Grid-Forming Inverters. *2022 IEEE Kansas Power and Energy Conference, KPEC 2022*, (July). https://doi.org/10.1109/KPEC54747.2022.9814774

Sahoo, S. K., Sinha, A. K., and Kishore, N. K., "Control Techniques in AC, DC, and Hybrid AC-DC Microgrid: A Review," IEEE J. Emerg. Sel. Top. Power Electron., vol. 6, no. 2, pp. 738–759, 2018.

Salem, Q., Munoz, O., and Xie, J., "An overall power flow algorithm to control the active power transfer at PCC in LV-distribution Network," 2018 IEEE International Conference on Industrial Technology (ICIT)At: Lyon, France, pp. 2–7, 2018.

Sraidi, S., Maaroufi, M., and Louzazni, M., "Energy Management in the Microgrid and Its Optimal Planning for Supplying Wireless Charging Electric Vehicle," J. Electr. Comput. Eng., vol. 2022, 2022.

Sateesh Kumar, M., Pavan Kumar, Y. V., John Pradeep, D., & Reddy, C. P. (2020). Analysis on the Effectiveness of Vertical Axis Wind Turbine for Domestic Consumers. *2020 International Symposium on Advanced Electrical and Communication Technologies, ISAECT 2020*, (c), 1–6. https://doi.org/10.1109/ISAECT50560.2020.9523698

Sayeed, F., et al., "A novel and comprehensive mechanism for the energy management of a

Hybrid Microgrid System," Energy Reports, vol. 8, pp. 847–862, 2022.

Semenov, D., Mirzaeva, G., Townsend, C. D., & Goodwin, G. C. (2018). Recent development in AC microgrid control-A survey. *2017 Australasian Universities Power Engineering Conference, AUPEC 2017*, *2017-Novem*(November), 1–6. https://doi.org/10.1109/AUPEC.2017.8282457

Serban, I., Teodorescu, R., & Marinescu, C. (2012). Analysis and optimization of the battery energy storage systems for frequency control in autonomous microgrids, by means of hardware-in-the-loop simulations. *Proceedings - 2012 3rd IEEE International Symposium on Power Electronics for Distributed Generation Systems, PEDG 2012*, 374–379. https://doi.org/10.1109/PEDG.2012.6254029

Shahgholian, G. (2021). A brief review on microgrids: Operation, applications, modeling, and control. *International Transactions on Electrical Energy Systems*, *31*(6), 1–28. https://doi.org/10.1002/2050-7038.12885

Shahzad, S., Abbasi, M. A., Chaudhry, M. A., & Hussain, M. M. (2022). Model Predictive Control Strategies in Microgrids: A Concise Revisit. *IEEE Access*, *10*(October), 122211–122225. https://doi.org/10.1109/ACCESS.2022.3223298

She, B., Li, F., Cui, H., Shuai, H., Oboreh-Snapps, O., Bo, R., … Tolbert, L. M. (2023). Inverter PQ Control with Trajectory Tracking Capability for Microgrids Based on Physics-informed Reinforcement Learning. *IEEE Transactions on Smart Grid*, *PP*, 1. https://doi.org/10.1109/TSG.2023.3277330

Shi, J., Ye, Z., Member, G. S., and Lyapunov, G. H. O., "Optimization in Online Battery Energy Storage System Control for Commercial Buildings," vol. 14, no. 1, pp. 328–340, 2023.

Silwal, S., Karimi-Ghartemani, M., Karimi, H., Davari, M., & Zadeh, S. M. H. (2022). A Multivariable Controller in Synchronous Frame Integrating Phase-Locked Loop to Enhance Performance of Three-Phase Grid-Connected Inverters in Weak Grids. *IEEE Transactions on Power Electronics*, *37*(9), 10348–10359. https://doi.org/10.1109/TPEL.2022.3164878

Singh, A. R., Ding, L., Kumar, A., Kheshti, M., Singh, R., & Bansal, R. (2019). Isolated microgrid voltage regulation using fuzzy-logic based inverter control. *IET Conference Publications*, *2019*(CP764), 29–33. https://doi.org/10.1049/cp.2019.0529

Soheli, S. N., Aney, U. S., & Mahmud, S. I. (2021). Designing A Highly Effective DC-DC Buck Converter for Sustainable Electronic Applications. *International Conference on Robotics, Electrical and Signal Processing Techniques*, 178–182. https://doi.org/10.1109/ICREST51555.2021.9331195

Thirunavukkarasu, G. S., Seyedmahmoudian, M., Jamei, E., Horan, B., Mekhilef, S., & Stojcevski, A. (2022). Role of optimization techniques in microgrid energy management systems—A review. *Energy Strategy Reviews*, *43*(June 2021), 100899. https://doi.org/10.1016/j.esr.2022.100899

Troops, G., Optimized, "Hybrid DC – AC Microgrid Energy Management System Using," Application of Intelligent Techniques in Power System Stability, Control and Protection), 2022.

Ufa, R. A., Malkova, Y. Y., Rudnik, V. E., Andreev, M. V., & Borisov, V. A. (2022). A review on distributed generation impacts on electric power system. *International Journal of Hydrogen Energy*, *47*(47), 20347–20361. https://doi.org/10.1016/j.ijhydene.2022.04.142

Venkatramanan, D., Singh, M. K., Ajala, O., Dominguez-Garcia, A., & Dhople, S. (2022). *Integrated System Models for Networks with Generators & Inverters*. 1–17. Retrieved from http://arxiv.org/abs/2203.08253

Waqas, M., Ahmed, T., Elavarasan, R. M., Waqar, A., Leong, K., Pugazhendhi, R., … Jeelani, M. W. (2021). DQ Transformation Based Control of Single-Phase Grid-Tied Inverter. *Proceedings of 2021 31st Australasian Universities Power Engineering Conference, AUPEC 2021*, 24–29. https://doi.org/10.1109/AUPEC52110.2021.9597712

Wong, L. A., and Ramachandaramurthy, V. K., "Optimal Allocation of Battery Energy Storage System Using Whale Optimization Algorithm," 2021 International Conference on Electrical, Computer, Communications and Mechatronics Engineering (ICECCME), pp. 7–8, 2021.

Wu, H., & Wang, X. (2023). Control of Grid-Forming VSCs: A Perspective of Adaptive Fast/Slow Internal Voltage Source. *IEEE Transactions on Power Electronics*, 1–13. https://doi.org/10.1109/TPEL.2023.3268374

Wynn, S. L. L., Boonraksa, T., Boonraksa, P., Pinthurat, W., and Marungsri, B., "Decentralized Energy Management System in Microgrid Considering Uncertainty and Demand Response," Electron., vol. 12, no. 1, pp. 1–19, 2023.

Xu, J., Qian, H., Hu, Y., Bian, S., & Xie, S. (2021). Overview of SOGI-Based Single-Phase Phase-Locked Loops for Grid Synchronization under Complex Grid Conditions. *IEEE Access*, *9*, 39275–39291. https://doi.org/10.1109/ACCESS.2021.3063774

Yadav, A., & Srivastava, L. (2014). Optimal placement of distributed generation: An overview and key issues. *2014 International Conference on Power Signals Control and Computations, EPSCICON 2014*, (January), 8–10. https://doi.org/10.1109/EPSCICON.2014.6887517

Yousef, M. Y., Mosa, M. A., Ali, A. A., El Masry, S. M., & Abdel Ghany, A. M. (2022).

Frequency stability enhancement of AC microgrid with high share of wind energy. *Proceedings of the 2022 5th International Conference on Advanced Systems and Emergent Technologies, IC_ASET 2022*, 155–160. https://doi.org/10.1109/IC_ASET53395.2022.9765889

Yuan, Q. F., Wang, Y. W., Liu, X. K., & Liu, Z. W. (2022). Prescribed Performance-Based Secondary Control for DC Microgrid. *IEEE Transactions on Energy Conversion*, 1–10. https://doi.org/10.1109/TEC.2022.3186633

Yusuf, S. S., & Abubakar, A. S. (2023). *A Comprehensive Review on Grid-forming Inverter : Potential and Future Trends*. *17*(1), 1–27. https://doi.org/10.30486/mjee.2023.1970278.0

Zaheeruddin, & Manas, M. (2015). Renewable energy management through microgrid central controller design: An approach to integrate solar, wind and biomass with battery. *Energy Reports*, *1*, 156–163. https://doi.org/10.1016/j.egyr.2015.06.003

Zamee, M. A., Han, D., & Won, D. (2023). Integrated grid forming-grid following inverter fractional order controller based on Monte Carlo Artificial Bee Colony Optimization. *Energy Reports*, *9*, 57–72. https://doi.org/10.1016/j.egyr.2022.11.149

Zhou, X., Liu, Q., Ma, Y., Li, W., & Xie, B. (2021). A modified ladrc-based dc-link voltage controller for photovoltaic grid-connected inverters. *Electronics (Switzerland)*, *10*(8). https://doi.org/10.3390/electronics10080877

Zia, M. F., Elbouchikhi, E., & Benbouzid, M. (2018). Microgrids energy management systems: A critical review on methods, solutions, and prospects. *Applied Energy*, *222*(May), 1033–1055. https://doi.org/10.1016/j.apenergy.2018.04.103

Zuo, Y., Yuan, Z., Sossan, F., Zecchino, A., Cherkaoui, R., & Paolone, M. (2021). Performance assessment of grid-forming and grid-following converter-interfaced battery energy storage systems on frequency regulation in low-inertia power grids. *Sustainable Energy, Grids and Networks*, *27*, 100496. https://doi.org/10.1016/j.segan.2021.100496

APPENDIX A. Additional Simulation Results for Article 4

Tables A.1 and A.2 provide concise summaries of the diverse operational modes within the three used scenarios.

Table A.1: Condition Table of the EMS

Description	Condition	1	2	3	4	5	6	7
Scenario 1 ($P_G = P_L$)								
Supply variable AC Load	$P_G = P_L$	**1**	0	0	0	0	0	0
Scenario 2 ($P_G > P_L$)								
Supply variable AC Load & Charge Battery	$\mathrm{SOC} < 100\%$	0	**1**	0	0	0	0	0
Supply variable AC Load & Utility grid	$\mathrm{SOC} = 100\%$	0	0	**1**	0	0	0	0
Scenario 3 ($P_G < P_L$)								
Discharge Battery	$\mathrm{SOC} > 20\%$	0	0	0	**1**	0	0	0
Disconnect Battery	$\mathrm{SOC} \leq 20\%$	0	0	0	0	**1**	0	0
Connect the utility grid if it is available	Utility grid availability = 1	0	0	0	0	0	**1**	0
Switch on the diesel generator if the utility grid is unavailable	Utility grid availability = 0	0	0	0	0	0	0	**1**

Where P_G is the power produced by the RESs and P_L is the AC variable load power.

Table A.2: Action Table of the EMS

N*	Description	Action
1	Variable AC Load supplied	**A1:** AC Load = **ON**;
2	Variable AC Load supplied & Battery charging	**A2:** AC Load & Battery = **ON**;
3	Variable AC Load & Utility grid supplied	**A3:** AC Load = **ON**; Battery = **OFF**; Utility grid = **ON**;
4	Battery discharging	**A4:** AC Load = **ON**; Battery = **ON**;
5	Battery disconnected	**A5:** Battery = **OFF**;
6	Utility grid connected	**A6:** AC Load = **ON**; Utility grid = **ON**;
7	Diesel generator switched on	**A7:** AC Load = **ON**; Diesel generator = **ON**;

The Stateflow logical programming environment is utilized to model and simulate dynamic systems, particularly systems with discrete event-driven behaviour. Its primary purpose is to provide a visual and intuitive way to represent and analyse the logical control and decision-making aspects of a system. Stateflow is a tool that aids the design, analysis, and implementation of a control logic for dynamic systems, providing a way to create clear, structured, and efficient control algorithms.

The State-Flow Logical Programming Environment is a powerful tool that offers a clear and effective platform for designing and implementing logical control systems. This environment provides a wide range of capabilities that facilitate the design, testing, and maintenance of control systems. One of the most notable aspects of the Stateflow Logical Programming Environment is its graphical interface, which enables the design of state components using block diagrams. This visual representation simplifies the understanding and communication of complex system behaviour. The ability to drag and drop objects and connect blocks with lines improves the overall user experience and speeds up the design process. The simulation capabilities allow testing and validation of the control systems' behaviour based on a variety of scenarios, ensuring robustness and reliability.

Scenario 1:

Figure A.1 shows the power production scheme in which the generated power is the same compared to the requirement of the load.

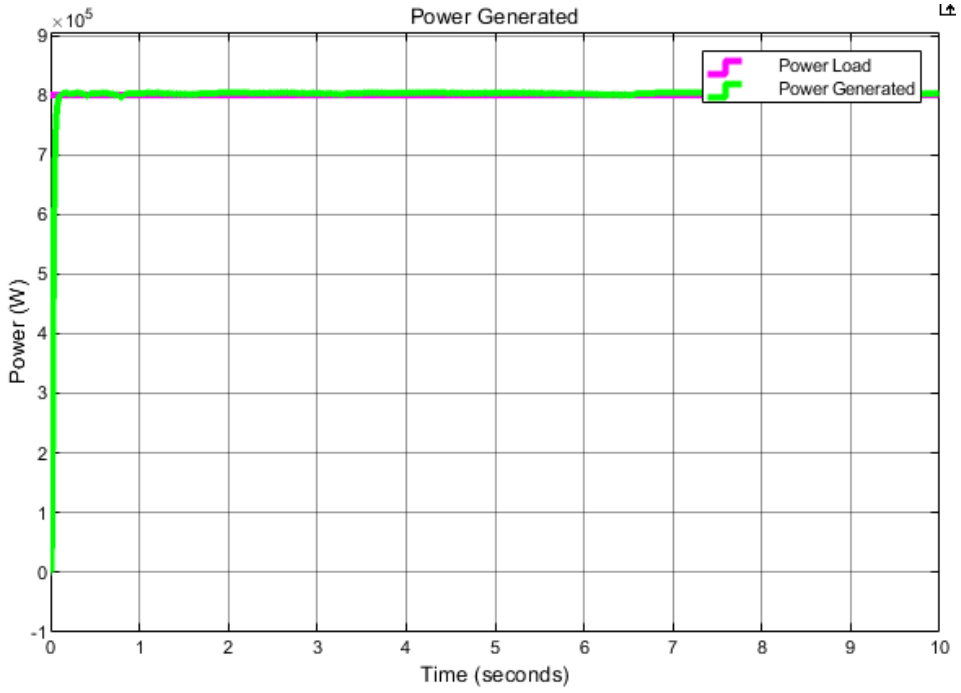


Figure A.1: Power produced by RESs (scenario 1).

Figure A.2 presents the Stateflow energy management block diagram. As the first scenario states, when the power produced and the load requirement are equal, it will be supplied without any interruption. On the block diagram, the load displays 1, which affirms that the

given condition is respected. The other outputs display 0, which indicates their inoperative state (disconnected from the system).

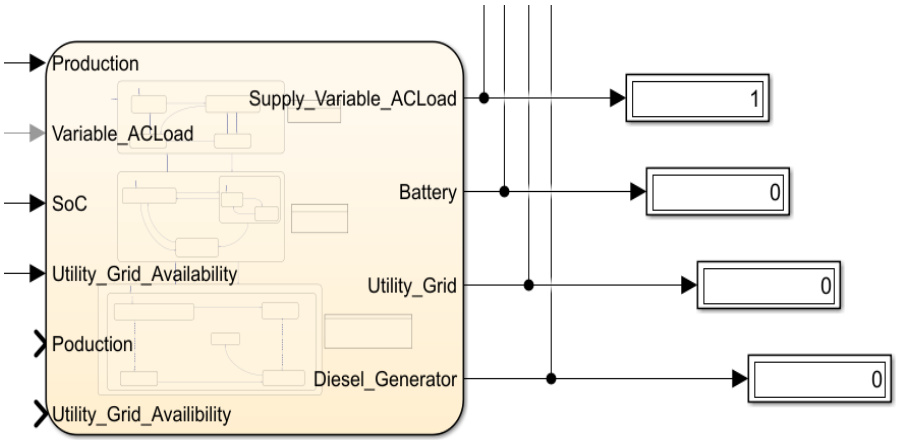


Figure A.2: Stateflow energy management block diagram.

The output results for this case are graphically presented in Figure A.3, presenting all the results visually. In this scenario, the load is receiving power, while the other outputs remain non-operational.

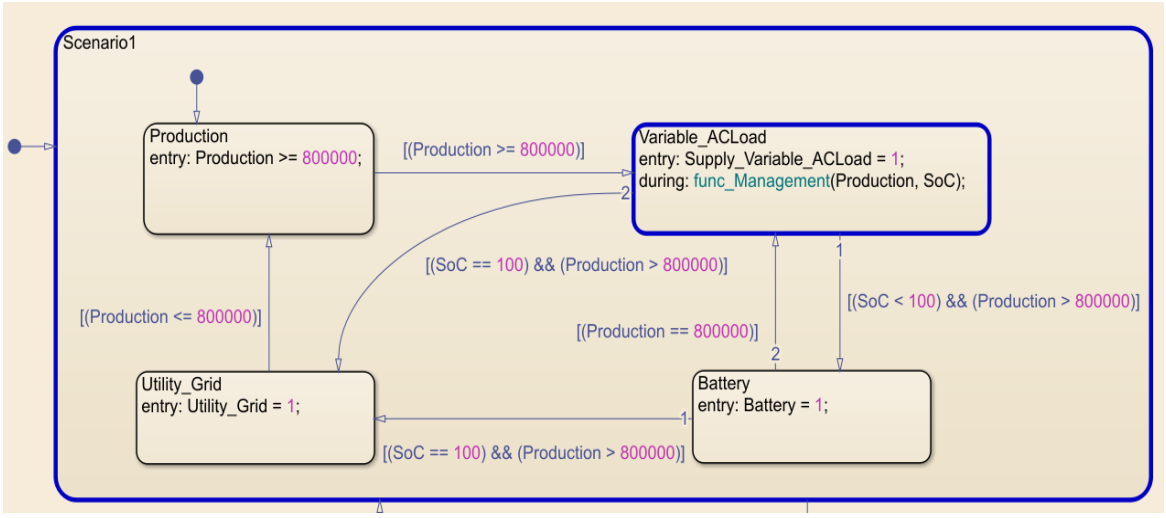


Figure A.3: Stateflow block transition.

Scenario 2: The generated power exceeds the load demand power in this situation, as Figure A.4 illustrates.

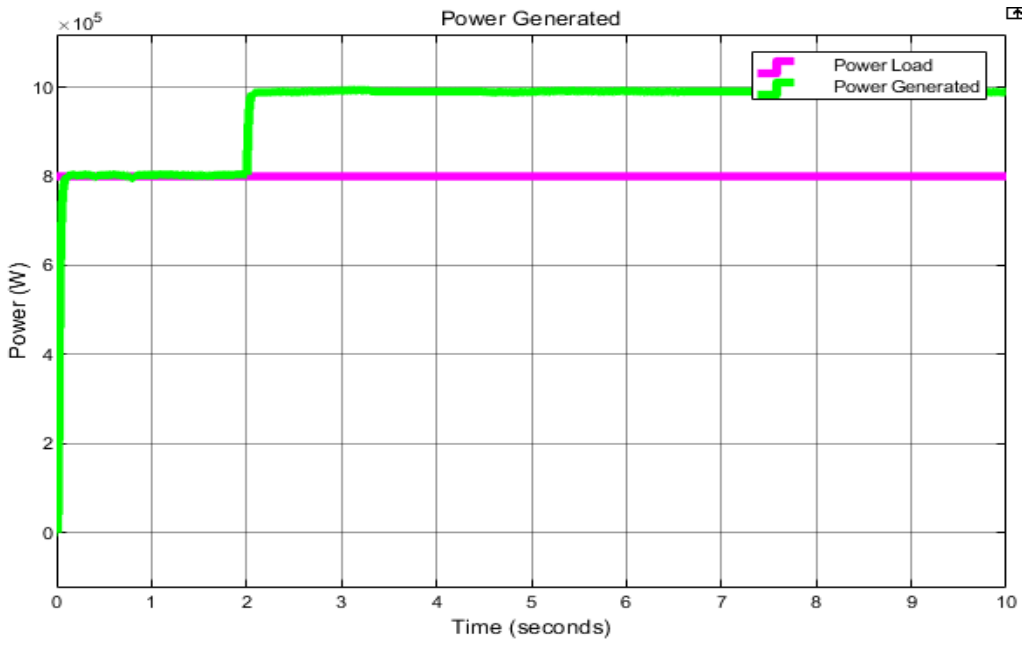


Figure A.4: Power produced by RESs (scenario 2)

Figure A.5 represents the condition/action diagram for this second scenario. When the power generated exceeds the requirement of the load, then the surplus of generation is going to be either stored in the battery or supplied to the grid according to the charging condition. Firstly, the SOC of the battery is checked to estimate its value (maximum or minimum). If the SOC is in a minimum value (≤ 20%), then the battery charges up to its maximum value (100%), after this value, the battery is disconnected, thus the rest of the production excess is supplied to the utility grid (grid connected mode).

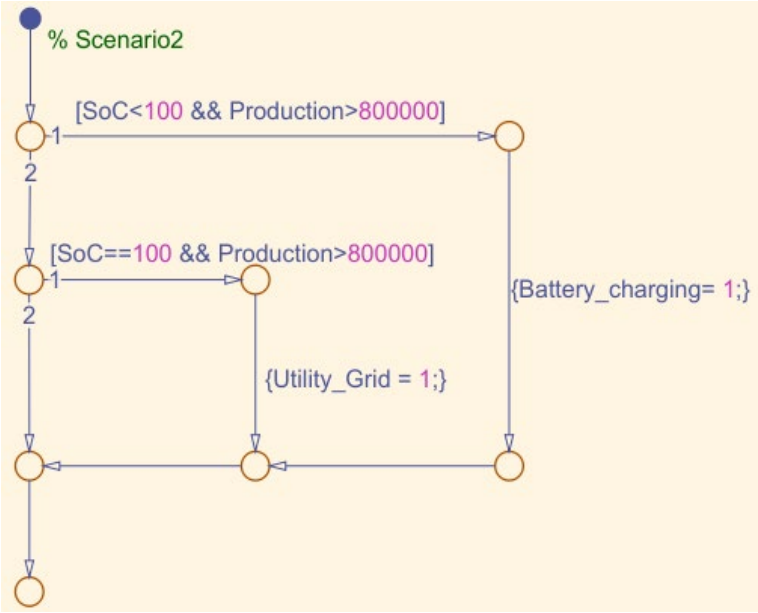


Figure A.5: Stateflow condition / action block

Figure A.6 represents the Stateflow energy management block diagram. As it is shown, the load is being supplied, while simultaneously, the battery is also charging; represented by 1 for the load demand and battery and 0 for the other outputs, meaning that they are not operating.

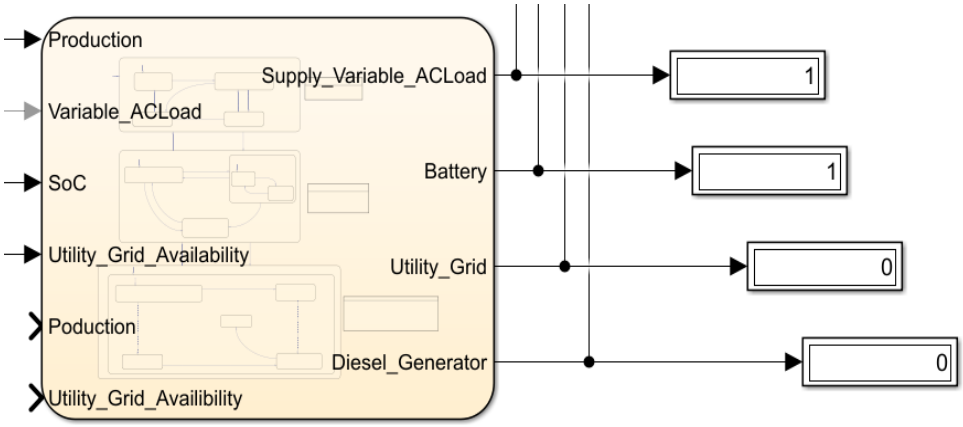


Figure A.6: Stateflow energy management block diagram

Figure A.7 shows that the transition block of the battery displays blue, which means that the state transited from the load demand block to the battery block showing that the demand of the load is satisfied and the battery is being charged.

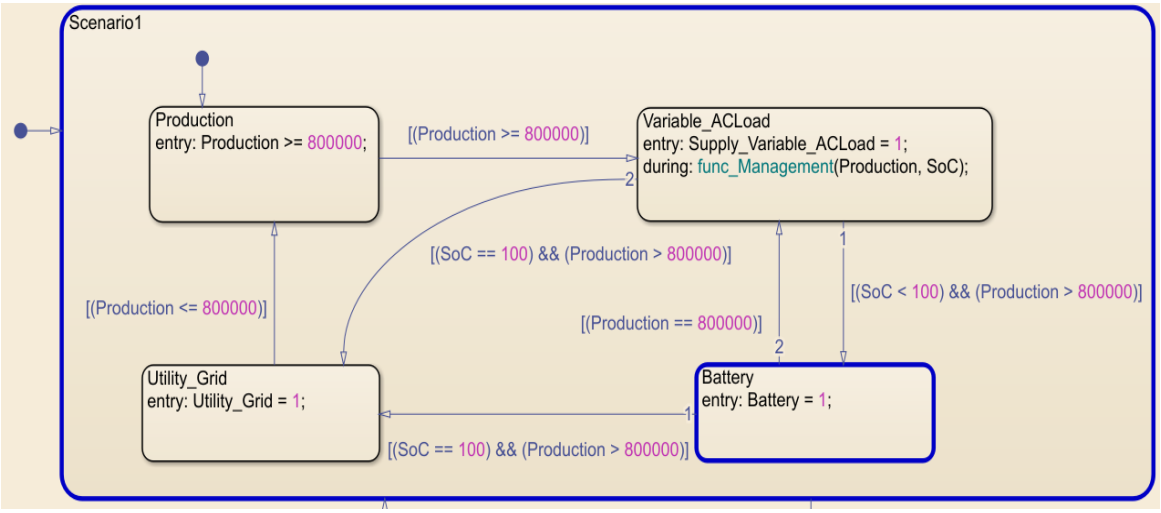


Figure A.7: Stateflow block transition

The results from the energy management block diagram are presented in Figure A.8. The variable AC load and utility grid display 1 and 0 for the battery, meaning that the battery is disconnected after reaching its maximum value (100%) and the diesel generator is also 0 which means it is not operating.

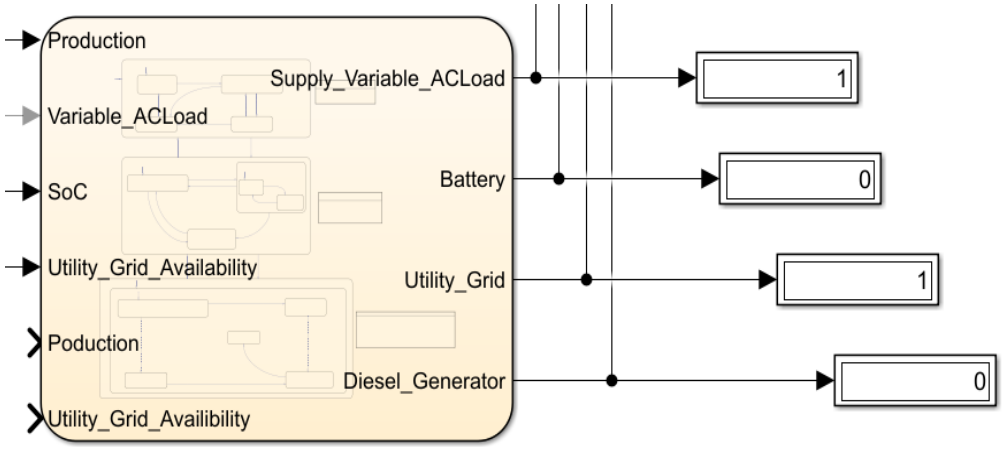


Figure A.8: Stateflow energy management block diagram

The Stateflow block transition graphical interface is shown in Figure A.9 below. As shown, the utility grid block diagram is displayed in blue, which means the state transited from the load demand, afterwards to the battery and then to the utility grid based on the EMS control. Only the utility grid and load blocks operate for this case.

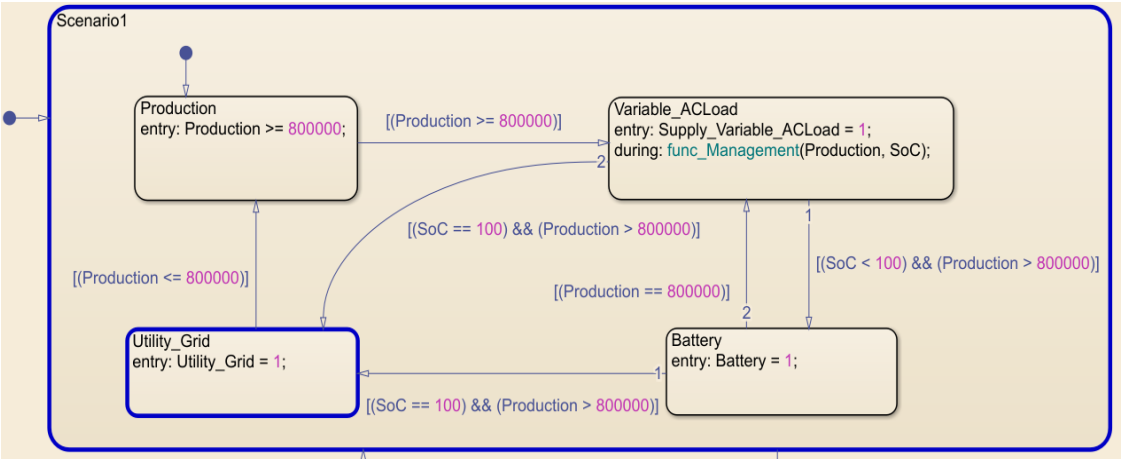


Figure A.9: Stateflow block transition

Scenario 3: The load requirements exceed the produced power in this scenario, as shown in Figure A.10. Consequently, the load requirements will be fulfilled with the assistance of the battery.

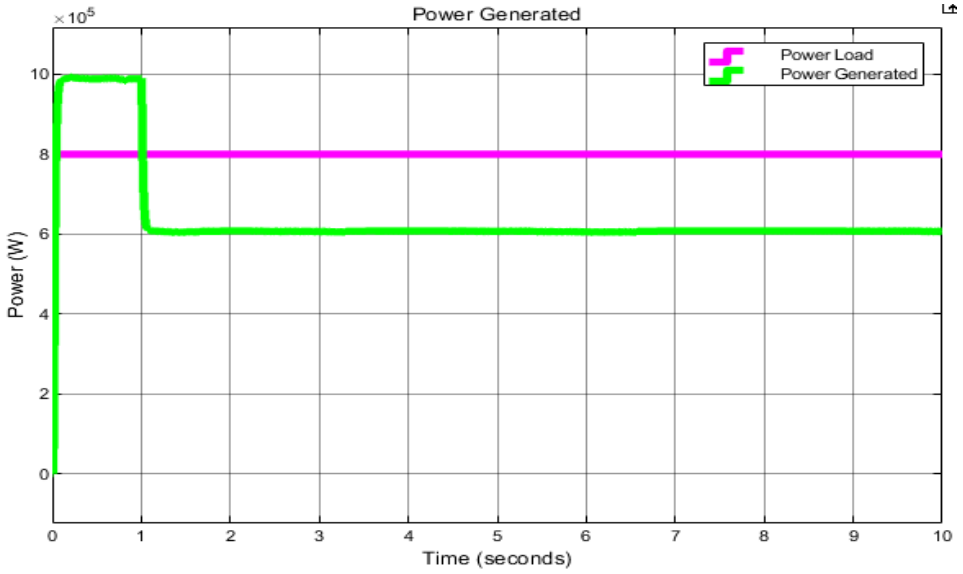


Figure A.10: Power supplied by RESs (third scenario)

Figure A.11 presents the condition / action block. The condition is that, the EMS algorithm firstly checks the available power in the battery storage by checking its maximum and

minimum values. If the SOC is over 20%, the battery discharges and when the SOC reaches its minimum value (≤ 20%), then the battery stops supplying and it is disconnected.

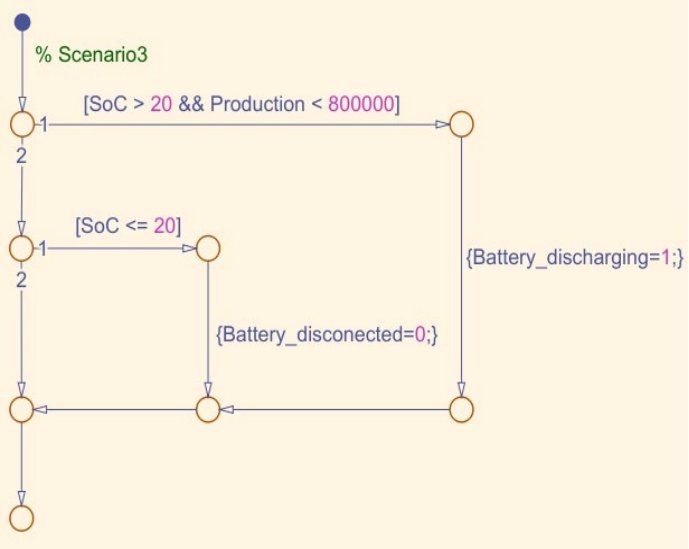


Figure A.11: Stateflow condition / action block

Figure A.12 presents the EMS algorithm block diagram; in which it is illustrated that the load demand is satisfied with the assistance of the battery. It is shown that the load is receiving power from the generated power and the battery, thus, the battery is discharging.

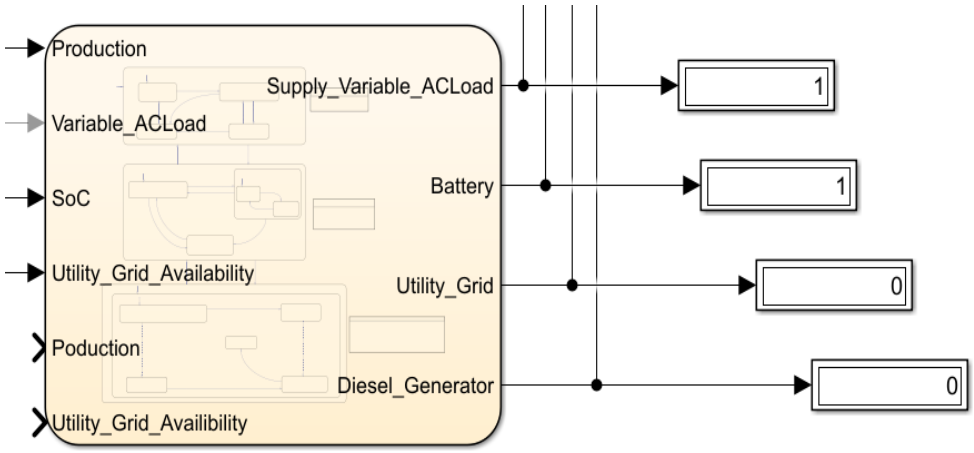


Figure A.12: Stateflow energy management system block diagram

The graphical interface of the third case is shown in Figure A.13. The load demand block diagram is displayed in blue, meaning its operating mode. The state transits from the production, then to the battery and goes to the load based on the EMS control.

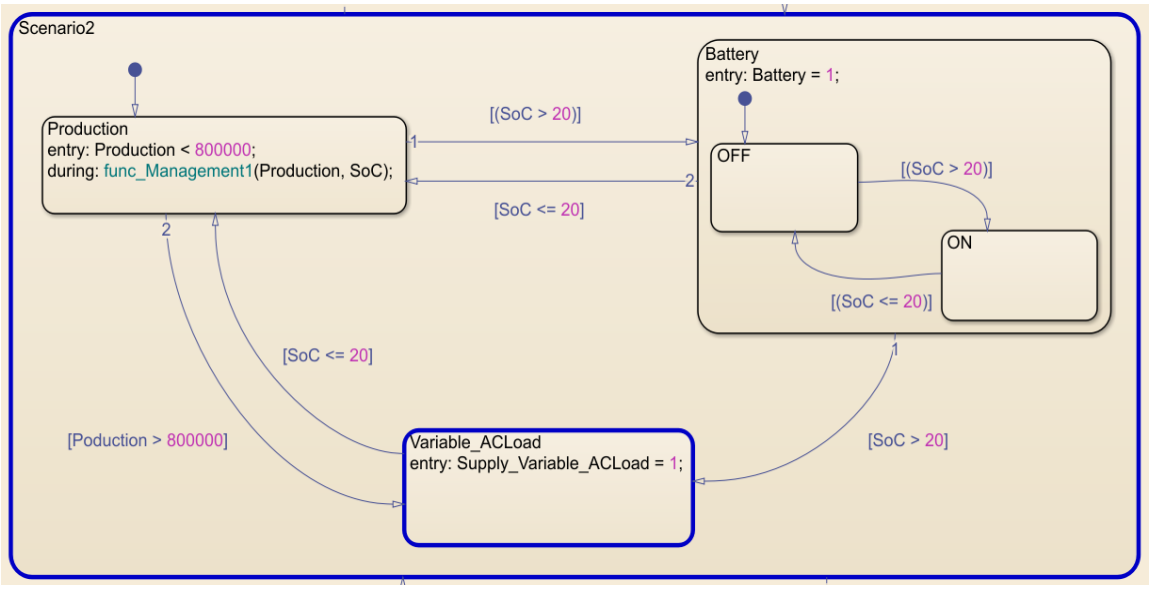


Figure A.13: Stateflow block transition.

The condition/action block for this case is shown in Figure A.14. The condition is based on the accessibility of the grid, when it is accessible, it provides power to meet the requirement of the load; if not, the diesel generator is activated to meet the load demand. As defined by the developed algorithm, the battery is allowed to charge when the generated power is greater than or equal to 20% of the production. The production is estimated at 1 MW, thus 20% of the production refers to 200 kW. Based on the condition, the battery is charged when the generation is ≥ 200 kW.

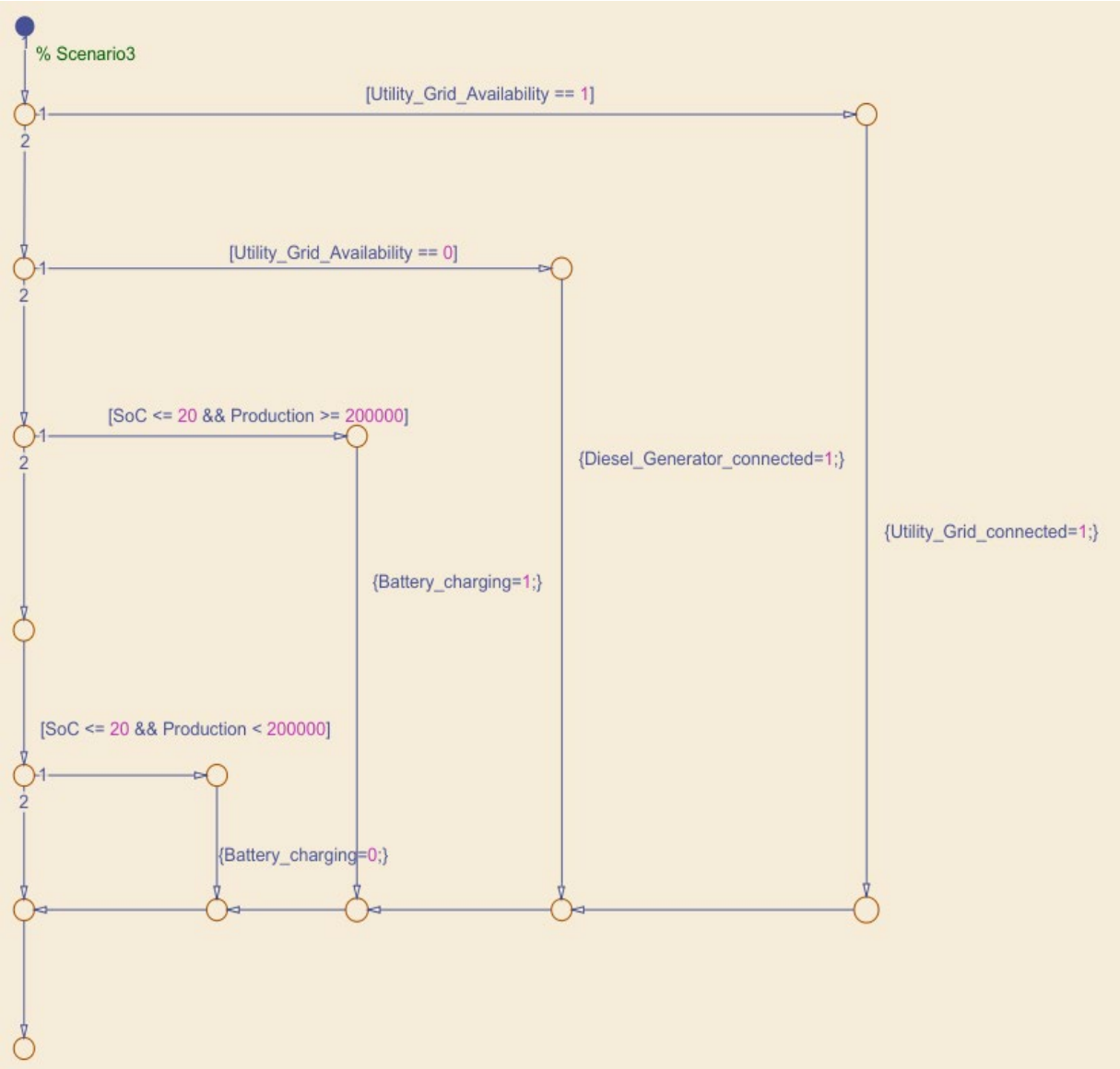


Figure A.14: Stateflow condition / action block

Figure A.15 presents the EMS algorithm block diagram. In this figure, it is illustrated that the requirement of the load is met with the help of the utility grid, while simultaneously, the battery is charging from the available power produced by renewable energy sources. This implies that the power supplied exceeds 20% of the production.

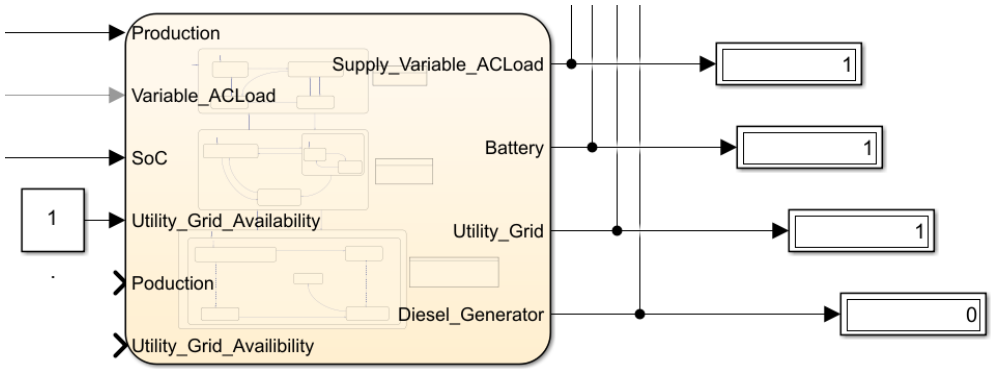


Figure A.15: Stateflow energy management block diagram

In Figure A.16, the transition block of this case is presented. It is seen that the battery block diagram displays blue, which explains the load and the battery operating mode. As stated previously, the transition state starts from one point to another. In this scenario, the load is supplied from the grid, thus the transition states from the grid block to the load block. Moreover, given that the production exceeds 200 kW, the battery is charging as shown in the transition block.

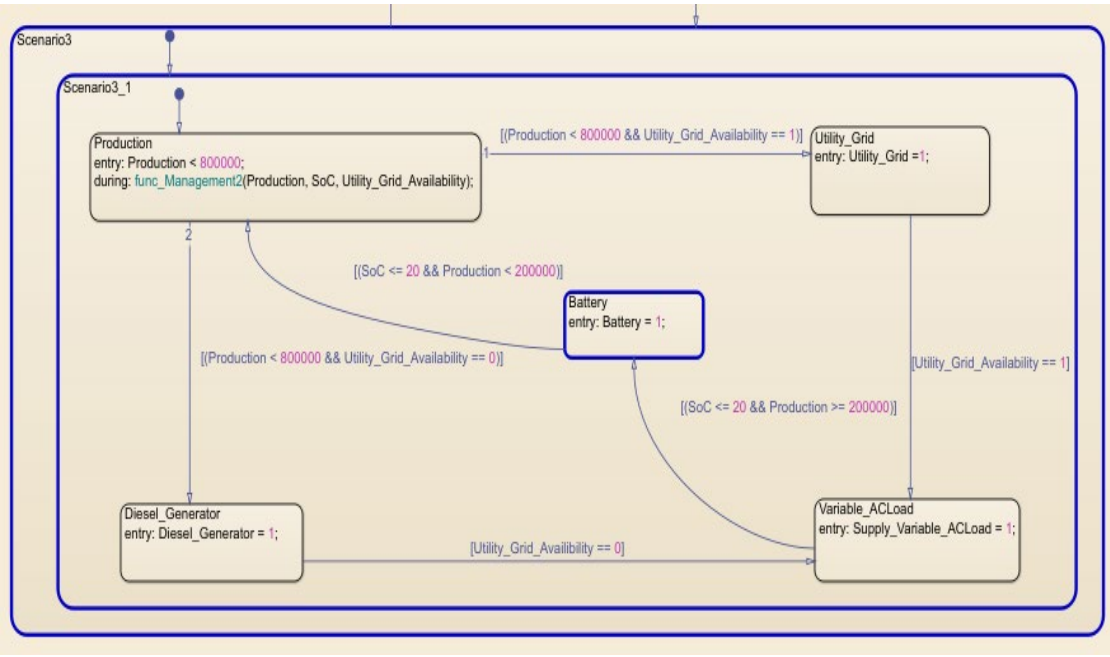


Figure A.16: Stateflow block transition.

Figure A.17 shows that the battery has been disconnected. Therefore, the demand for the load is met by the utility grid and the produced power.

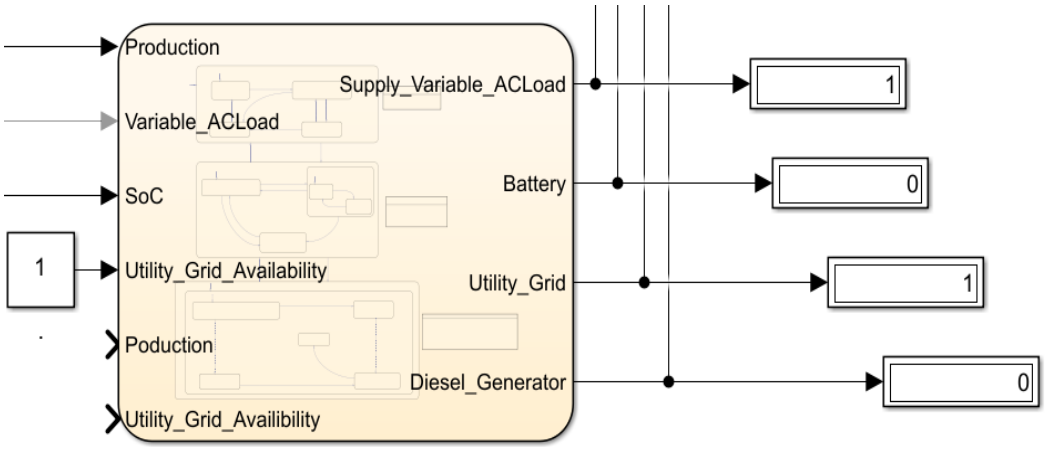


Figure A.17: Stateflow energy management block diagram.

Figure A.18 presents the graphical interface of the discussed case. It is shown that the load block diagram is displayed in blue, which explains its operating mode and the state transits from the grid block to the load demand block.

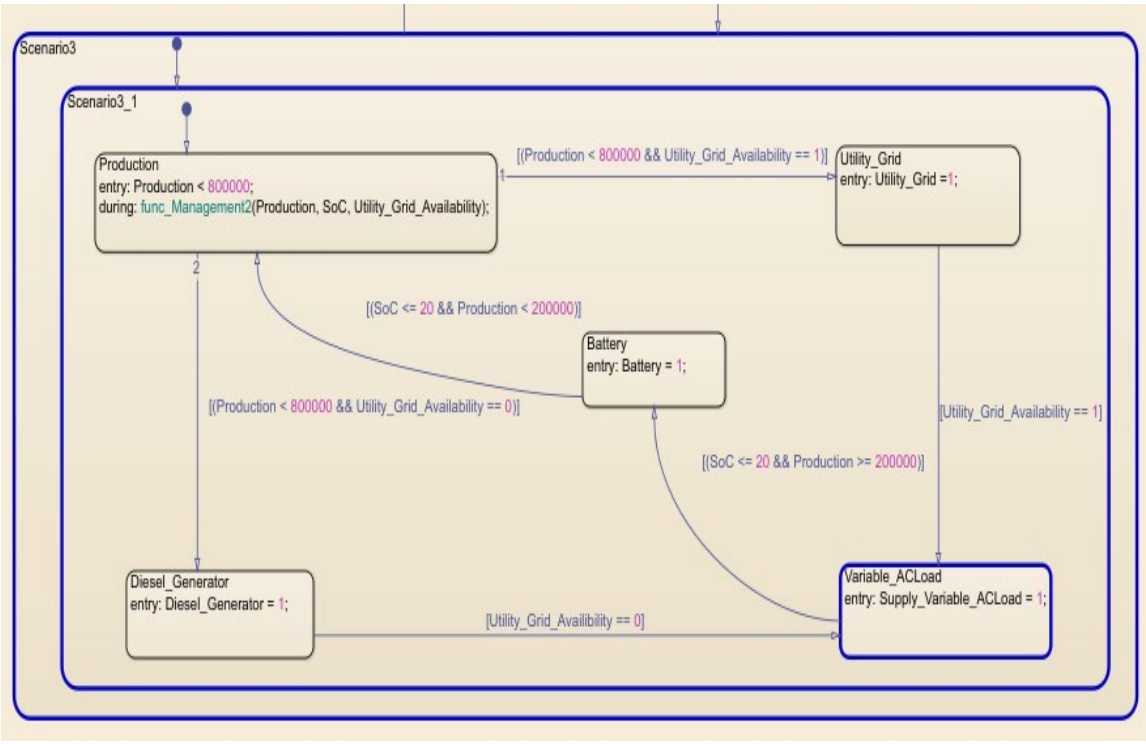


Figure A.18: Stateflow block transition.

As illustrated in Figure A.19, the diesel generator provides power to the load, and the production power is used to charge the battery. The battery is charged because the production power in this case exceeds 20% of the production (≥ 200 kW).

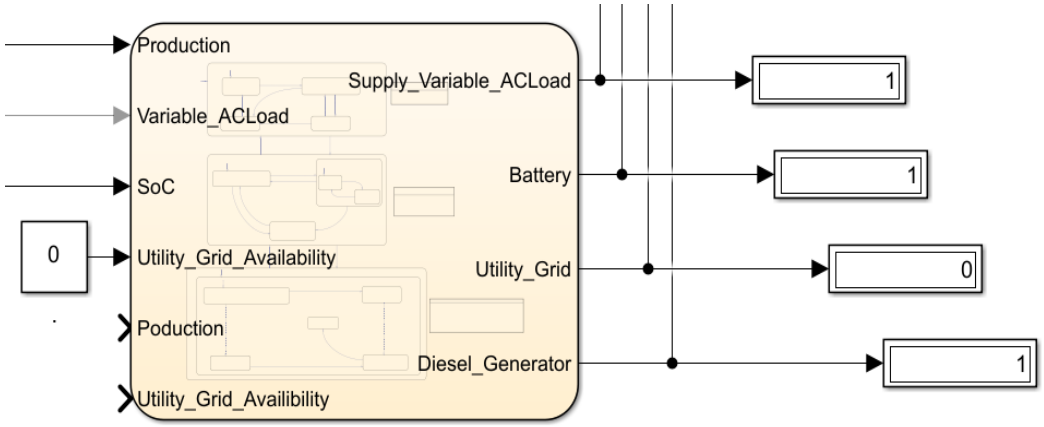


Figure A.19: Stateflow energy management block diagram.

In Figure A.20, the transition block of this case is presented, where the utility grid is not accessible and the diesel generator is activated. It is seen that the battery block diagram displays blue, which explains the operating mode of the battery and the load. The demand of the load is met by the diesel generator, thus the transition states from the diesel generator block to the load demand block. Moreover, given that the power supplied by the renewable energy sources exceeds 200 kW, then the battery charges as shown in the transition block in Figure A.21.

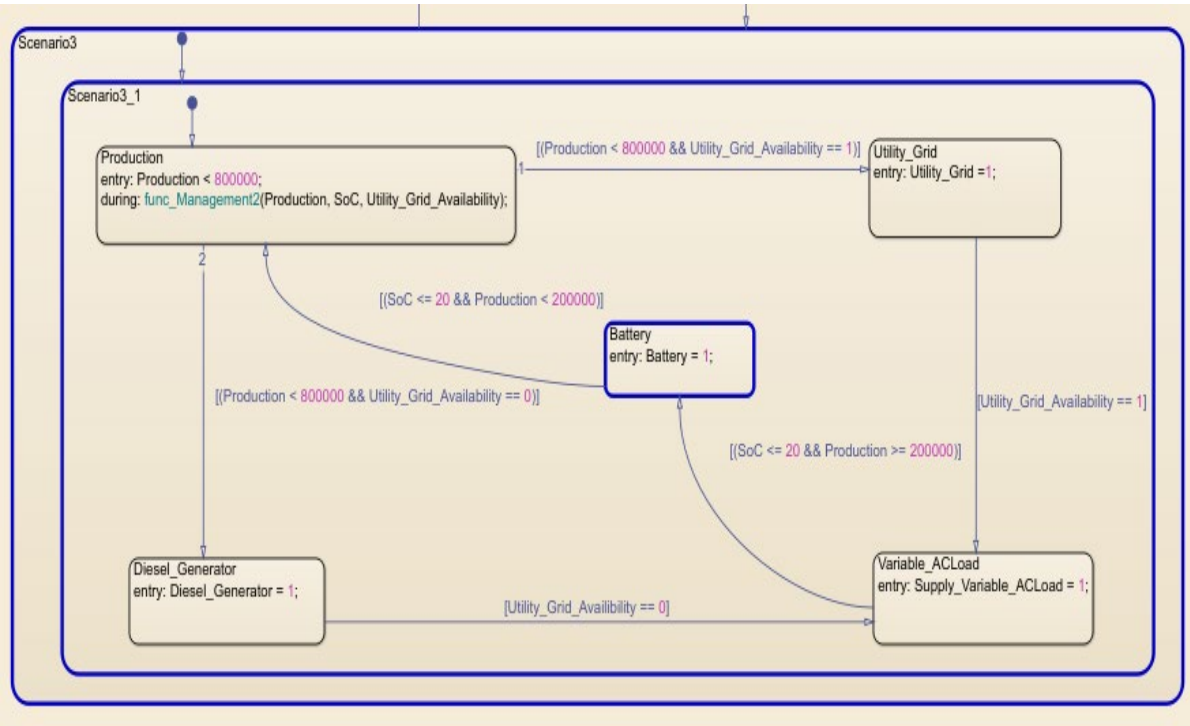


Figure A.20: Stateflow block transition

In Figure A.21, the results indicate that the battery has been disconnected. Therefore, the production power combined with the diesel generator supply power to the load.

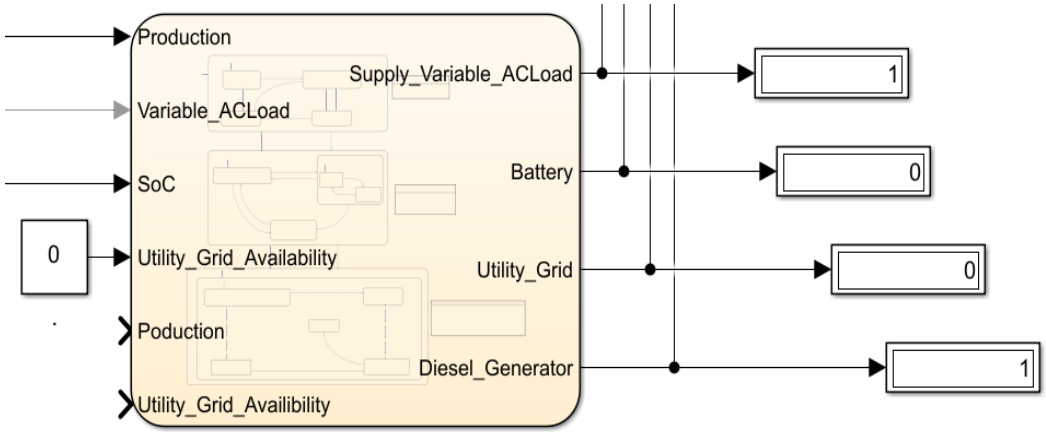


Figure A.21: Stateflow energy management block diagram.

The graphical interface of the discussed case is shown in Figure A.22.

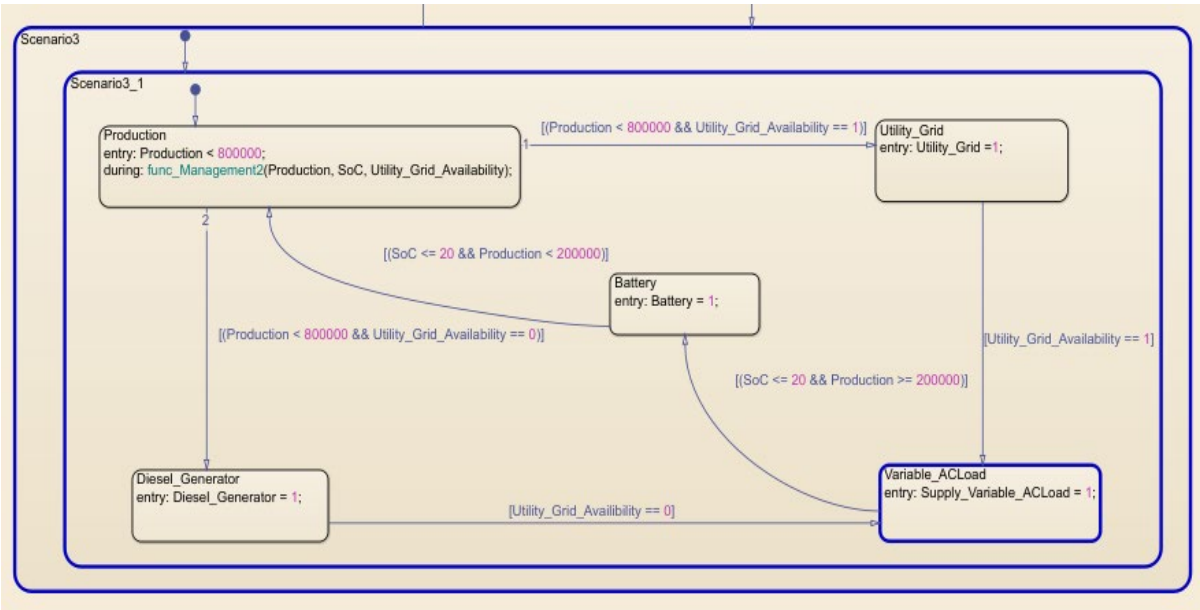


Figure A.22: Stateflow block transition.

It is seen that the load demand block diagram displays blue, which explains its operating mode and the state that transits from the diesel generator block to the load demand block. The demand is met using the production power combined with the diesel generator, and the developed EMS algorithm consistently monitors the production power as well as the grid accessibility. As soon as the utility grid becomes or the produced power is sufficient to meet the requirement of the load, the diesel generator is deactivated. This strategy is persistently employed to provide an uninterrupted power supply to the variable AC load. Through the implementation of these control algorithm conditions, the power balance of the system is attained, and the state of charge of the battery is maintained at the necessary level to prolong battery life.

APPENDIX B. Additional Simulation Results for Article 5

Typhoon HIL software was used to physically build the developed hybrid micro-grid and EMS control, to test, validate and optimize its performance. Each circuit element is represented by corresponding model blocks, which are provided in the software.

B.1: Wind Power Plant Model Simulation

To verify the design of the model, its quality performances are estimated and analysed using simulation. This model has a rotational speed of 18 rpm, as shown in Figure B.1. The system has a maximum power of 500 kW, and a maximum voltage of 380 Vac. The wind power simulation results are shown in Figure B.2.

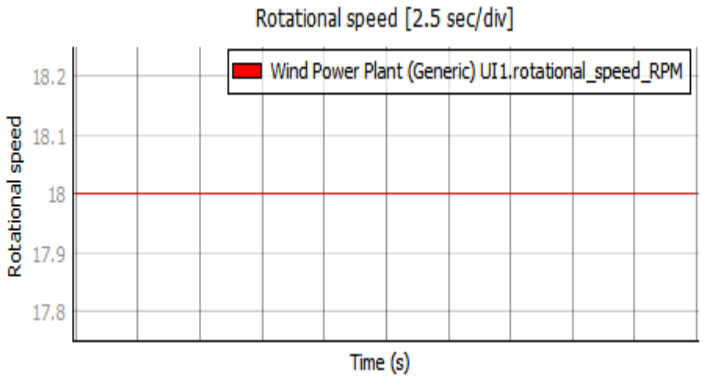


Figure B.1: Wind power plant rotational speed.

Figure B.1 shows the rotational speed of the wind power plant. To guarantee safe and effective wind turbine operation, the rotational speed is adjusted in the simulation model, thus reducing downtime and increasing energy output. Figure B.2, presents the HIL SCADA panel of the wind power plant. The Typhoon HIL system has a graphical user interface called the HIL SCADA panel that enables users to monitor and control the HIL simulation in real-time. It gives users a thorough overview of the simulated power system and enables them to visualize data, conduct analysis, and interact with the simulation. It also enables the monitoring of power flows, voltage and frequency waveforms, and other relevant parameters.

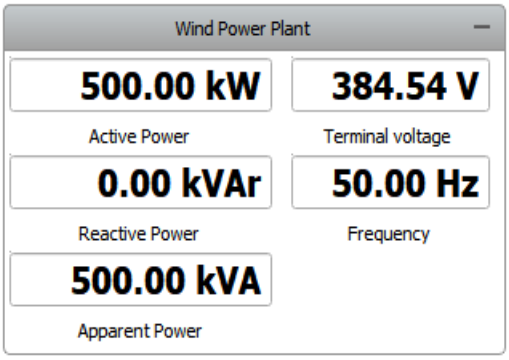


Figure B.2: Wind power plant HIL SCADA panel.

As can be seen in Figure B.3, the panel includes features for setting up alarms and monitoring system events.

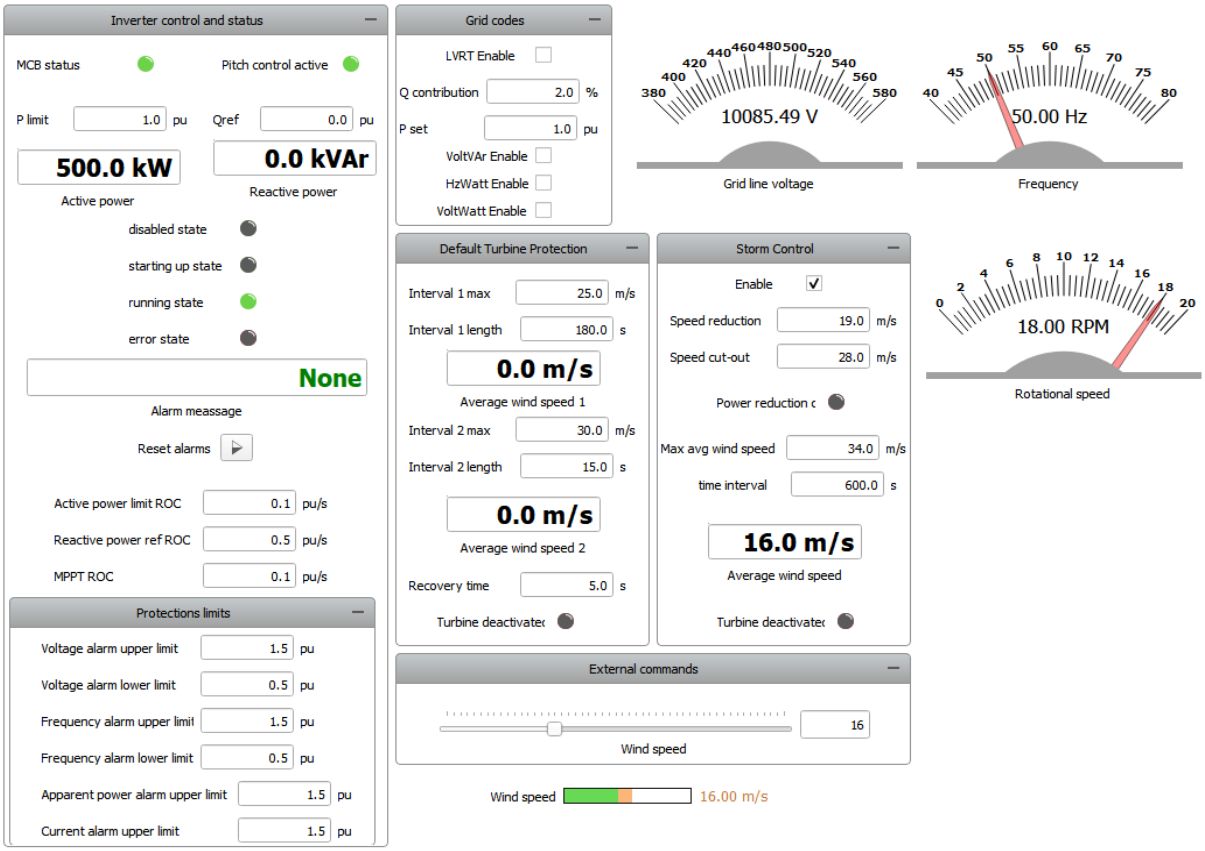


Figure B.3: Wind power plant HIL SCADA interface.

The voltage and power outputs are illustrated in Figure B.4 and Figure B.5. The results demonstrate that the voltage and power outputs remain constant with very small ripples. The average wind power values for the output voltage are 384.5 V and 500 kW for the output power.

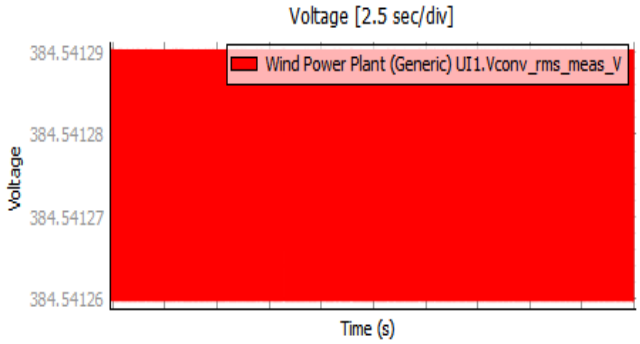


Figure B.4: Wind turbine output voltage.

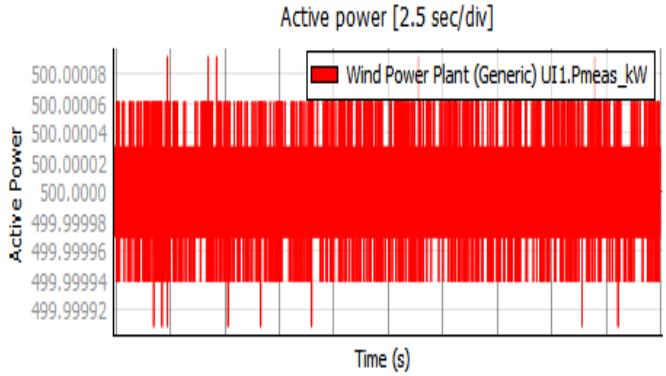


Figure B.5: Wind turbine output power.

B.2: Photovoltaic Power Plant Model Simulation

To generate the required power, the PV module must be connected in a considerable quantity of solar cells both in parallel and series. In this simulation, the temperature was maintained constant at 25°C while the solar irradiation was expected to vary depending on various scenarios. The PV power plant HIL SCADA is shown in Figure B.6 in which all the data are visualized. On this panel, different data such as terminal voltage, frequency, active power, reactive power and apparent power are presented.

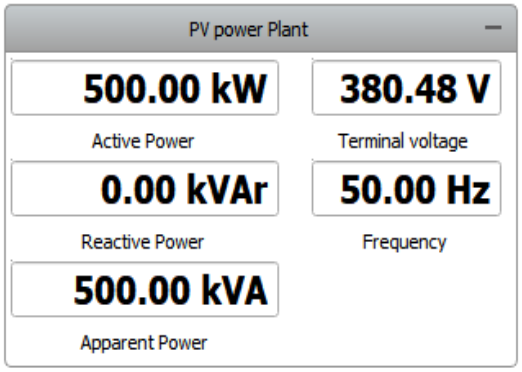


Figure B.6: PV power plant HIL SCADA panel.

Figure B.6 shows the PV plant output power from the inverter as a function of simulation time. The result shows that output power is remained constant at 500 kW with minimum ripples

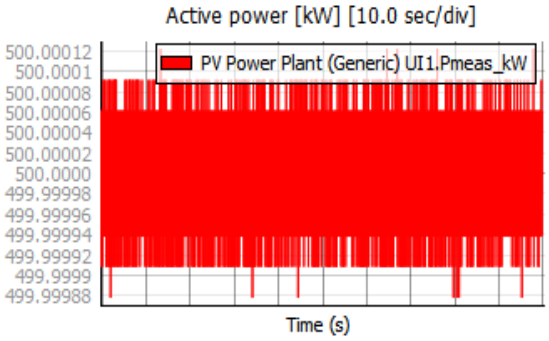


Figure B.7: PV power plant output power.

The PV power plant HIL SCADA interface is shown in Figure B.8. Different parameters are seen in the interface including the active power for each phase, the inverter control and the external commands which represent the slider micro widget component that allows to vary the solar irradiance.

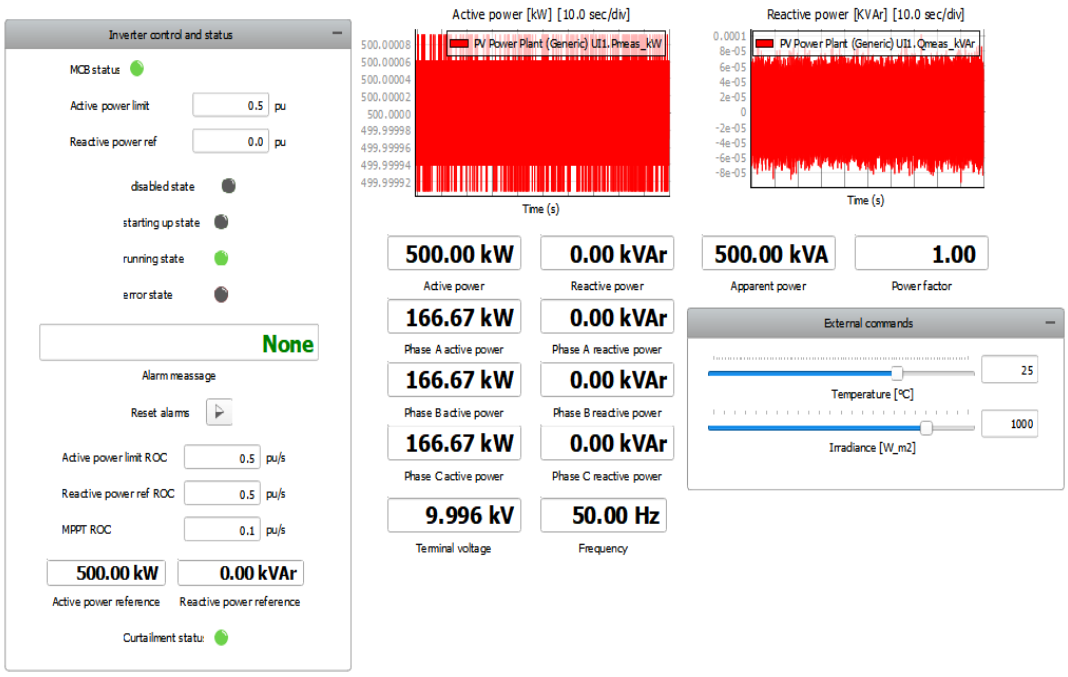


Figure B.8: PV power plant HIL SCADA interface.

B.3: Diesel Generator Model Simulation

As seen in Figure B.9, the maximum generator speed is 1800 rpm. The diesel generator has a maximum output power of 1.5 MW and 380 V_{ac}. The following Figures present the simulation results. Figure B.9 shows the generator rotational speed, which has a maximum speed of 1800 rpm. This speed represents the maximum value at which the diesel generator generates the maximum power.

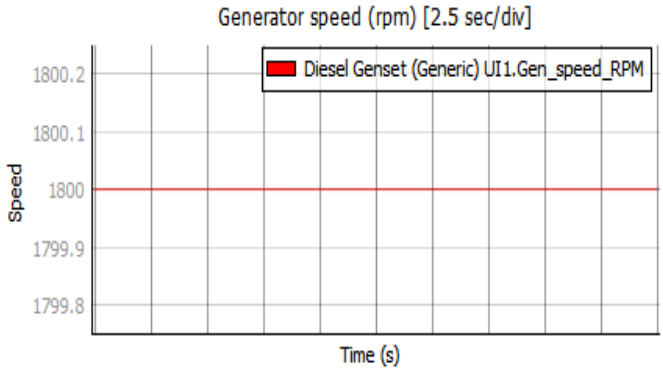


Figure B.9: Generator speed.

Figure B.10 presents the diesel generator HIL SCADA panel in which all the parameter values are visualized. In this panel, different data are shown such as active and reactive powers, terminal voltage, frequency as well as apparent power.

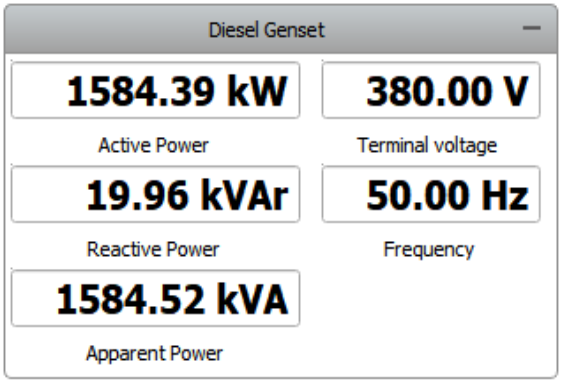


Figure B.10: Diesel generator HIL SCADA panel.

The output voltage of the diesel generator is shown in Figure B.11. The result shows that the output voltage remains constant with very small ripples, which are insignificant.

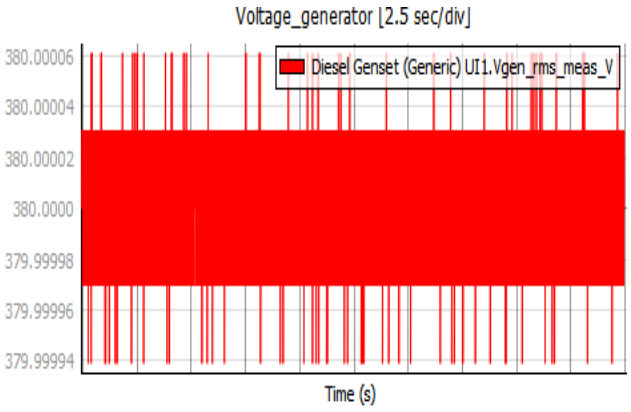


Figure B.11: Diesel generator output voltage.

In Figure B.12, the maximum diesel generator output power is presented and this value is constant with very small ripples, which are negligible.

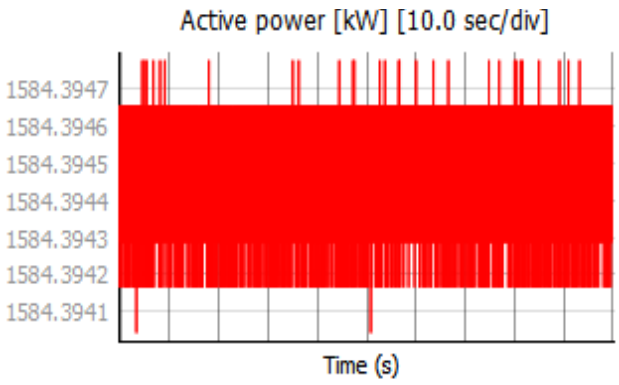


Figure B.12: Diesel generator output power.

In Figure B.13, the HIL SCADA interface of the diesel generator is presented, which includes different relevant parameters.

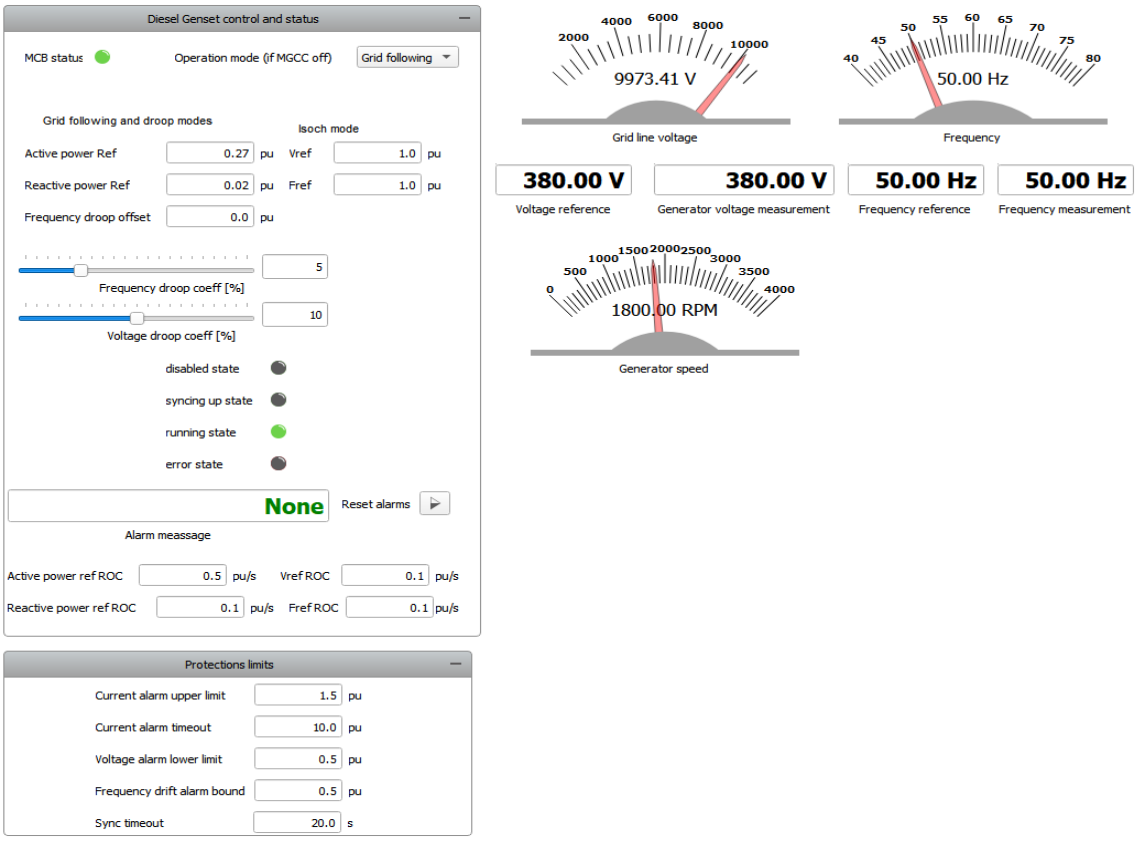


Figure B.13: Diesel generator HIL SCADA interface.

B.4. Battery Energy Storage Model Simulation

The maximum capacity of the battery is 900 Ah and a 380 V_{ac}. A bidirectional converter was used to step down the battery system input voltage for charging and to step up the output voltage for discharging. The results of the simulation are presented in the following Figures. Figure B.14 is the HIL SCADA panel of the battery inverter in which all the parameter values are visualized. In this panel, all the parameter values are shown in the HIL simulation in real-time. Various data are shown such as active and reactive powers, terminal voltage, frequency, SOC as well as apparent power.

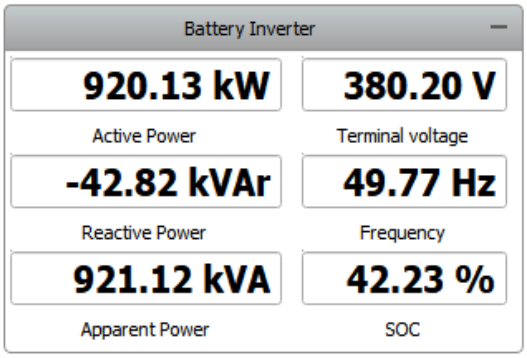


Figure B.14: Battery inverter HIL SCADA panel.

Figure B.15 shows the battery inverter output power, demonstrating its consistency with minor fluctuations. The average generated power is 920.12 kW, and Figure B.16 shows the corresponding output voltage.

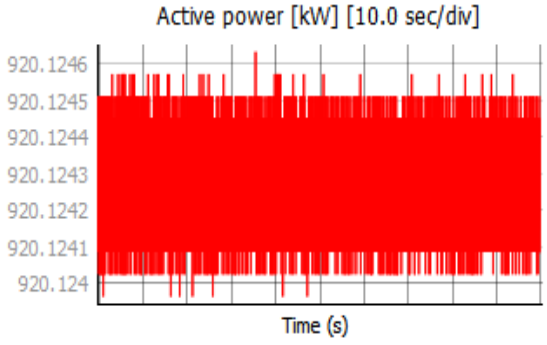


Figure B.15: Battery output power from the inverter.

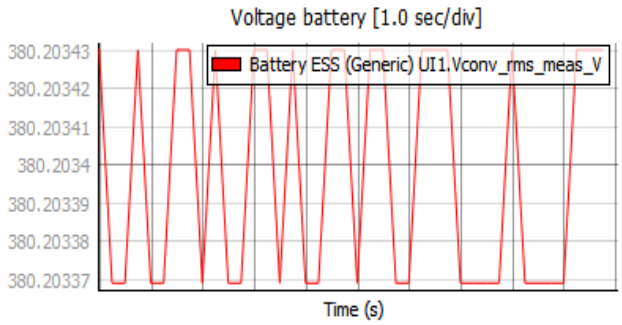


Figure B.16: Battery output voltage from the inverter.

Figure B.17 presents the HIL SCADA interface of the battery inverter, which includes different parameters and allows to interact with the simulation. Thresholds can be set in this interface or conditions that trigger alerts when specific events occur, such as overvoltage, overcurrent, or abnormal behaviour.

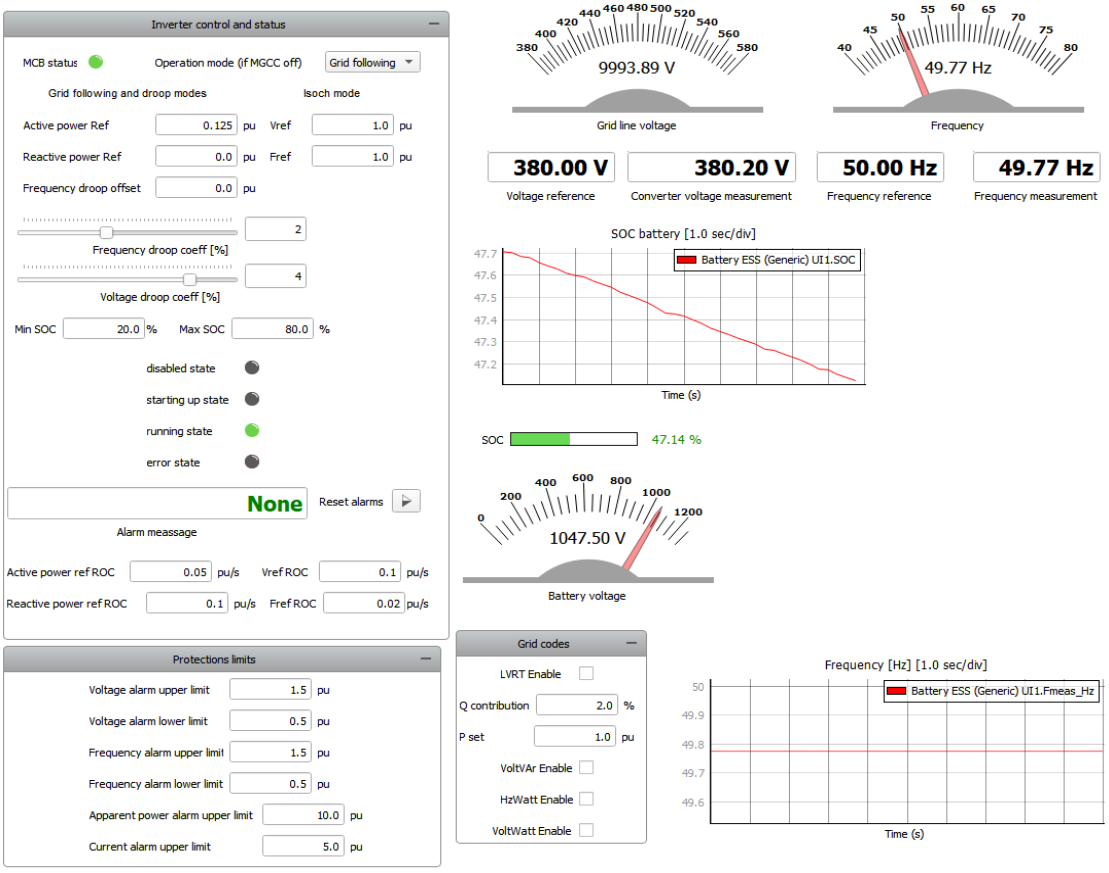


Figure B.17: Battery HIL SCADA interface

APPENDIX C: PQ control model / MATLAB/Simulink environment

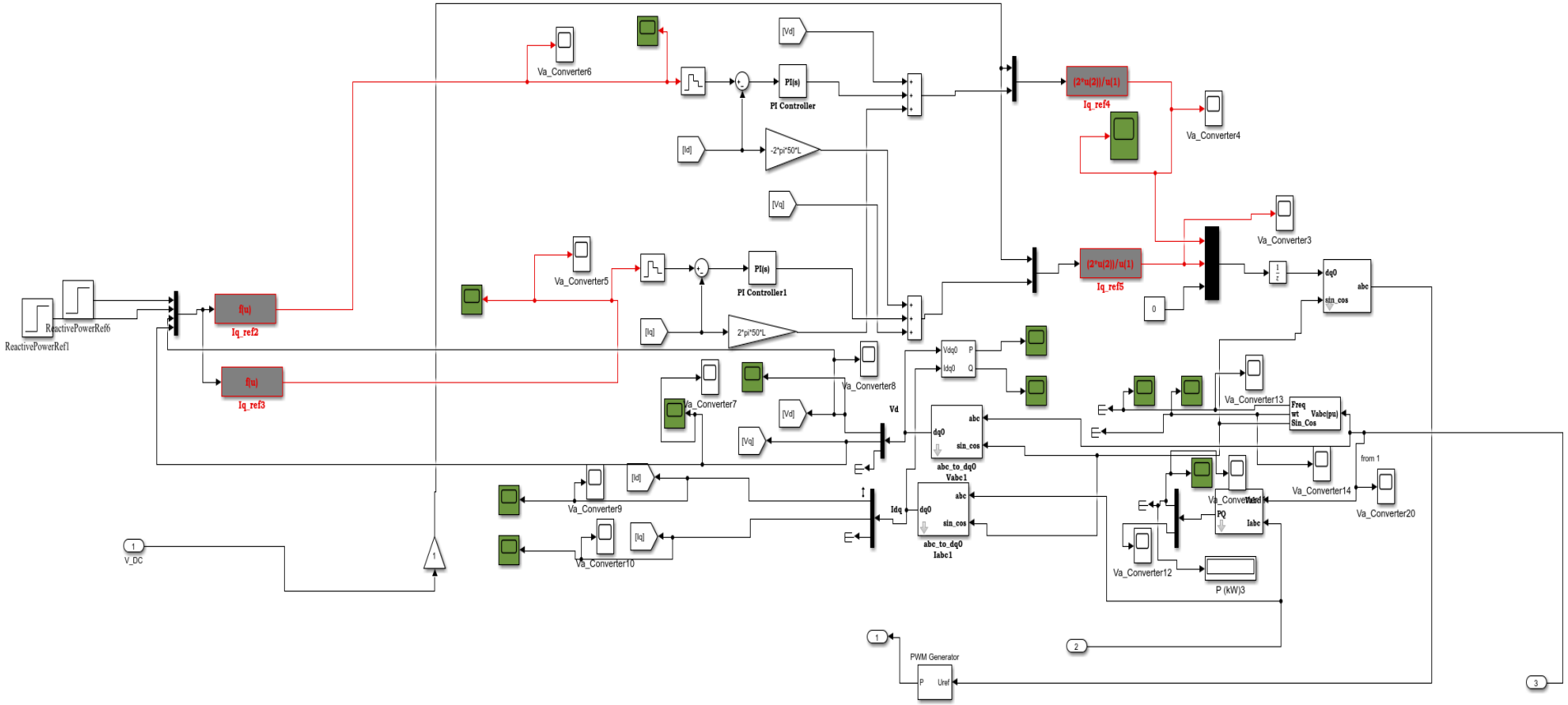


Figure C: DC voltage regulator control diagram

APPENDIX D: Hybrid Micro-Grid Controller / Typhoon HIL

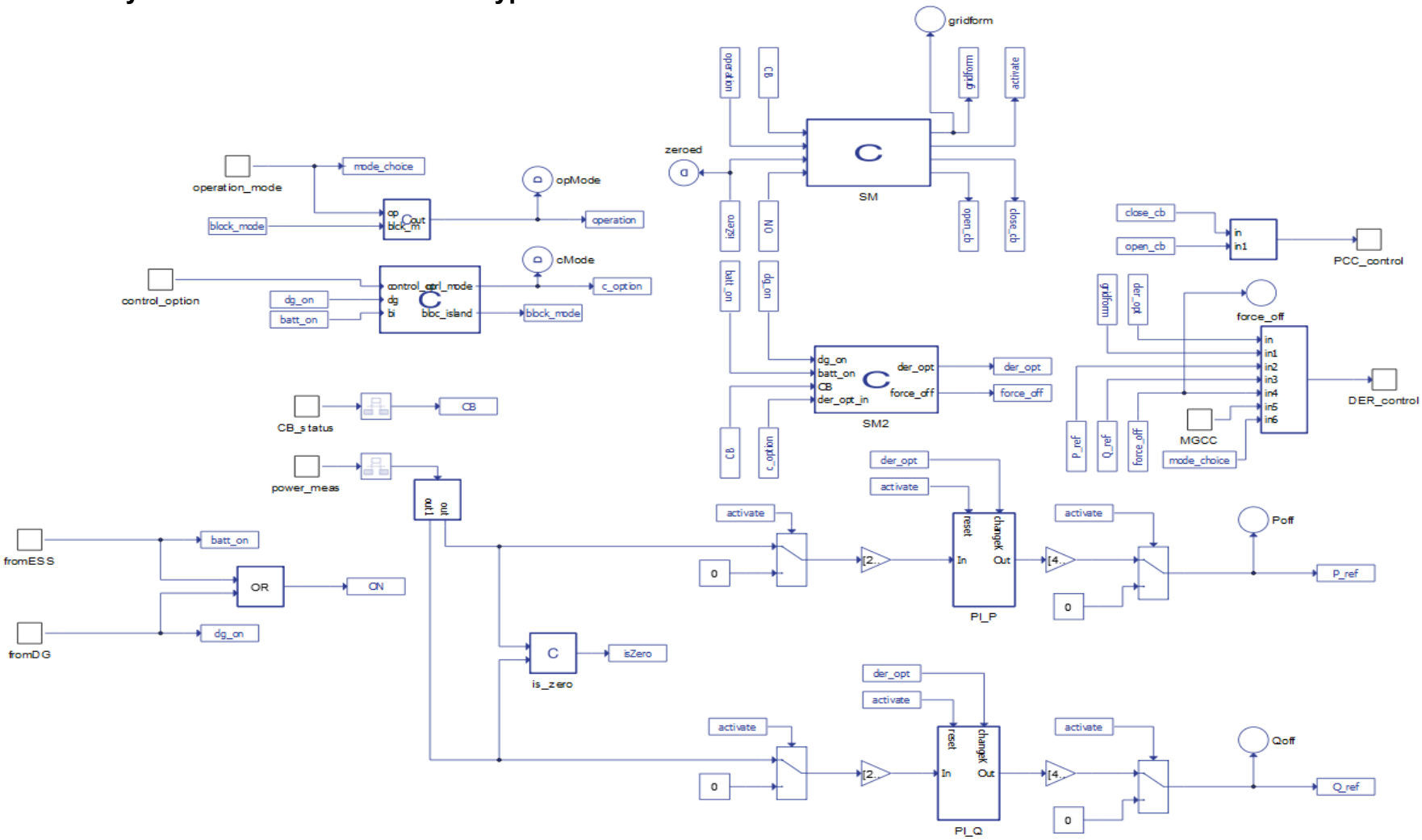


Figure D: Energy management control / Typhoon HIL

APPENDIX E: Hybrid Micro-Grid / Typhoon HIL

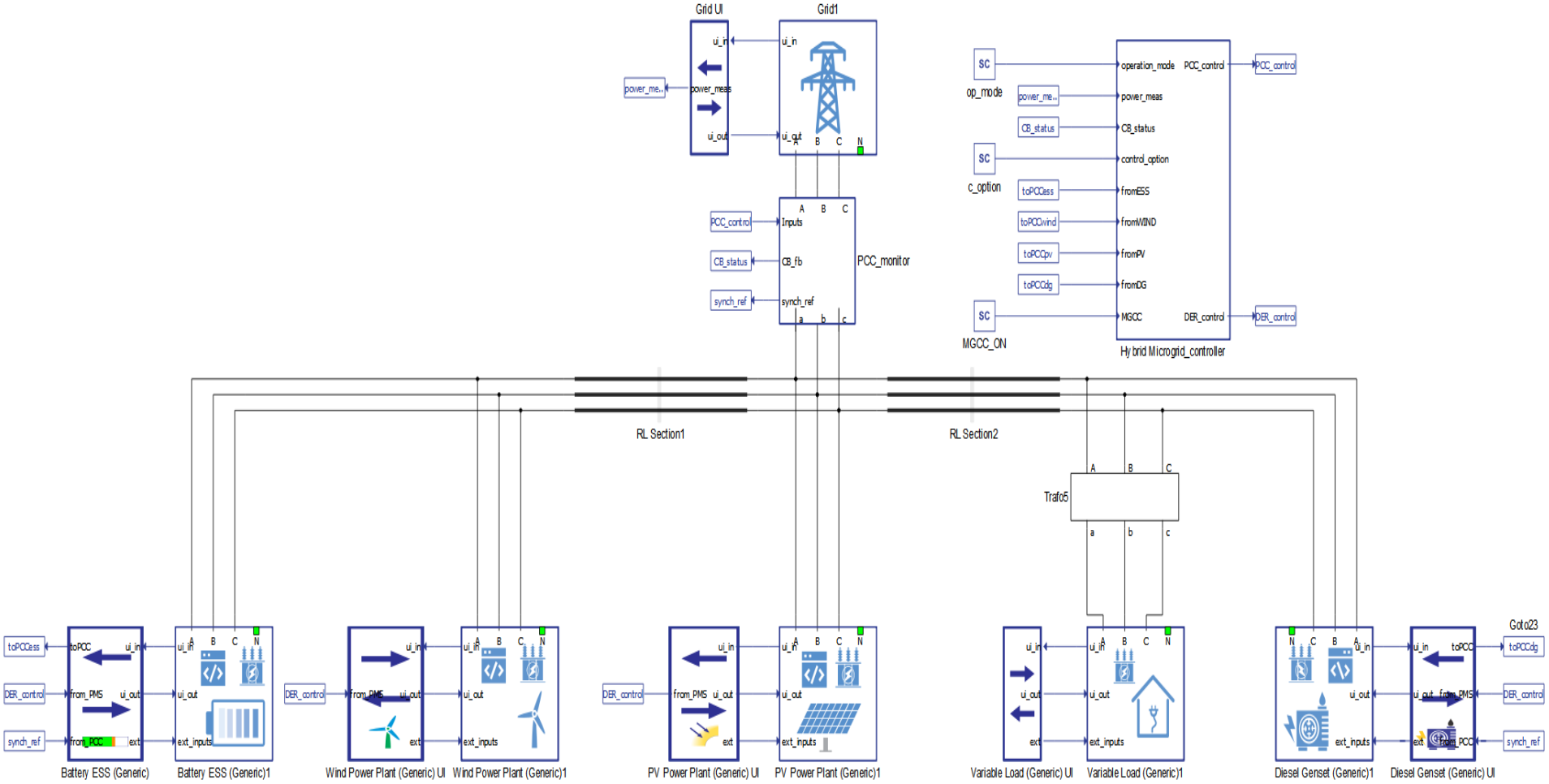


Figure E: Developed Hybrid micro-grid.